

# Spectral Transmittance Simulation for the ILAS Infrared (830-1,650 $\text{cm}^{-1}$ ) and Visible (12,740-13,280 $\text{cm}^{-1}$ ) Regions

by Tatsuya Yokota<sup>1</sup> and Jae H. Park<sup>2</sup>

1: The National Institute for Environmental Studies

2: NASA Langley Research Center  
Hampton, VA 23665 USA

The National Institute for Environmental Studies

環境庁 国立環境研究所

## Preface

Environment Agency has been developing a satellite-borne instrument for observing distribution of atmospheric constituents related to the stratospheric ozone layer chemistry. The instrument is called Improved Limb Atmospheric Spectrometer (ILAS), which is based on the principle of solar occultation technique in the infrared and visible region. The ILAS will be installed on the Advanced Earth Observing Satellite (ADEOS) which is planned for launch in early 1995.

The ILAS measurement gases are ozone, methane, nitrous oxide, nitric acid, water vapor, nitrogen dioxide and CFC11. Vertical profiles of these constituents are derived from transmittance measurements in the infrared (850-1610  $\text{cm}^{-1}$ ) wavelength region. Forty-four elements of pyroelectric array detectors are used for the infrared measurements.

Temperature and pressure profiles will be obtained from transmittance measurements in the oxygen A-band in the visible (12755-13280  $\text{cm}^{-1}$ ) region. Aerosol information is also obtained from the visible region. A detector for the visible channel is a MOS photodiode array with 1024 elements.

The National Institute for Environmental Studies (NIES) is responsible for developing a software system for processing the ILAS data. This will include spectrum fitting and inversion software for integral equations of multiple-channel data.

This report was prepared as one of the early steps for that purpose and is intended to provide, for not only researchers involved in the ILAS data processing algorithms but also future potential users of the ILAS products, with detailed information on atmospheric absorption spectrum in the ILAS infrared and visible regions.

The report has been prepared by Dr. T. Yokota (NIES) and Dr. J. H. Park (NASA Langley Research Center) during Dr. Yokota's one-year stay (1990-1991) at NASA Langley Research Center.

We hope this report would be of great help to those who are interested in the ILAS instrument and its products.

Yasuhiro Sasano  
ILAS Science Team Leader

## Contents

Preface

Introduction .....	1
Atlas of the Infrared Absorption Spectrum .....	15
Atlas of the Visible O <sub>2</sub> Absorption Spectrum .....	183
Appendices .....	213

## Introduction

Presented in this report are the simulations of spectral transmittance over the 830 to 1,650  $\text{cm}^{-1}$  range (infrared region) and over the 12,740 to 13,280  $\text{cm}^{-1}$  range (visible region).

Temperature and pressure profiles (Fig. 1 and Table 1) are for the northern hemisphere sub-arctic (52.6°N) winter condition. The model atmosphere is adopted from ATMOS Standard Profiles for  $\text{NO}_2$ ,  $\text{HNO}_3$ , CFC-11, and CFC-12, and from HALOE SIDS (Simulated Instrument Data Set) Atmosphere for the temperature, pressure, and the other gases. Gas mixing ratio profiles of nine species ( $\text{H}_2\text{O}$ ,  $\text{CO}_2$ ,  $\text{O}_3$ ,  $\text{N}_2\text{O}$ ,  $\text{CH}_4$ ,  $\text{NO}_2$ ,  $\text{HNO}_3$ , CFC-11( $\text{CFCl}_3$ ), and CFC-12 ( $\text{CF}_2\text{Cl}_2$ )) are shown in Fig. 2 and Table 1. A constant mixing ratio 0.21 is assumed for  $\text{O}_2$ .

The atmosphere is divided into 10 km thick homogeneous layers with the top of the atmosphere at 50 km (Fig. 3). Optical path refraction through the atmosphere is not considered in this simulation. The 1986 AFGL line database for the seven gases is used for the simulations. Absorption lines whose intensities ( $SL$  [ $\text{cm}^{-1}/(\text{molec}\cdot\text{cm}^{-2}) @ 296\text{K}$ ]) are less than  $SL_{\text{min}}$  are ignored in the cross section calculation;  $SL_{\text{min}}(\text{H}_2\text{O})=1\times 10^{-24}$ ,  $SL_{\text{min}}(\text{O}_3)=1\times 10^{-24}$ ,  $SL_{\text{min}}(\text{N}_2\text{O})=4\times 10^{-24}$ ,  $SL_{\text{min}}(\text{CH}_4)=4\times 10^{-24}$ ,  $SL_{\text{min}}(\text{CO}_2)=1\times 10^{-26}$ ,  $SL_{\text{min}}(\text{NO}_2)=1\times 10^{-24}$ , and  $SL_{\text{min}}(\text{HNO}_3)=4\times 10^{-24}$ . CFC-11 and CFC-12 are provided not by the line intensities but by the cross section data in the AFGL database. All  $\text{O}_2$  lines in the AFGL database are included in the calculations.

### Infrared Region

Shown in each page are transmittances calculated at 0.002  $\text{cm}^{-1}$  intervals and then averaged over 0.004  $\text{cm}^{-1}$  for every 10  $\text{cm}^{-1}$  interval at tangent altitudes of 10, 20, 30, 40, 50 km. In the opposite page are transmittances for individual gases at a tangent altitude of 20 km. Transmittances for CFC-11 and CFC-12 are magnified 25 times in the upper charts, and they are shown only in the spectral range of 830~940  $\text{cm}^{-1}$  and 1,060~1,180  $\text{cm}^{-1}$ .

### Visible Region

Transmittances are calculated for every 0.004  $\text{cm}^{-1}$  interval. Shown each page are transmittances (averaged over 0.008  $\text{cm}^{-1}$ ) for every 20  $\text{cm}^{-1}$  interval at tangent altitudes of 10, 20, 30, 40, 50 km. No aerosols are included in this simulation. Temperature dependence of  $\text{O}_2$  band absorption is shown in Figs. 4 through 9, because this channel is used for pressure and temperature sensing of the atmosphere.

These simulations were performed on the VAX 11/785 (HALOE VAX) and VAX 11/780 (ASD (Atmospheric Sciences Division) VAX) systems in cooperation with NASA Langley Research Center. Summary of the time for calculation is shown in Appendices A, B, and C. FORTRAN programs TRN. FOR ; 50, TRNS. FOR ; 51, TRNF. FOR ; 55, TRNFS. FOR ; 54,

and TRNV. FOR ; 54 were used for the infrared and visible calculation, which were coded by T. Yokota by modifying Jae Park's program. The transmittance charts were produced by using the IDL graphic utility package.

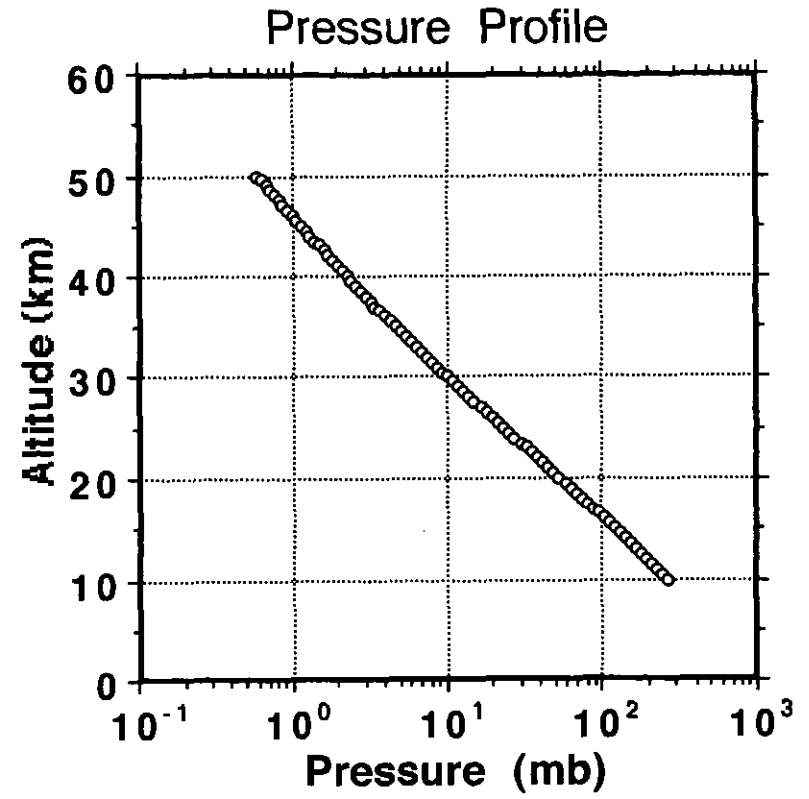
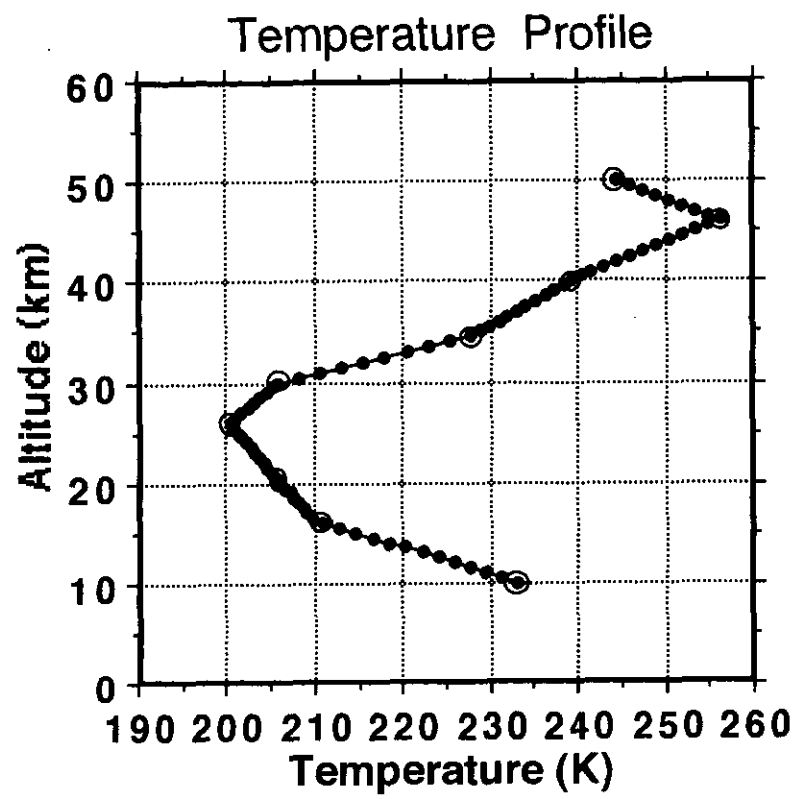


Fig.1 Temperature and Pressure Profiles (from HALOE SIDSATM\_N.DAT)

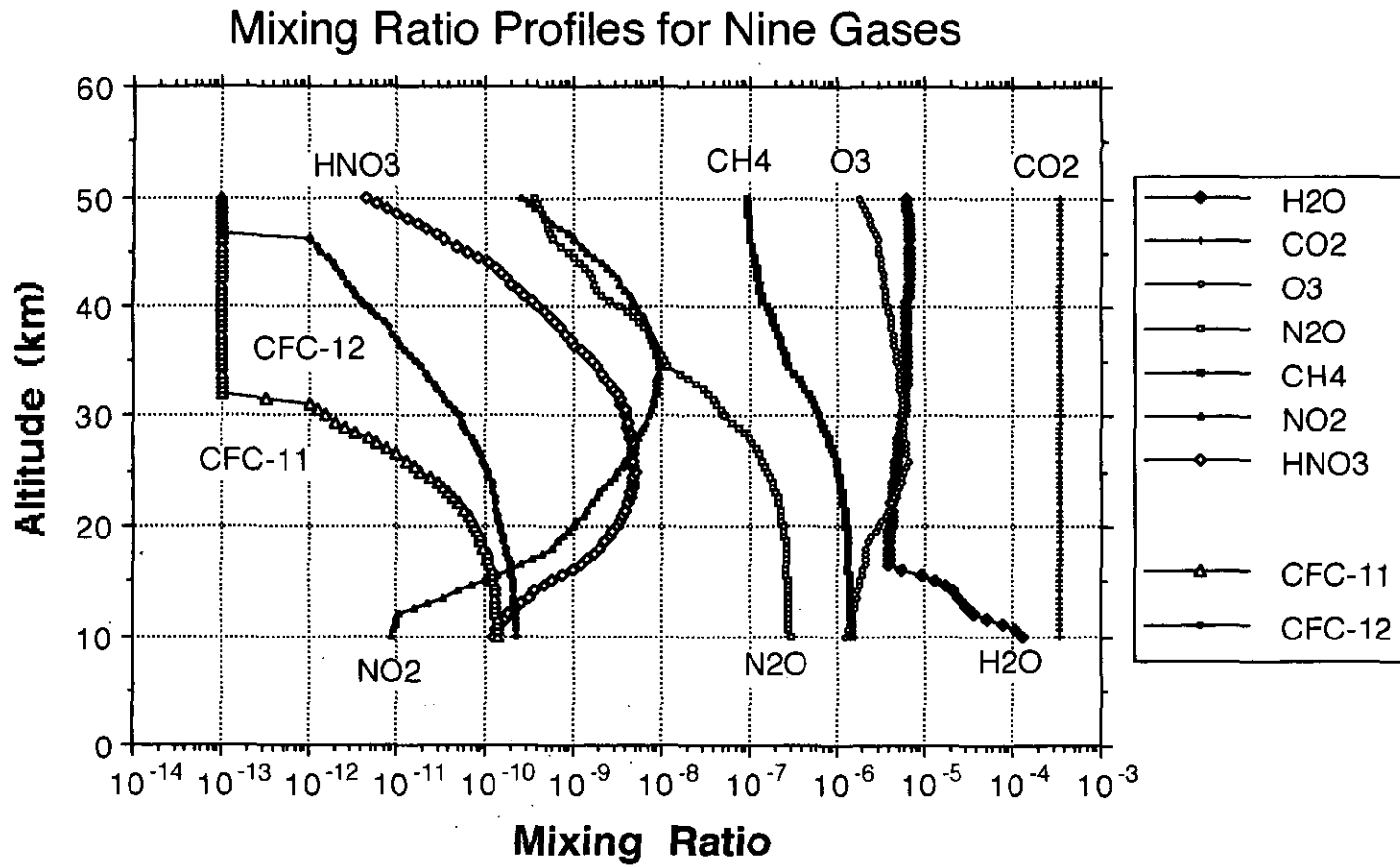


Fig.2 Mixing Ratio Profiles (from HALOE SIDSATM\_N.DAT for H<sub>2</sub>O, CO<sub>2</sub>, O<sub>3</sub>, NO<sub>2</sub>, CH<sub>4</sub>), (from ATMOS Standard Profiles for NO<sub>2</sub>, HNO<sub>3</sub>, CFC-11, CFC-12)

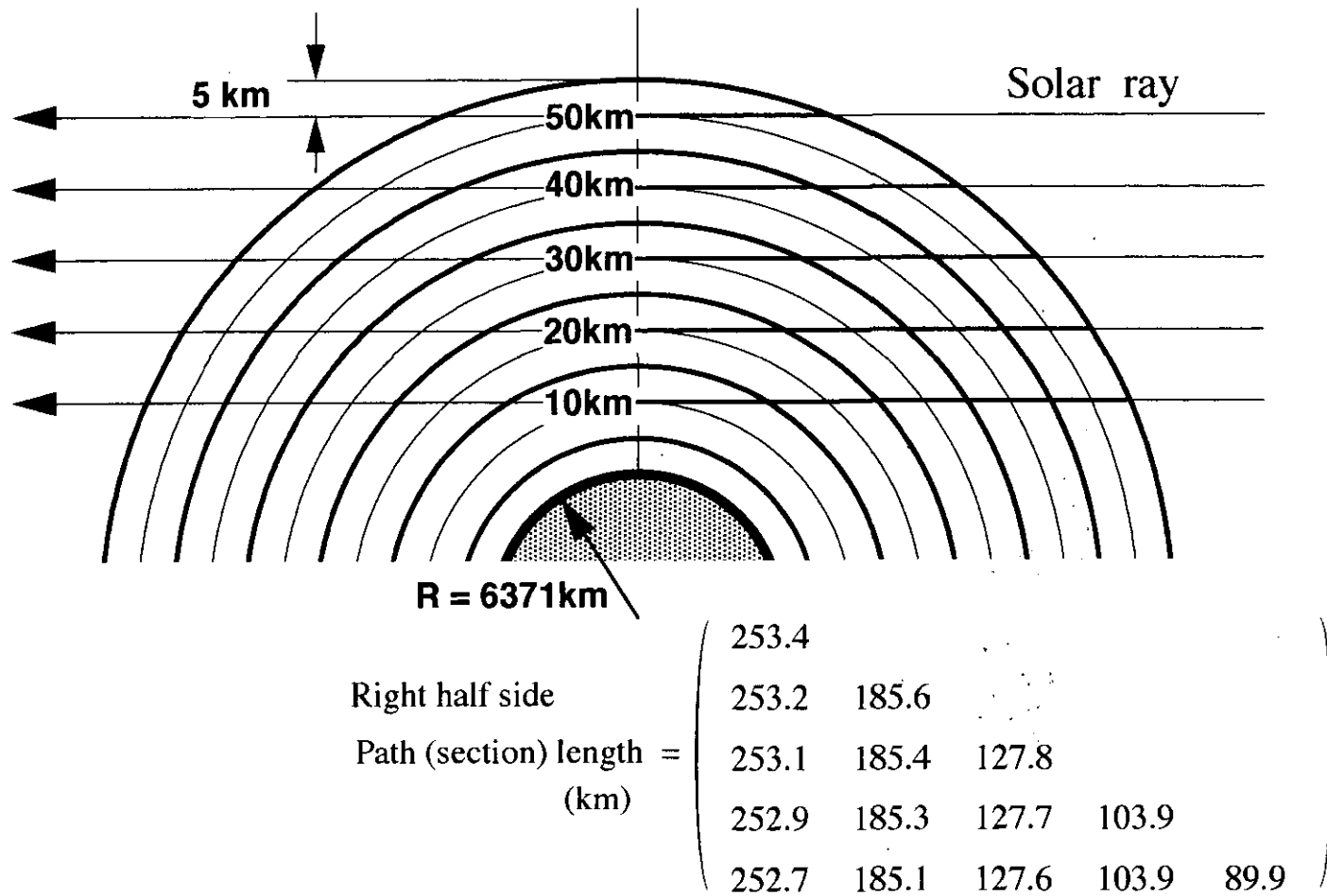


Fig.3 Limb Transmission Geometry (Homogeneous layer thickness = 10 km)



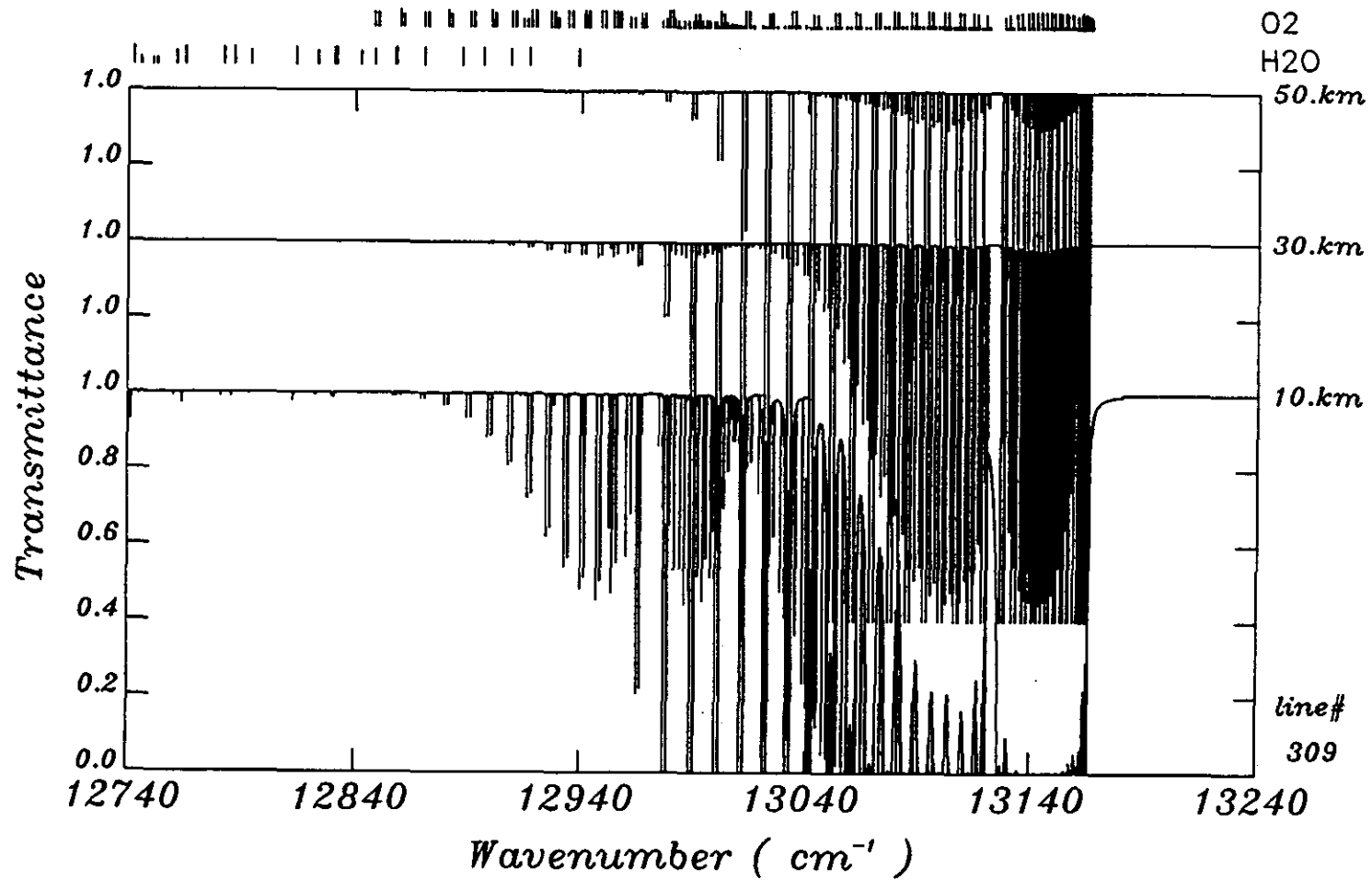


Fig.4 Transmittances in the visible spectral region at tangent altitudes of 10, 30, and 50 km (with standard temperature).

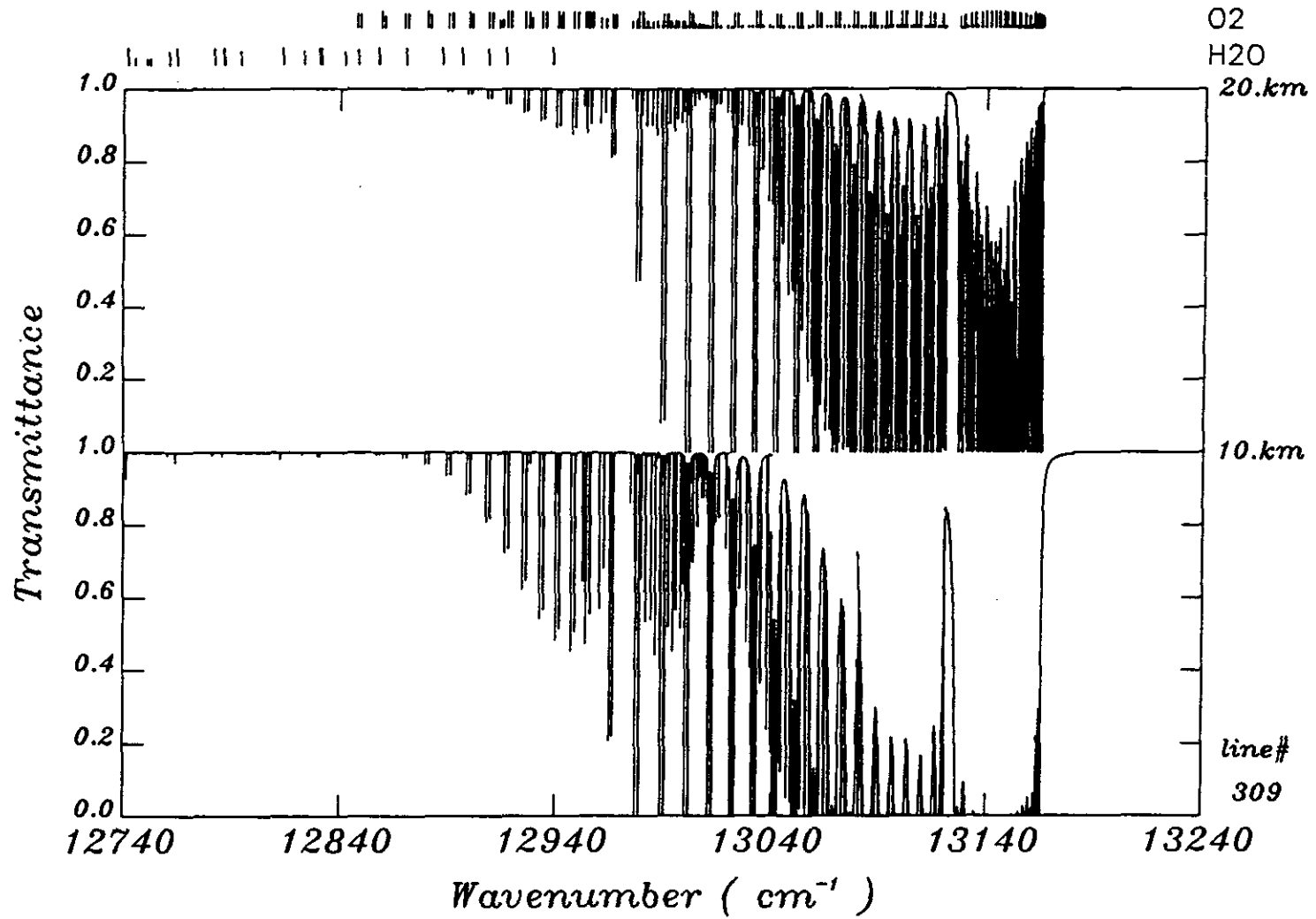


Fig.5 Transmittance comparison between 10 km and 20 km altitudes.

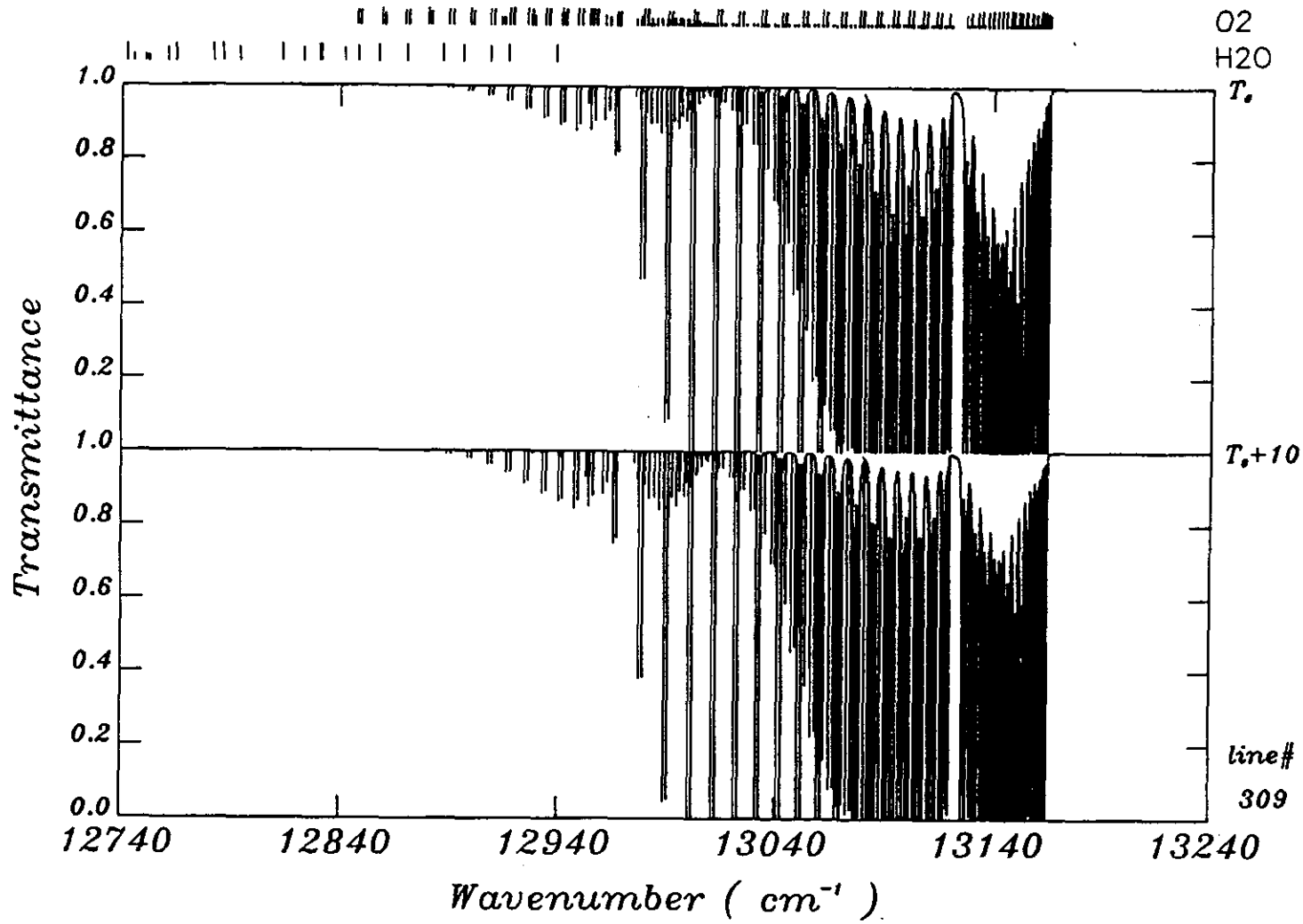


Fig.6 Transmittance comparison between standard temperature ( $T_0$ ) and 10 degree increased temperature ( $T_0 + 10$ ) at a tangent altitude of 20 km.

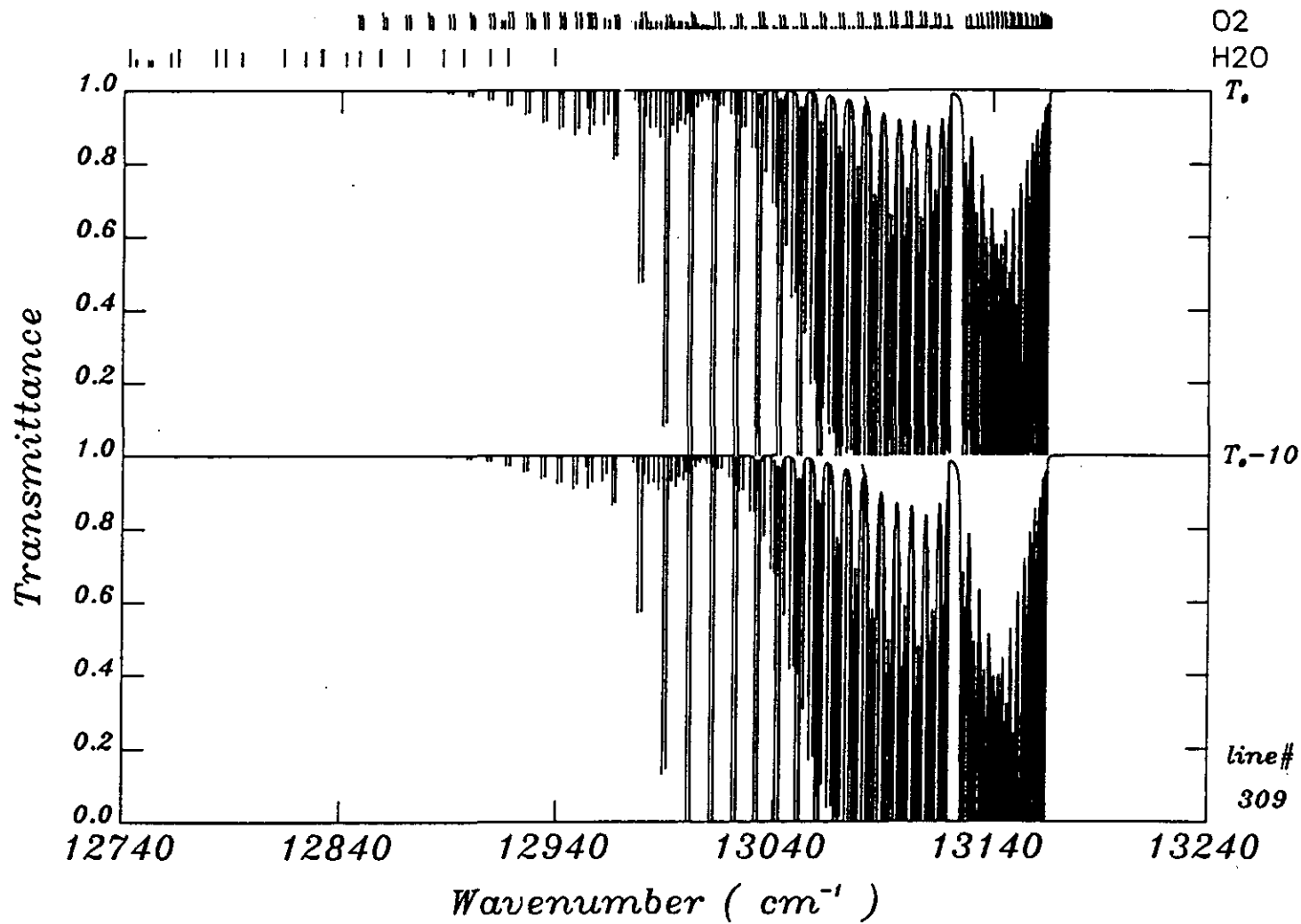


Fig.7 Transmittance comparison between standard temperature ( $T_0$ ) and 10 degree decreased temperature ( $T_0 - 10$ ) at a tangent altitude of 20 km.

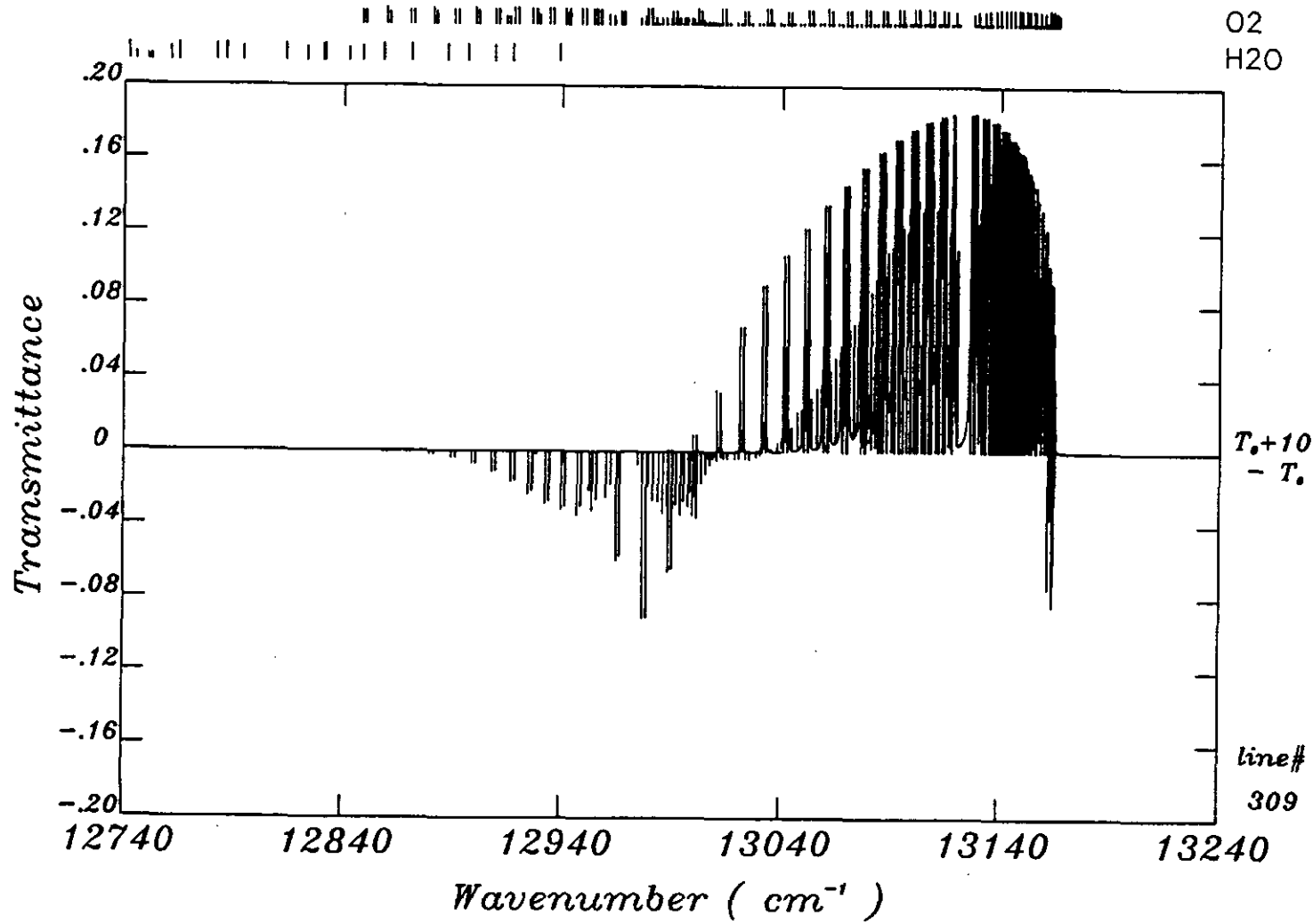


Fig.8 Transmittance difference between standard temperature ( $T_0$ ) and 10 degree increased temperature ( $T_0 + 10$ ) at a tangent altitude of 20 km.

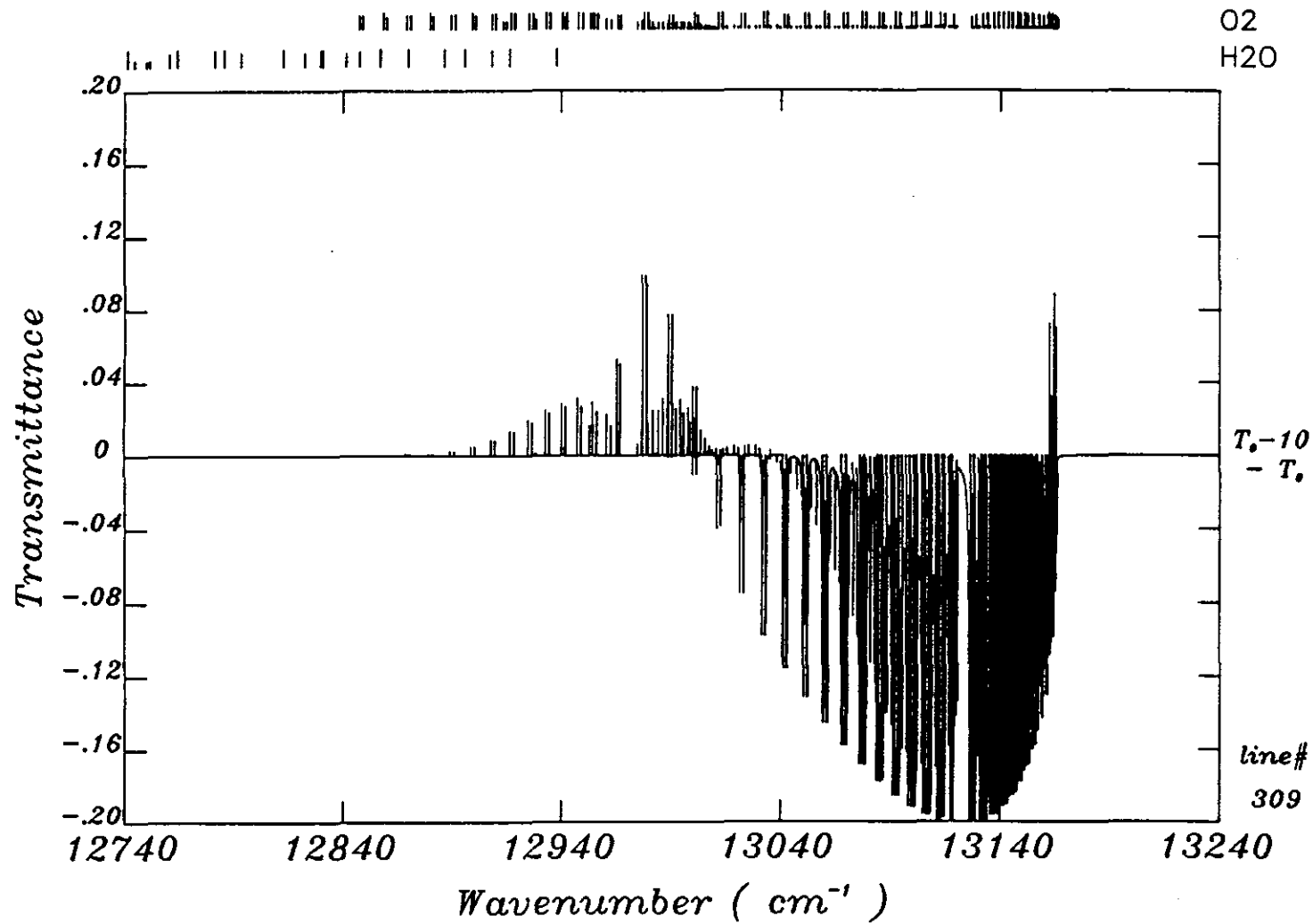


Fig.9 Transmittance difference between standard temperature ( $T_0$ ) and 10 degree decreased temperature ( $T_0 - 10$ ) at a tangent altitude of 20 km.

Table 1-1 Atmospheric Model Profiles (1)

Z(km)	P(mb)	T(K)	H2O	CO2	O3	N2O	CH4	NO2	HNO3	CFC-11	CFC-12
50.0	0.58	244.53	6.41E-6	3.3E-4	1.82E-6	3.63E-10	9.19E-8	2.60E-10	4.5E-12	1.0E-13	1.0E-13
49.5	0.62	246.00	6.42E-6	3.3E-4	1.96E-6	3.90E-10	9.32E-8	3.10E-10	5.9E-12	1.0E-13	1.0E-13
49.0	0.67	247.48	6.43E-6	3.3E-4	2.09E-6	4.17E-10	9.45E-8	3.60E-10	7.6E-12	1.0E-13	1.0E-13
48.5	0.72	248.95	6.44E-6	3.3E-4	2.22E-6	4.44E-10	9.58E-8	4.30E-10	1.0E-11	1.0E-13	1.0E-13
48.0	0.77	250.43	6.46E-6	3.3E-4	2.35E-6	4.71E-10	9.71E-8	5.10E-10	1.3E-11	1.0E-13	1.0E-13
47.5	0.82	251.90	6.47E-6	3.3E-4	2.48E-6	4.98E-10	9.83E-8	6.00E-10	1.7E-11	1.0E-13	1.0E-13
47.0	0.88	253.37	6.48E-6	3.3E-4	2.61E-6	5.25E-10	9.96E-8	7.10E-10	2.1E-11	1.0E-13	1.0E-13
46.5	0.93	254.85	6.49E-6	3.3E-4	2.75E-6	5.52E-10	1.01E-7	8.50E-10	2.7E-11	1.0E-13	1.0E-13
46.0	1.00	256.32	6.50E-6	3.3E-4	2.88E-6	5.79E-10	1.02E-7	1.00E-9	3.4E-11	1.0E-13	1.0E-12
45.5	1.07	254.92	6.50E-6	3.3E-4	2.95E-6	7.23E-10	1.06E-7	1.20E-9	4.6E-11	1.0E-13	1.2E-12
45.0	1.14	253.44	6.49E-6	3.3E-4	3.02E-6	8.70E-10	1.09E-7	1.40E-9	6.1E-11	1.0E-13	1.3E-12
44.5	1.22	251.96	6.49E-6	3.3E-4	3.09E-6	1.02E-9	1.12E-7	1.70E-9	8.2E-11	1.0E-13	1.6E-12
44.0	1.30	250.48	6.48E-6	3.3E-4	3.17E-6	1.16E-9	1.16E-7	2.10E-9	1.1E-10	1.0E-13	1.8E-12
43.5	1.39	249.00	6.48E-6	3.3E-4	3.24E-6	1.31E-9	1.19E-7	2.40E-9	1.3E-10	1.0E-13	2.0E-12
43.0	1.49	247.52	6.47E-6	3.3E-4	3.31E-6	1.46E-9	1.22E-7	2.70E-9	1.5E-10	1.0E-13	2.2E-12
42.5	1.60	246.04	6.46E-6	3.3E-4	3.38E-6	1.60E-9	1.26E-7	3.10E-9	1.7E-10	1.0E-13	2.4E-12
42.0	1.71	244.56	6.46E-6	3.3E-4	3.45E-6	1.75E-9	1.29E-7	3.50E-9	2.0E-10	1.0E-13	2.7E-12
41.5	1.83	243.08	6.45E-6	3.3E-4	3.53E-6	1.90E-9	1.33E-7	3.90E-9	2.4E-10	1.0E-13	3.1E-12
41.0	1.97	241.60	6.44E-6	3.3E-4	3.60E-6	2.04E-9	1.36E-7	4.30E-9	2.8E-10	1.0E-13	3.5E-12
40.5	2.11	240.44	6.43E-6	3.3E-4	3.70E-6	2.62E-9	1.45E-7	4.70E-9	3.4E-10	1.0E-13	4.0E-12
40.0	2.26	239.39	6.42E-6	3.3E-4	3.81E-6	3.34E-9	1.56E-7	5.20E-9	4.0E-10	1.0E-13	4.5E-12
39.5	2.43	238.34	6.41E-6	3.3E-4	3.92E-6	4.06E-9	1.67E-7	5.60E-9	4.6E-10	1.0E-13	5.2E-12
39.0	2.61	237.28	6.39E-6	3.3E-4	4.03E-6	4.77E-9	1.78E-7	6.10E-9	5.3E-10	1.0E-13	6.0E-12
38.5	2.80	236.23	6.38E-6	3.3E-4	4.14E-6	5.49E-9	1.88E-7	6.60E-9	6.1E-10	1.0E-13	6.9E-12
38.0	3.01	235.17	6.36E-6	3.3E-4	4.25E-6	6.21E-9	1.99E-7	7.20E-9	7.0E-10	1.0E-13	8.0E-12
37.5	3.23	234.12	6.35E-6	3.3E-4	4.36E-6	6.93E-9	2.10E-7	7.60E-9	8.0E-10	1.0E-13	8.9E-12
37.0	3.47	233.06	6.34E-6	3.3E-4	4.47E-6	7.64E-9	2.21E-7	8.00E-9	9.2E-10	1.0E-13	9.8E-12
36.5	3.74	232.01	6.32E-6	3.3E-4	4.58E-6	8.36E-9	2.32E-7	8.50E-9	1.0E-9	1.0E-13	1.1E-11
36.0	4.02	230.96	6.31E-6	3.3E-4	4.69E-6	9.08E-9	2.43E-7	9.00E-9	1.2E-9	1.0E-13	1.2E-11
35.5	4.32	229.90	6.30E-6	3.3E-4	4.80E-6	9.80E-9	2.54E-7	9.00E-9	1.4E-9	1.0E-13	1.4E-11
35.0	4.66	228.85	6.28E-6	3.3E-4	4.91E-6	1.05E-8	2.64E-7	9.05E-9	1.6E-9	1.0E-13	1.6E-11
34.5	5.01	227.73	6.27E-6	3.3E-4	5.02E-6	1.14E-8	2.76E-7	9.10E-9	1.8E-9	1.0E-13	1.8E-11
34.0	5.40	225.28	6.19E-6	3.3E-4	5.08E-6	1.58E-8	3.14E-7	9.10E-9	2.1E-9	1.0E-13	2.1E-11
33.5	5.83	222.82	6.12E-6	3.3E-4	5.13E-6	2.02E-8	3.51E-7	9.00E-9	2.3E-9	1.0E-13	2.3E-11
33.0	6.29	220.37	6.05E-6	3.3E-4	5.19E-6	2.47E-8	3.88E-7	8.95E-9	2.6E-9	1.0E-13	2.6E-11
32.5	6.79	217.92	5.98E-6	3.3E-4	5.24E-6	2.91E-8	4.26E-7	8.90E-9	2.8E-9	1.0E-13	2.8E-11
32.0	7.34	215.46	5.91E-6	3.3E-4	5.30E-6	3.35E-8	4.63E-7	8.80E-9	3.1E-9	1.0E-13	3.1E-11
31.5	7.95	213.01	5.83E-6	3.3E-4	5.35E-6	3.79E-8	5.00E-7	8.40E-9	3.3E-9	3.2E-13	3.5E-11
31.0	8.61	210.56	5.76E-6	3.3E-4	5.41E-6	4.24E-8	5.38E-7	8.00E-9	3.5E-9	1.0E-12	3.9E-11
30.5	9.33	208.10	5.69E-6	3.3E-4	5.46E-6	4.68E-8	5.75E-7	7.65E-9	3.8E-9	1.2E-12	4.4E-11
30.0	10.13	205.94	5.61E-6	3.3E-4	5.53E-6	5.23E-8	6.13E-7	7.30E-9	4.0E-9	1.5E-12	5.0E-11

Table 1-2 Atmospheric Model Profiles (2)

Z(km)	P(mb)	T(K)	H2O	CO2	O3	N2O	CH4	NO2	HNO3	CFC-11	CFC-12
30.0	10.13	205.94	5.61E-6	3.3E-4	5.53E-6	5.23E-8	6.13E-7	7.30E-9	4.0E-9	1.5E-12	5.0E-11
29.5	11.00	205.24	5.52E-6	3.3E-4	5.64E-6	6.37E-8	6.58E-7	6.80E-9	4.1E-9	2.0E-12	5.4E-11
29.0	11.95	204.55	5.42E-6	3.3E-4	5.76E-6	7.50E-8	7.02E-7	6.30E-9	4.2E-9	2.6E-12	5.9E-11
28.5	12.98	203.85	5.32E-6	3.3E-4	5.88E-6	8.64E-8	7.46E-7	5.90E-9	4.4E-9	3.5E-12	6.4E-11
28.0	14.11	203.16	5.22E-6	3.3E-4	5.99E-6	9.77E-8	7.91E-7	5.50E-9	4.5E-9	4.6E-12	7.0E-11
27.5	15.34	202.46	5.12E-6	3.3E-4	6.11E-6	1.09E-7	8.35E-7	5.10E-9	4.6E-9	6.0E-12	7.5E-11
27.0	16.68	201.77	5.03E-6	3.3E-4	6.23E-6	1.20E-7	8.79E-7	4.70E-9	4.7E-9	7.7E-12	8.0E-11
26.5	18.14	201.07	4.93E-6	3.3E-4	6.34E-6	1.32E-7	9.24E-7	4.30E-9	4.8E-9	1.0E-11	8.6E-11
26.0	19.74	200.38	4.83E-6	3.3E-4	6.46E-6	1.43E-7	9.68E-7	4.00E-9	4.9E-9	1.3E-11	9.2E-11
25.5	21.48	200.72	4.75E-6	3.3E-4	6.21E-6	1.52E-7	9.97E-7	3.60E-9	4.9E-9	1.6E-11	9.8E-11
25.0	23.37	201.23	4.68E-6	3.3E-4	5.90E-6	1.61E-7	1.02E-6	3.20E-9	5.0E-9	1.9E-11	1.1E-10
24.5	25.43	201.74	4.60E-6	3.3E-4	5.60E-6	1.70E-7	1.05E-6	2.90E-9	4.9E-9	2.4E-11	1.1E-10
24.0	27.65	202.25	4.53E-6	3.3E-4	5.29E-6	1.79E-7	1.08E-6	2.60E-9	4.9E-9	2.9E-11	1.2E-10
23.5	30.07	202.76	4.46E-6	3.3E-4	4.98E-6	1.87E-7	1.10E-6	2.30E-9	4.7E-9	3.3E-11	1.22E-10
23.0	32.69	203.27	4.38E-6	3.3E-4	4.68E-6	1.96E-7	1.13E-6	2.00E-9	4.5E-9	3.8E-11	1.25E-10
22.5	35.53	203.78	4.31E-6	3.3E-4	4.37E-6	2.05E-7	1.16E-6	1.80E-9	4.3E-9	4.4E-11	1.27E-10
22.0	38.62	204.29	4.23E-6	3.3E-4	4.06E-6	2.14E-7	1.18E-6	1.60E-9	4.1E-9	5.0E-11	1.3E-10
21.5	41.96	204.79	4.17E-6	3.3E-4	3.78E-6	2.20E-7	1.20E-6	1.40E-9	3.8E-9	5.7E-11	1.35E-10
21.0	45.58	205.27	4.12E-6	3.3E-4	3.52E-6	2.25E-7	1.22E-6	1.30E-9	3.6E-9	6.5E-11	1.4E-10
20.5	49.51	205.76	4.07E-6	3.3E-4	3.26E-6	2.30E-7	1.23E-6	1.10E-9	3.3E-9	7.0E-11	1.45E-10
20.0	53.76	206.25	4.01E-6	3.3E-4	3.00E-6	2.35E-7	1.25E-6	1.00E-9	3.1E-9	7.5E-11	1.5E-10
19.5	58.37	206.73	3.96E-6	3.3E-4	2.73E-6	2.41E-7	1.27E-6	8.70E-10	2.8E-9	8.1E-11	1.55E-10
19.0	63.37	207.22	3.91E-6	3.3E-4	2.47E-6	2.46E-7	1.28E-6	7.60E-10	2.5E-9	8.7E-11	1.6E-10
18.5	68.78	207.71	3.86E-6	3.3E-4	2.21E-6	2.51E-7	1.30E-6	6.65E-10	2.2E-9	8.9E-11	1.65E-10
18.0	74.63	208.20	3.83E-6	3.3E-4	2.14E-6	2.54E-7	1.31E-6	5.80E-10	2.0E-9	9.2E-11	1.7E-10
17.5	80.97	208.71	3.81E-6	3.3E-4	2.12E-6	2.56E-7	1.32E-6	4.40E-10	1.7E-9	1.05E-10	1.77E-10
17.0	87.84	209.21	3.79E-6	3.3E-4	2.09E-6	2.58E-7	1.33E-6	3.40E-10	1.4E-9	1.1E-10	1.84E-10
16.5	95.26	209.71	3.77E-6	3.3E-4	2.07E-6	2.61E-7	1.34E-6	2.60E-10	1.2E-9	1.15E-10	1.92E-10
16.0	103.30	210.80	5.37E-6	3.3E-4	2.03E-6	2.63E-7	1.35E-6	2.00E-10	1.0E-9	1.2E-10	2.0E-10
15.5	111.90	212.70	9.18E-6	3.3E-4	1.96E-6	2.65E-7	1.36E-6	1.40E-10	7.7E-10	1.22E-10	2.02E-10
15.0	121.20	214.59	1.30E-5	3.3E-4	1.90E-6	2.67E-7	1.37E-6	1.00E-10	6.0E-10	1.25E-10	2.05E-10
14.5	131.20	216.48	1.68E-5	3.3E-4	1.83E-6	2.69E-7	1.39E-6	7.10E-11	4.6E-10	1.27E-10	2.07E-10
14.0	141.80	218.38	2.06E-5	3.3E-4	1.76E-6	2.71E-7	1.40E-6	5.00E-11	3.6E-10	1.3E-10	2.1E-10
13.5	153.30	220.27	2.44E-5	3.3E-4	1.70E-6	2.73E-7	1.41E-6	3.40E-11	3.1E-10	1.31E-10	2.12E-10
13.0	165.50	222.16	2.83E-5	3.3E-4	1.63E-6	2.75E-7	1.42E-6	2.30E-11	2.6E-10	1.32E-10	2.15E-10
12.5	178.70	224.06	3.21E-5	3.3E-4	1.56E-6	2.77E-7	1.43E-6	1.60E-11	2.2E-10	1.33E-10	2.17E-10
12.0	192.70	225.95	3.59E-5	3.3E-4	1.49E-6	2.79E-7	1.45E-6	1.10E-11	1.9E-10	1.35E-10	2.2E-10
11.5	207.70	227.78	5.16E-5	3.3E-4	1.43E-6	2.81E-7	1.46E-6	1.00E-11	1.7E-10	1.36E-10	2.21E-10
11.0	223.80	229.56	7.83E-5	3.3E-4	1.37E-6	2.82E-7	1.47E-6	9.70E-12	1.5E-10	1.37E-10	2.22E-10
10.5	241.00	231.33	1.05E-4	3.3E-4	1.30E-6	2.84E-7	1.48E-6	9.10E-12	1.3E-10	1.38E-10	2.24E-10
10.0	259.30	233.10	1.32E-4	3.3E-4	1.24E-6	2.86E-7	1.49E-6	8.50E-12	1.2E-10	1.4E-10	2.25E-10

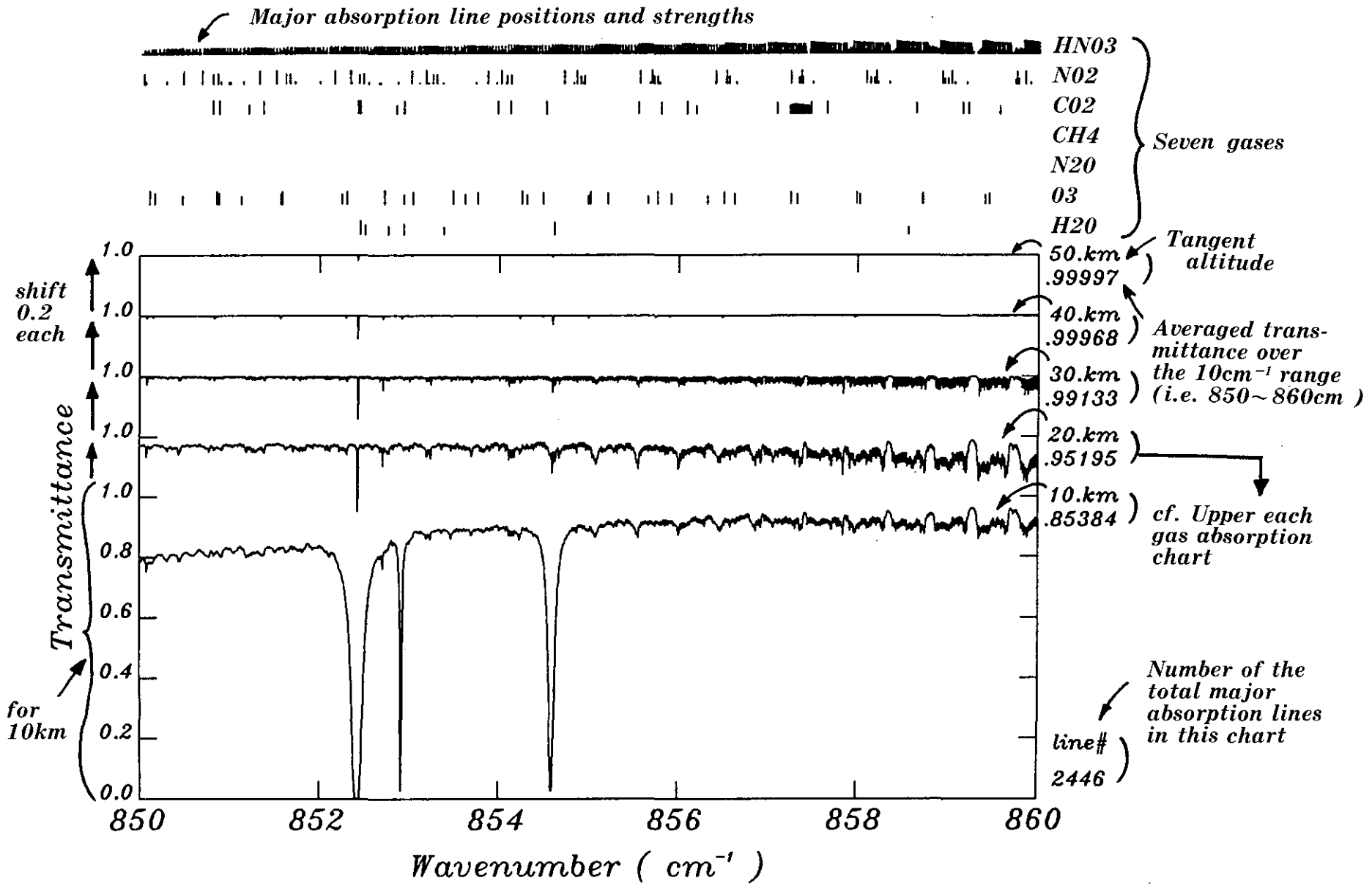


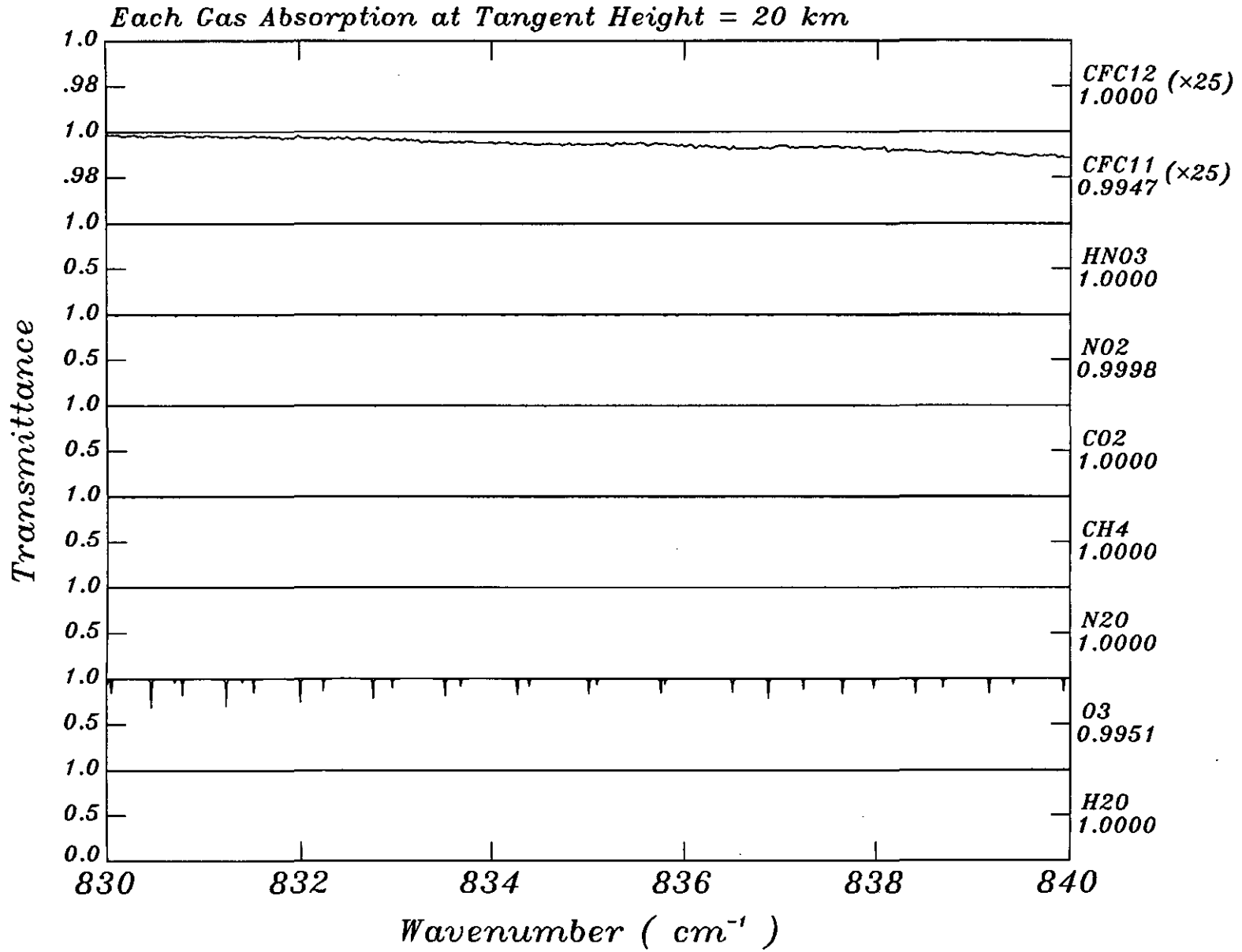


Atlas of the Infrared

Absorption Spectrum

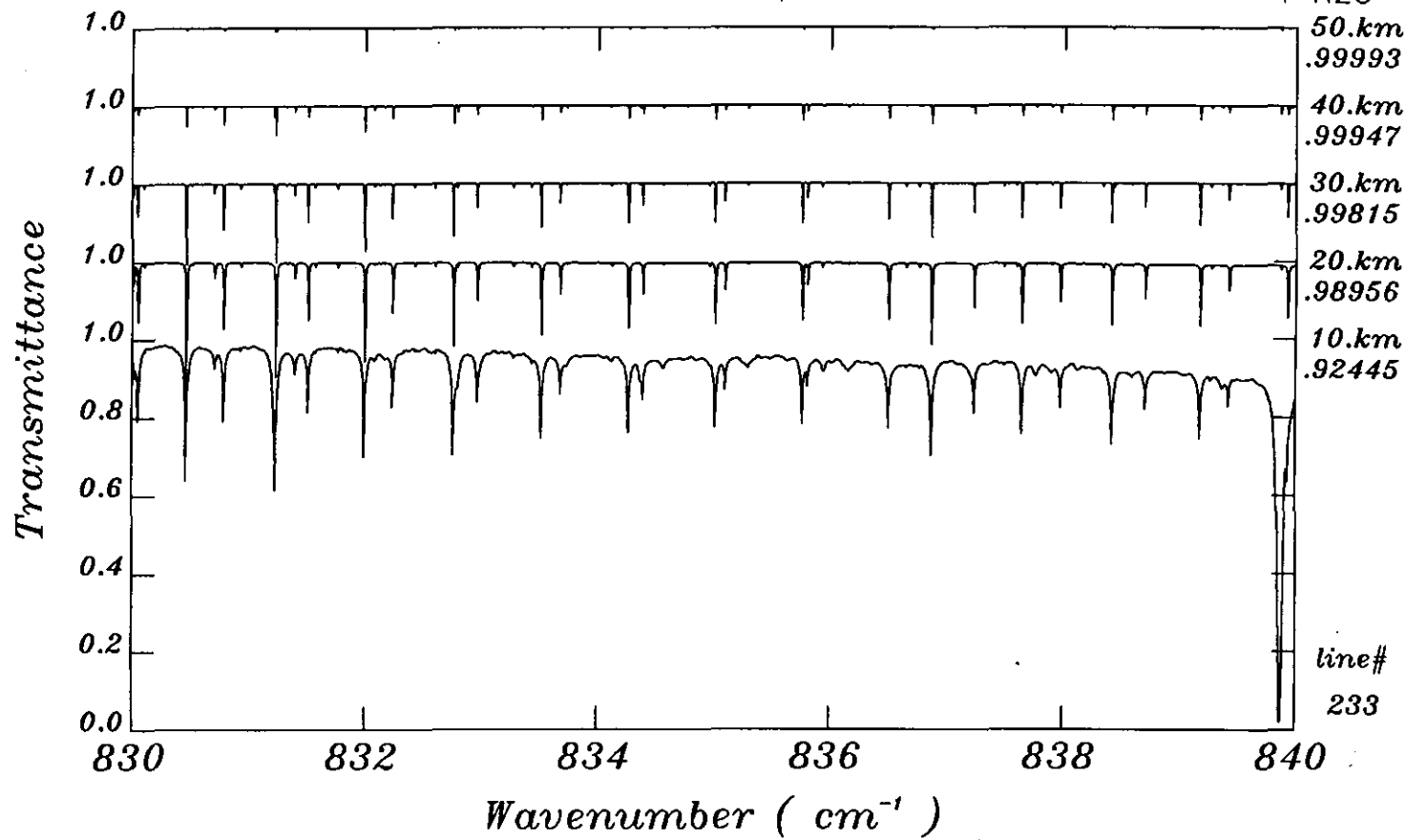
(Sample)



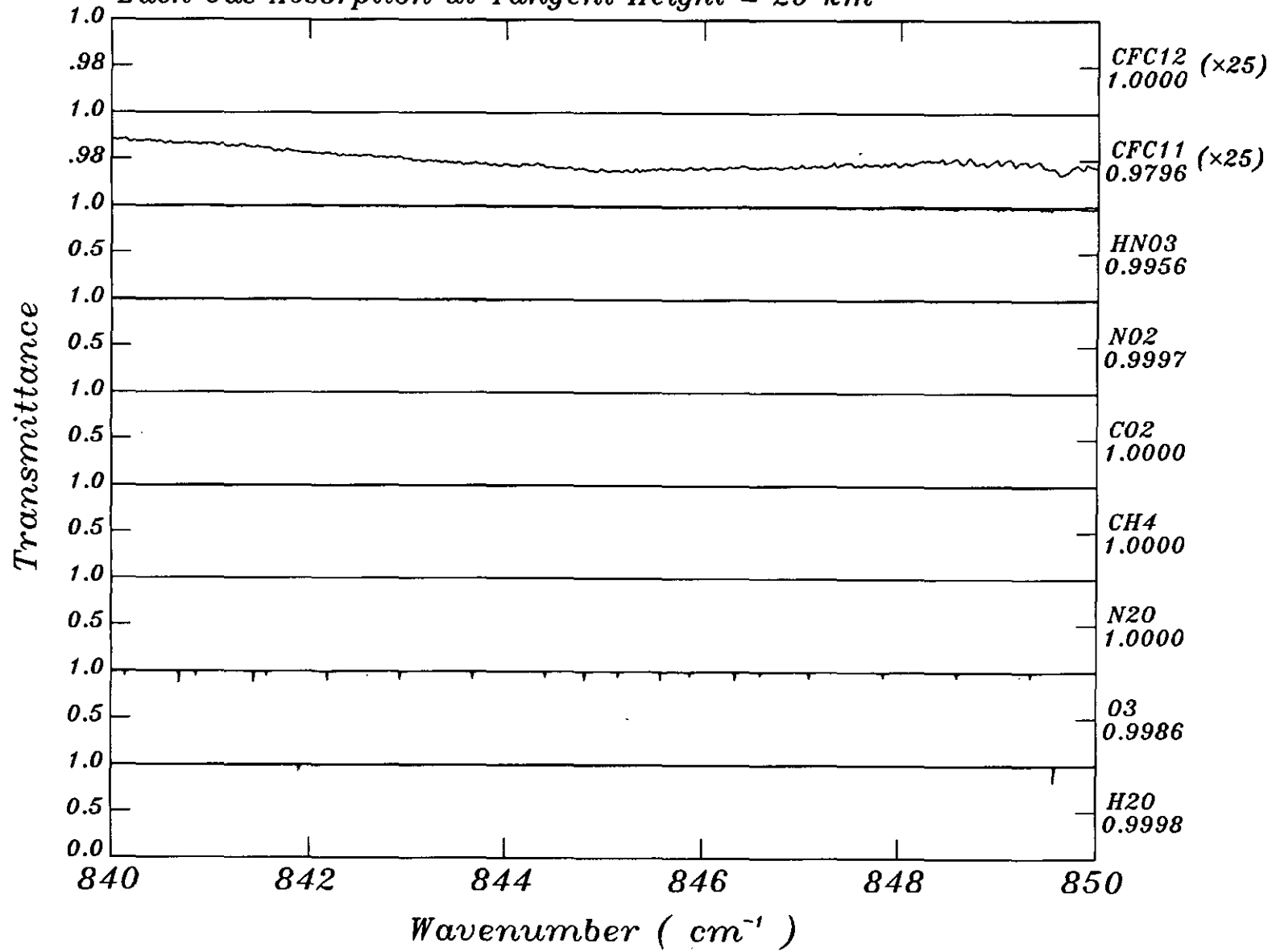


NO2  
CO2

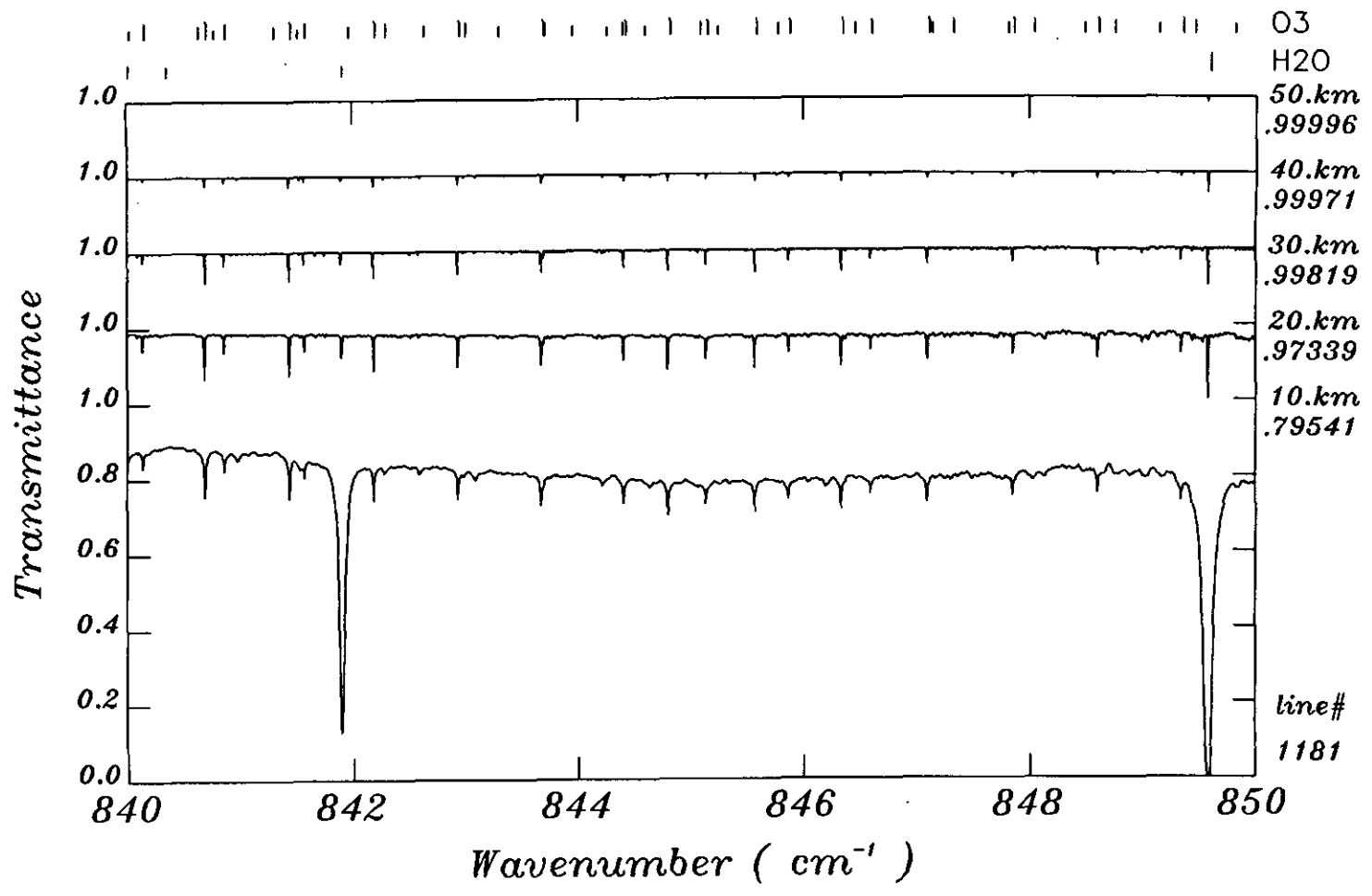
O3  
H2O



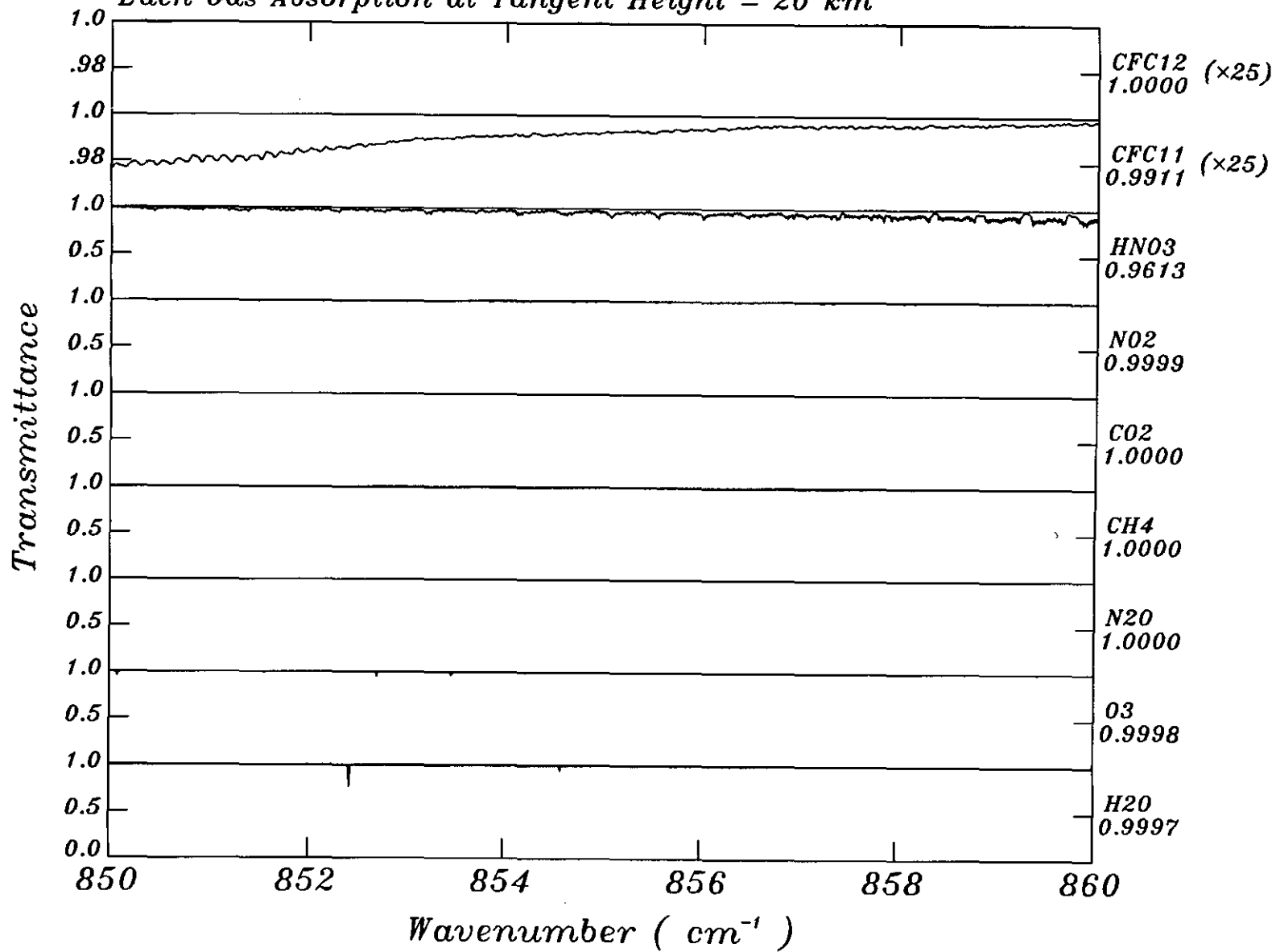
Each Gas Absorption at Tangent Height = 20 km



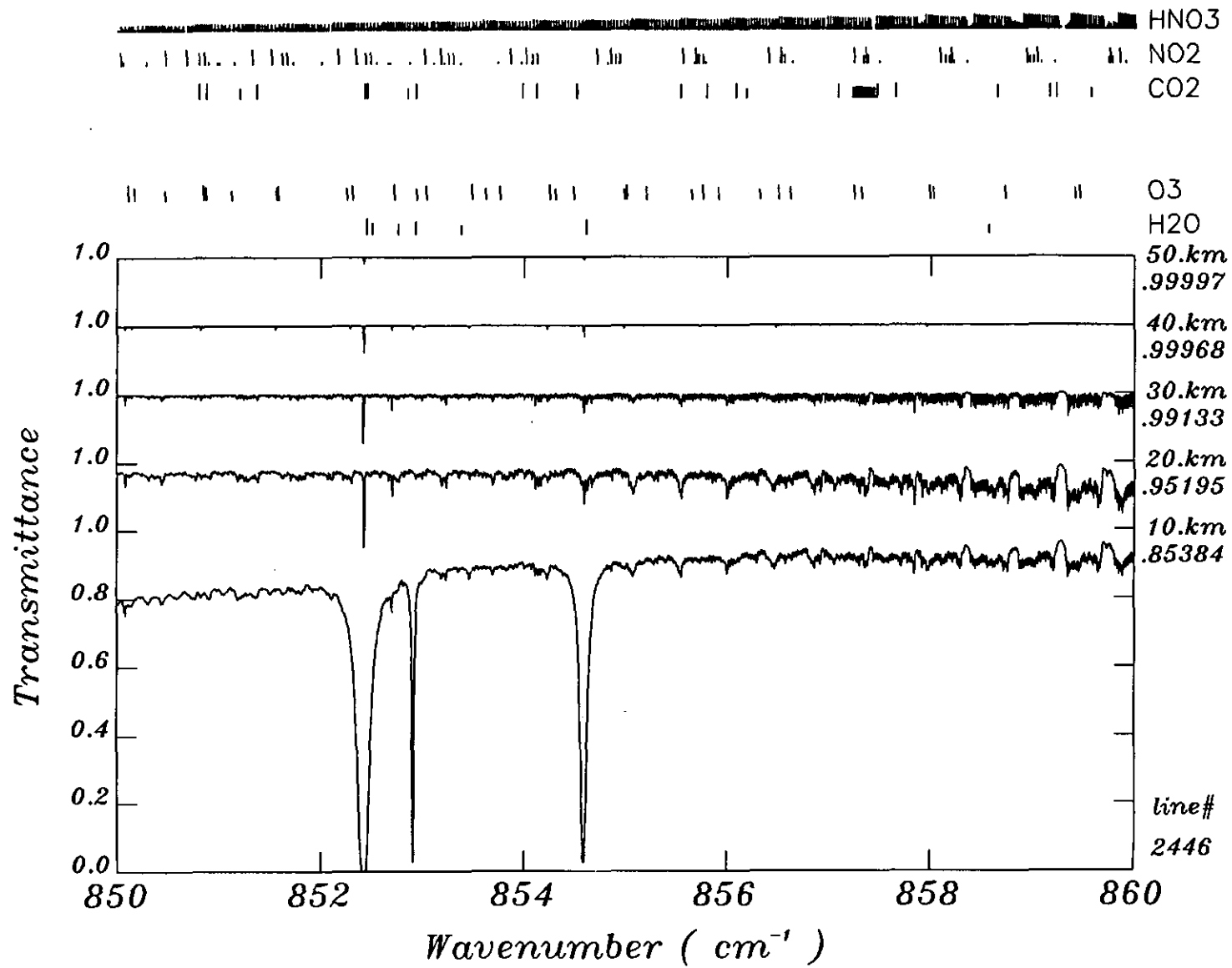
HNO3  
NO2  
CO2

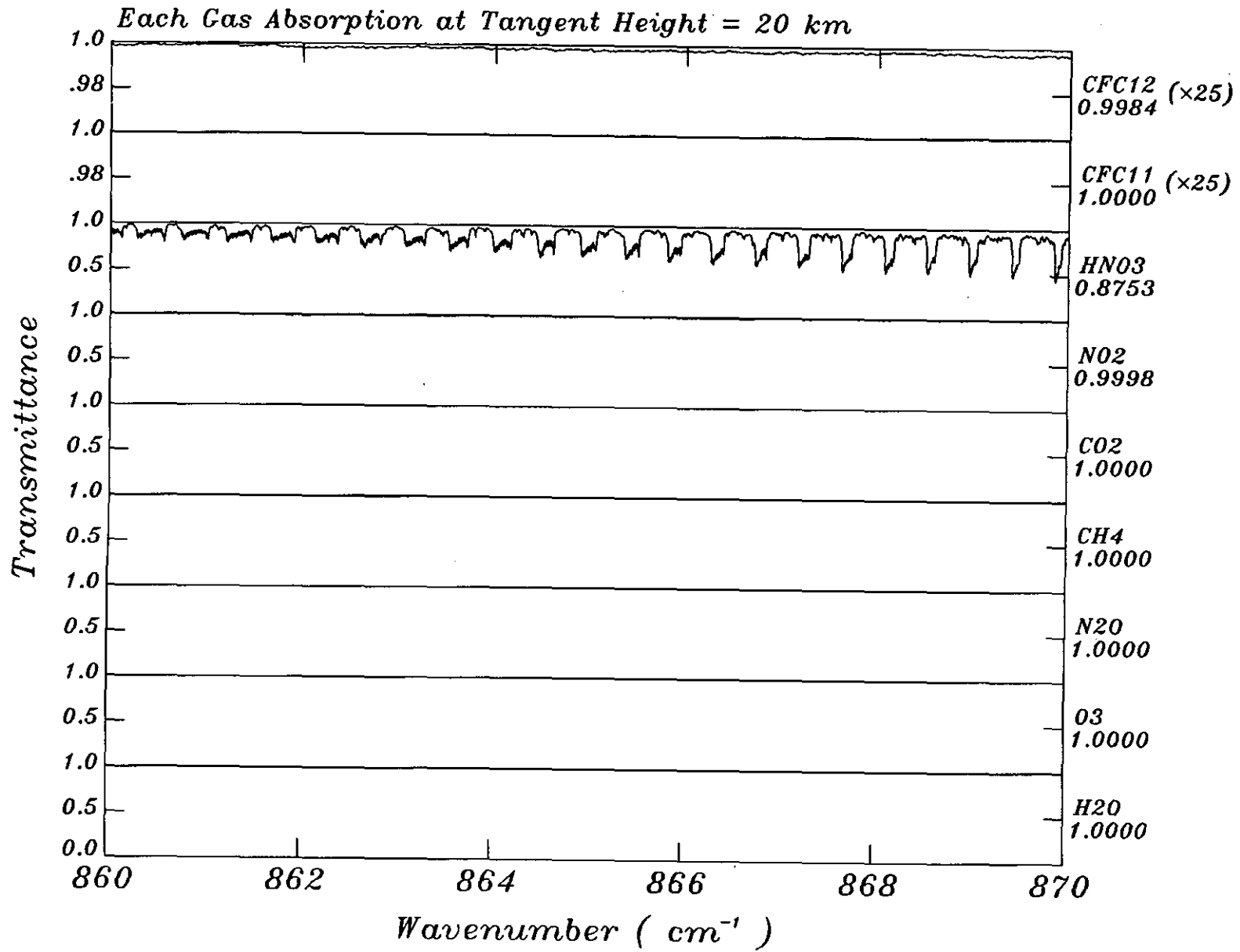


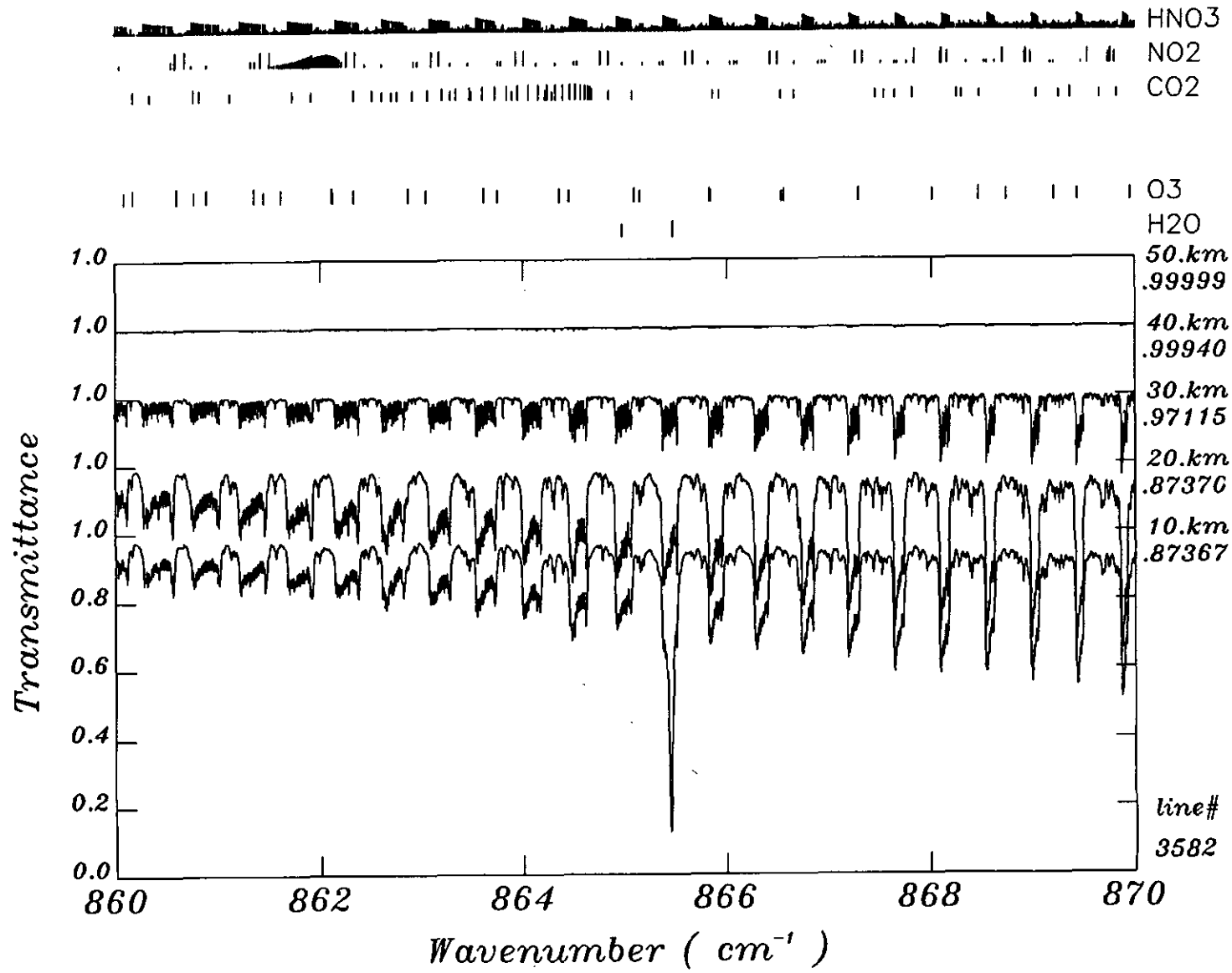
Each Gas Absorption at Tangent Height = 20 km



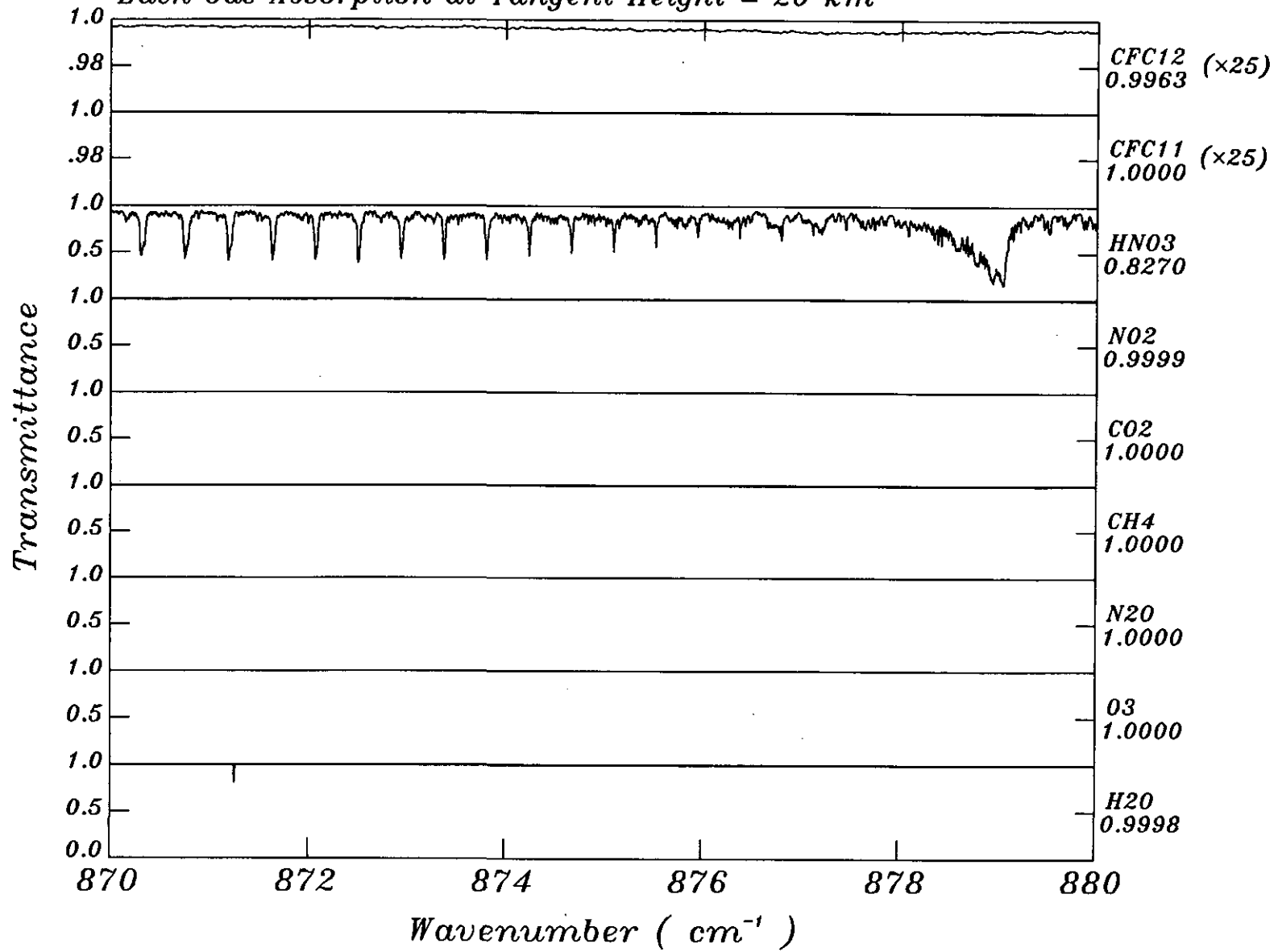


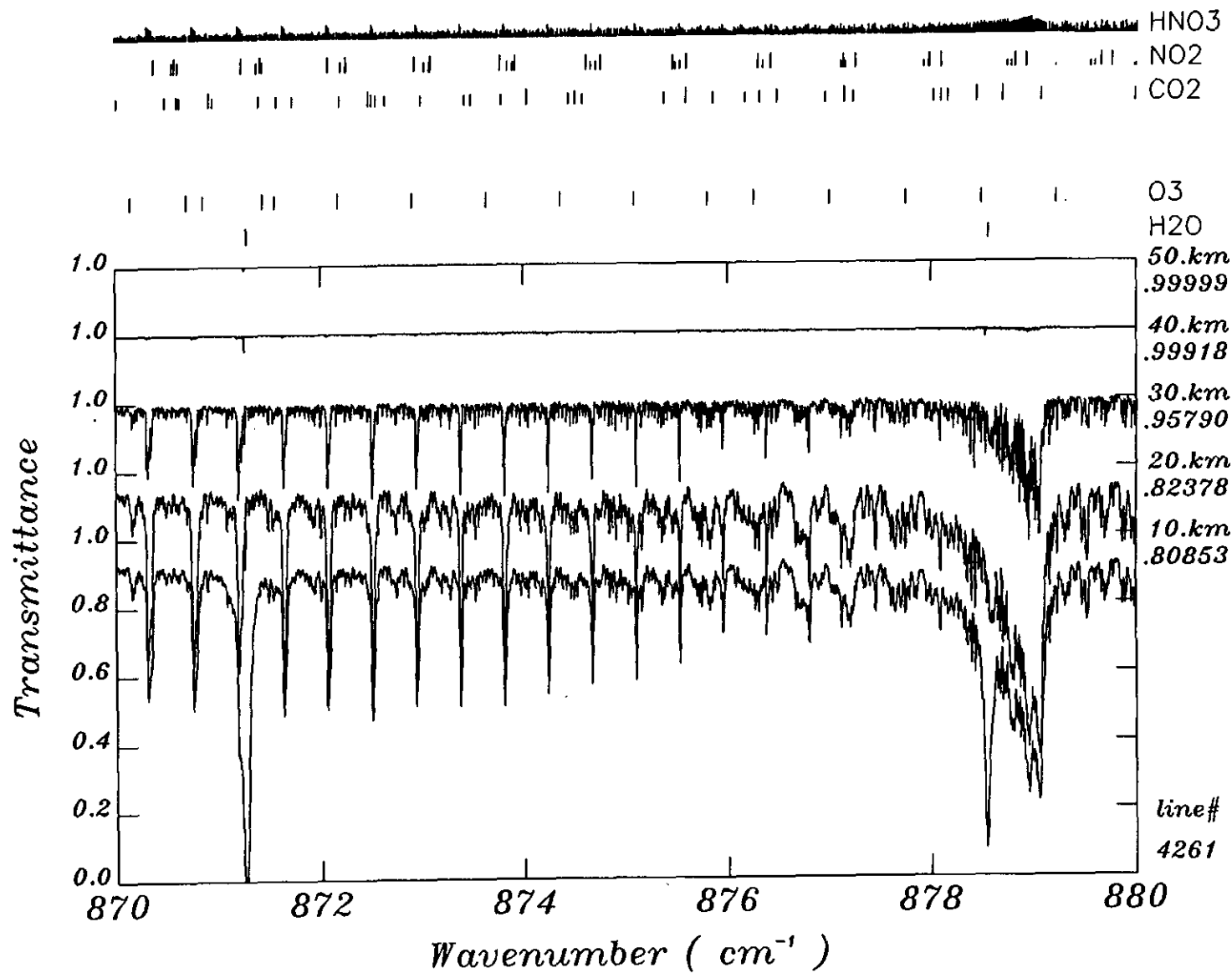


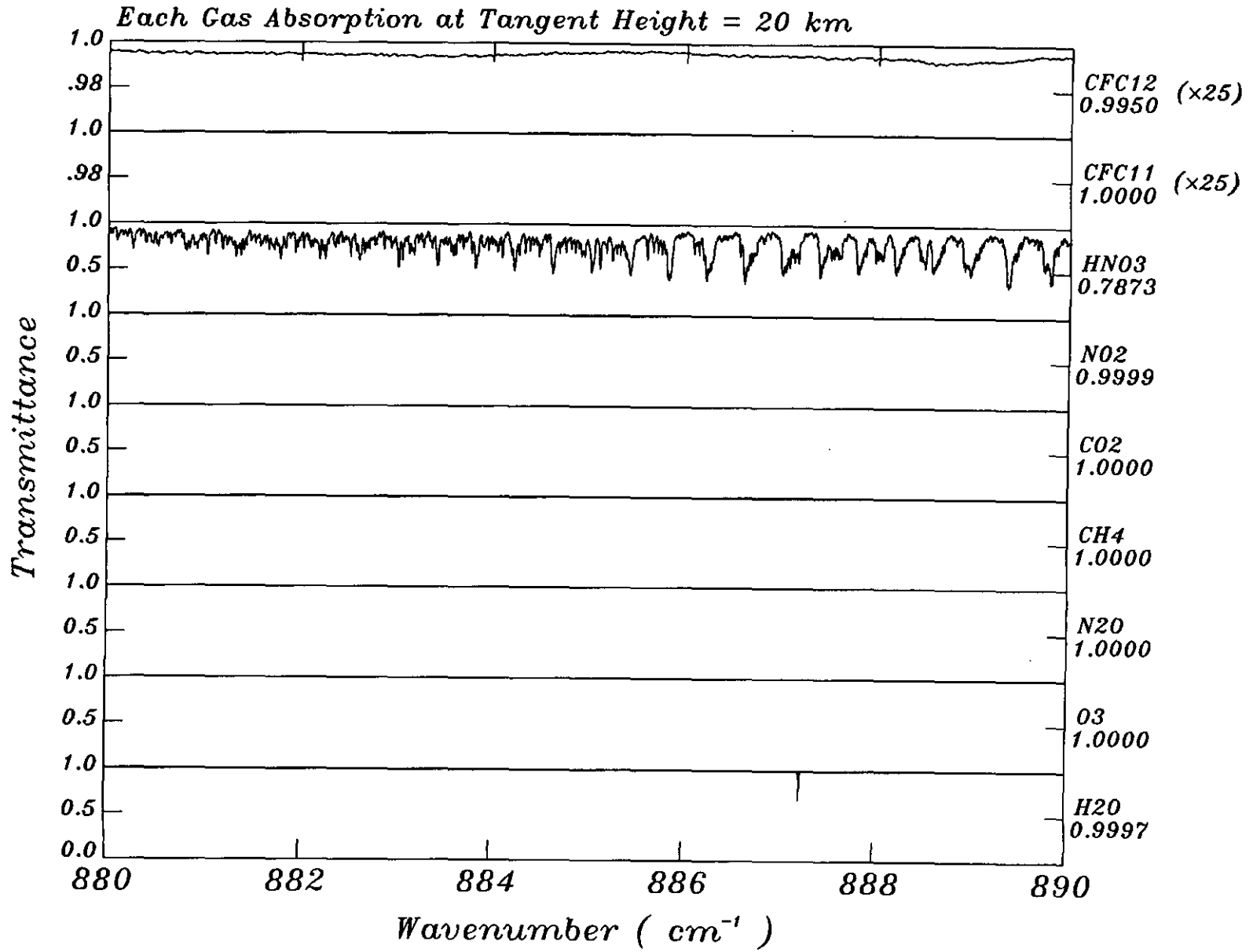


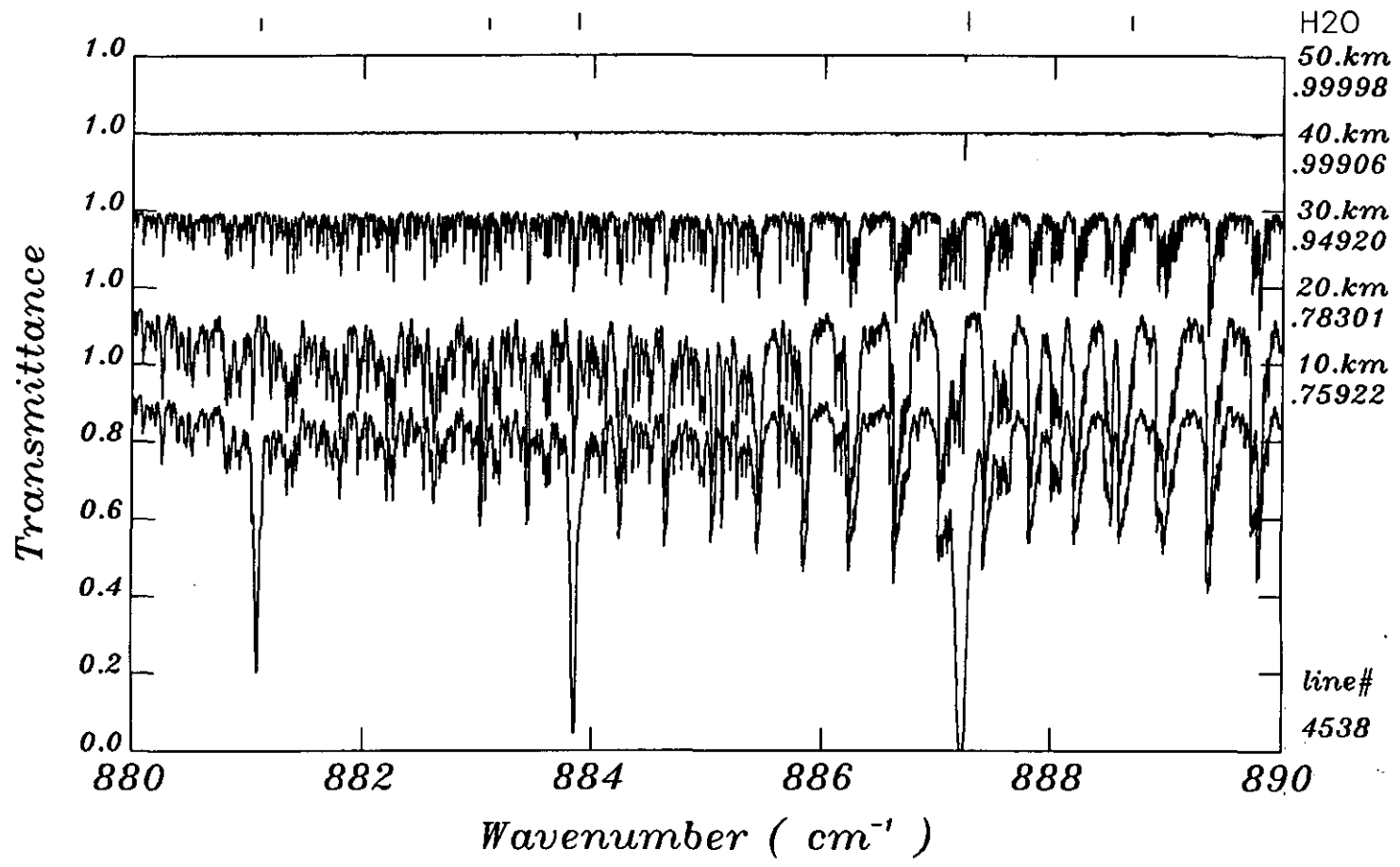


Each Gas Absorption at Tangent Height = 20 km

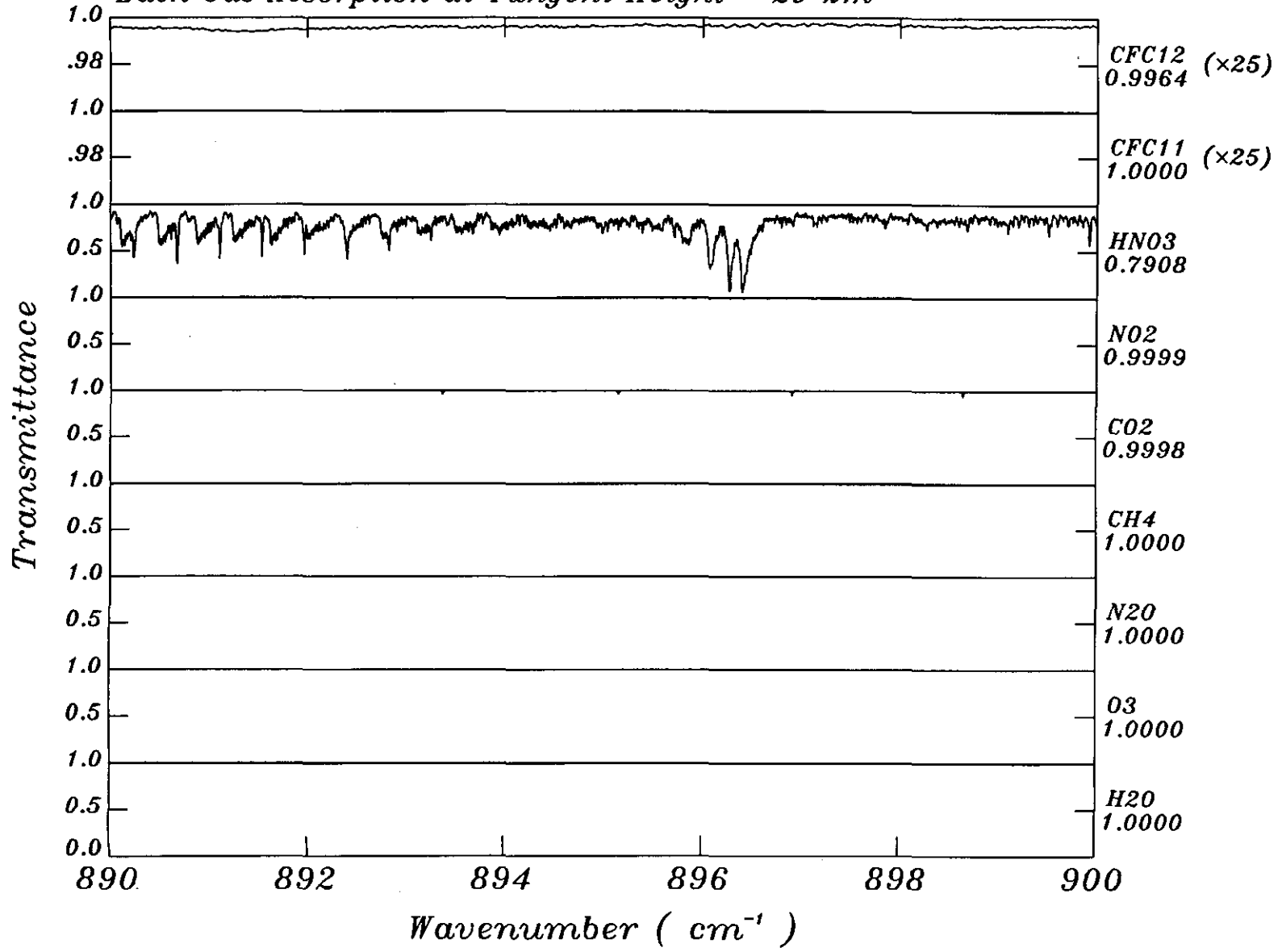






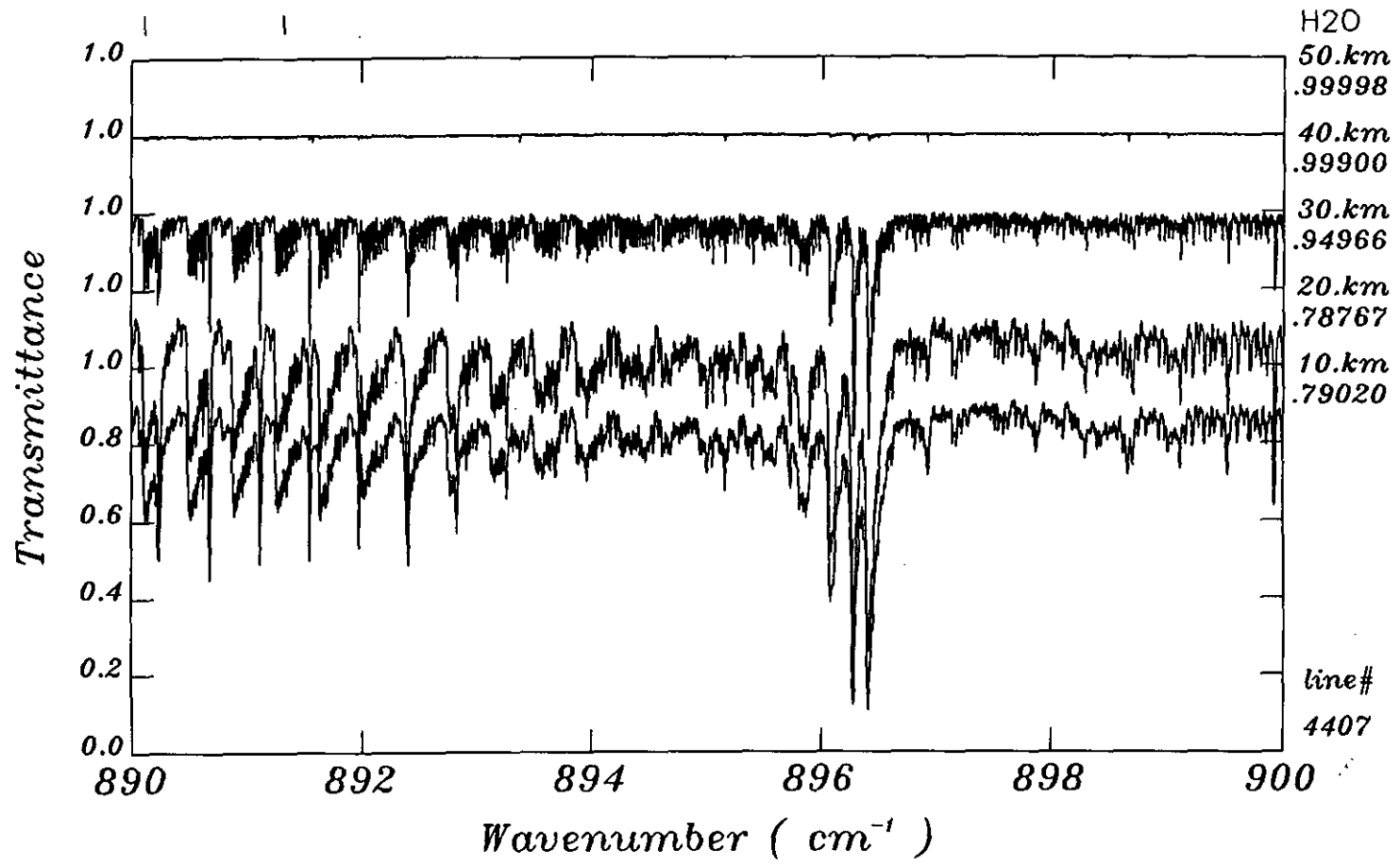


Each Gas Absorption at Tangent Height = 20 km

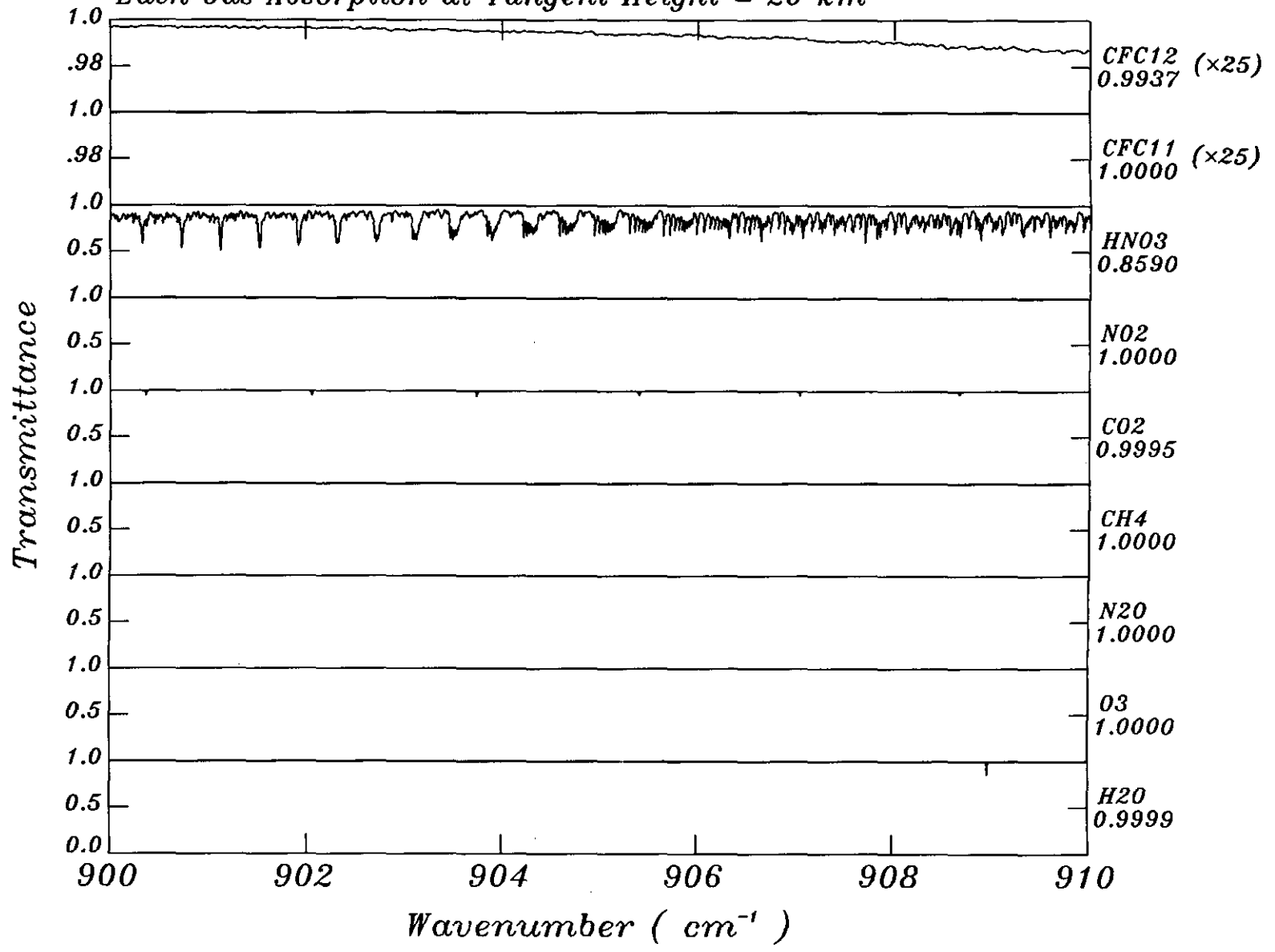


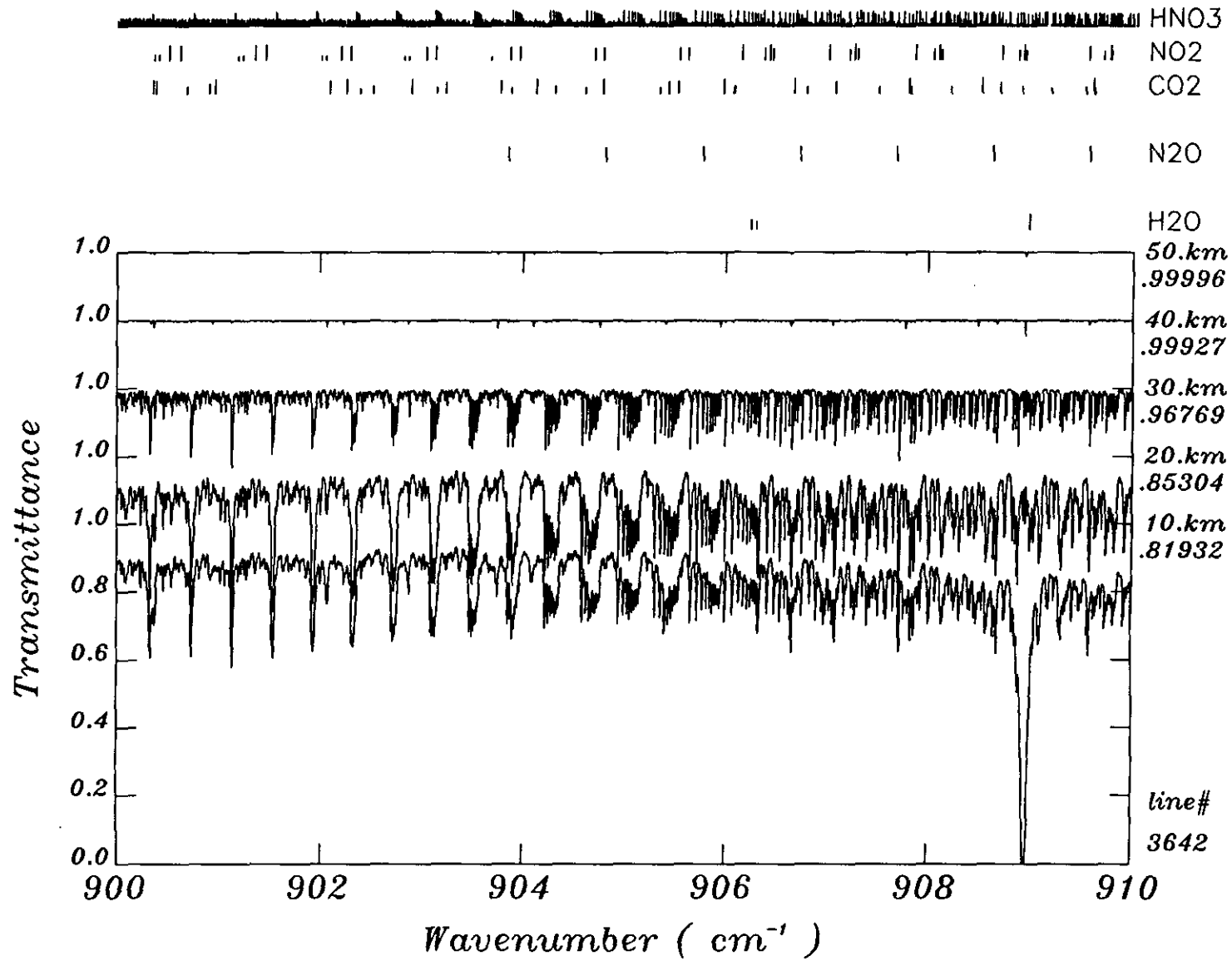


HNO3  
 NO2  
 CO2

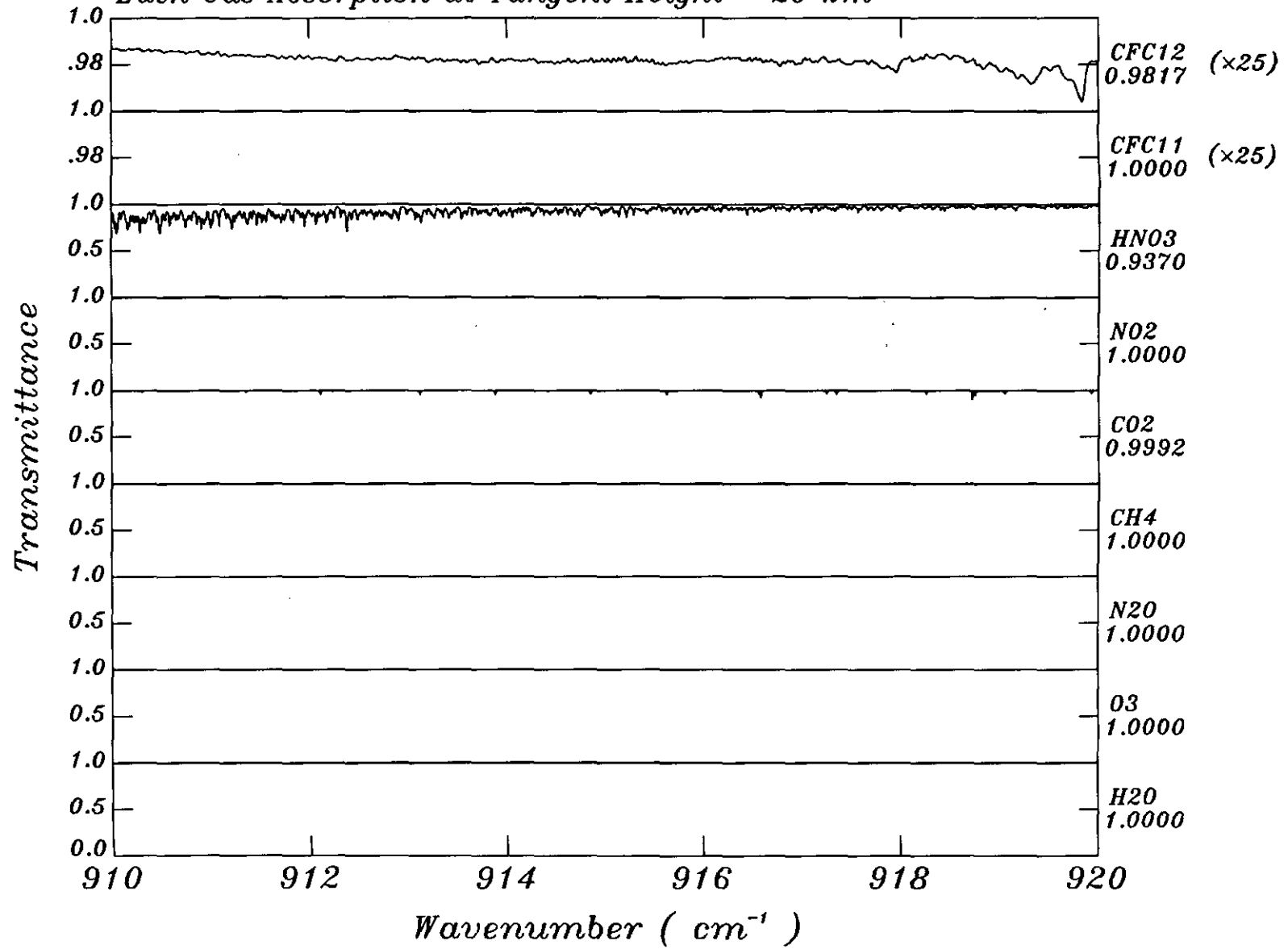


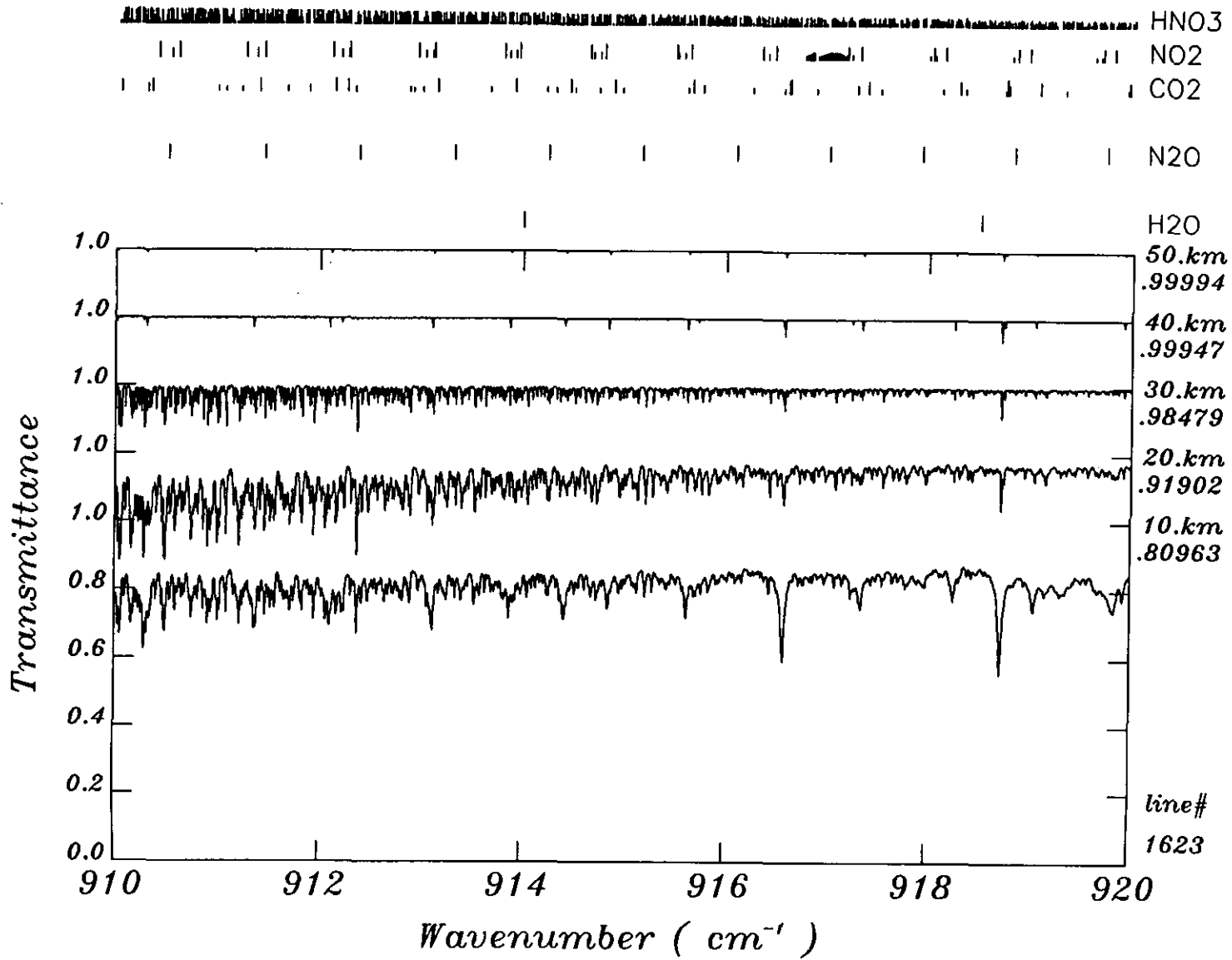
*Each Gas Absorption at Tangent Height = 20 km*

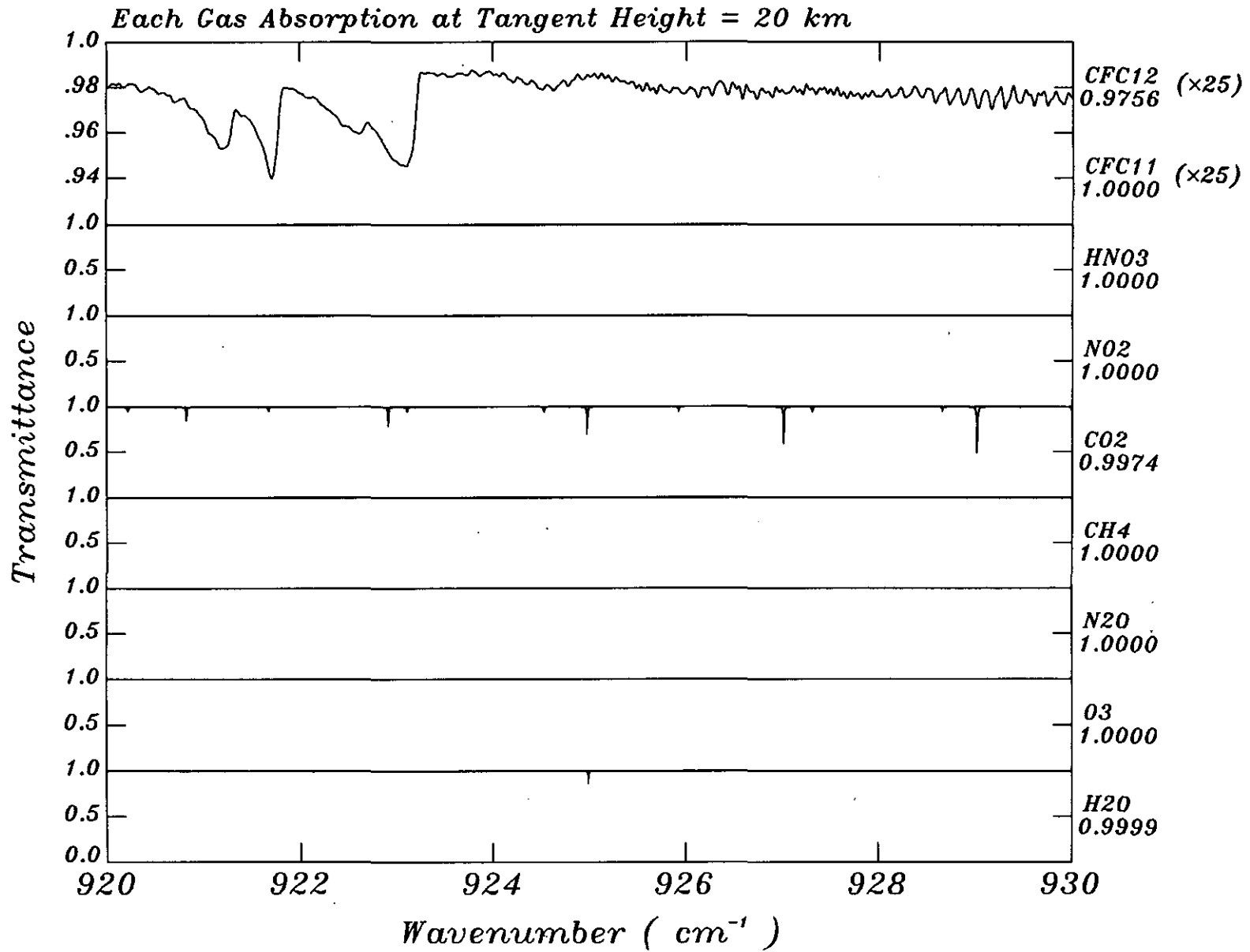


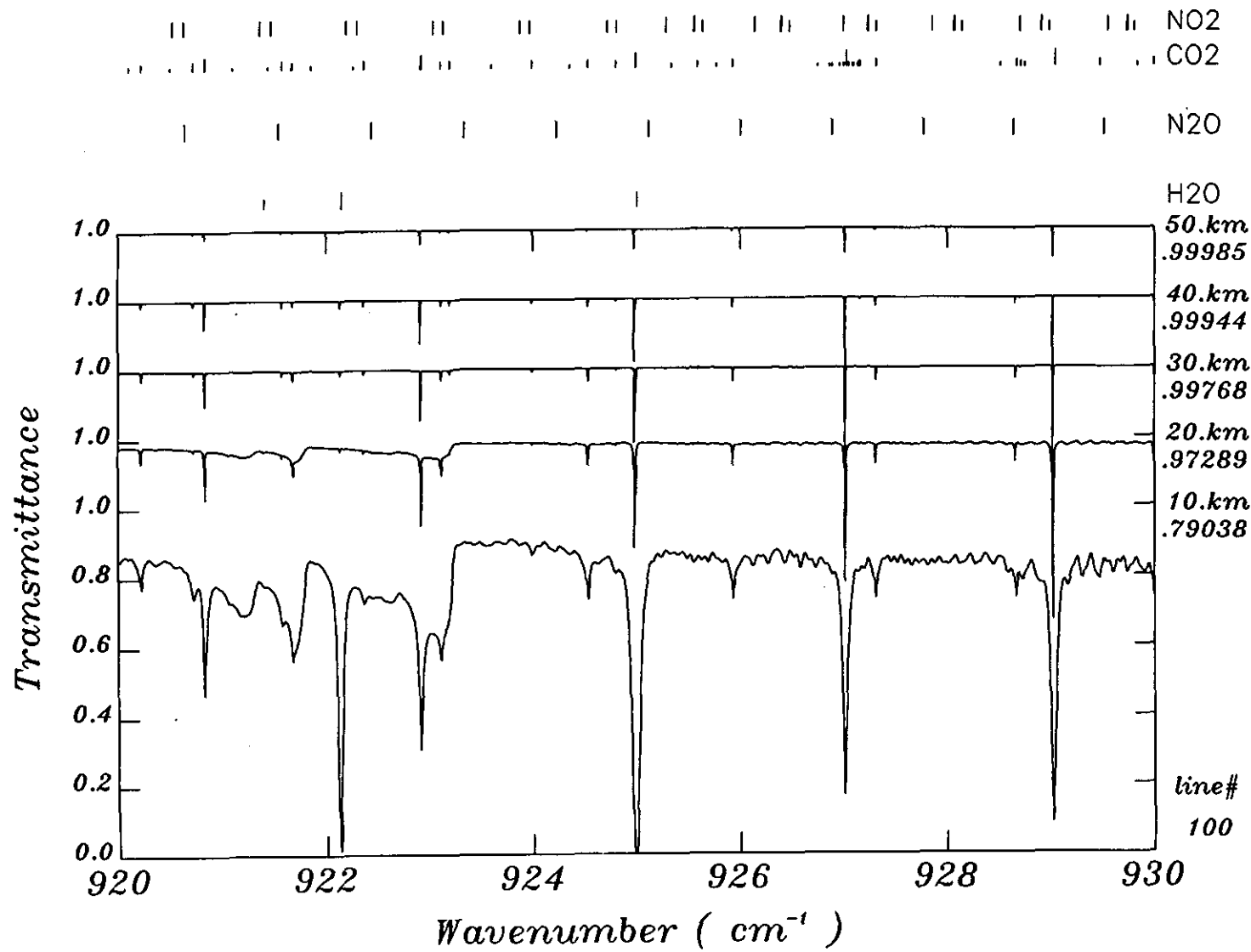


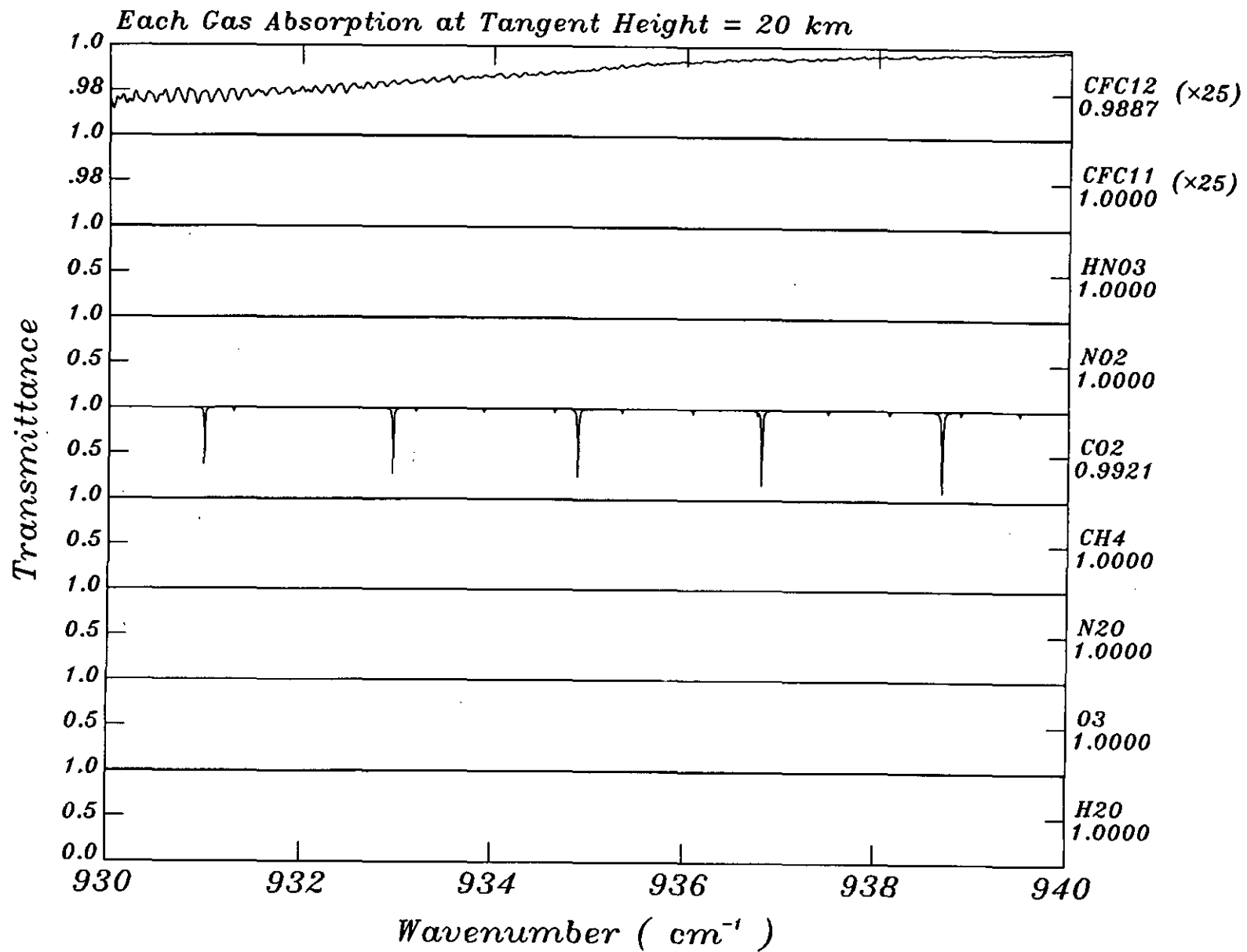
Each Gas Absorption at Tangent Height = 20 km





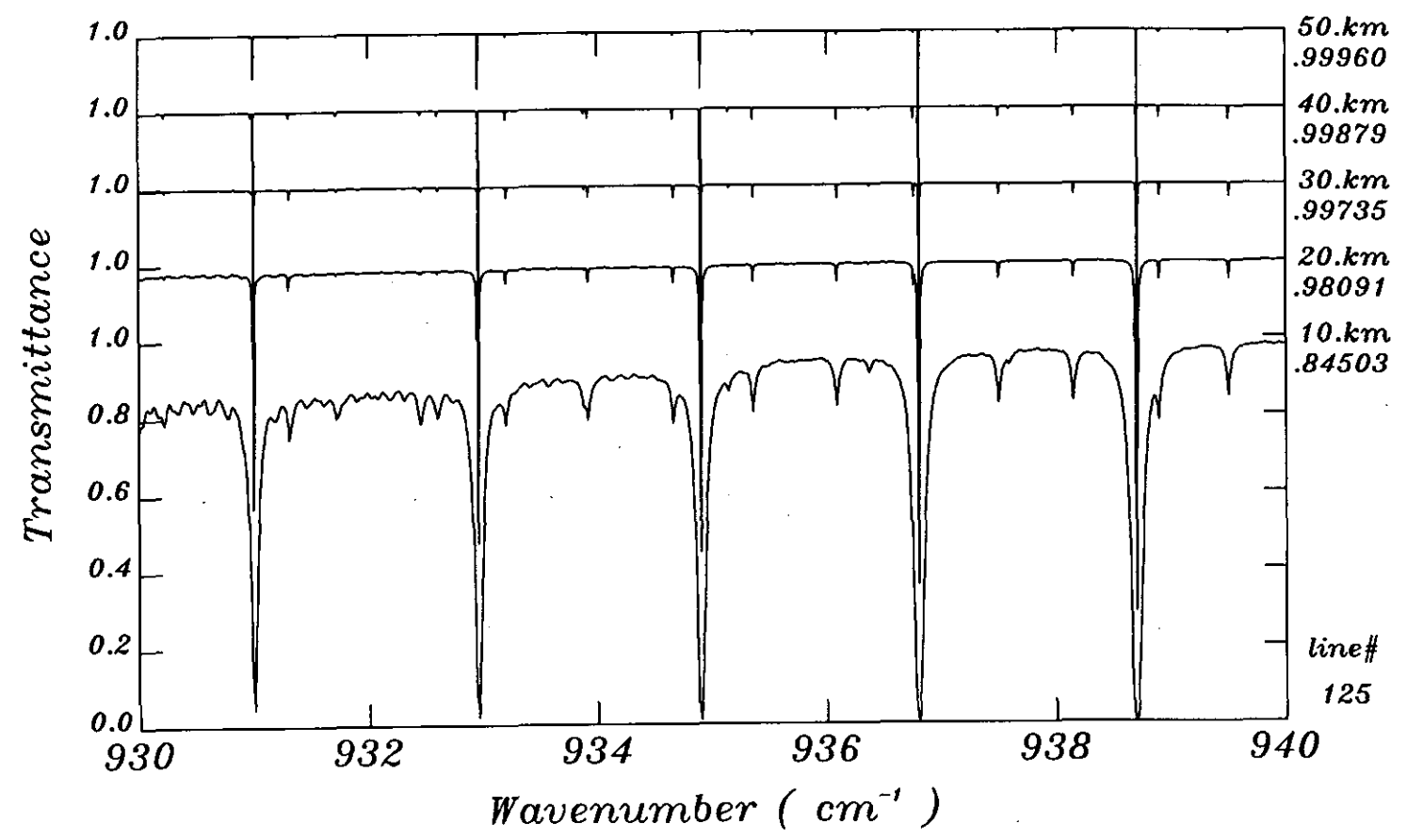




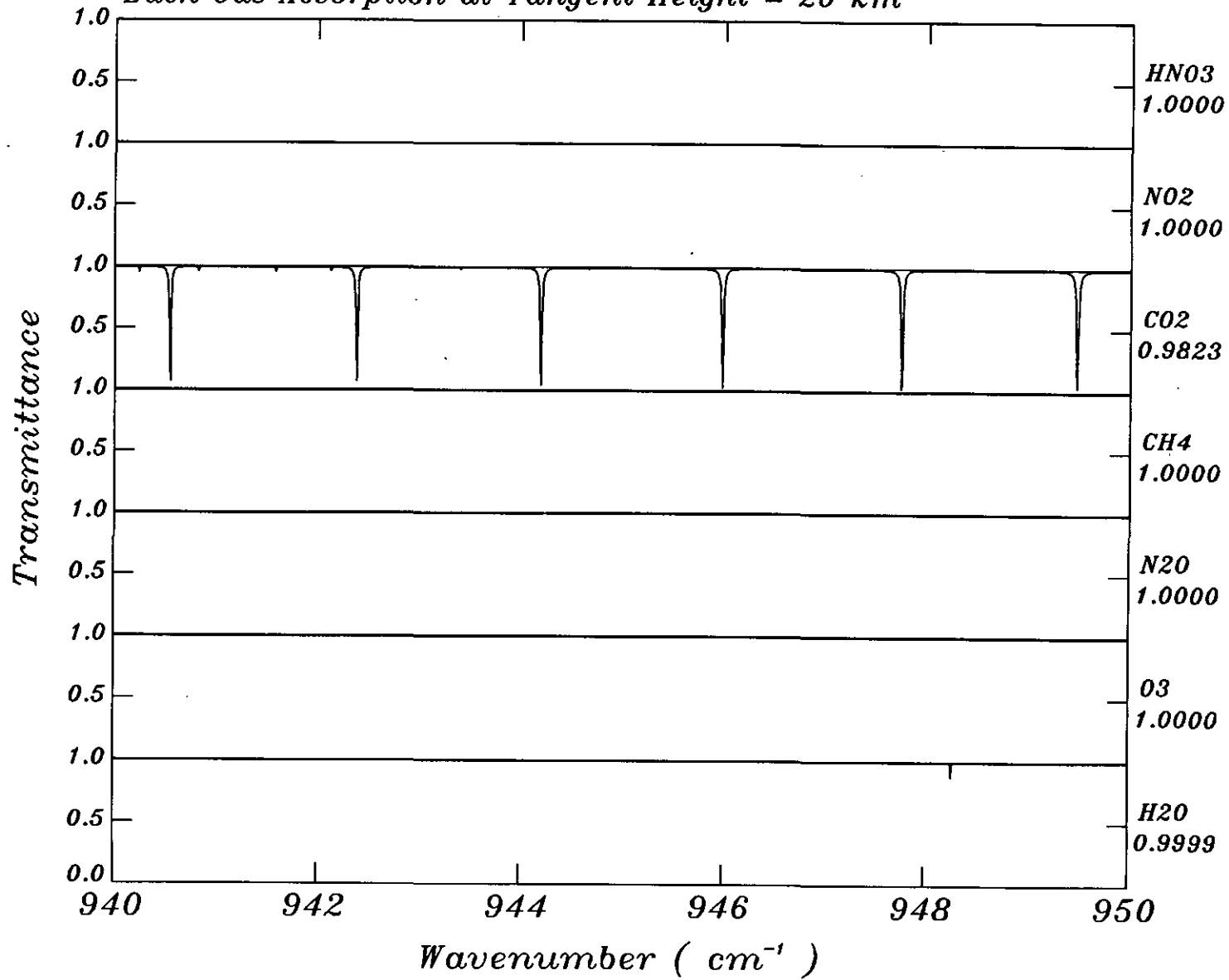


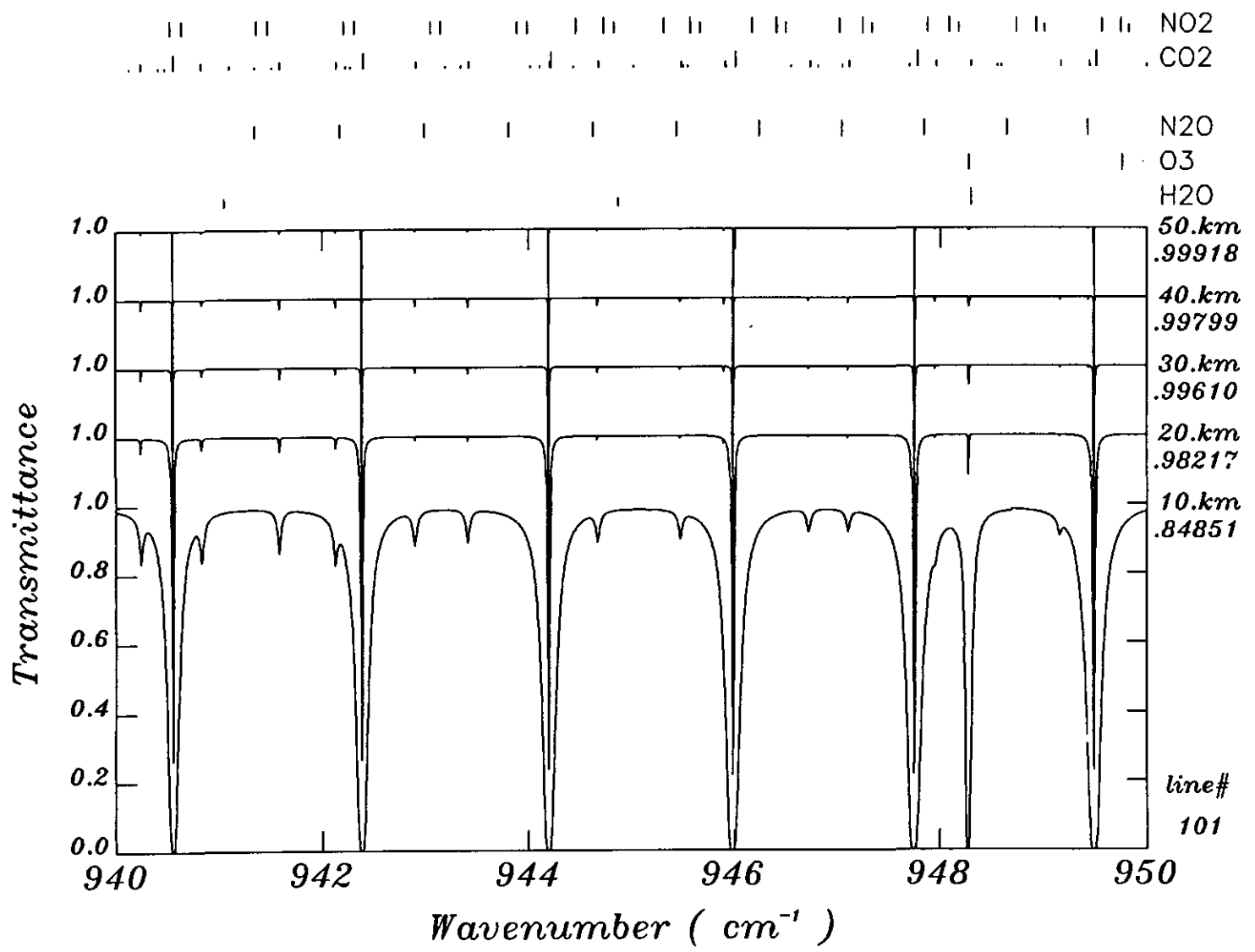


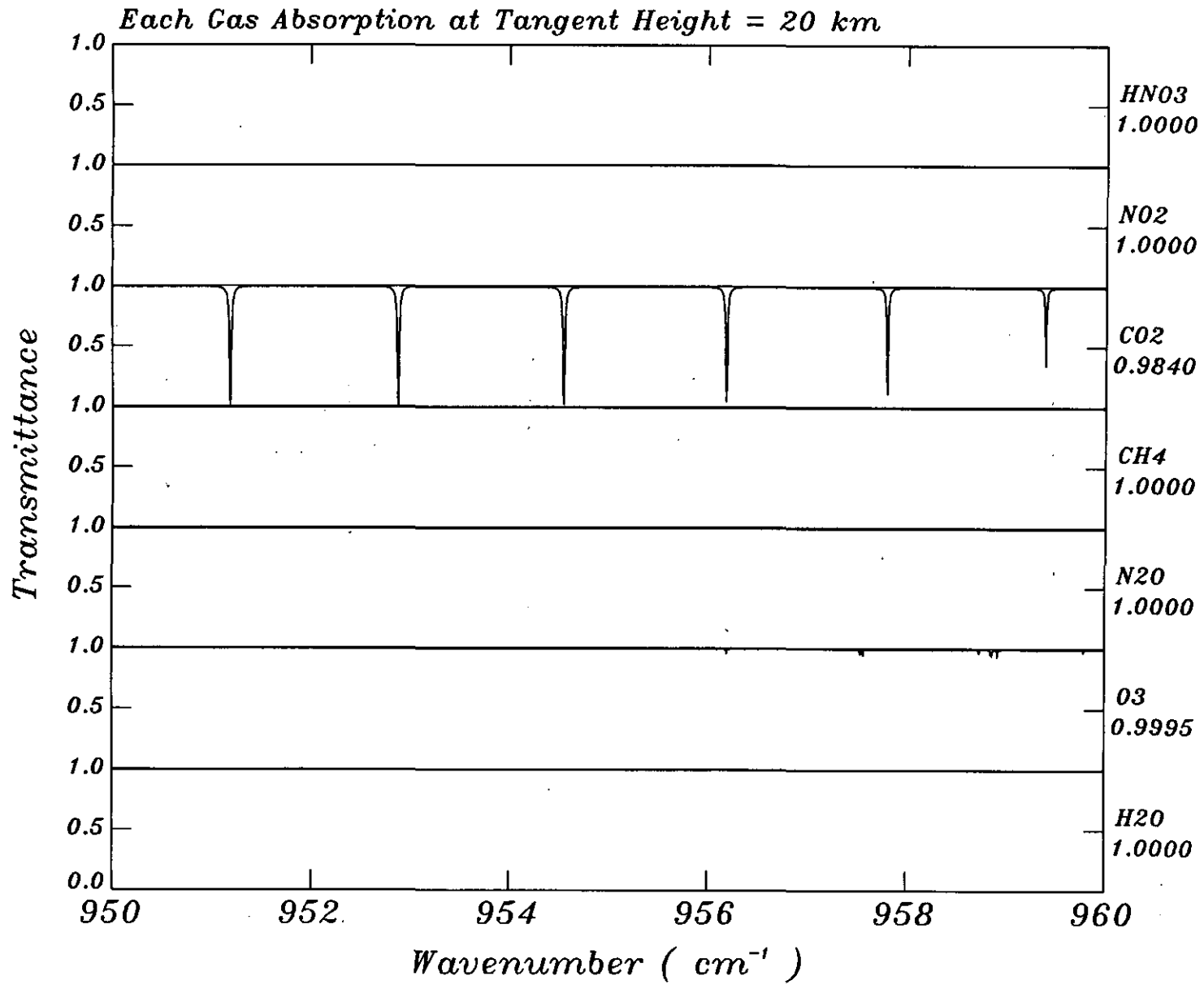
NO2  
 CO2  
 N2O

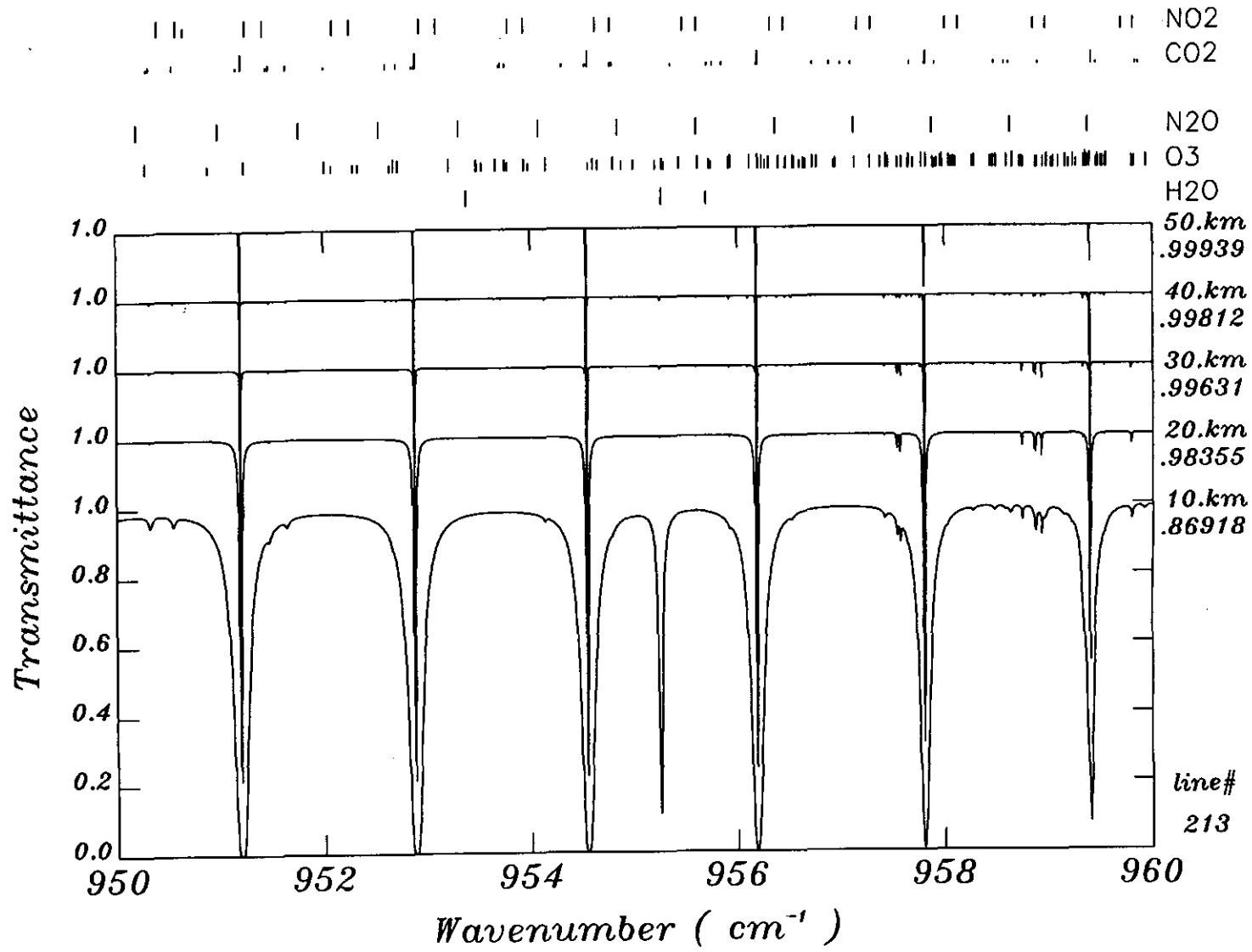


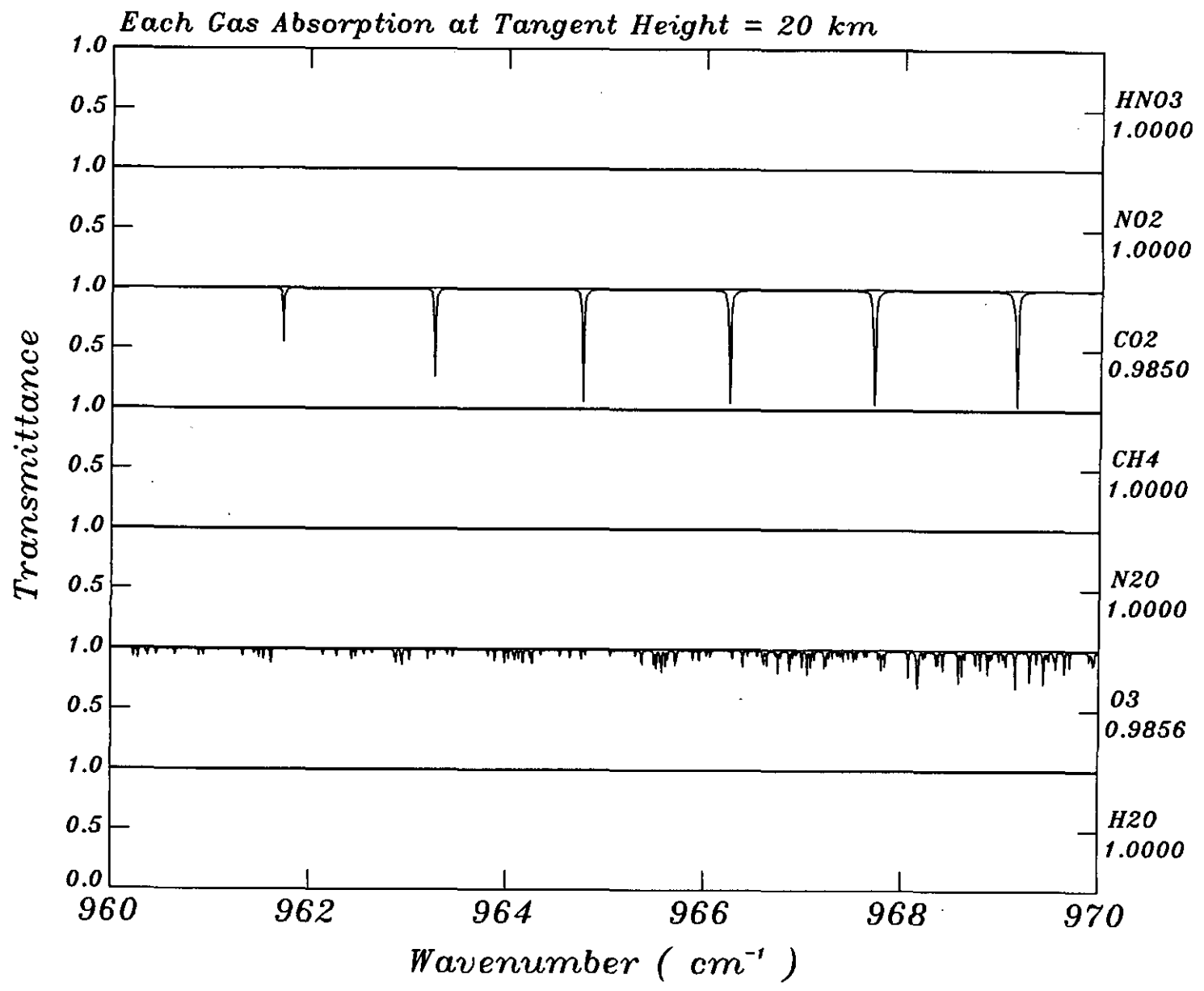
*Each Gas Absorption at Tangent Height = 20 km*

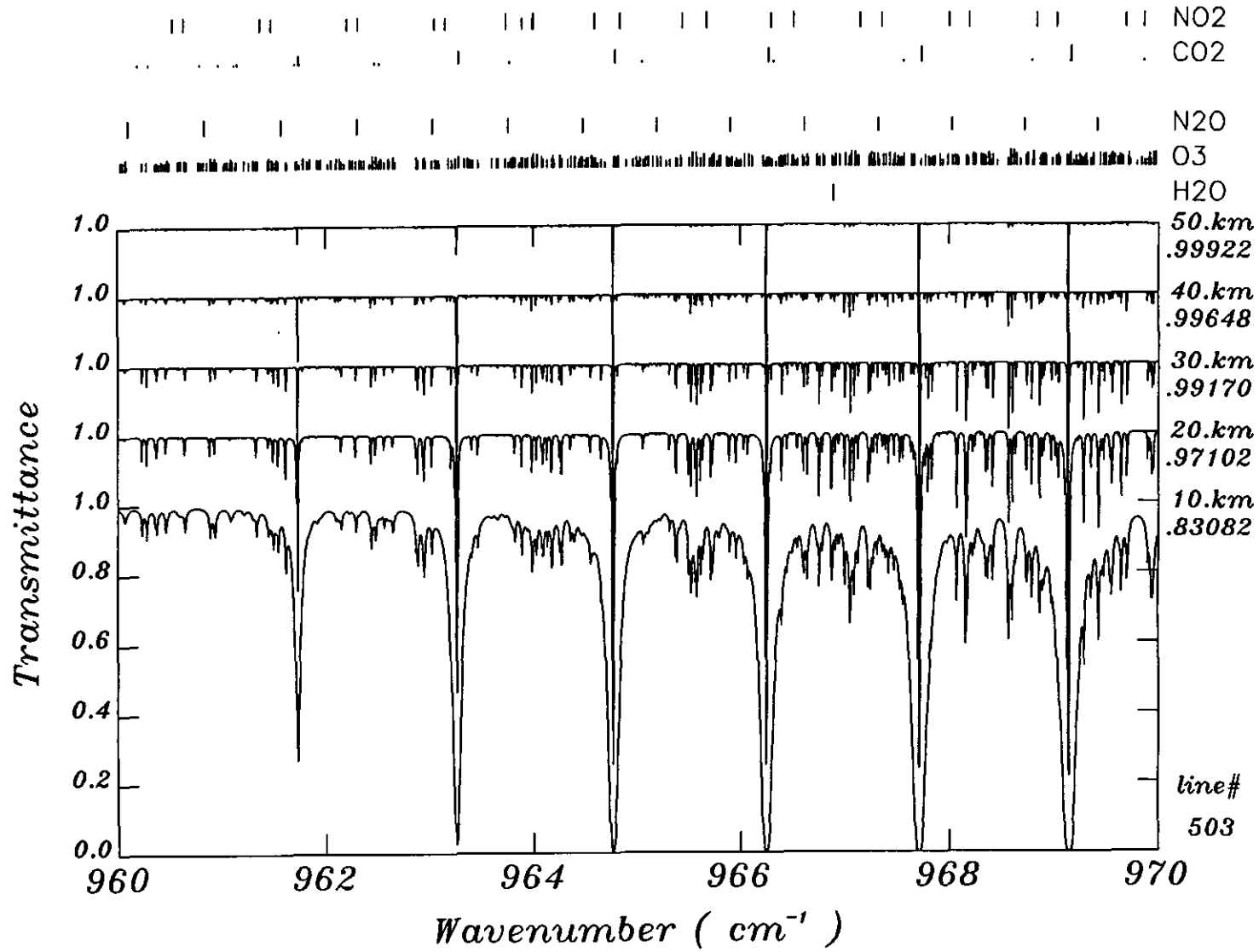




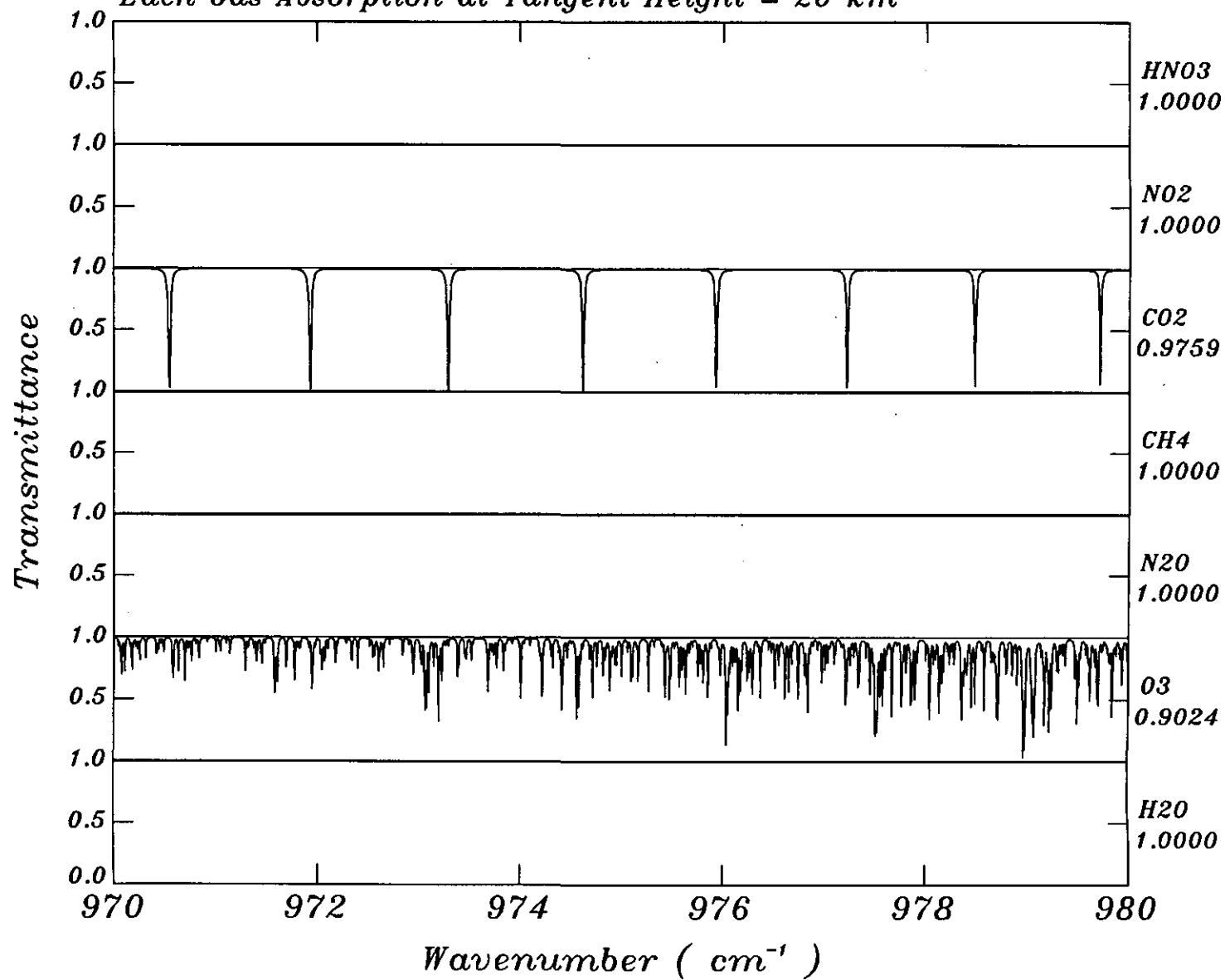




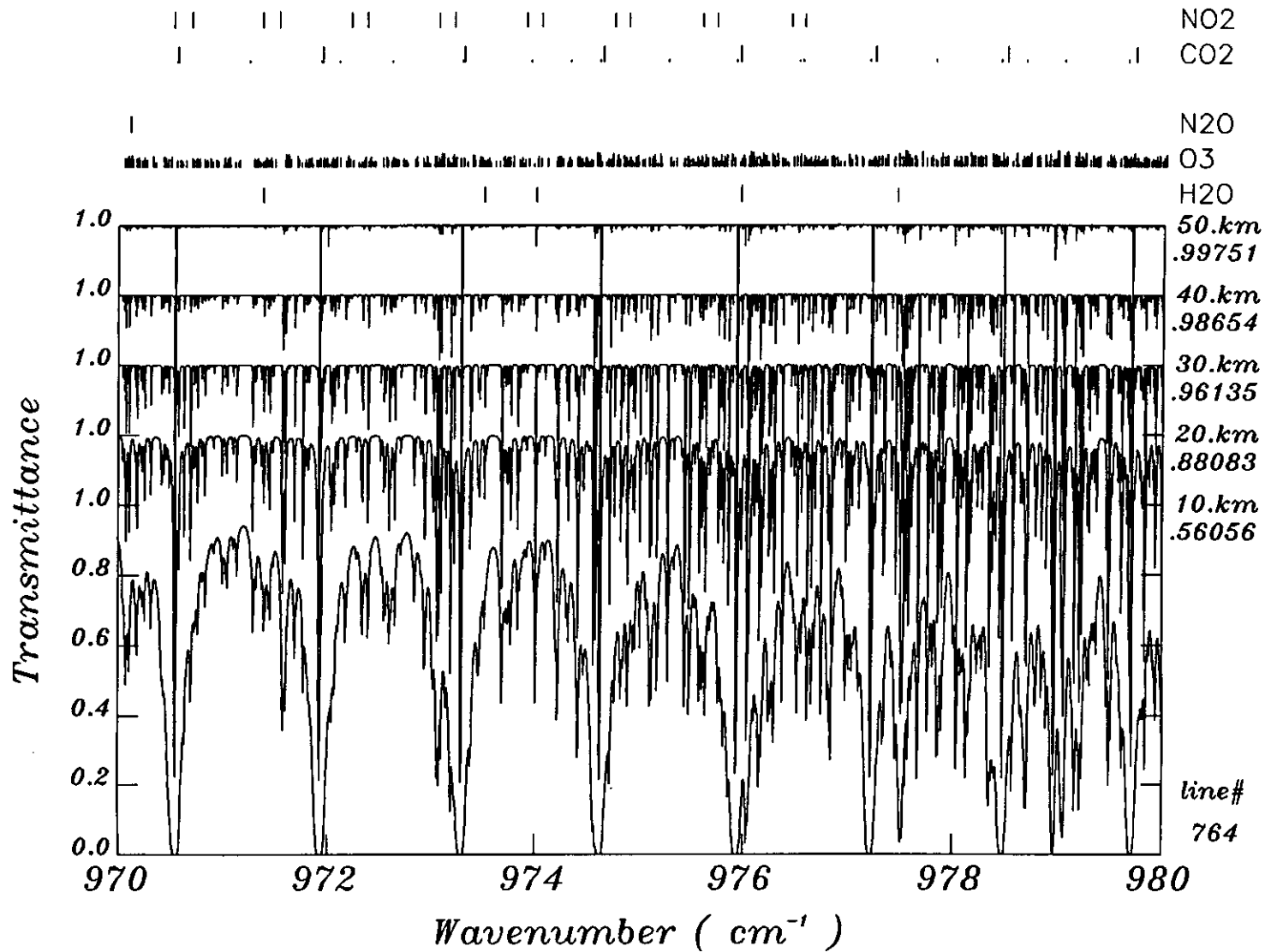


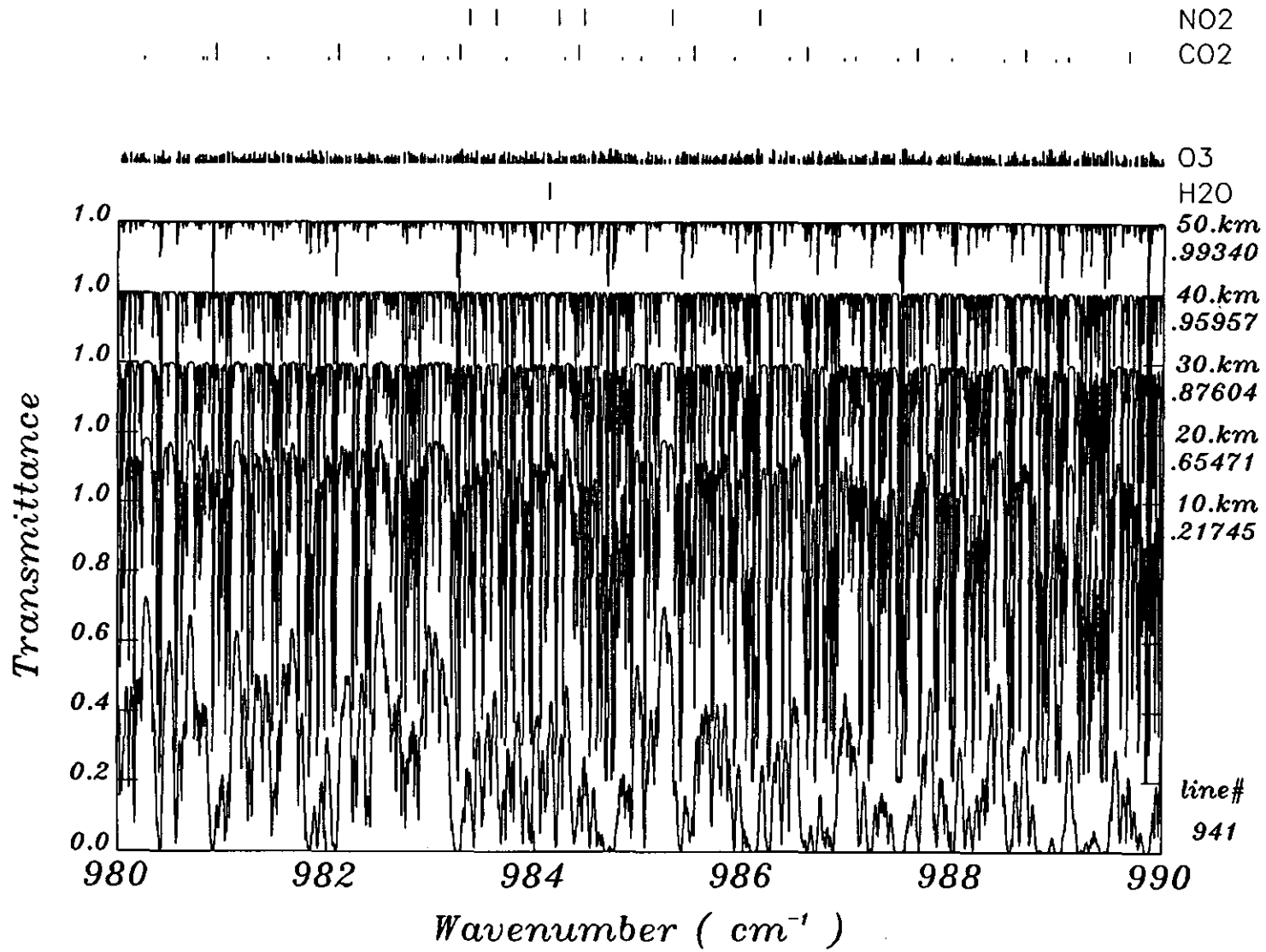


Each Gas Absorption at Tangent Height = 20 km

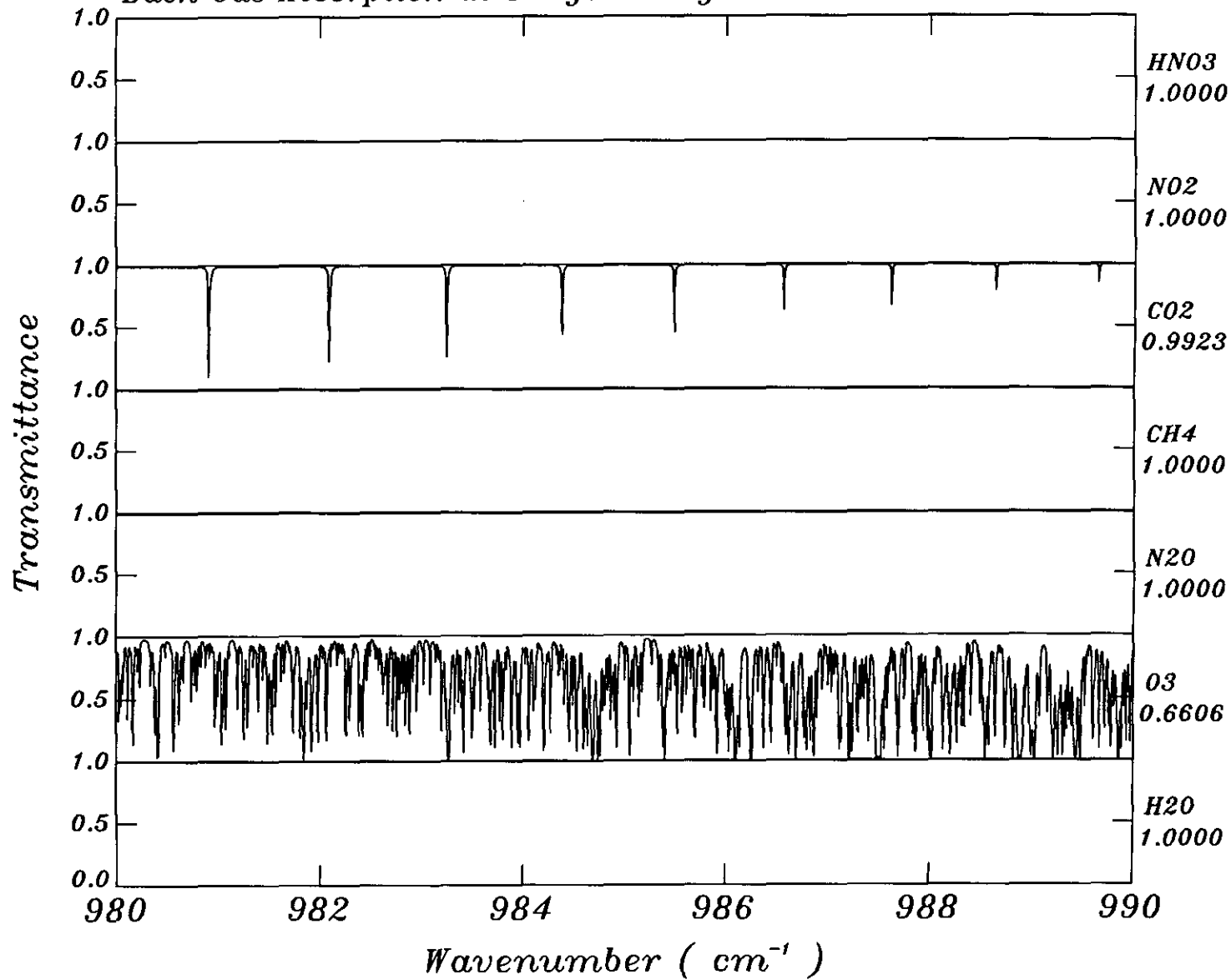


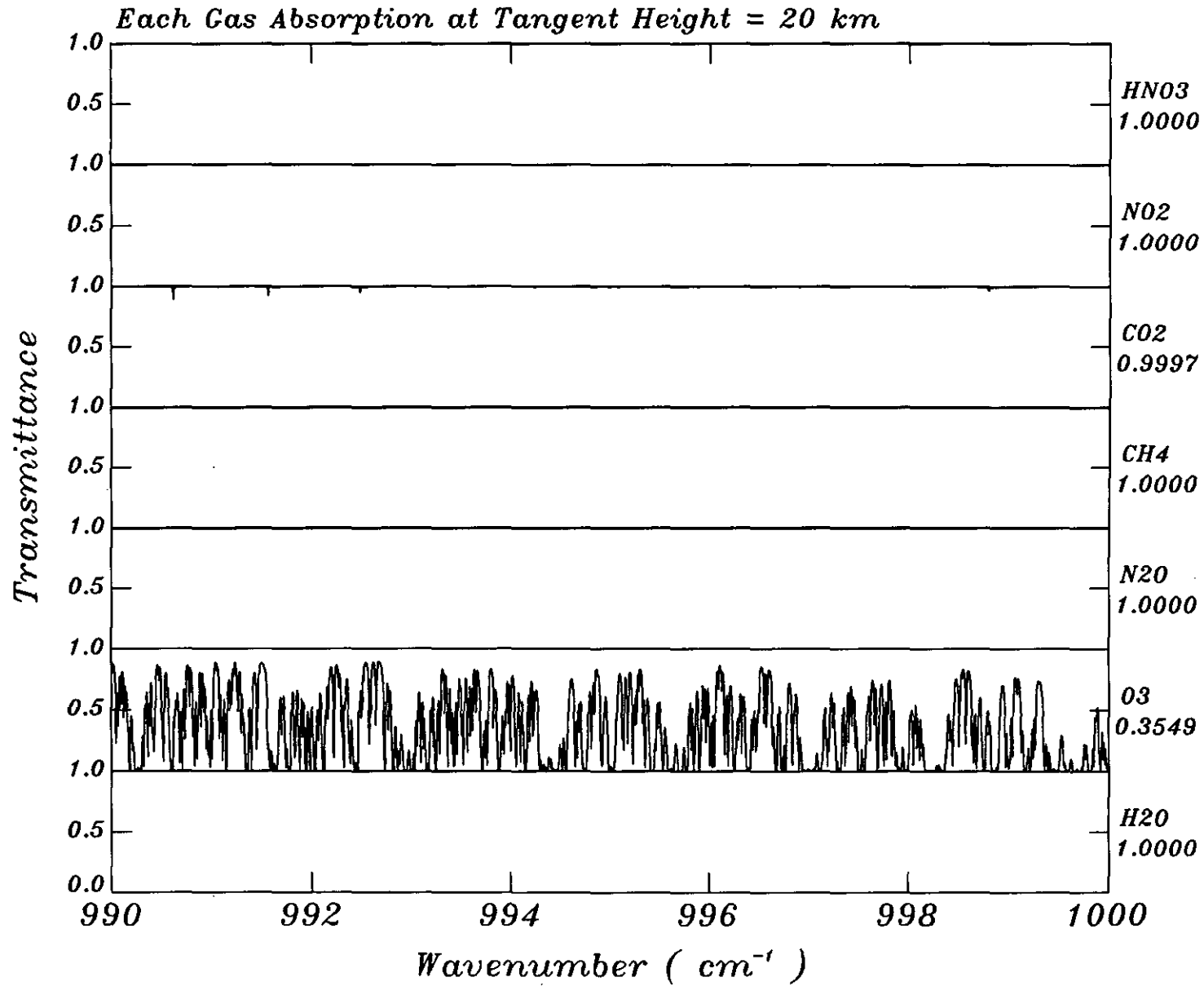


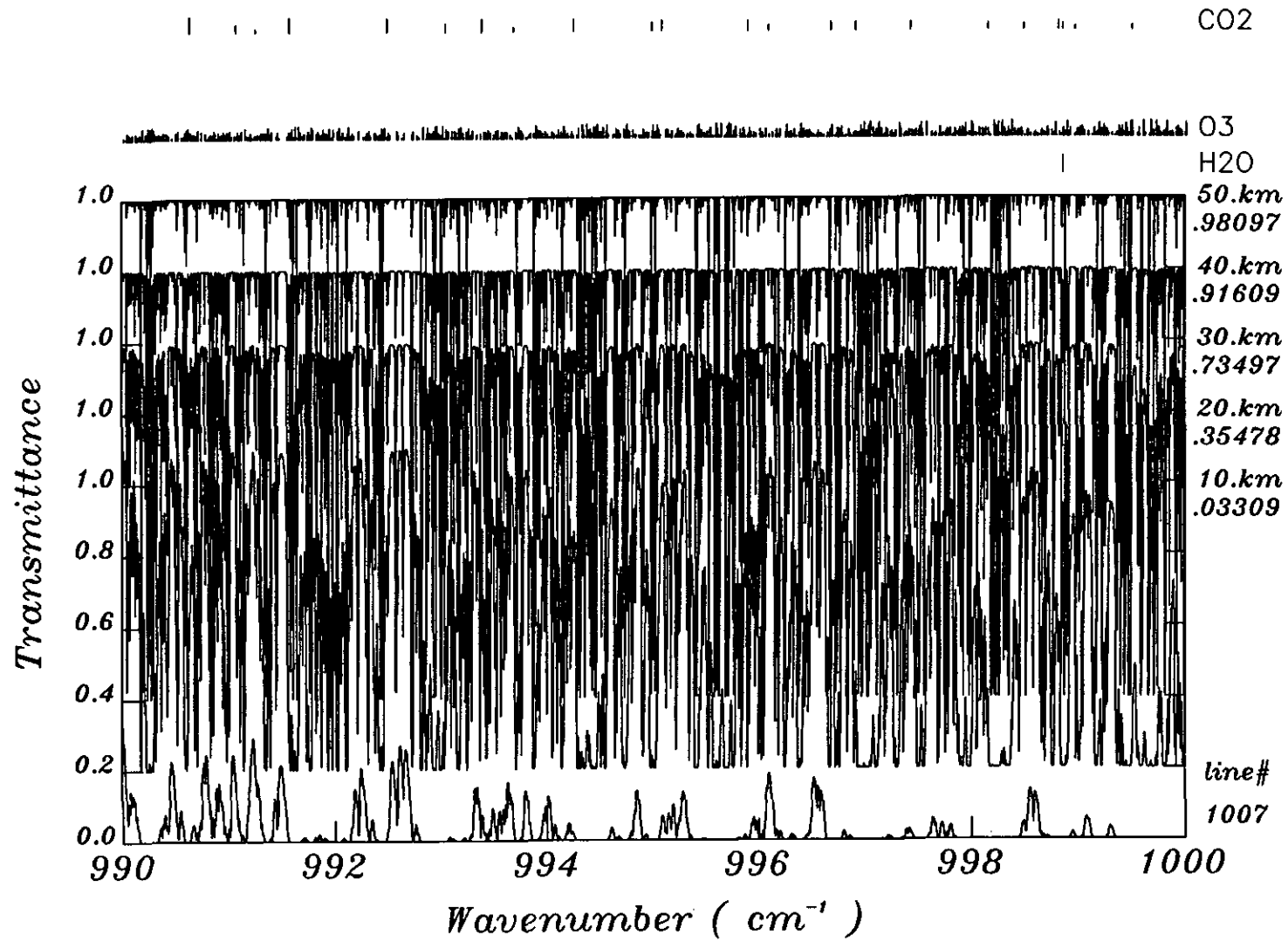




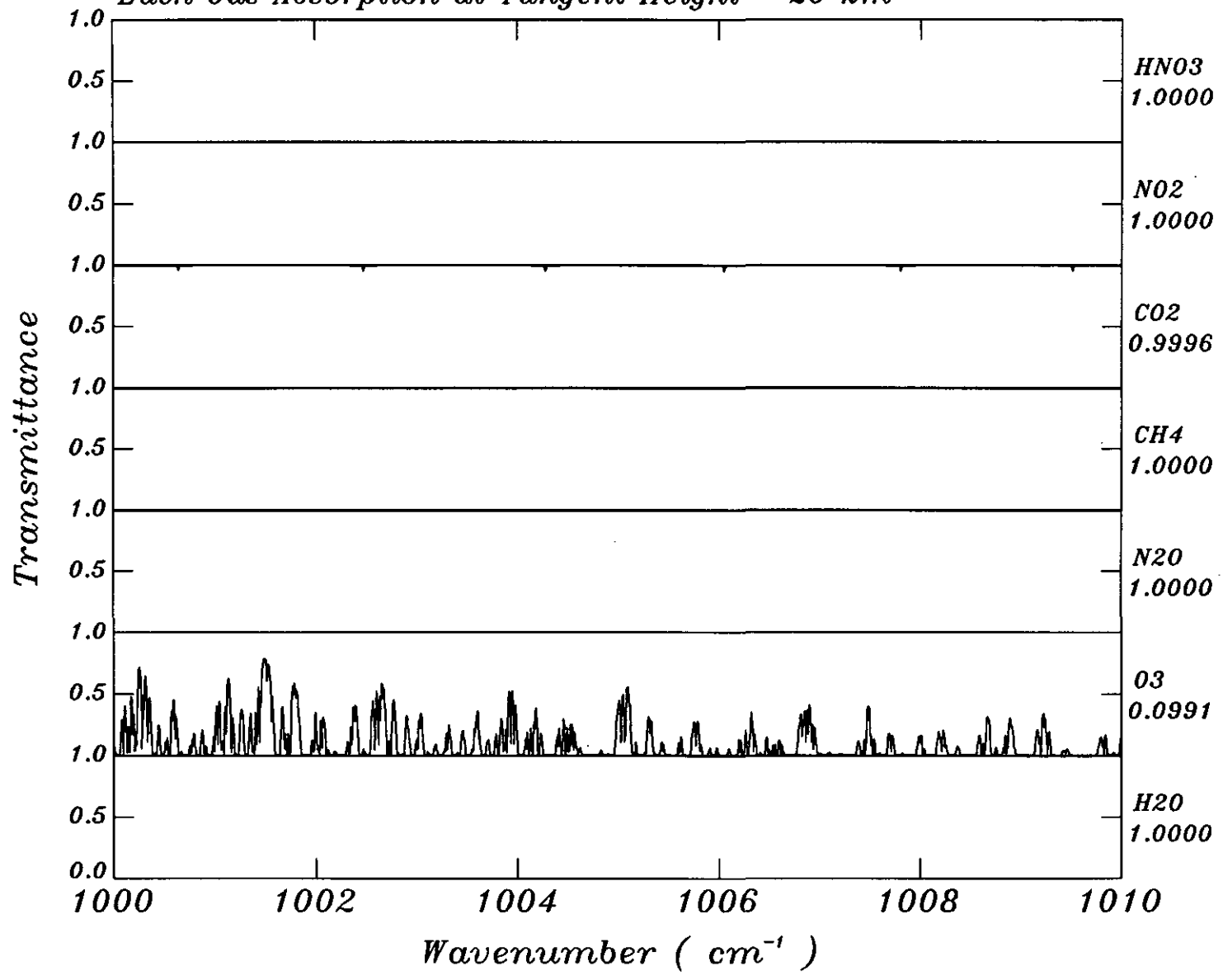
Each Gas Absorption at Tangent Height = 20 km

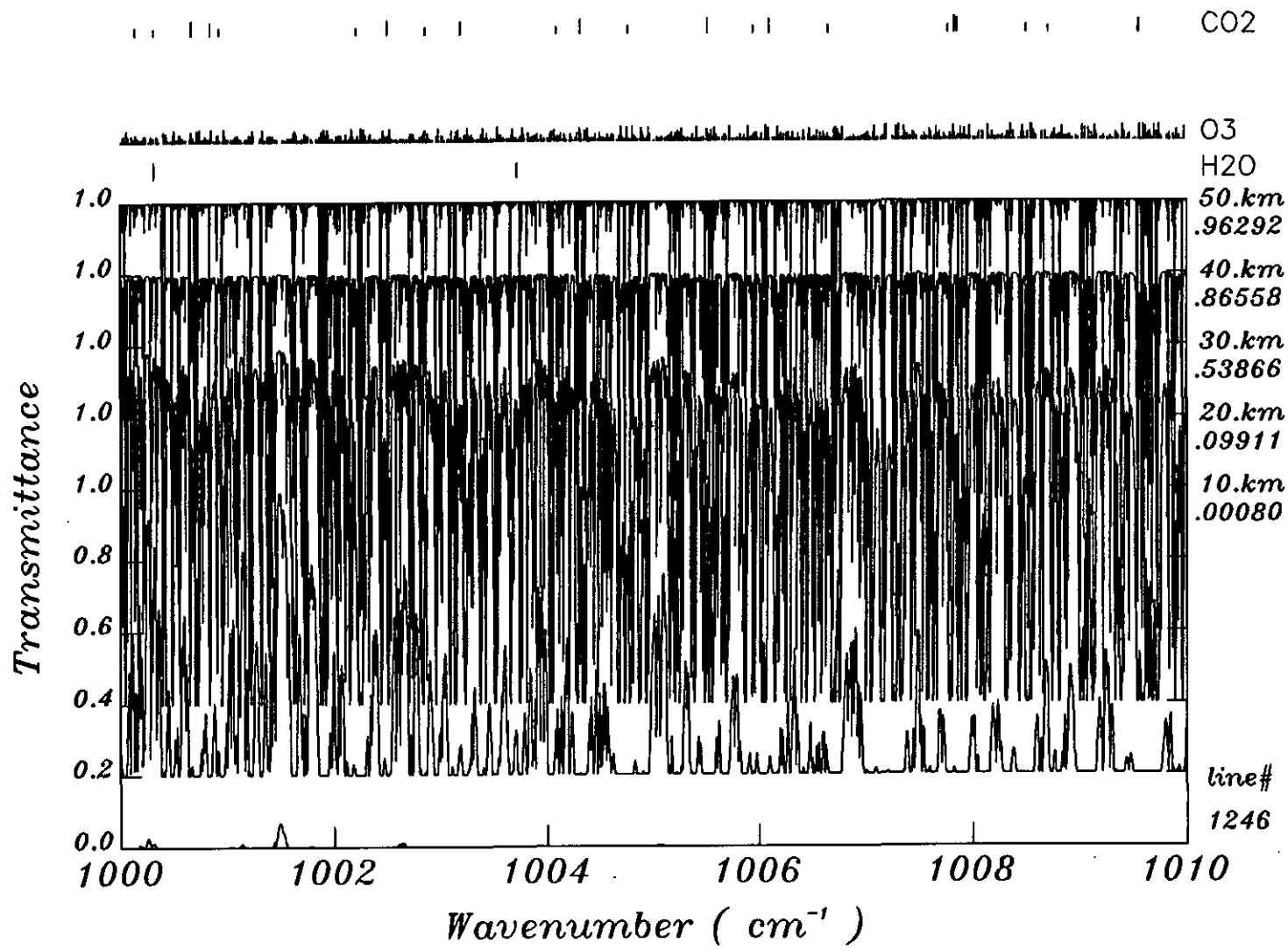




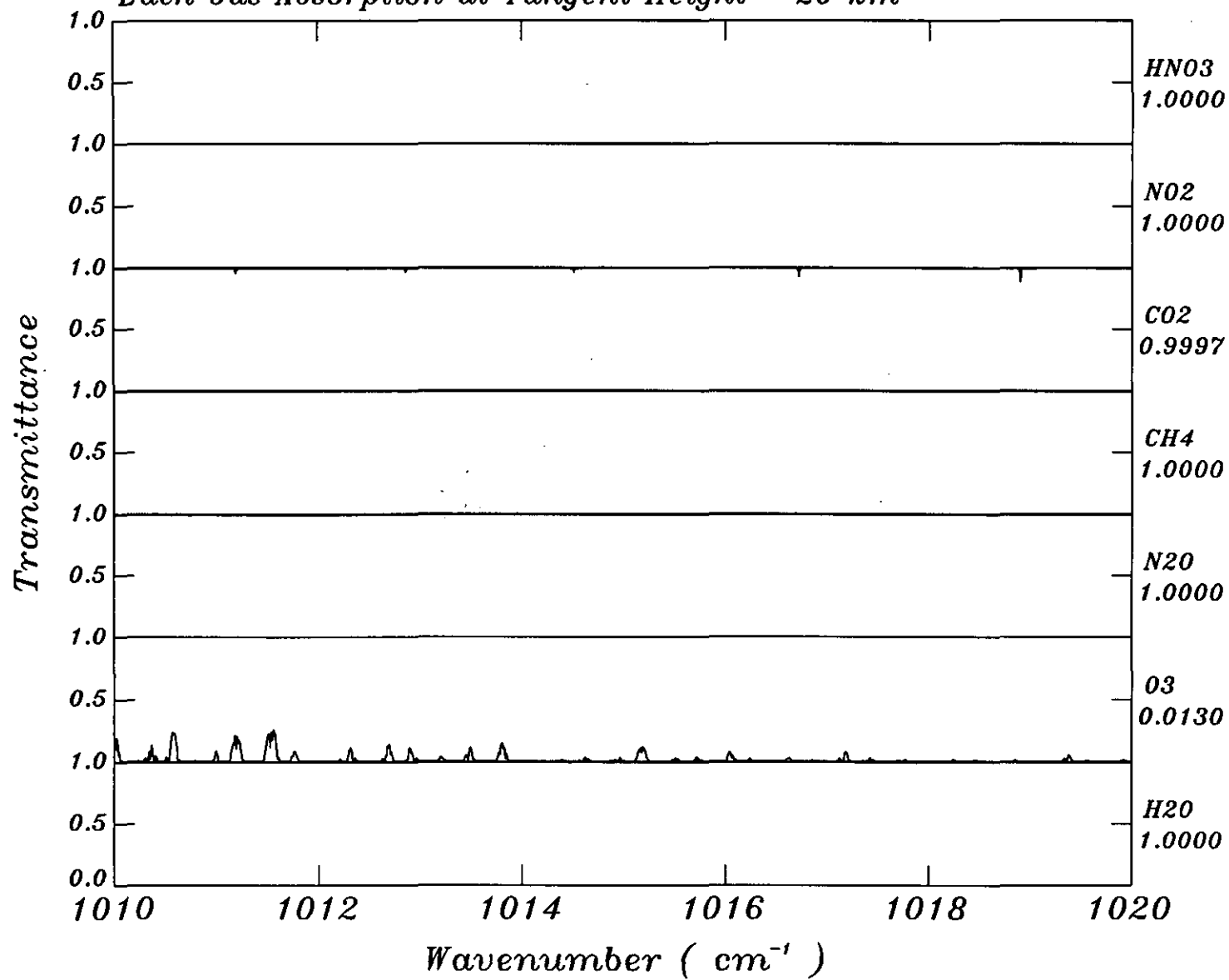


*Each Gas Absorption at Tangent Height = 20 km*

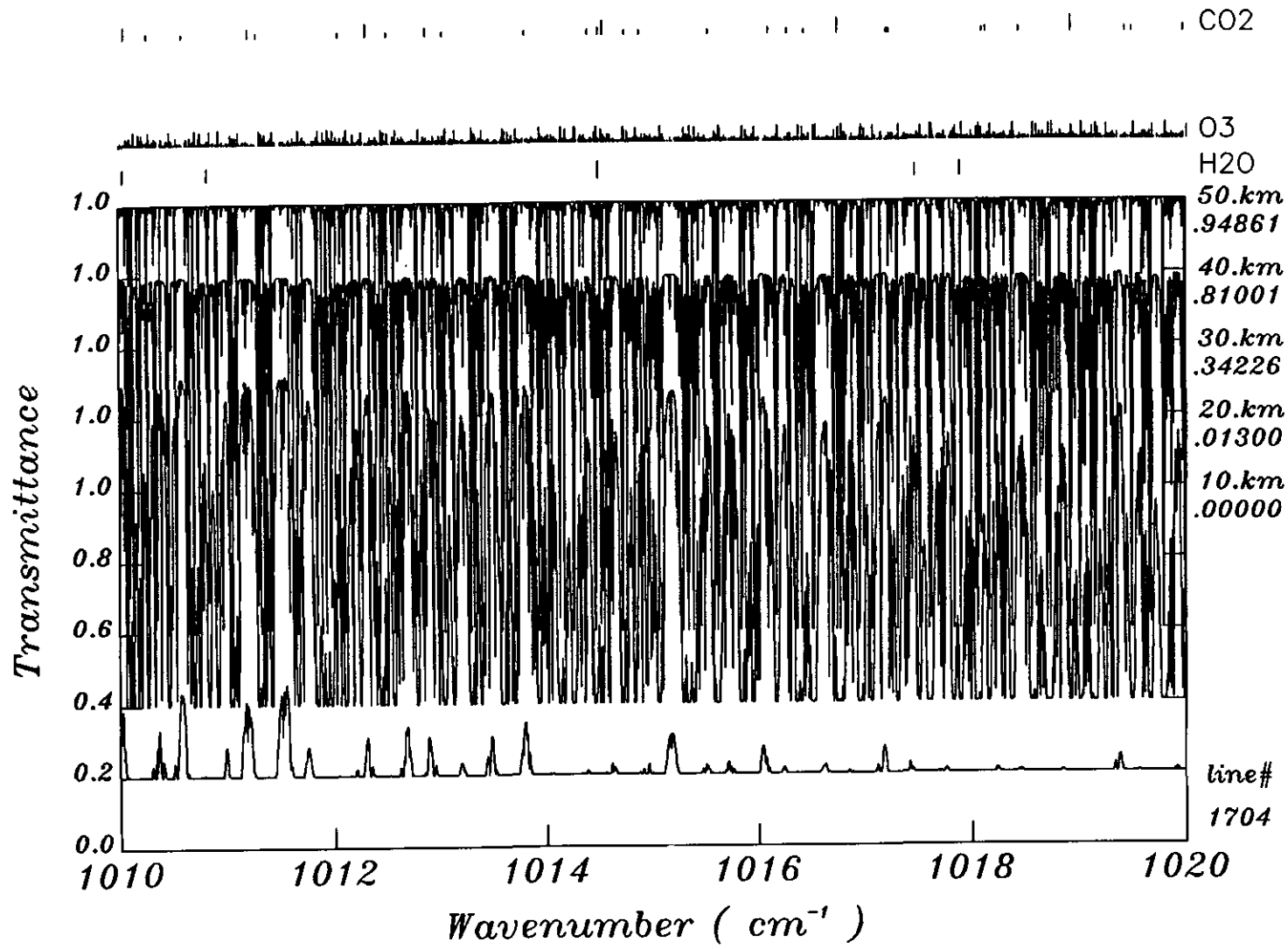




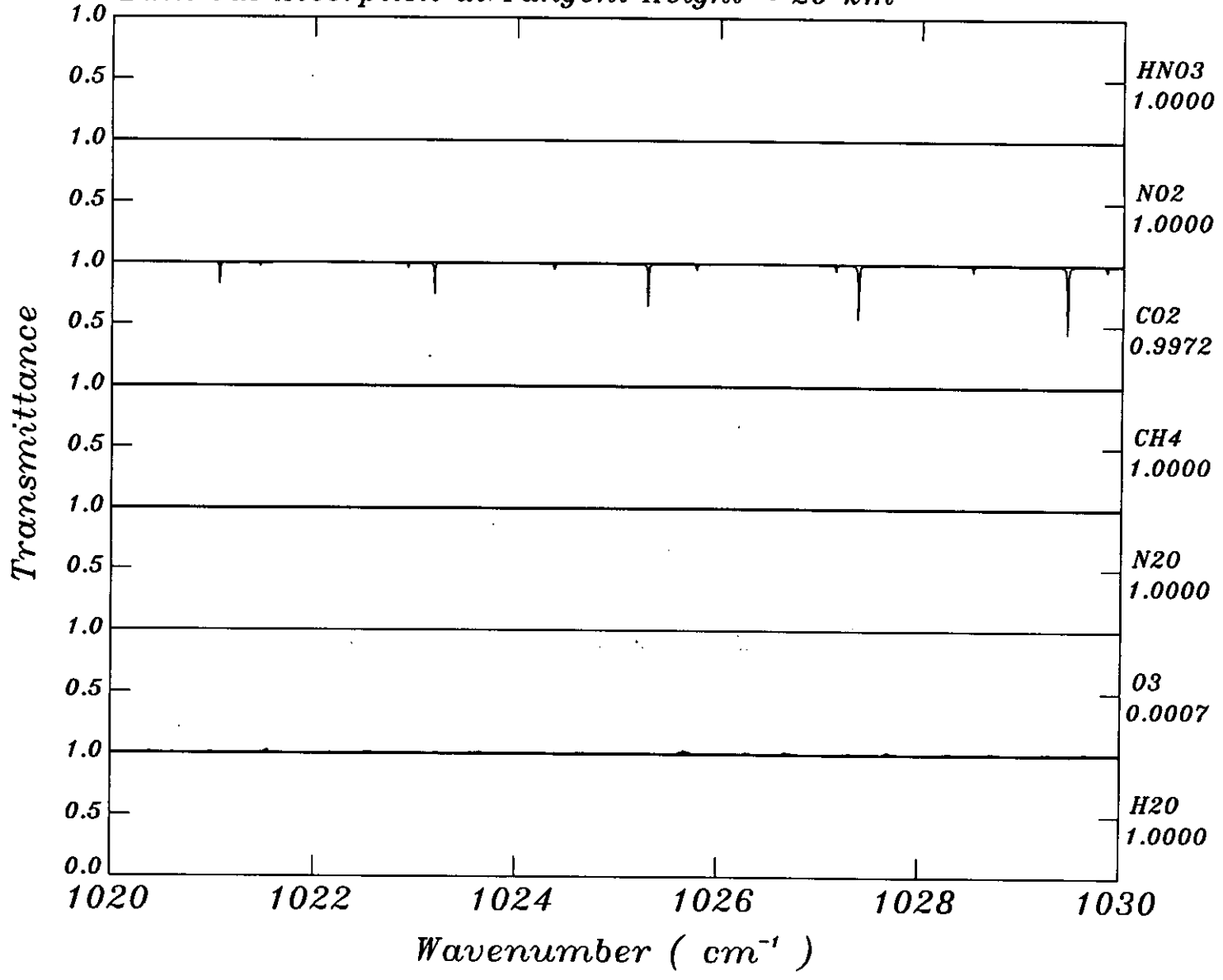
*Each Gas Absorption at Tangent Height = 20 km*



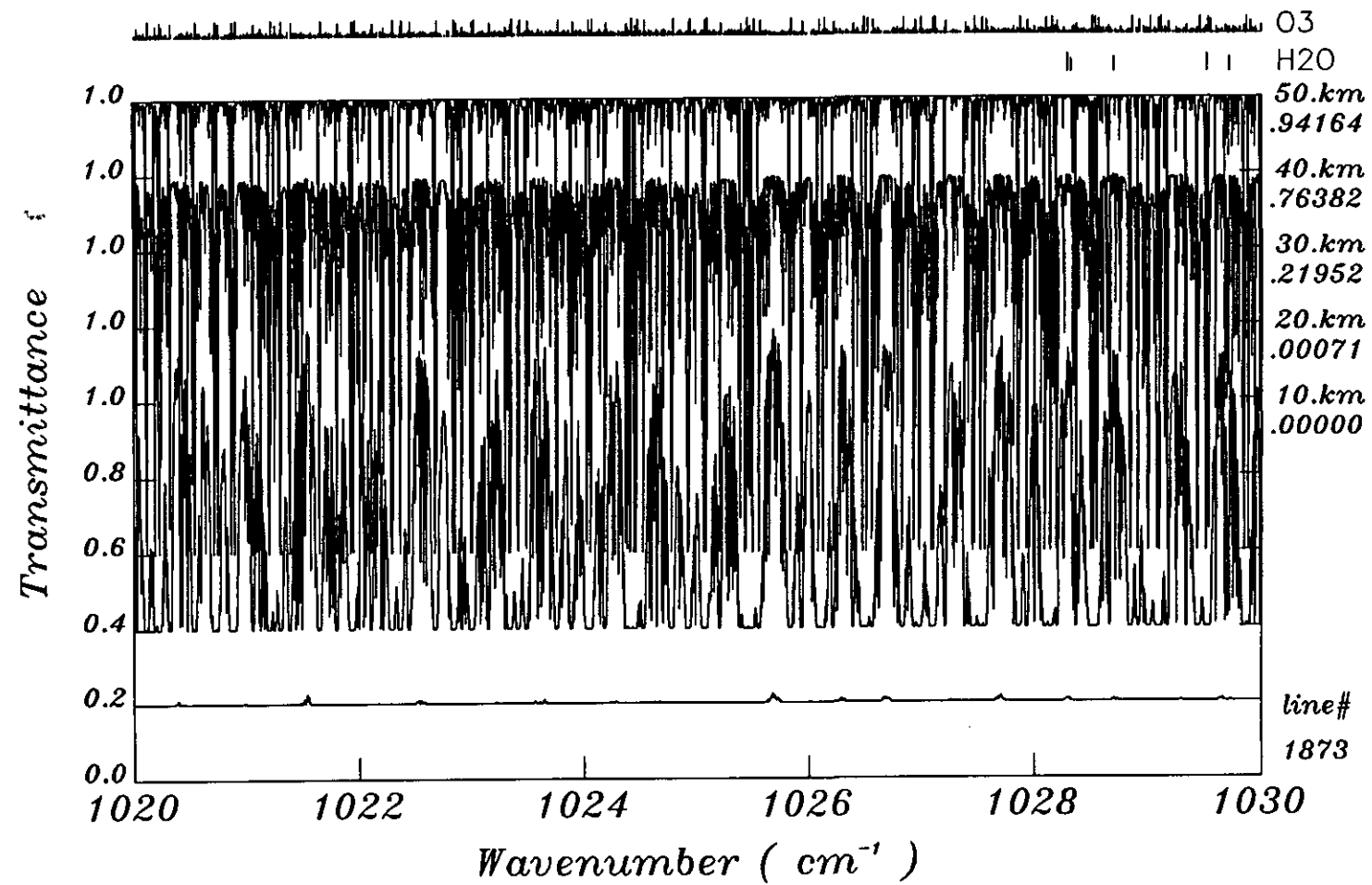




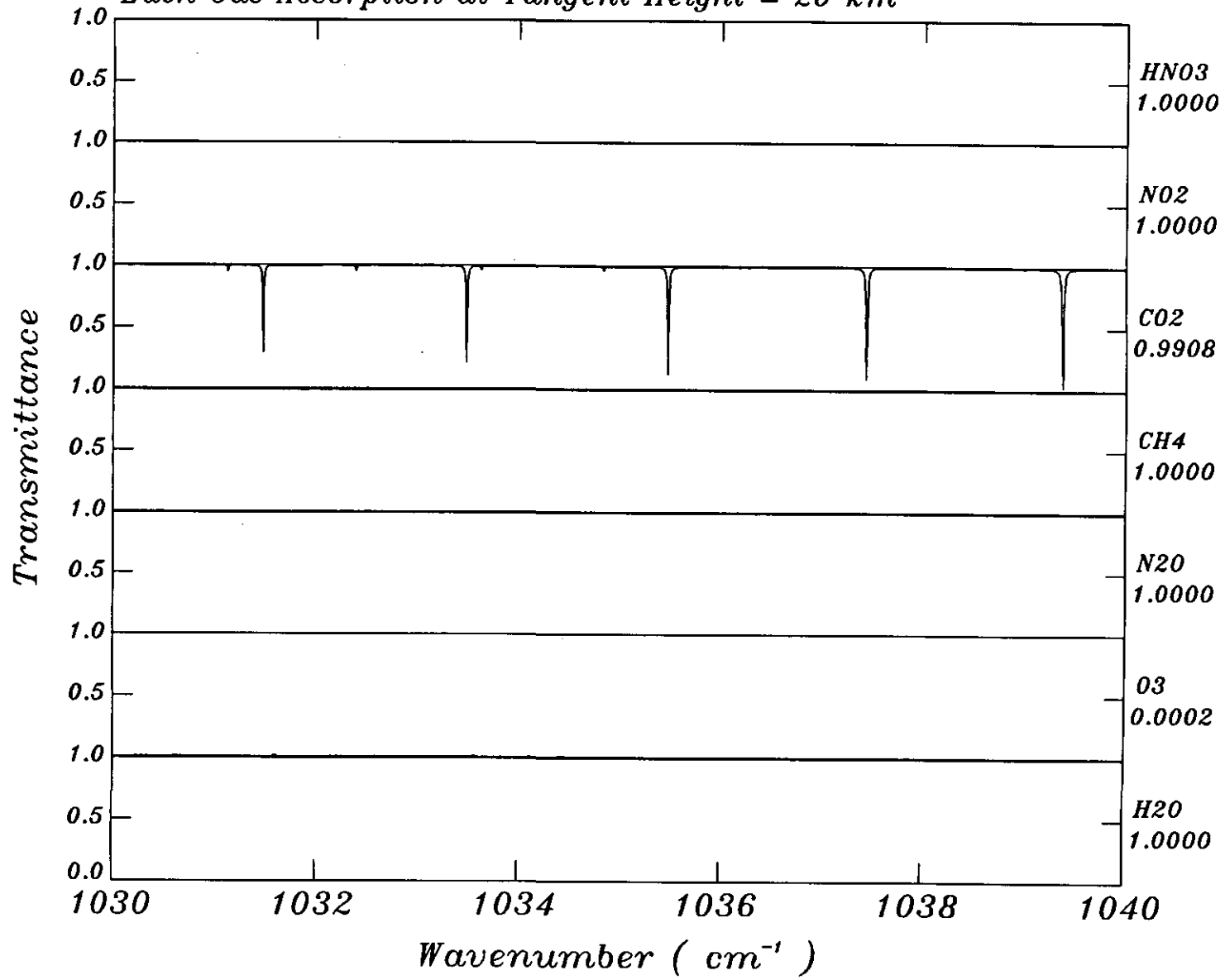
*Each Gas Absorption at Tangent Height = 20 km*

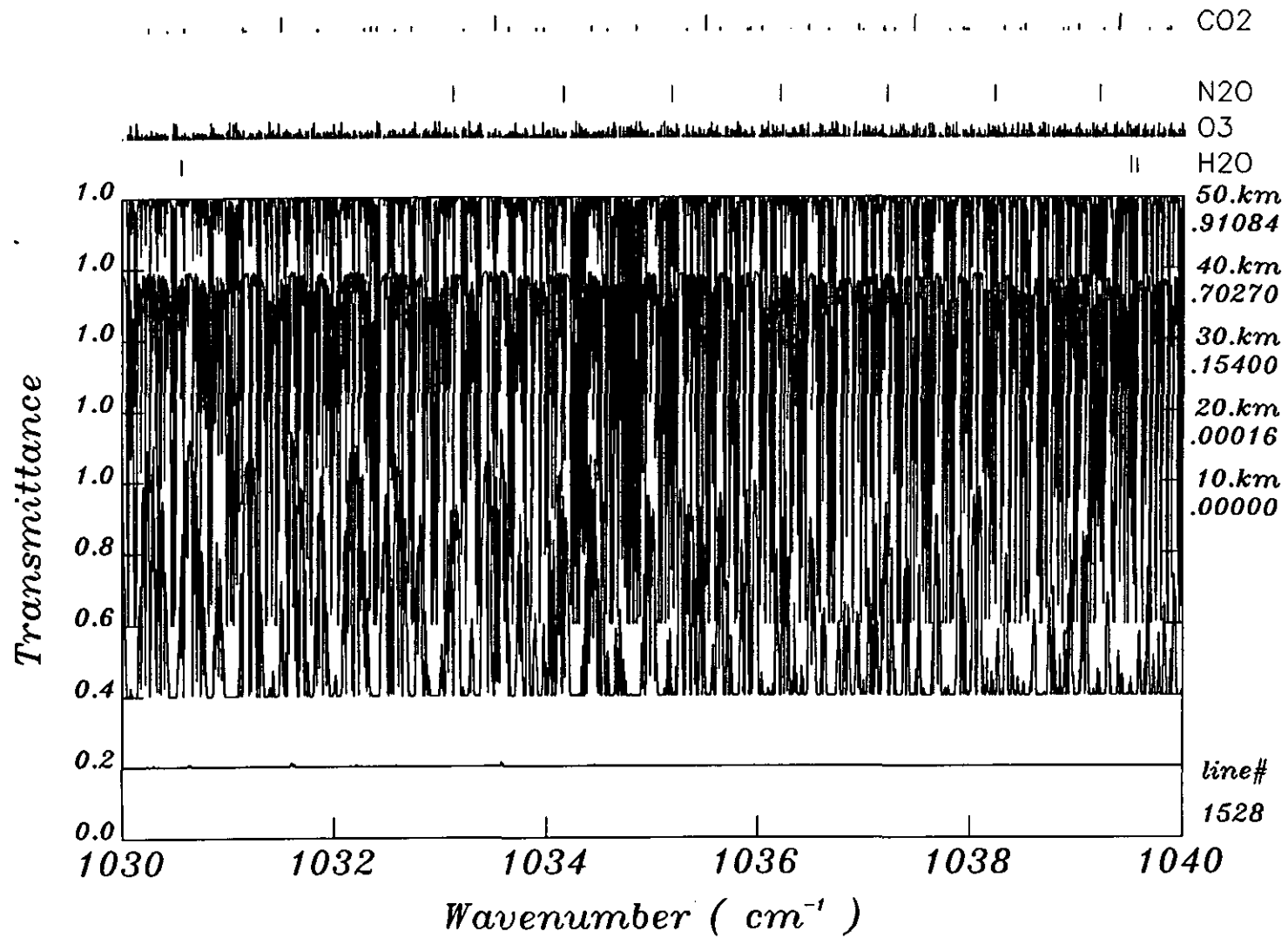


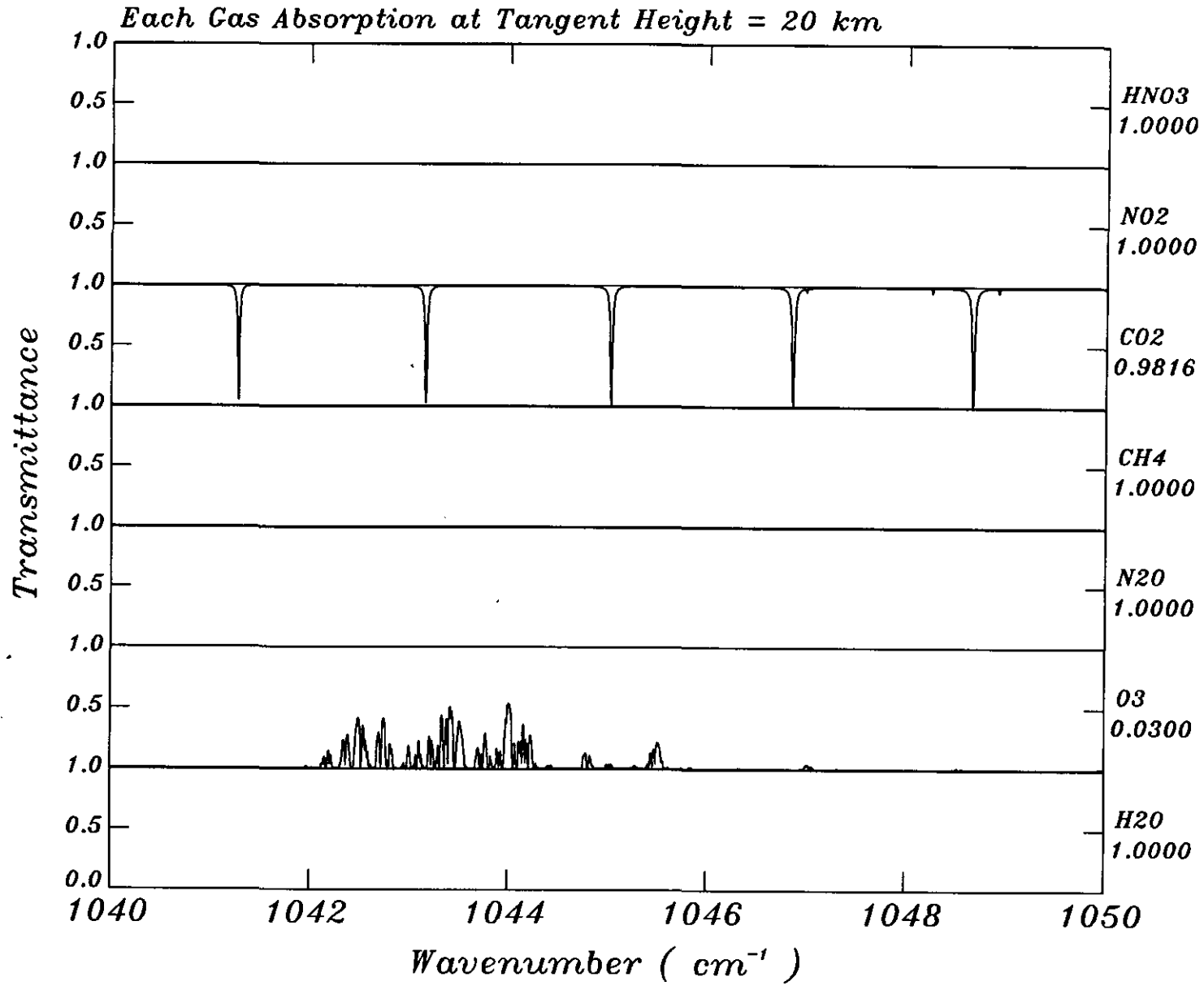
CO2

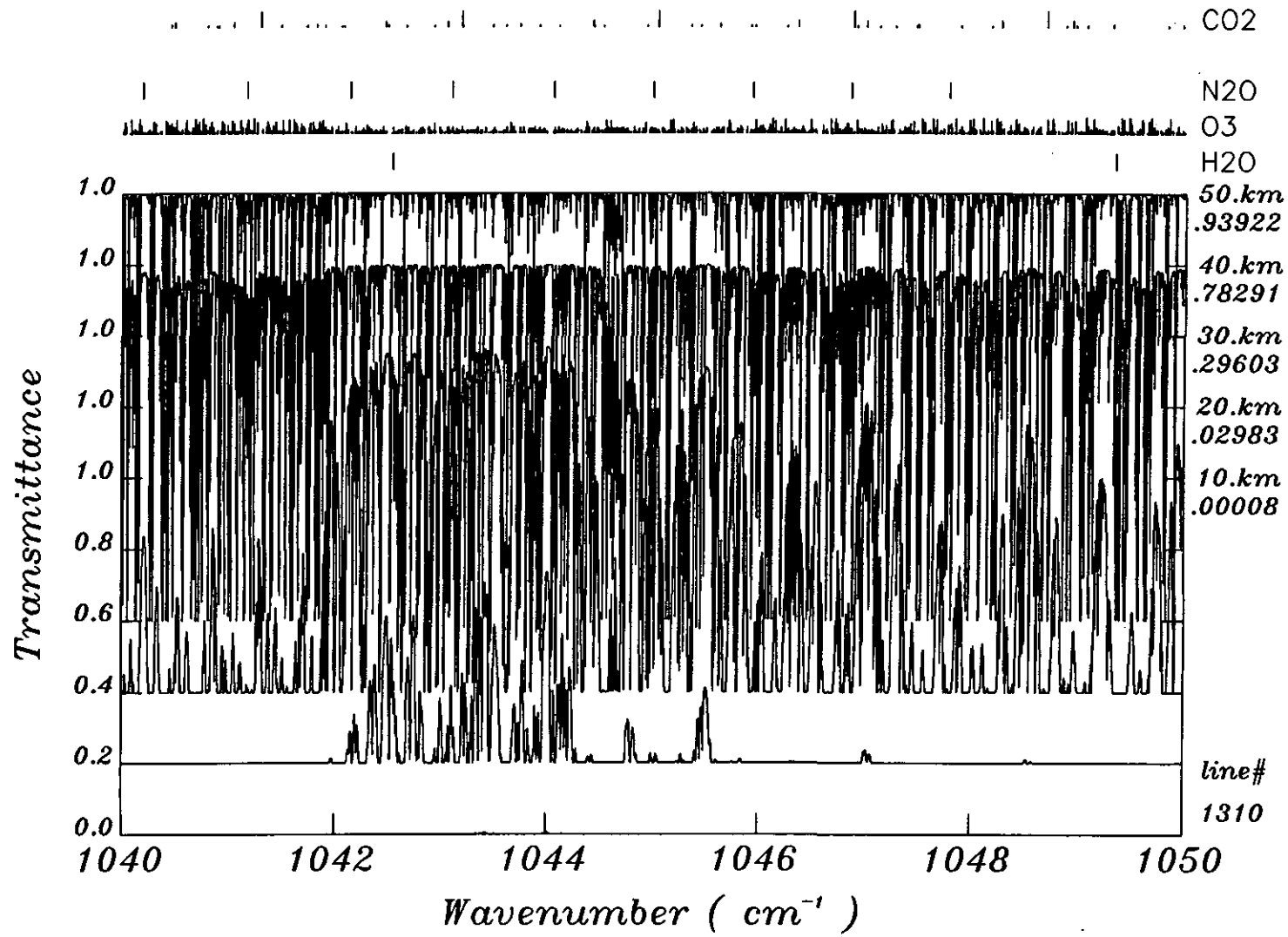


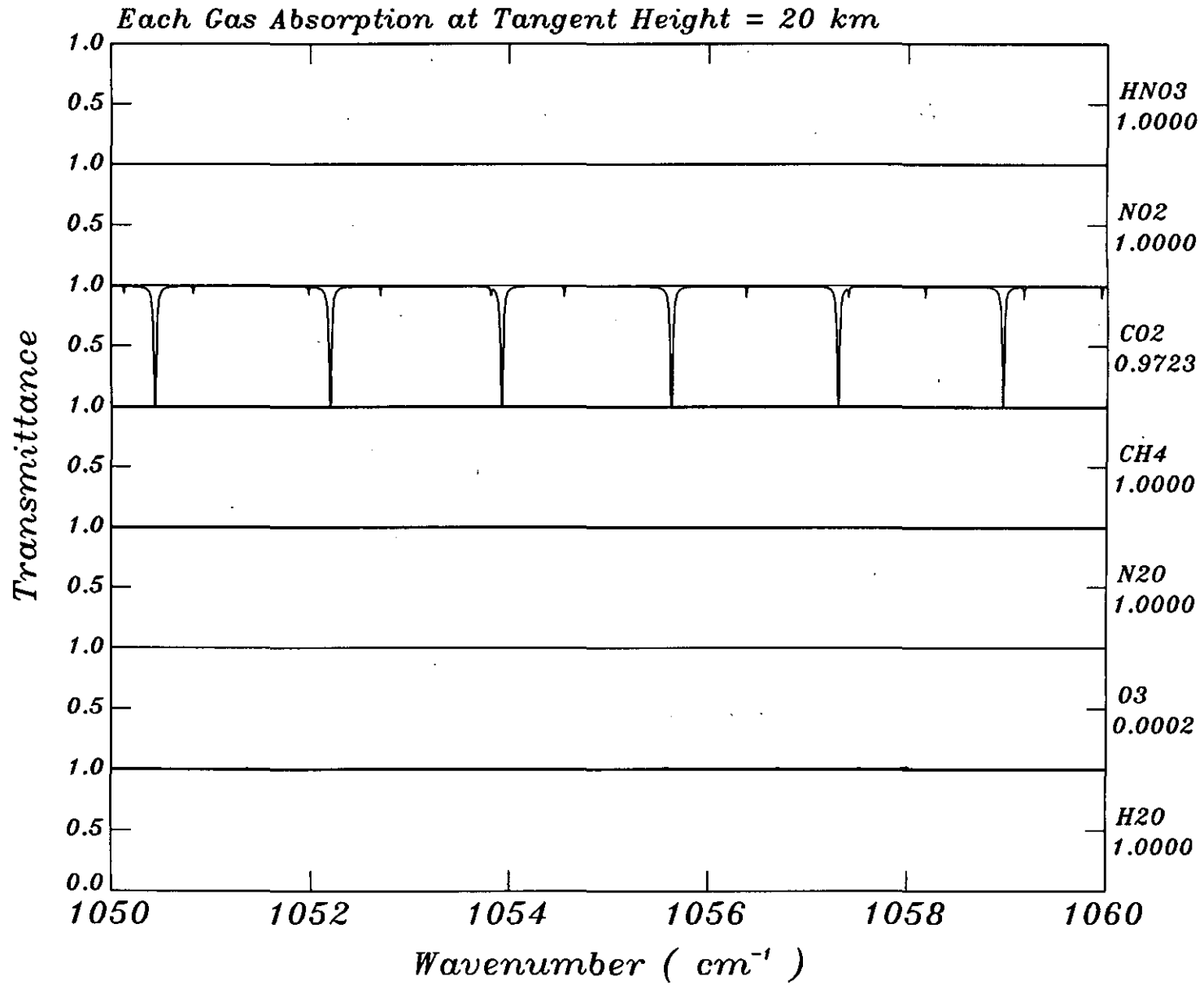
*Each Gas Absorption at Tangent Height = 20 km*



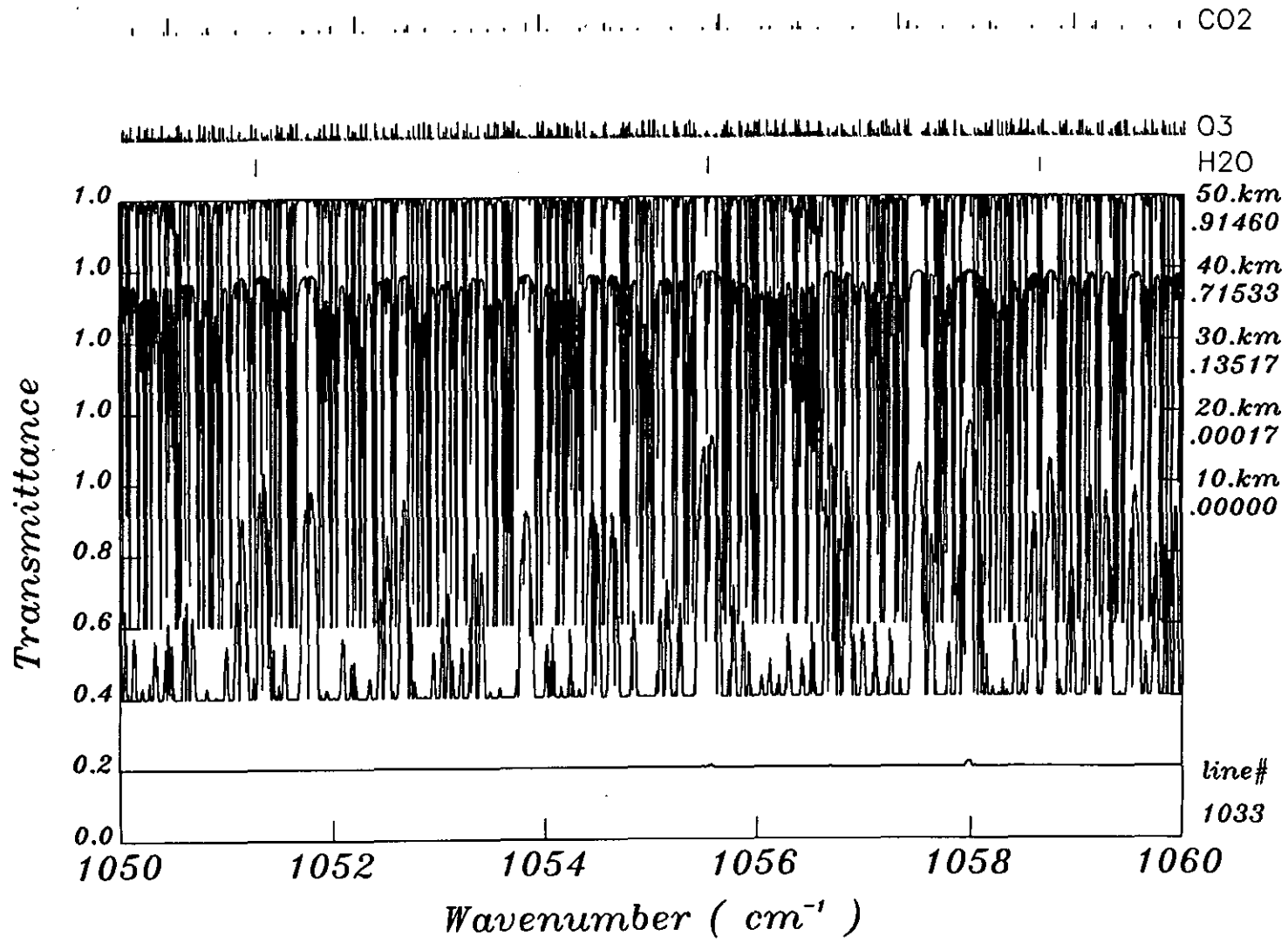


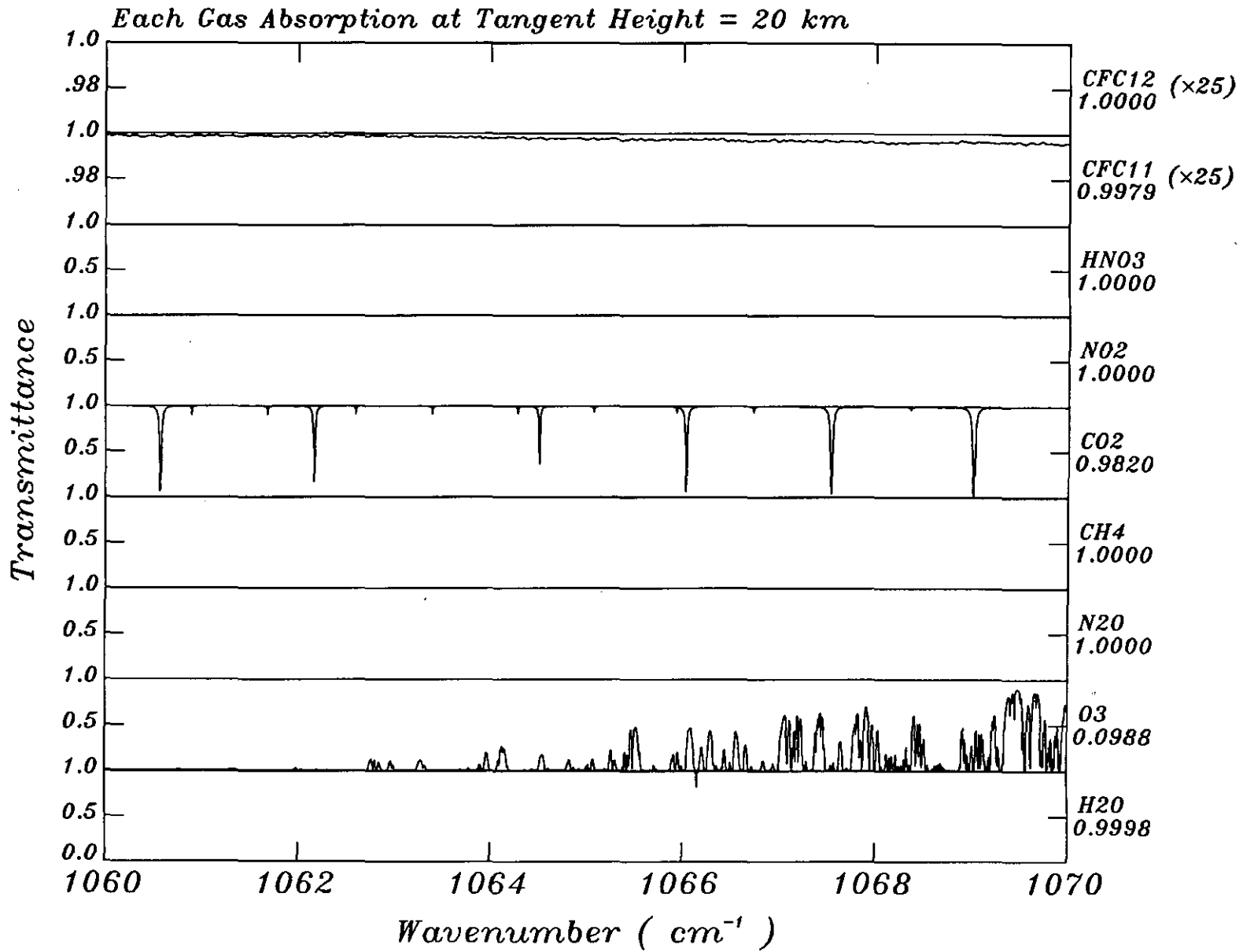


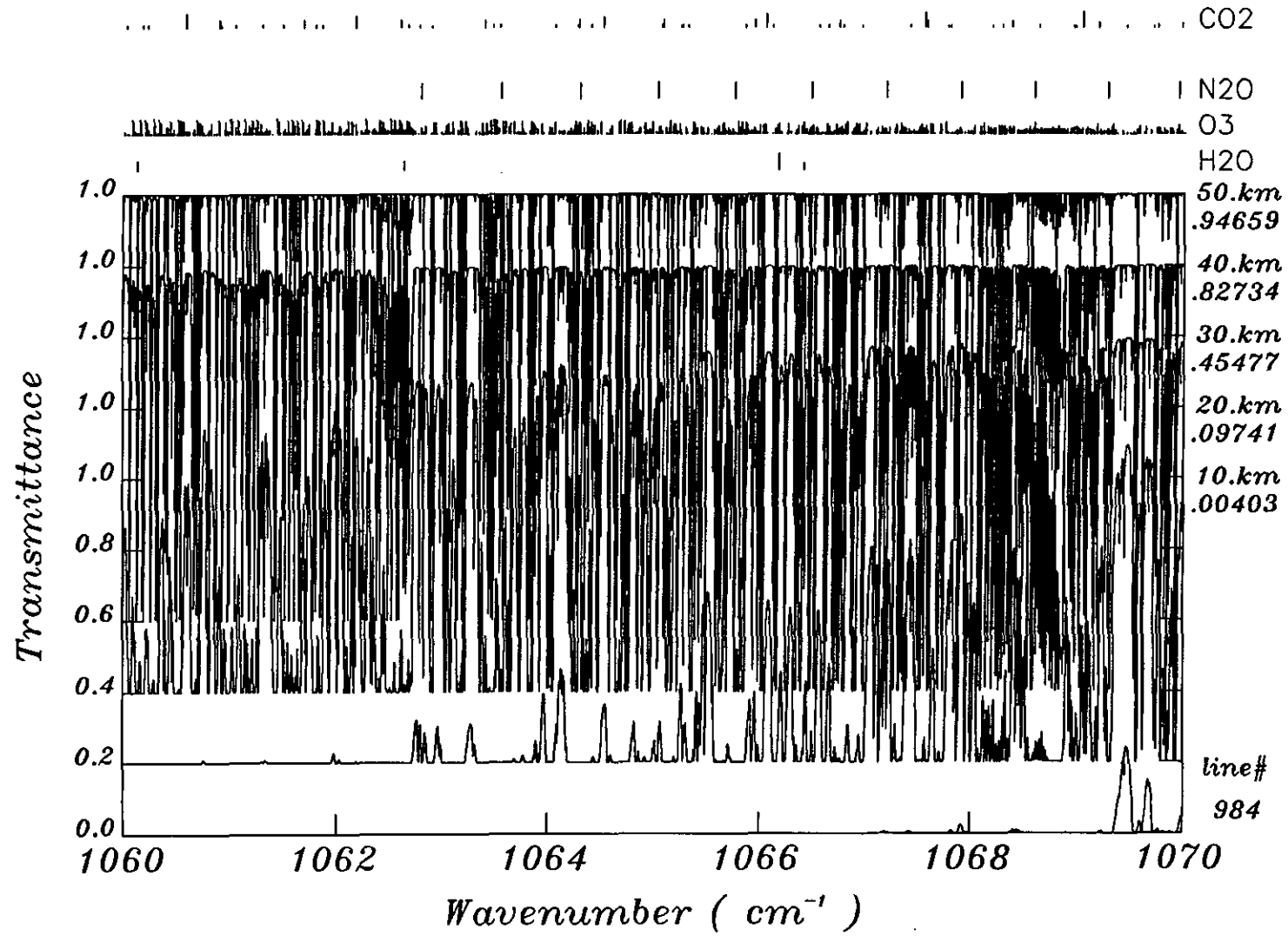


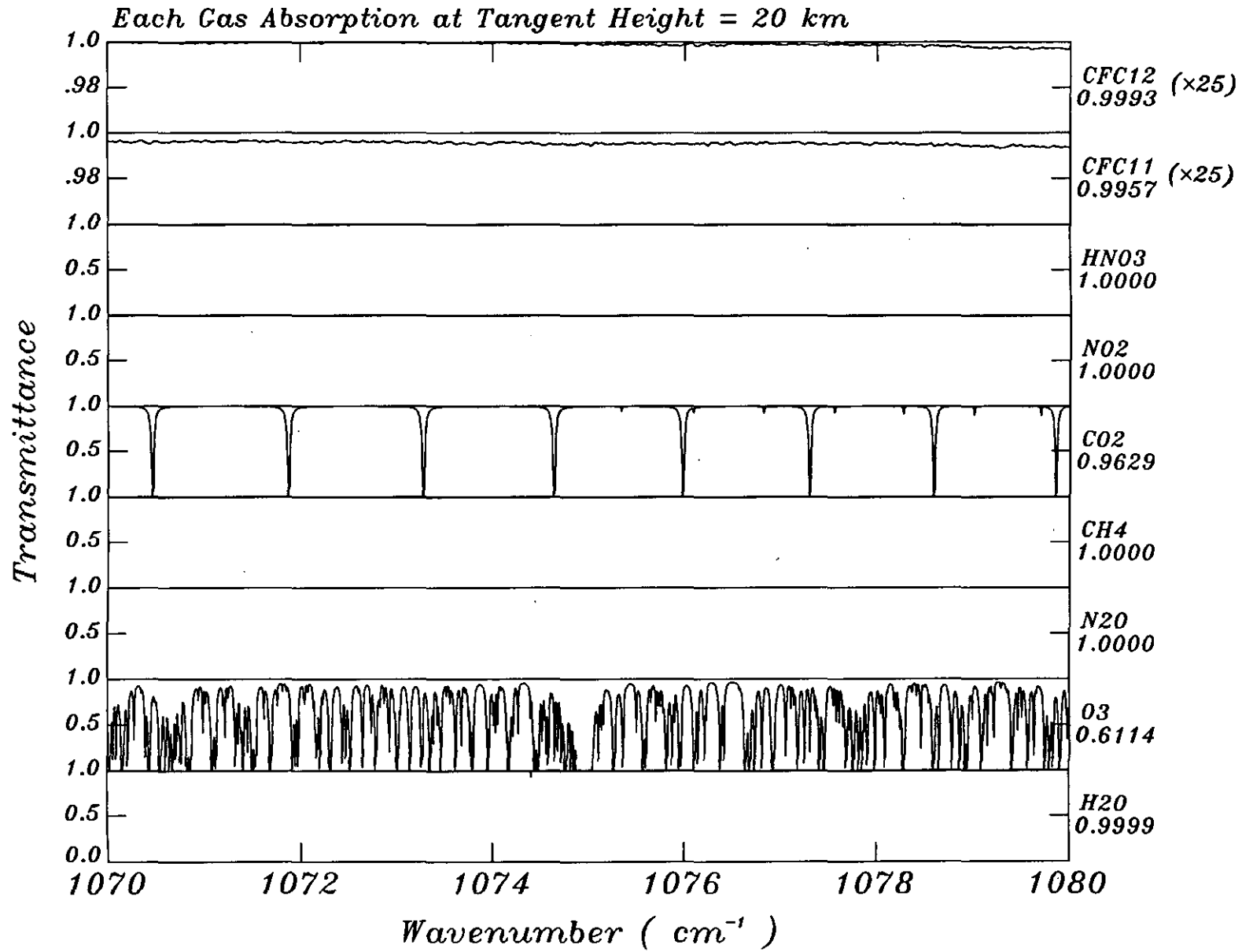


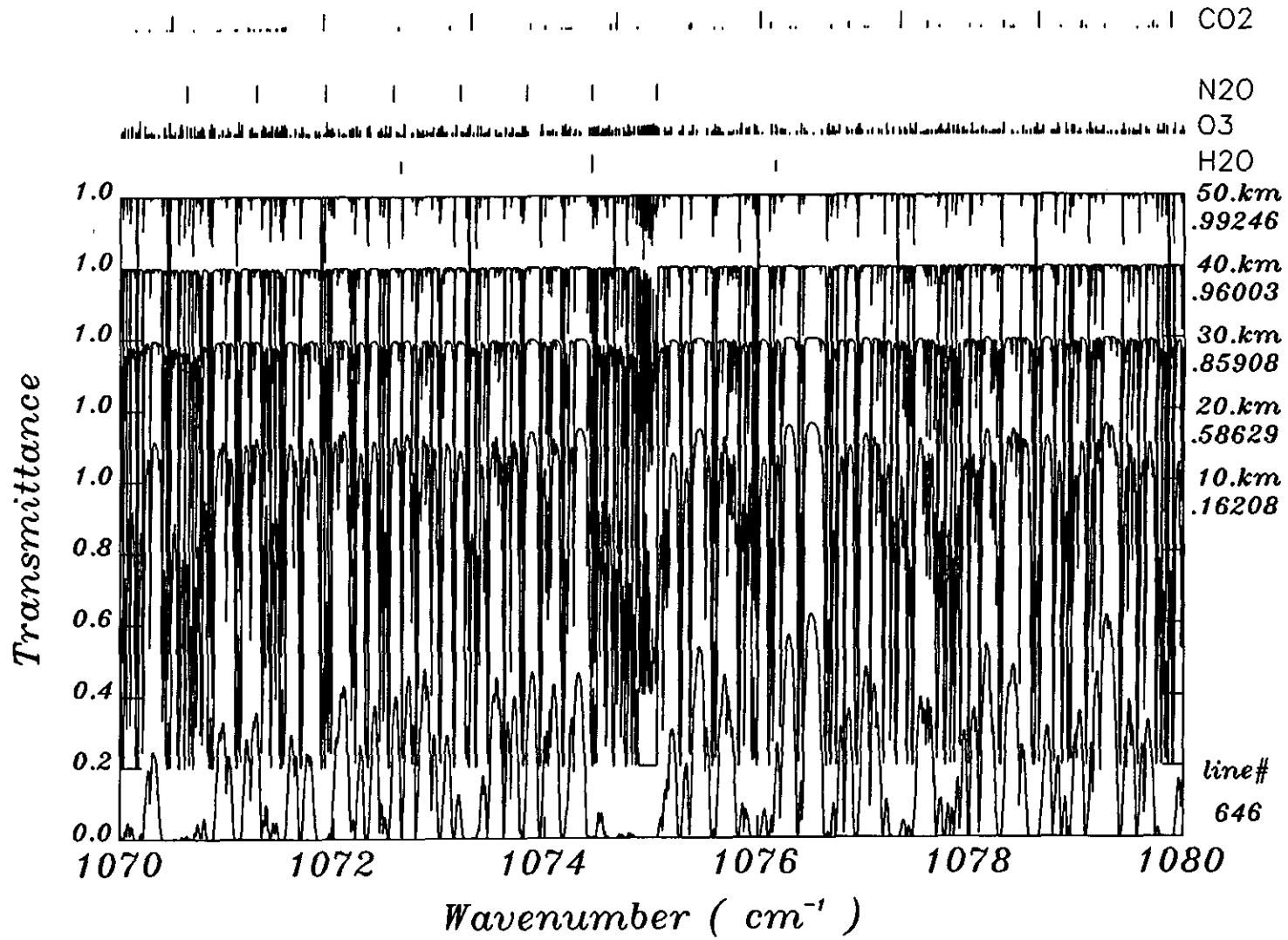


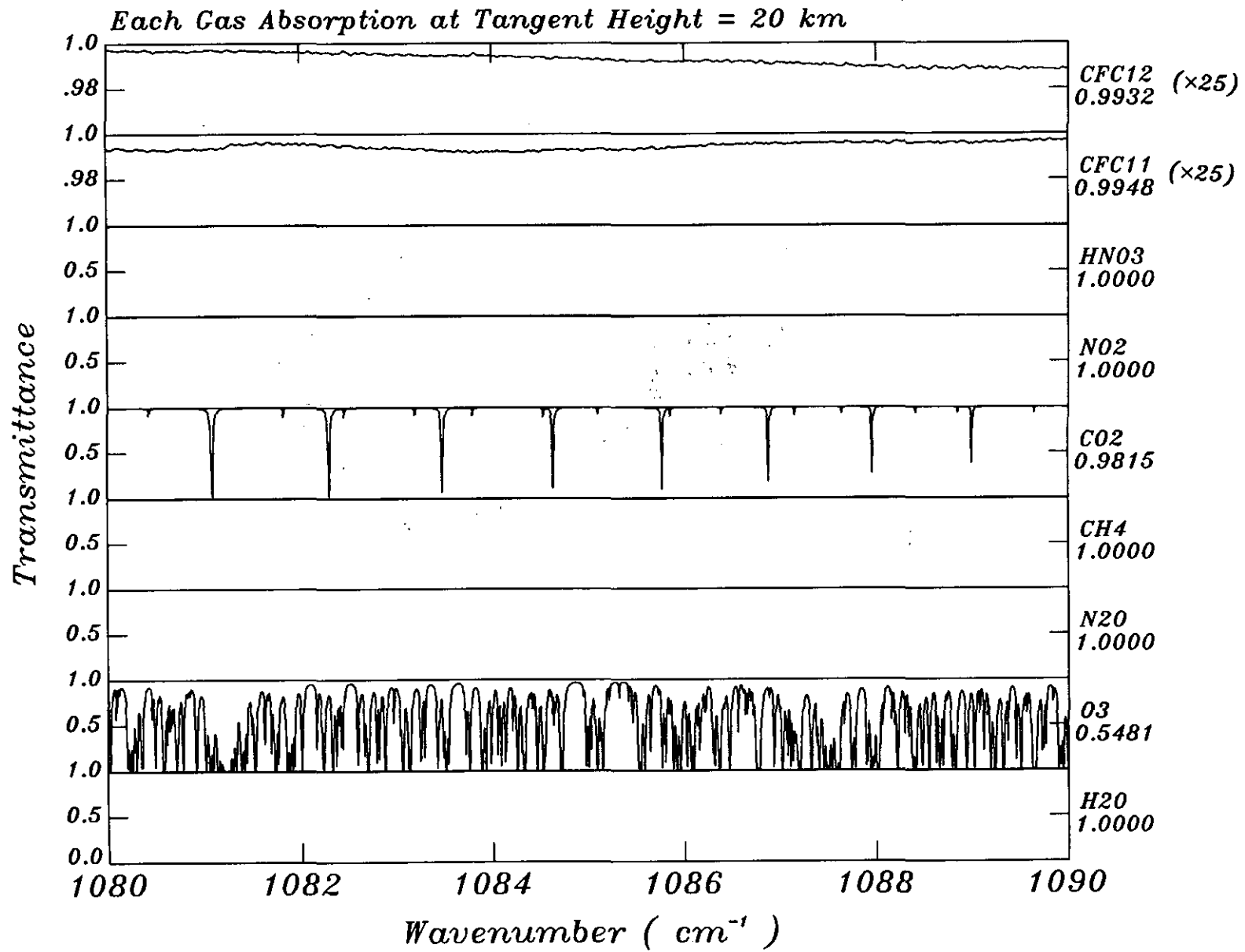


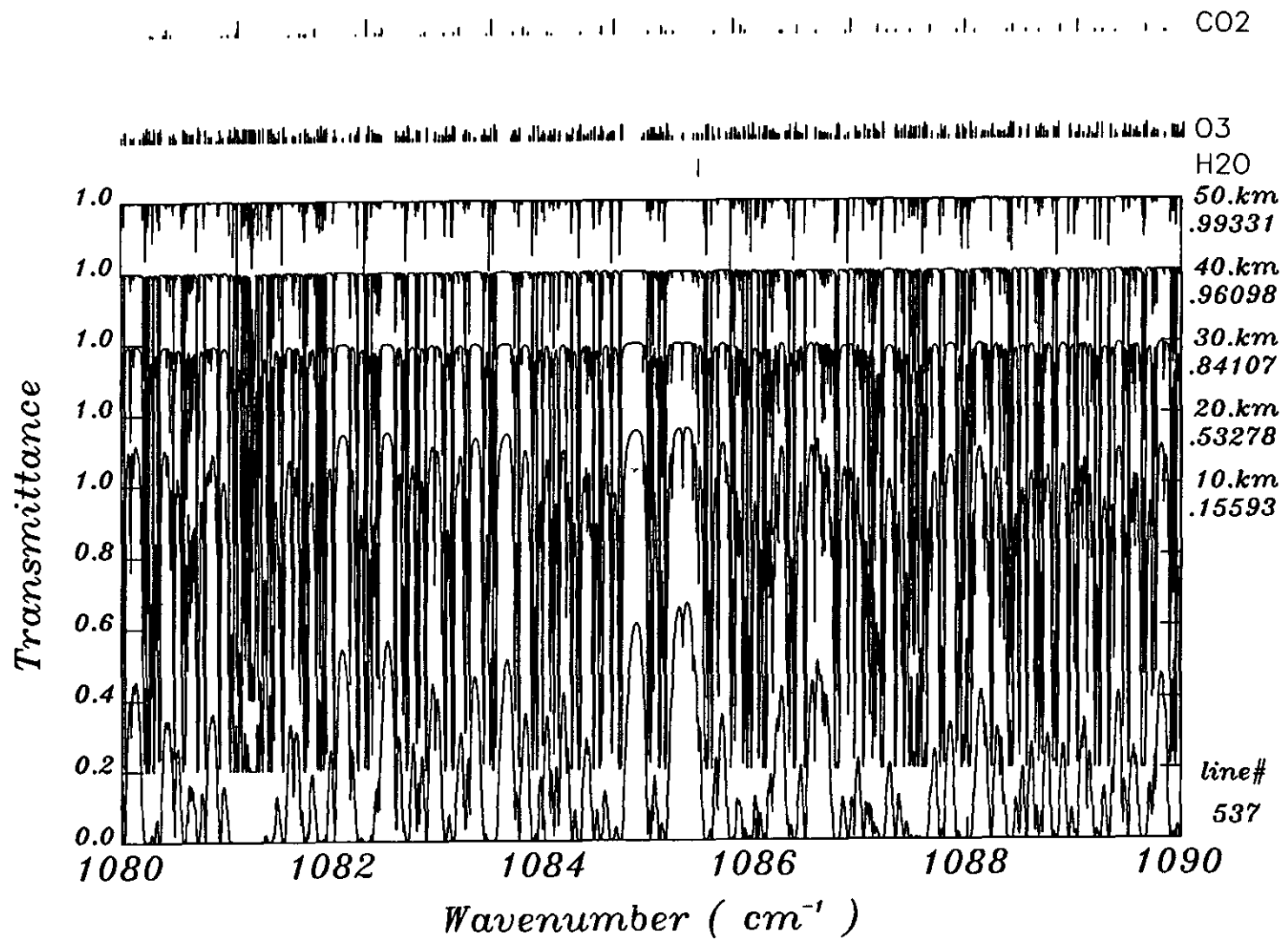




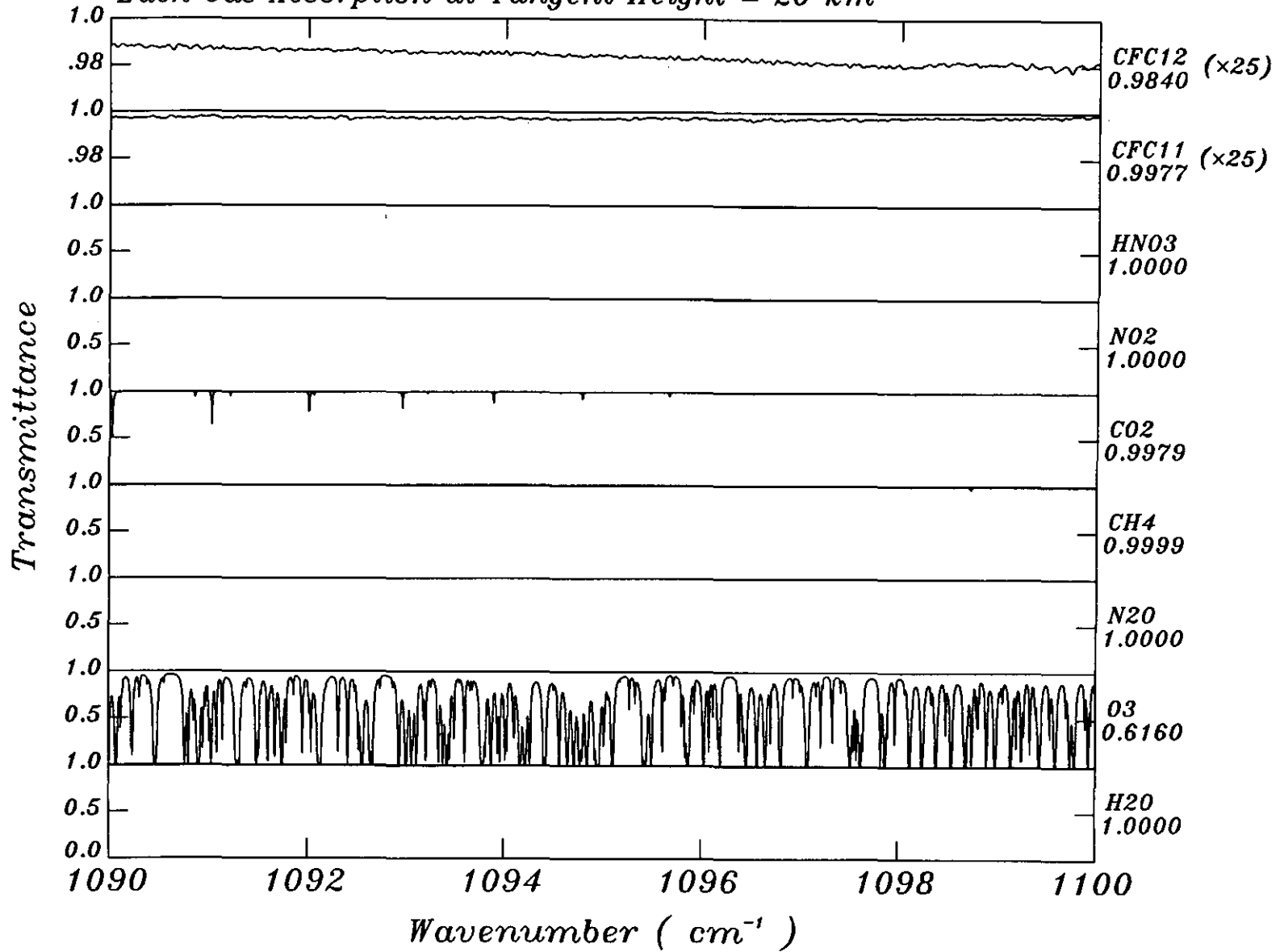




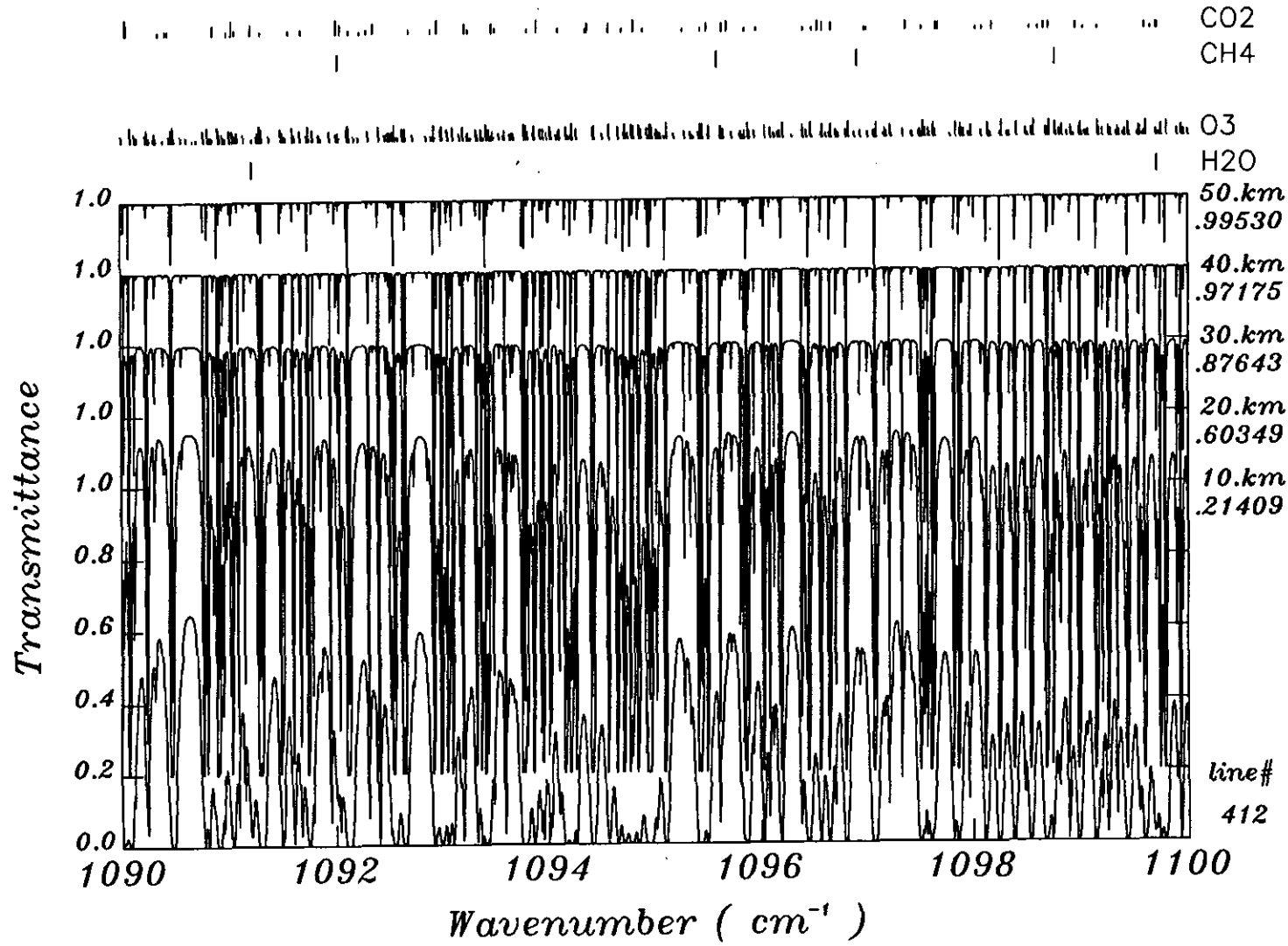




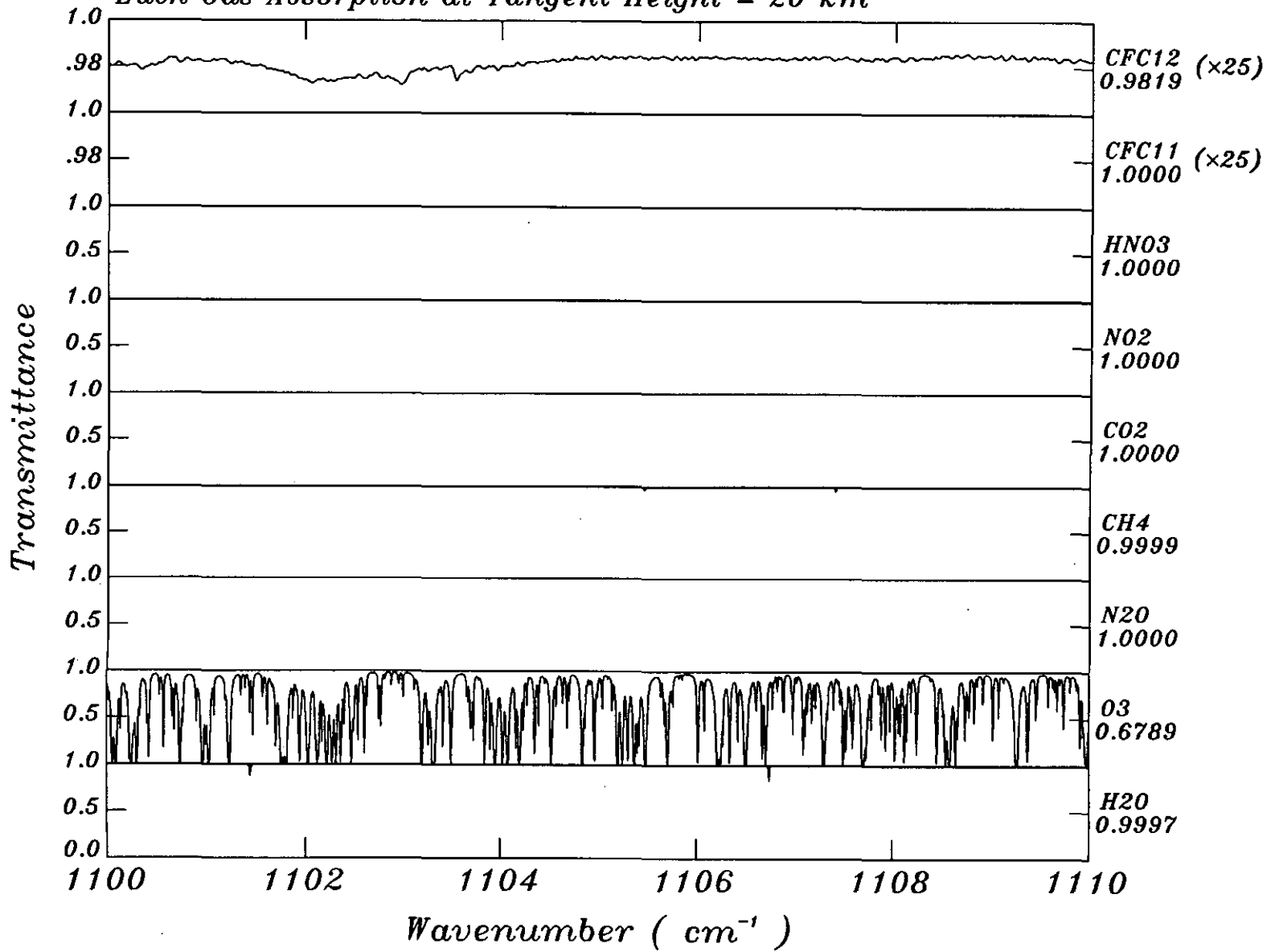
*Each Gas Absorption at Tangent Height = 20 km*

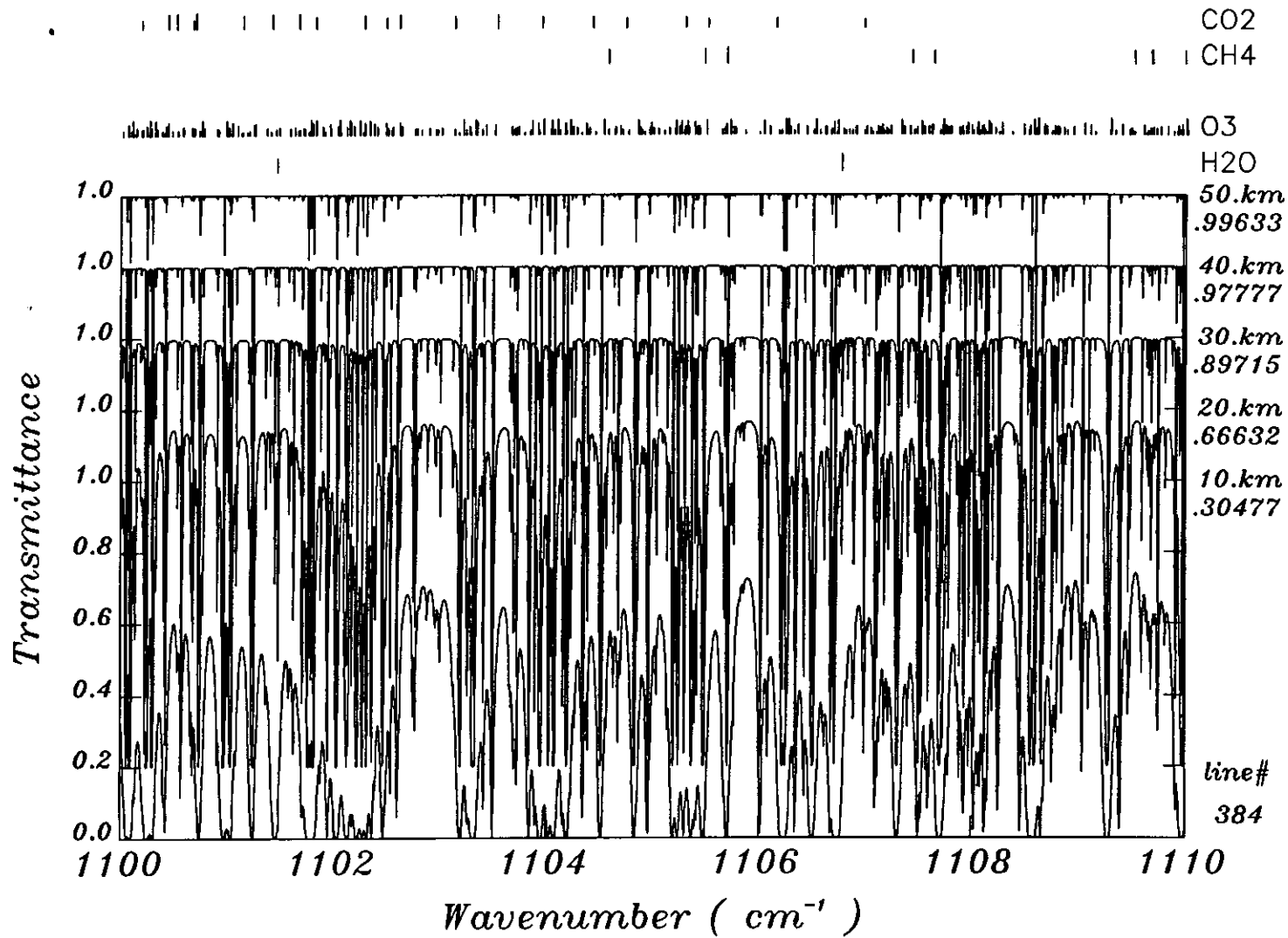


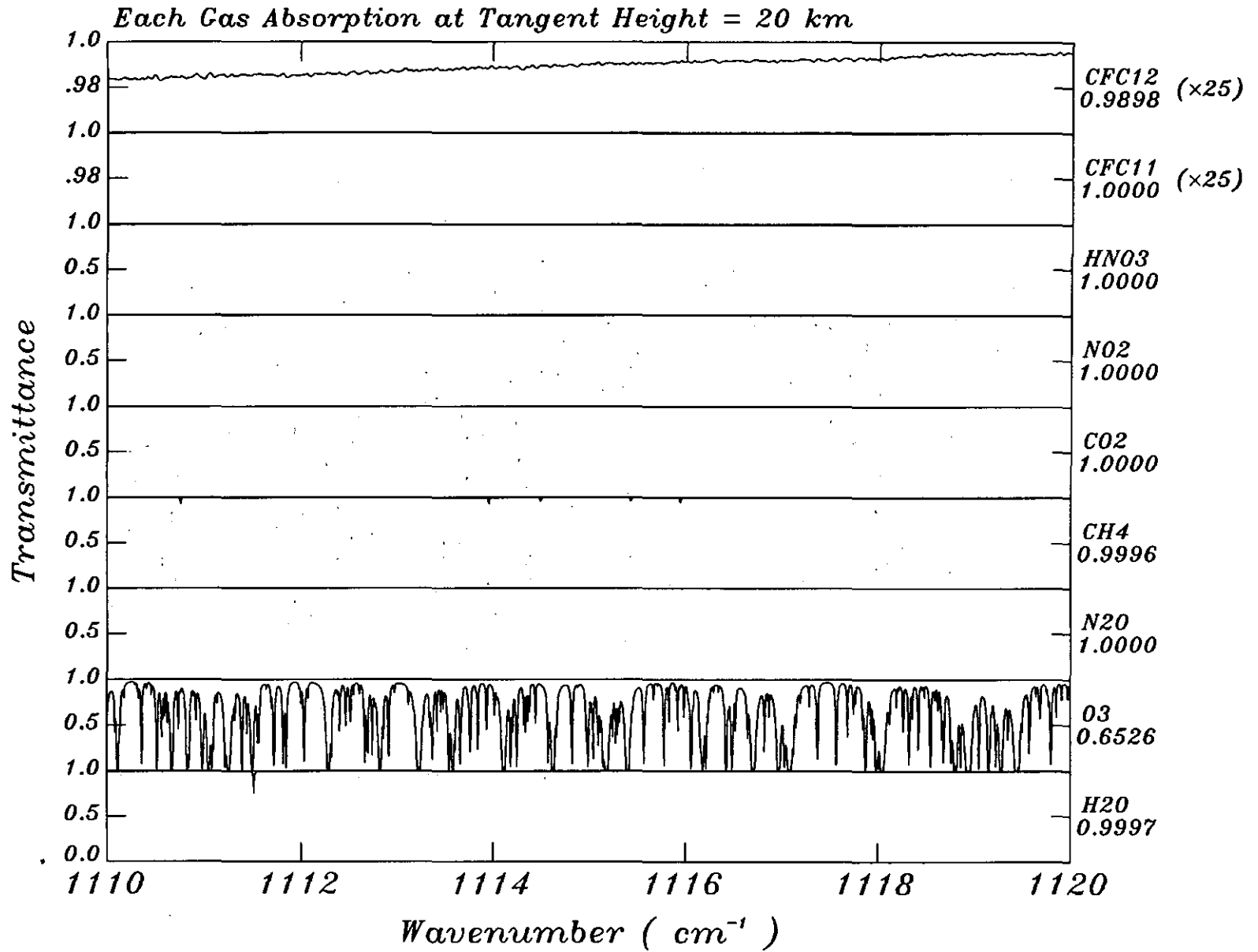


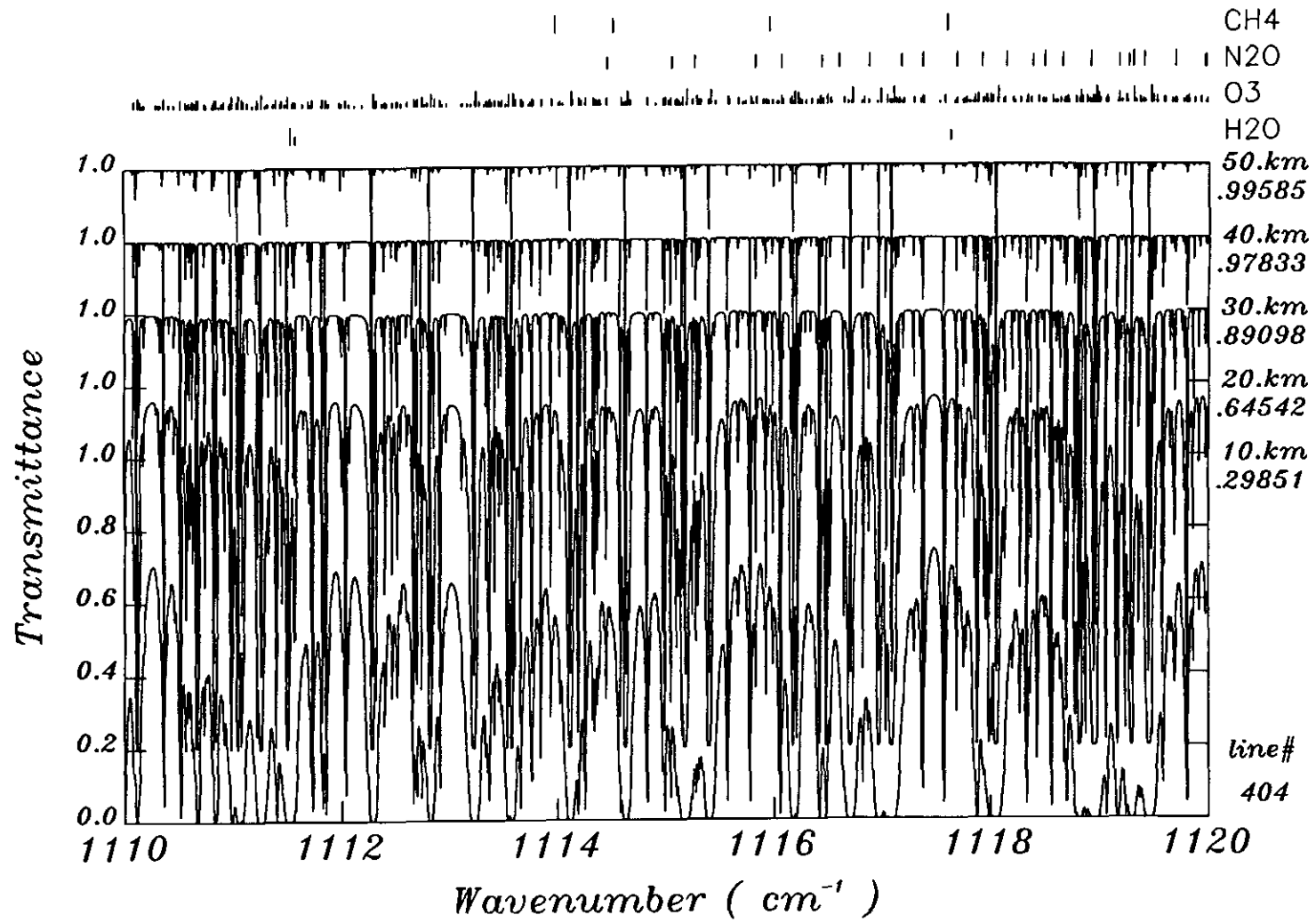


Each Gas Absorption at Tangent Height = 20 km

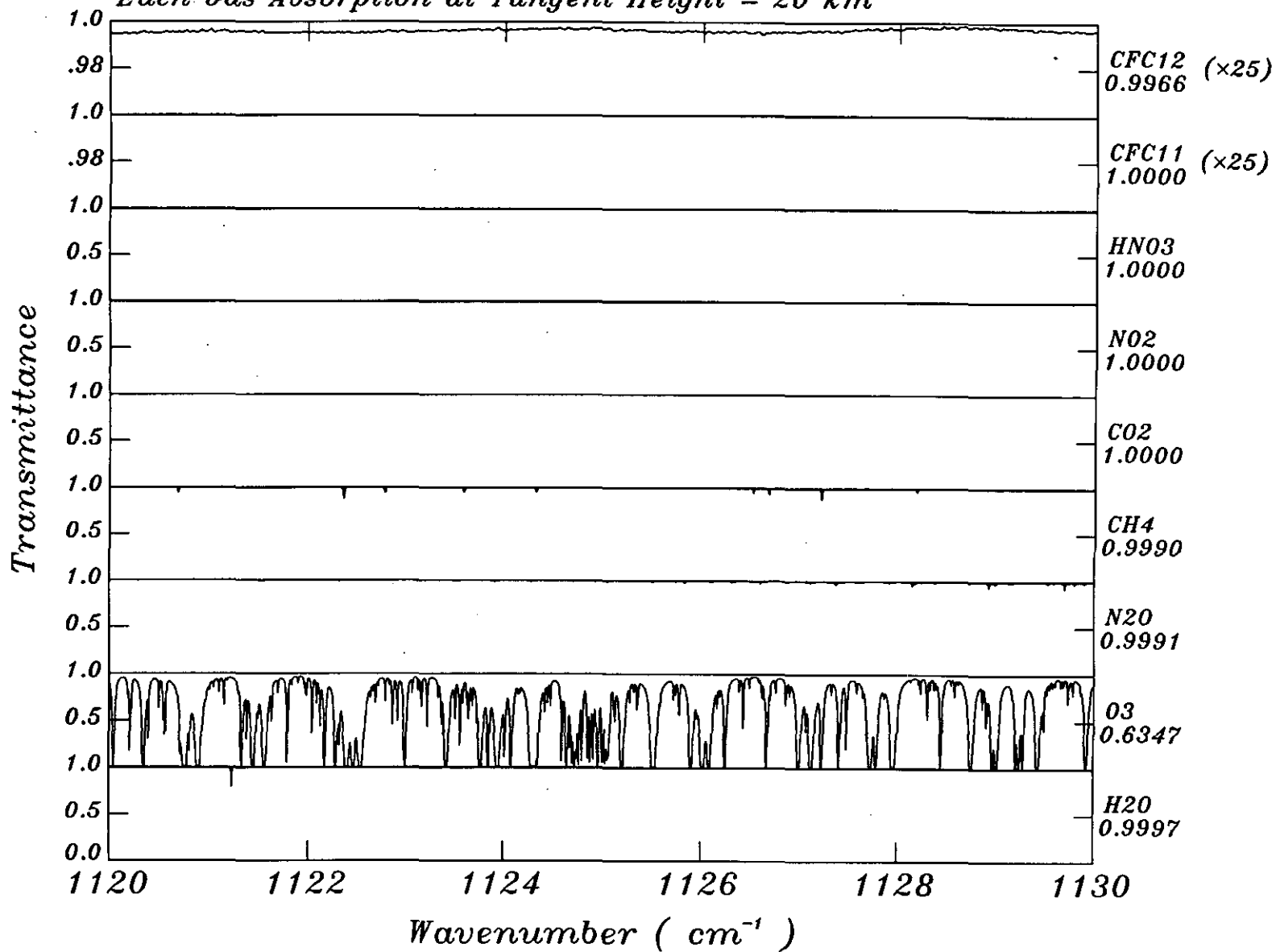


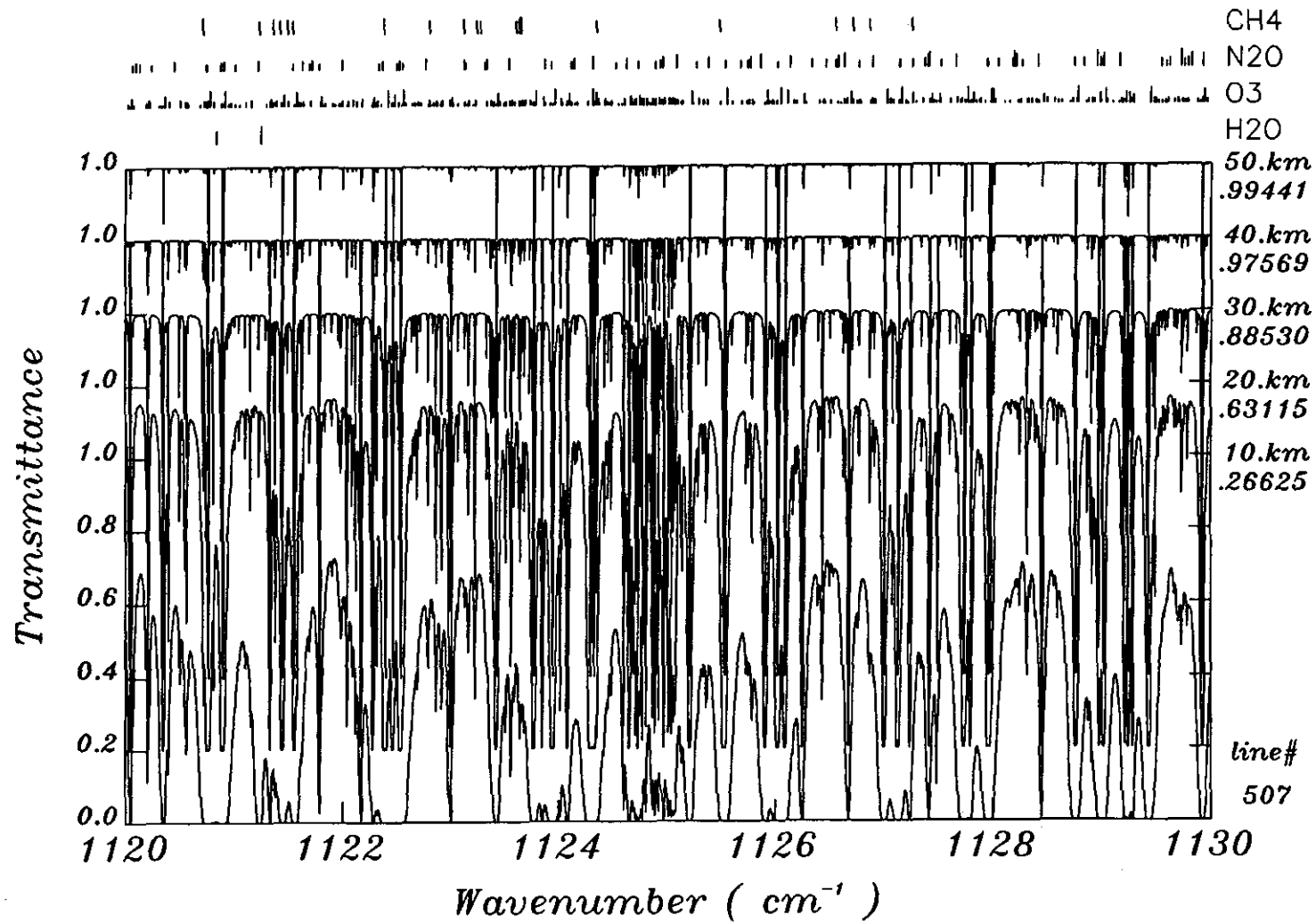




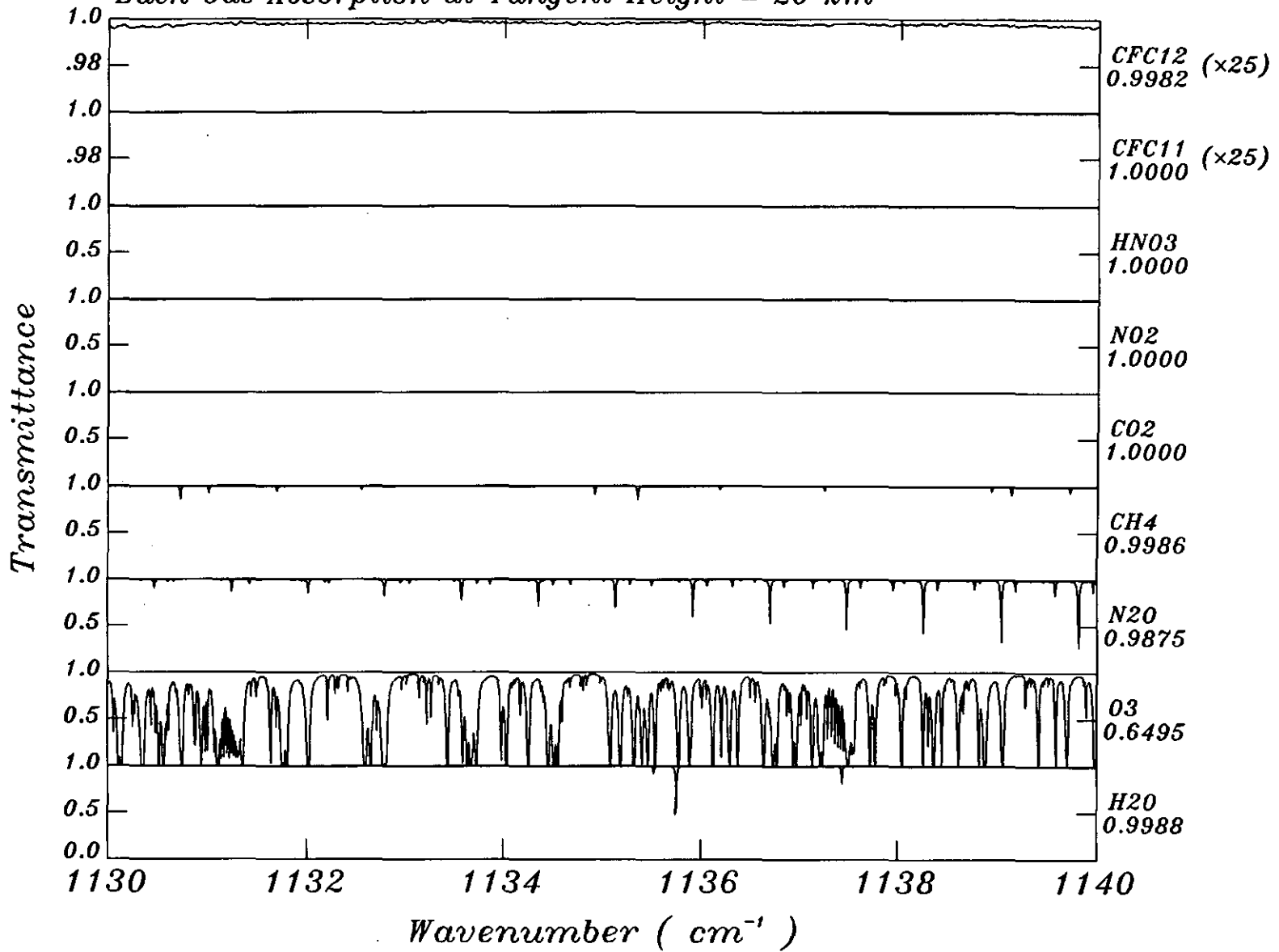


Each Gas Absorption at Tangent Height = 20 km

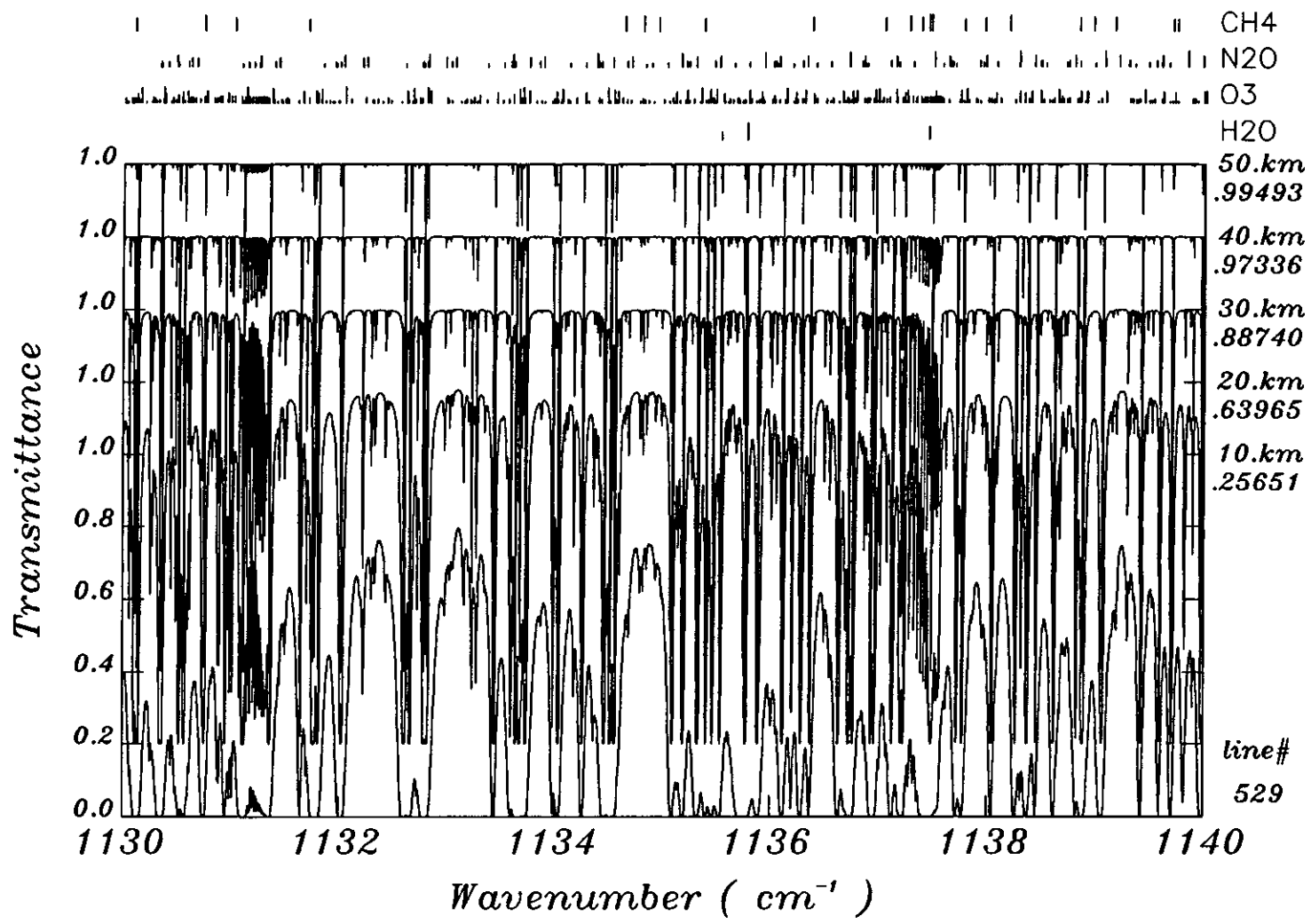


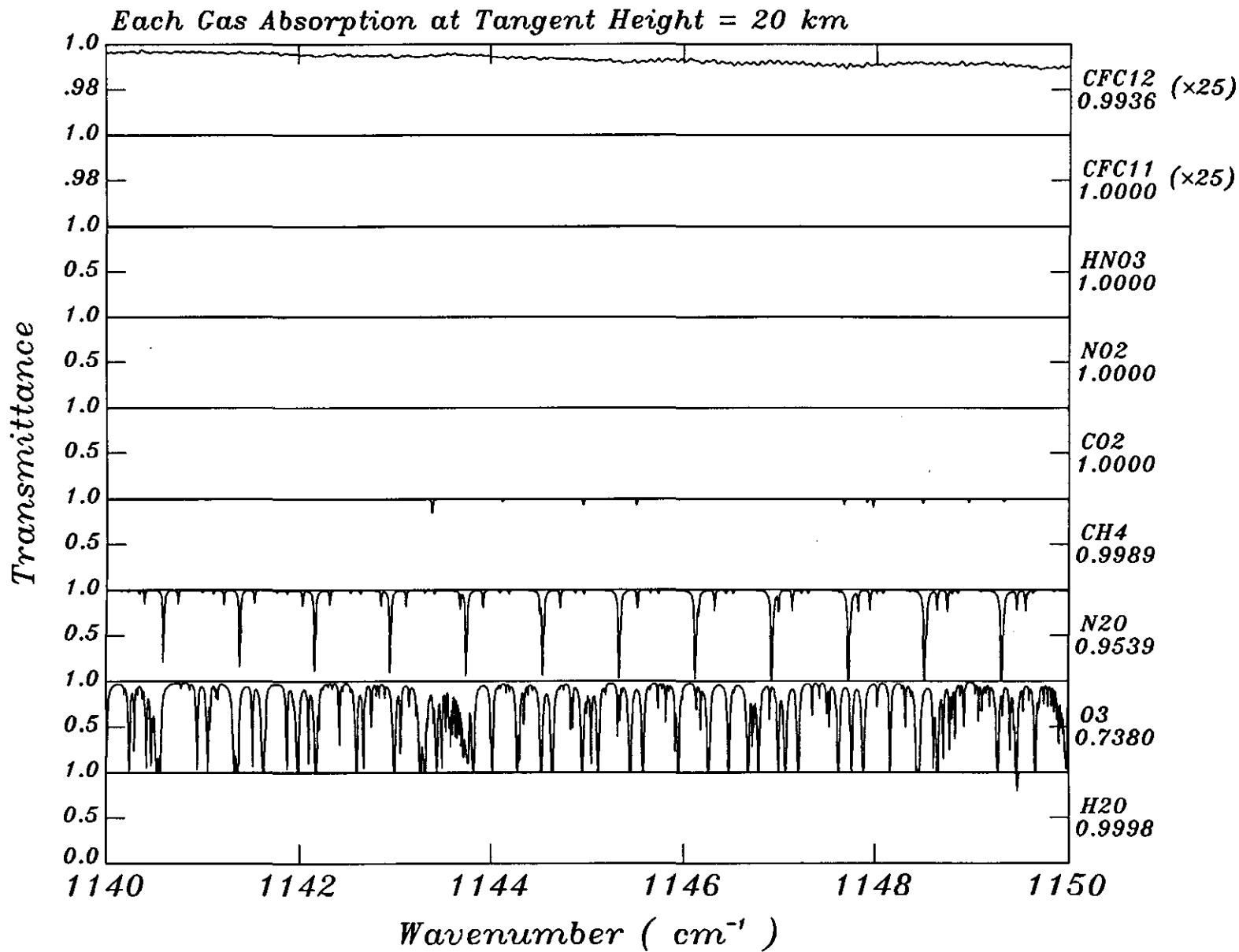


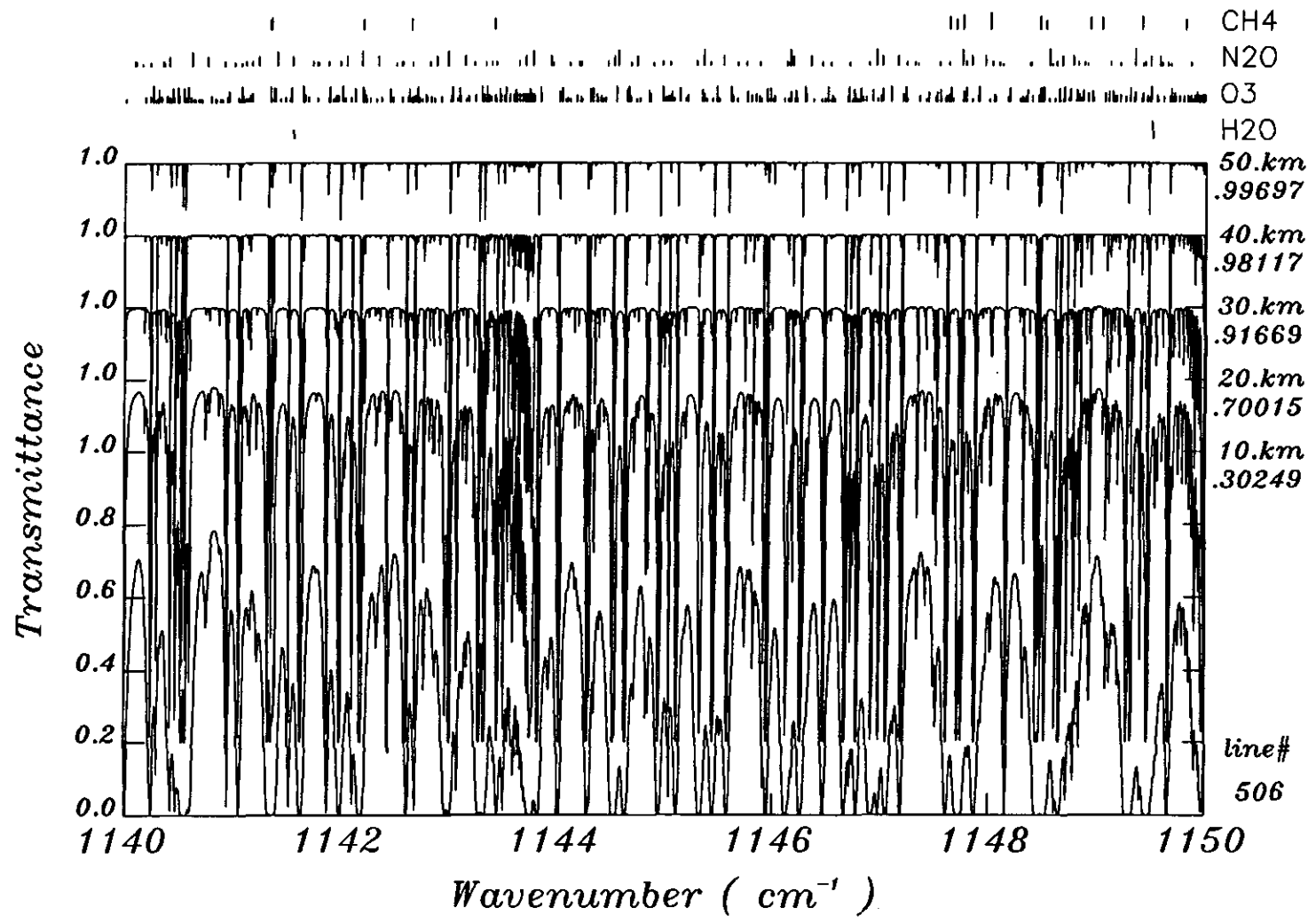
Each Gas Absorption at Tangent Height = 20 km



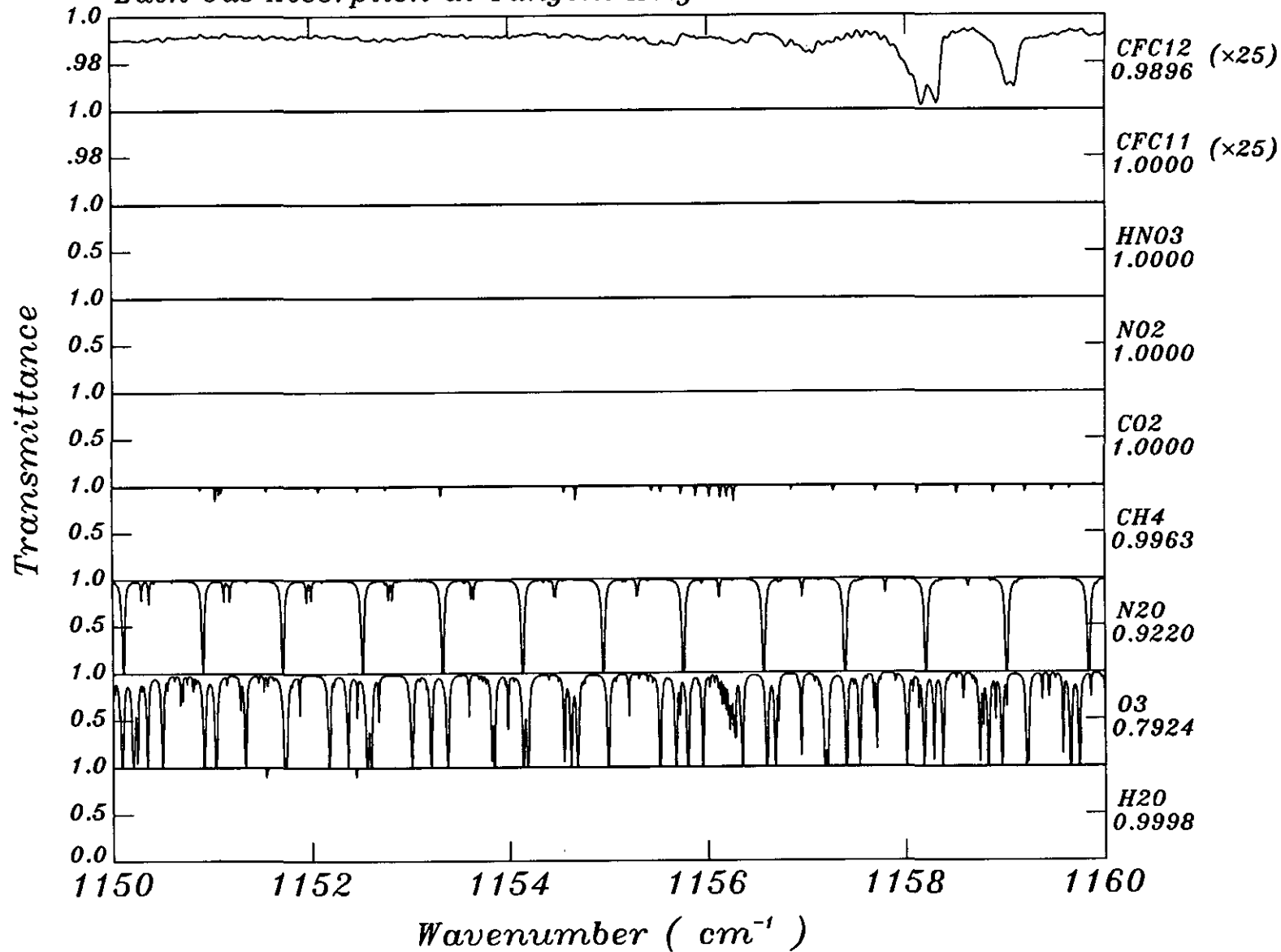


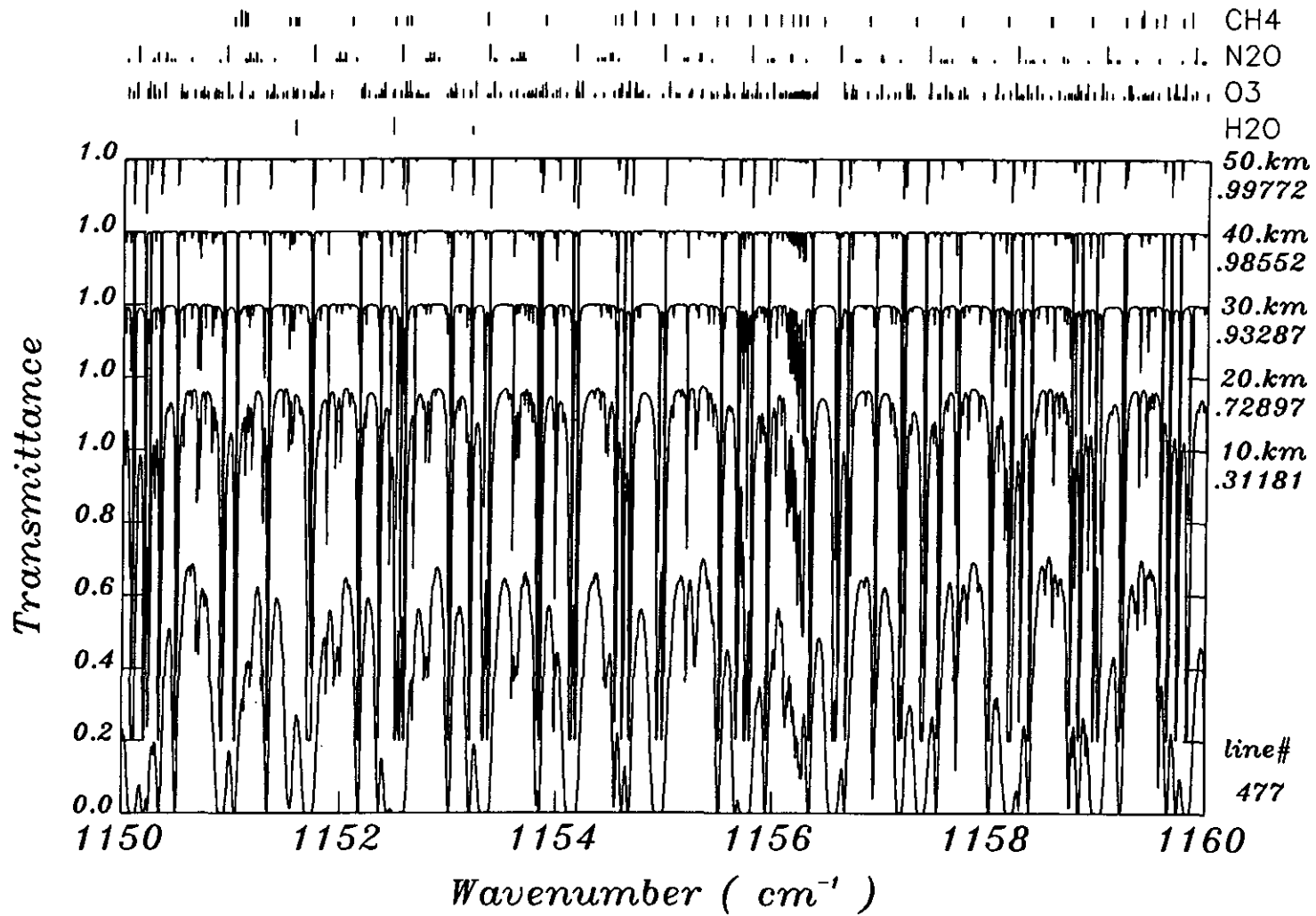


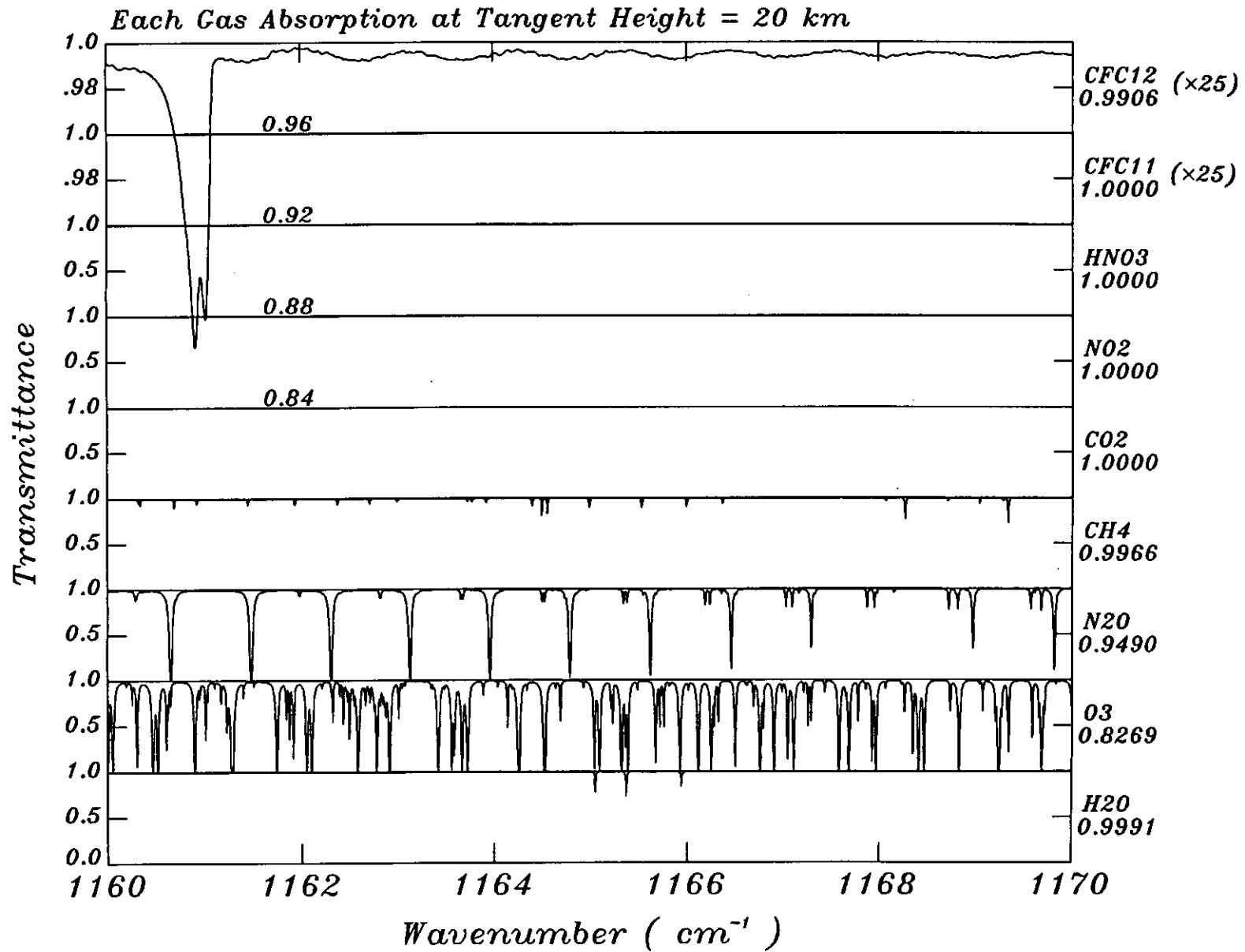


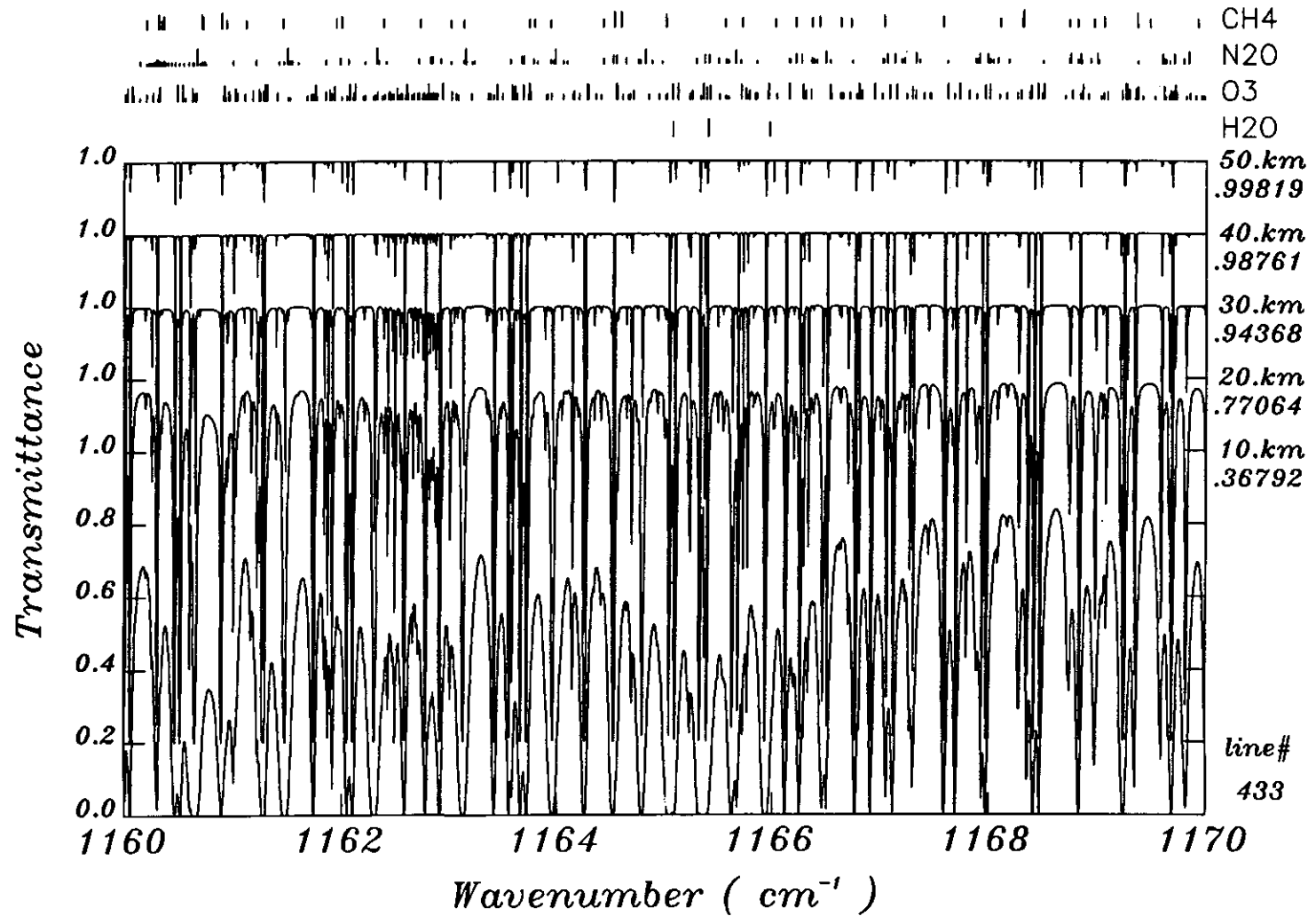


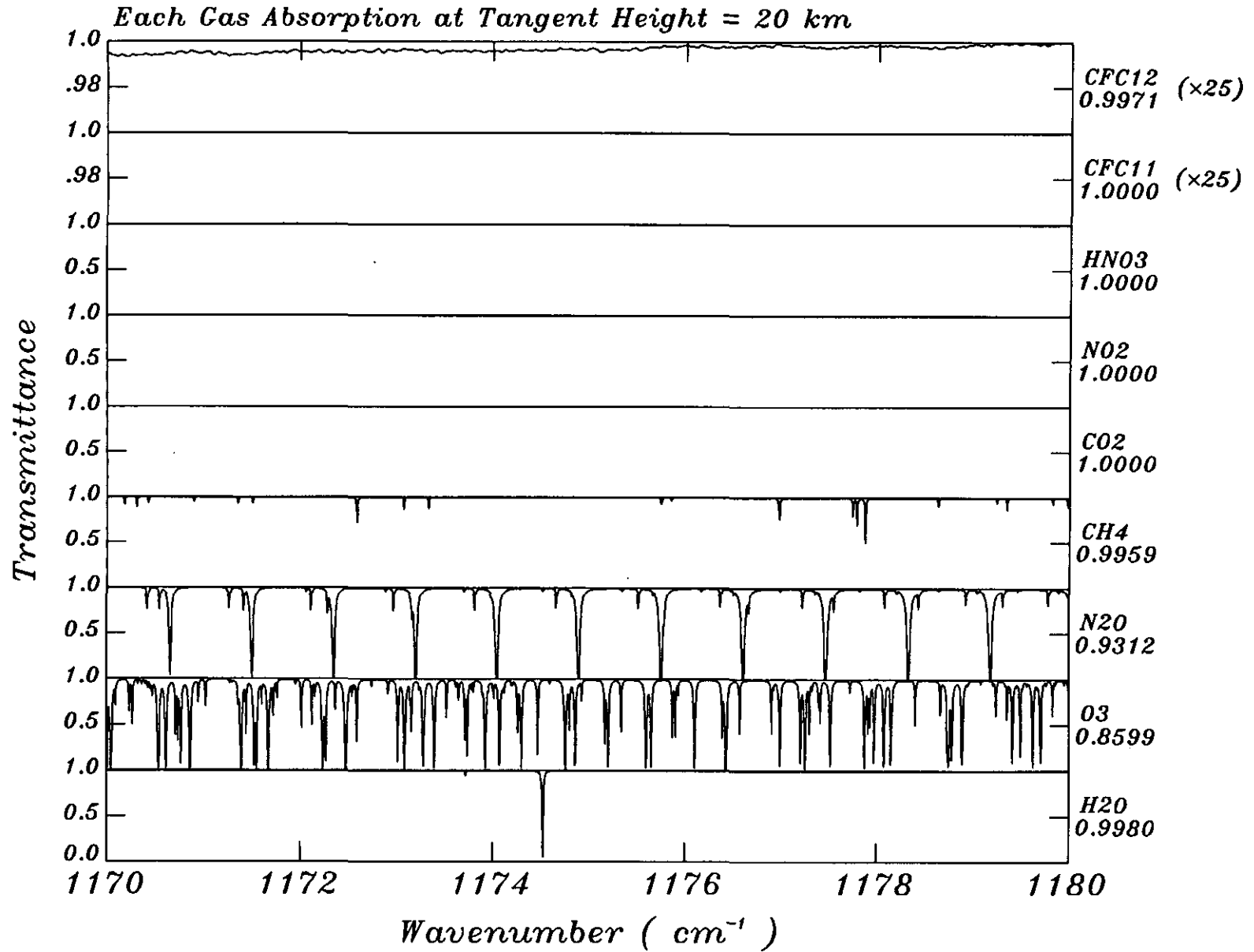
Each Gas Absorption at Tangent Height = 20 km



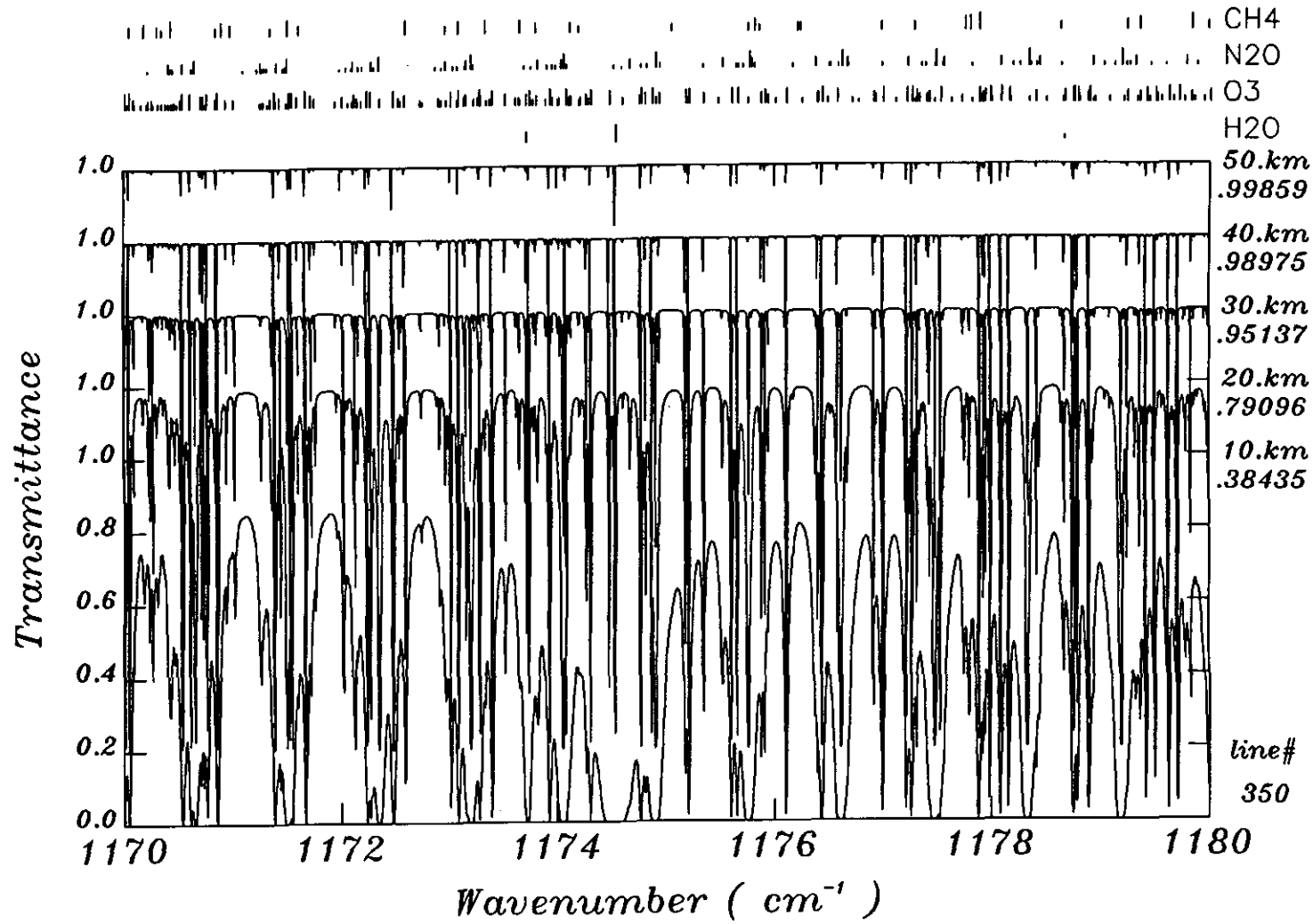


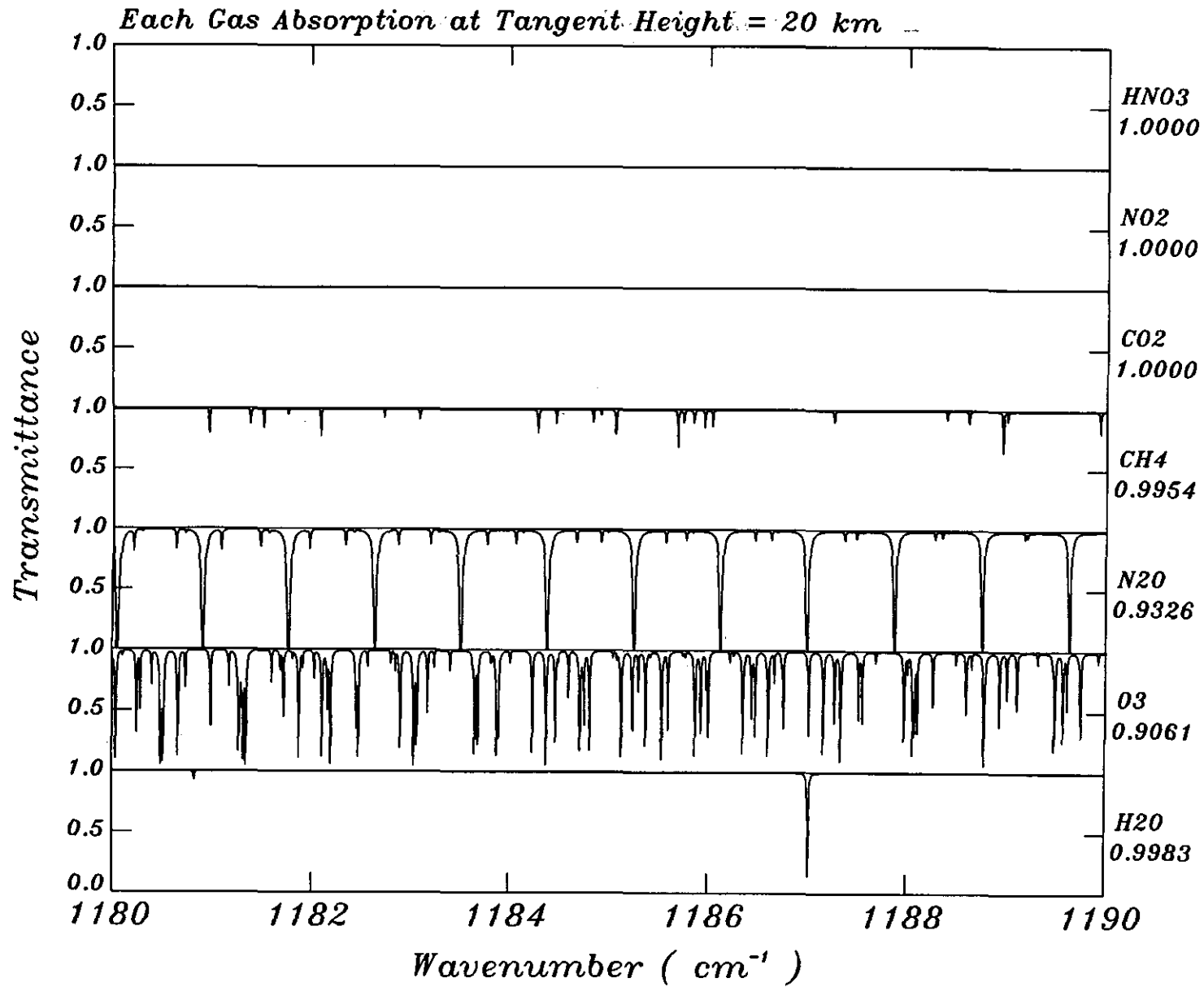


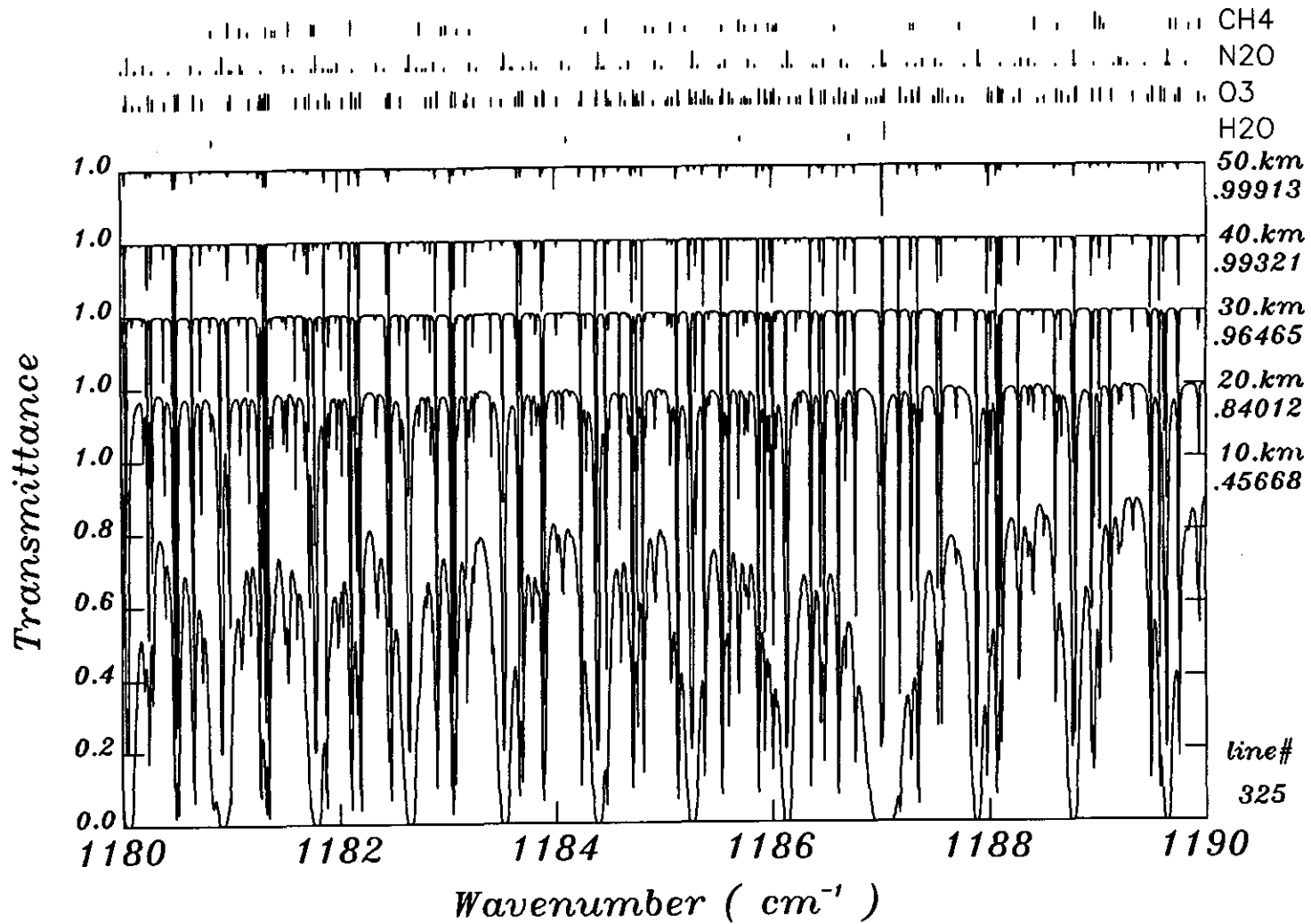


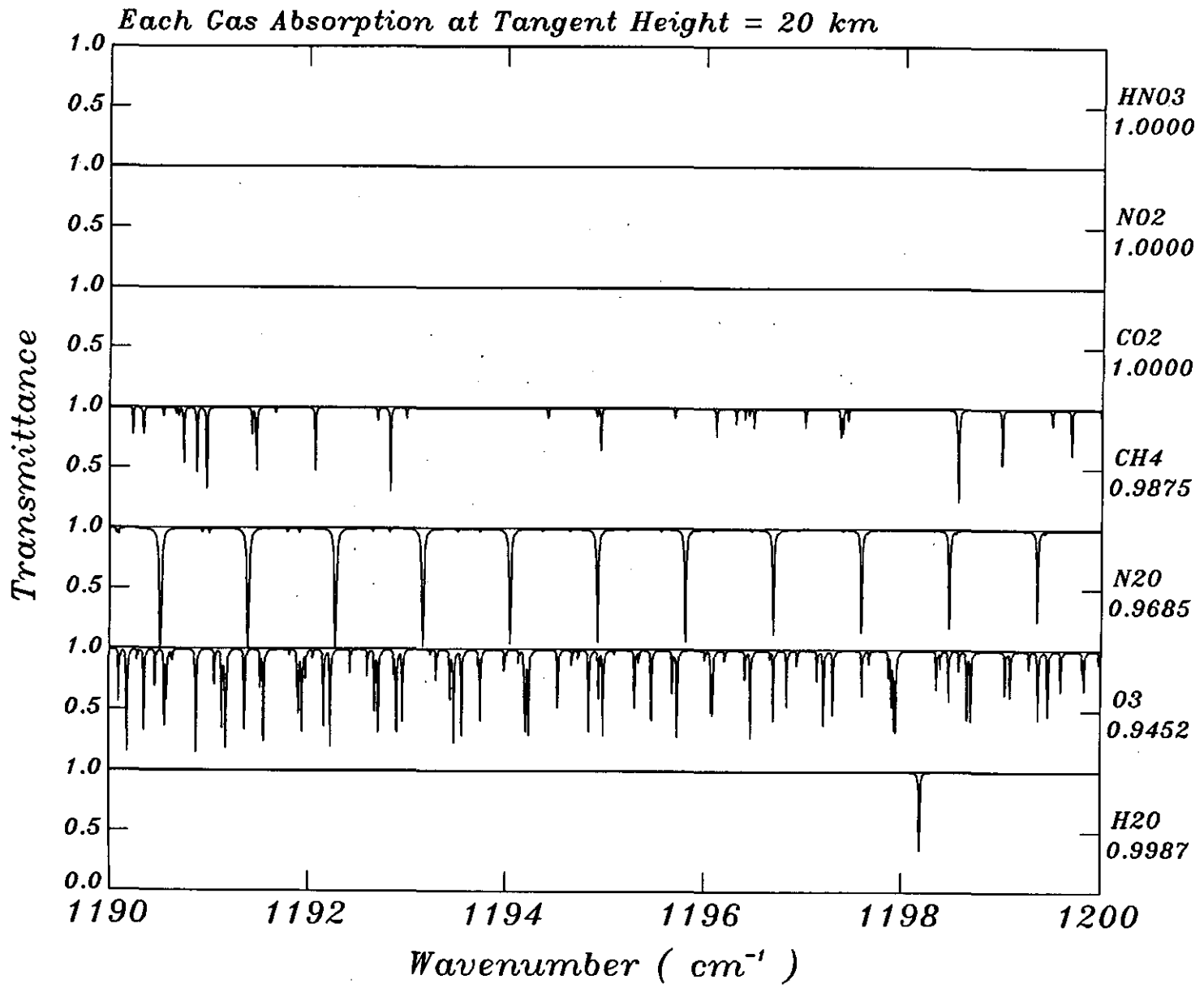


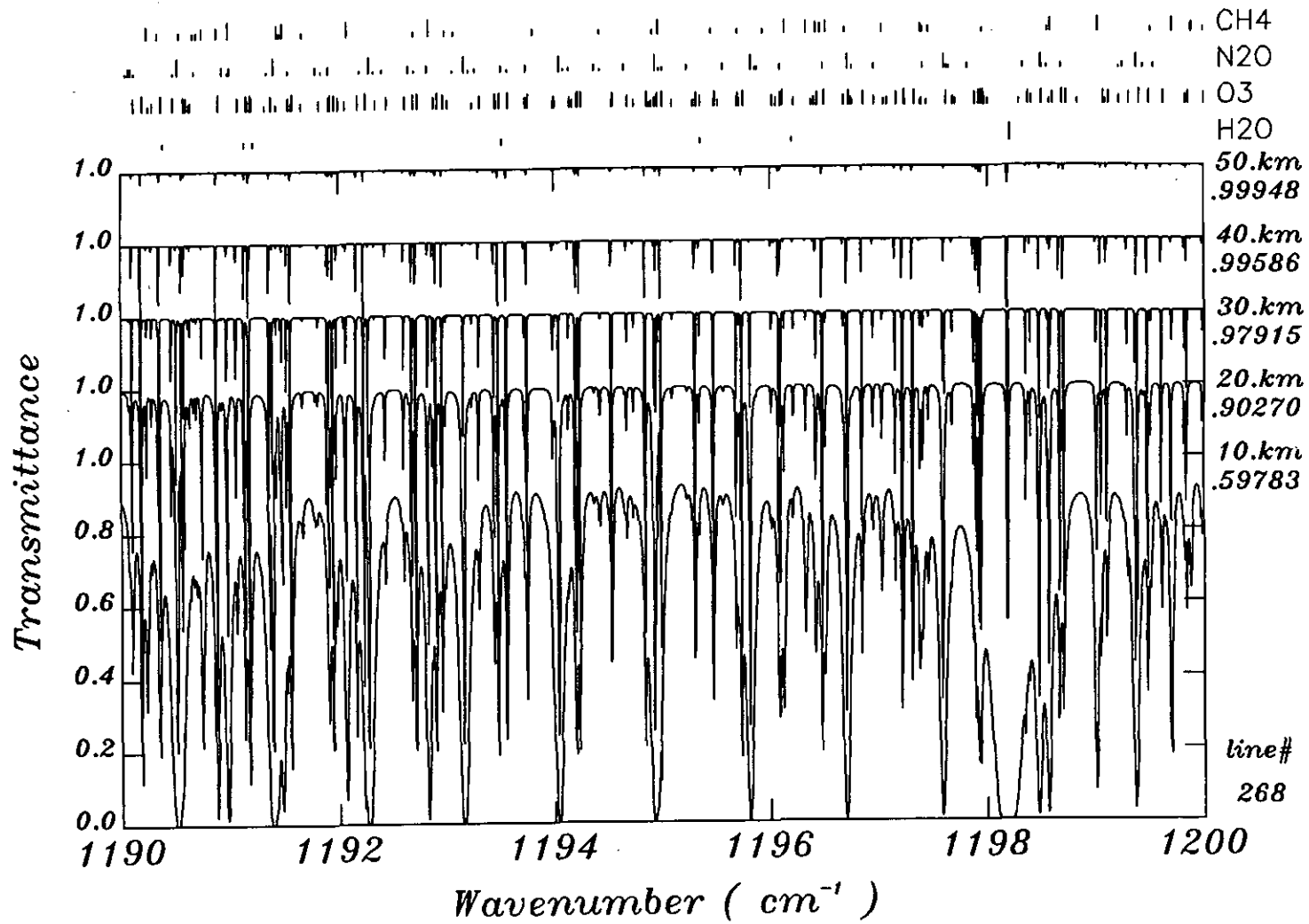




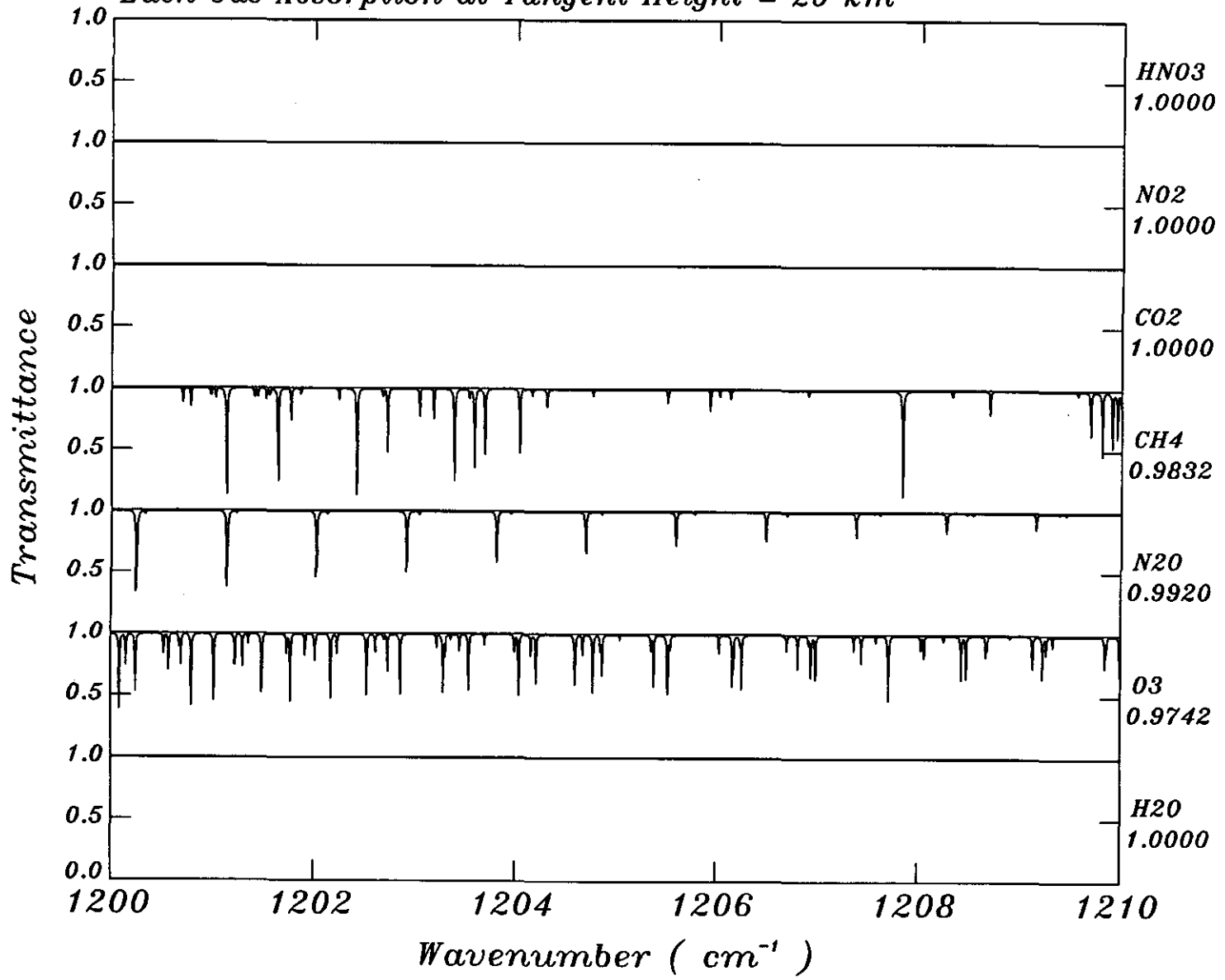


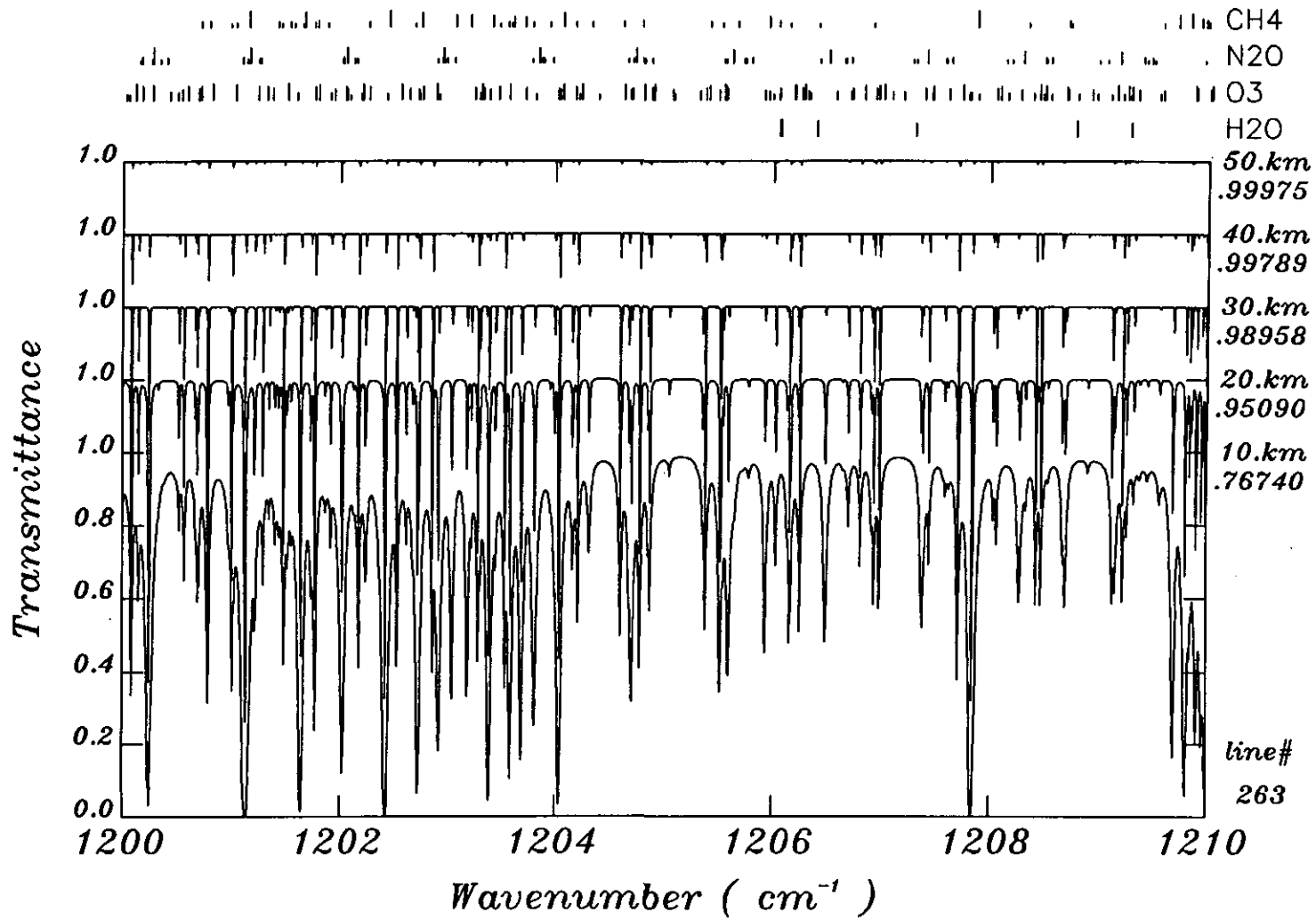




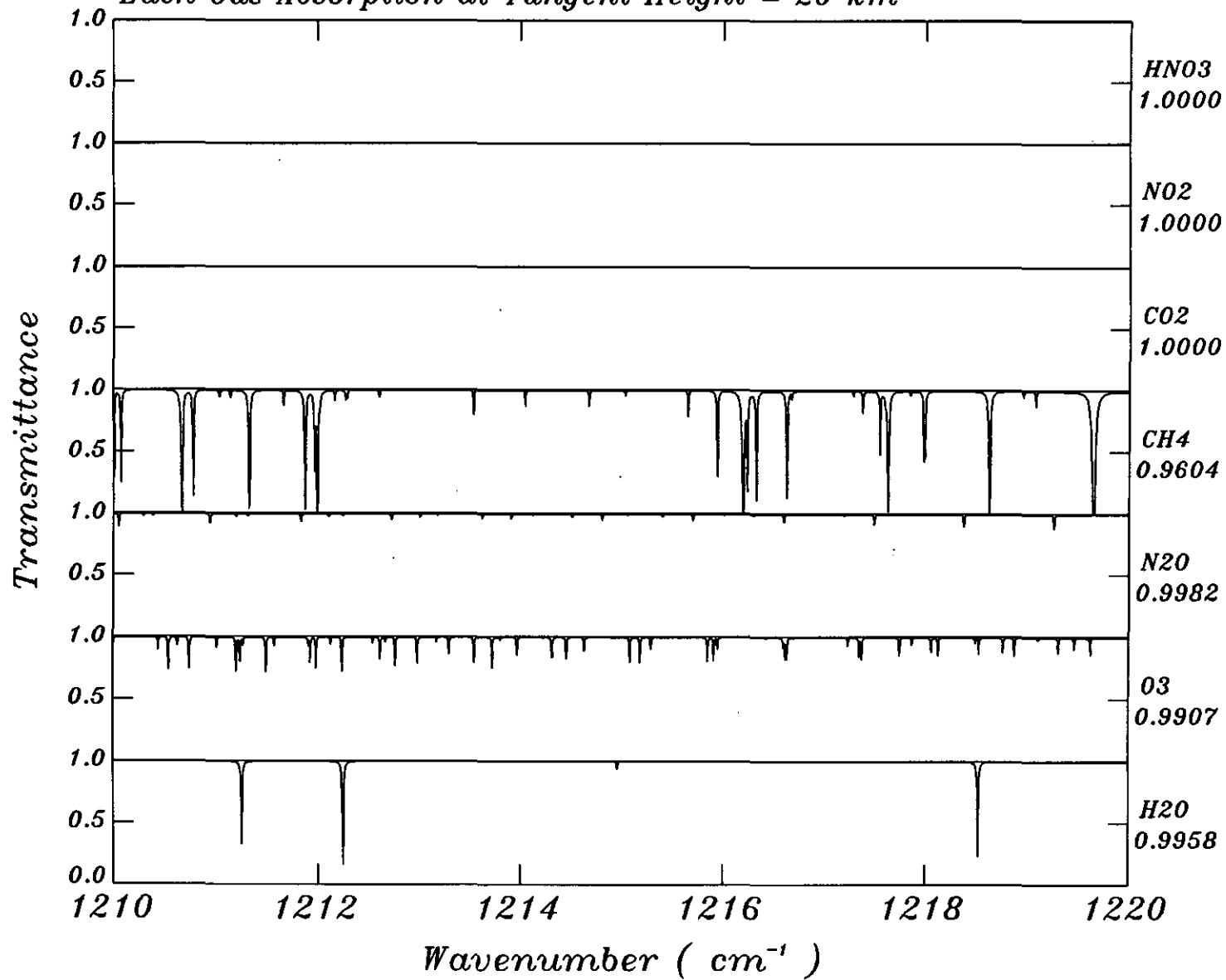


*Each Gas Absorption at Tangent Height = 20 km*

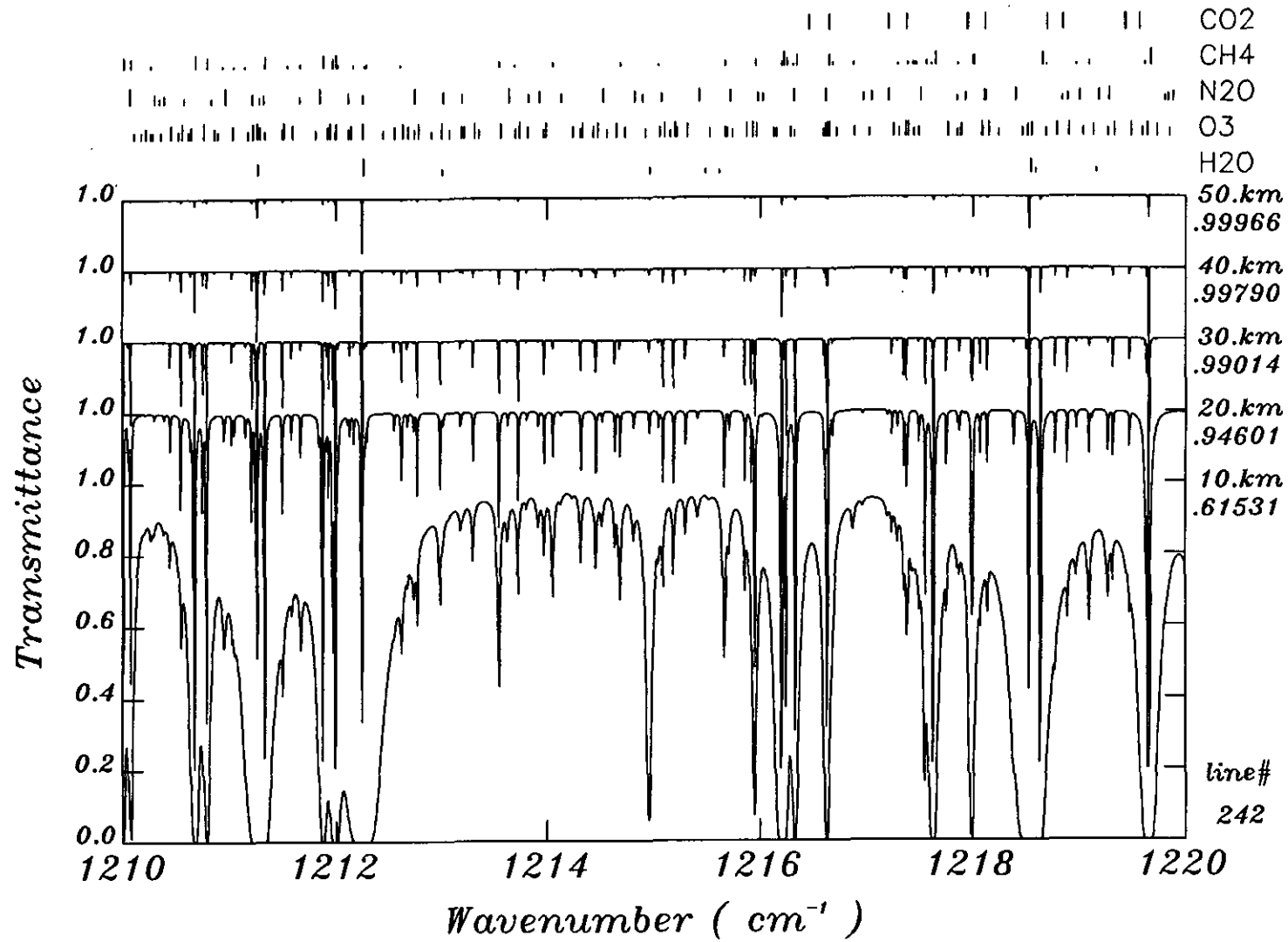


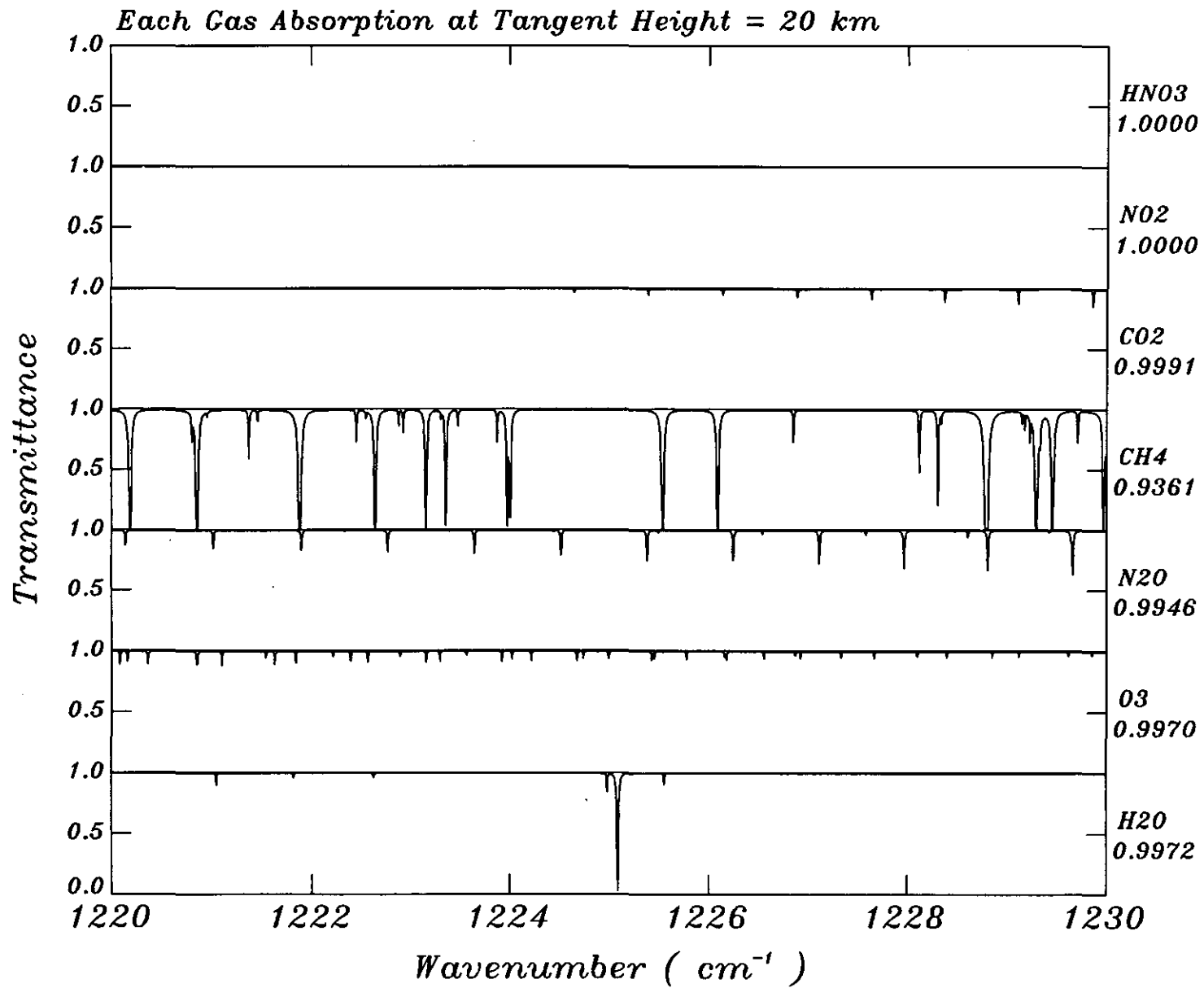


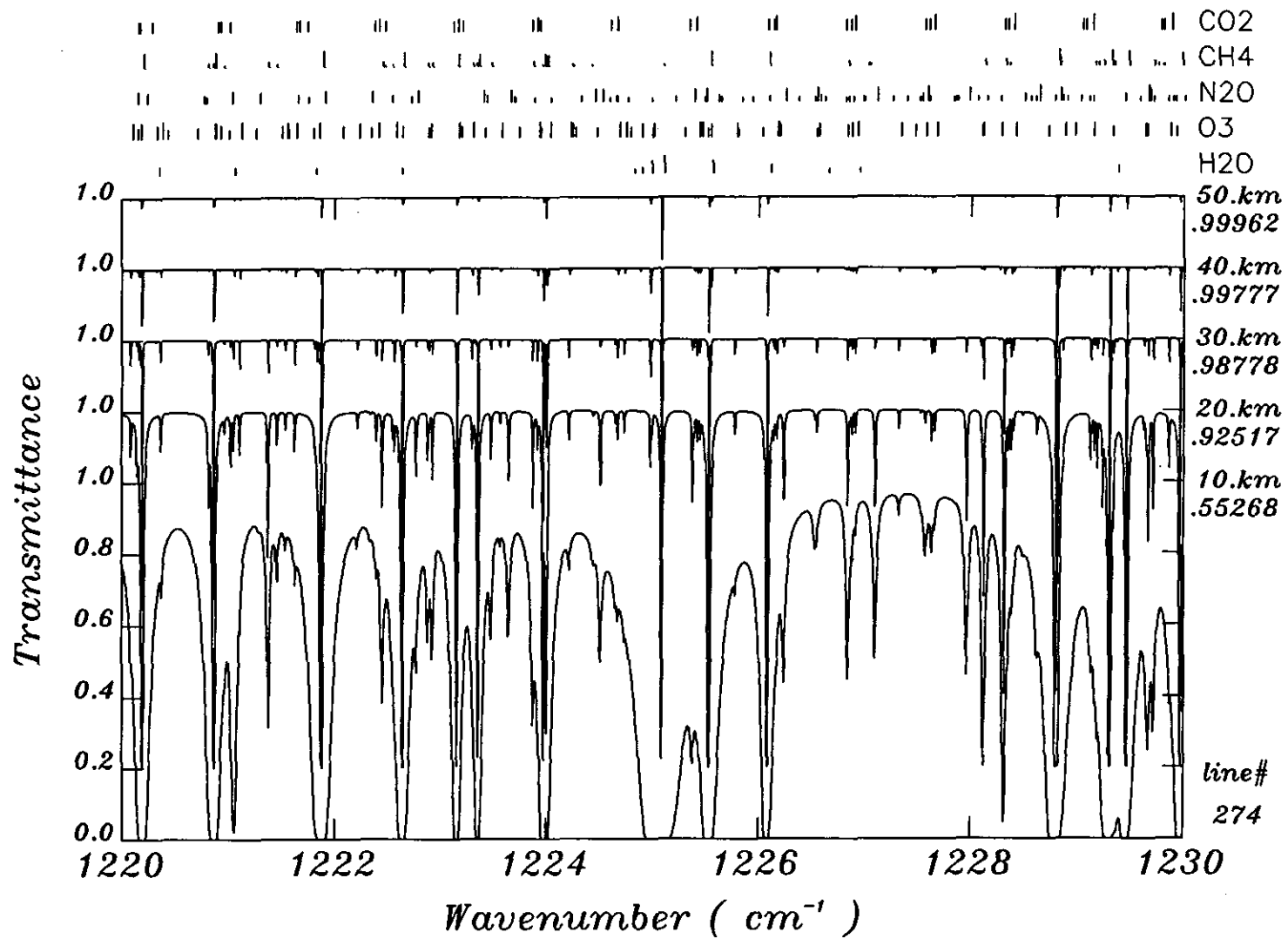
Each Gas Absorption at Tangent Height = 20 km

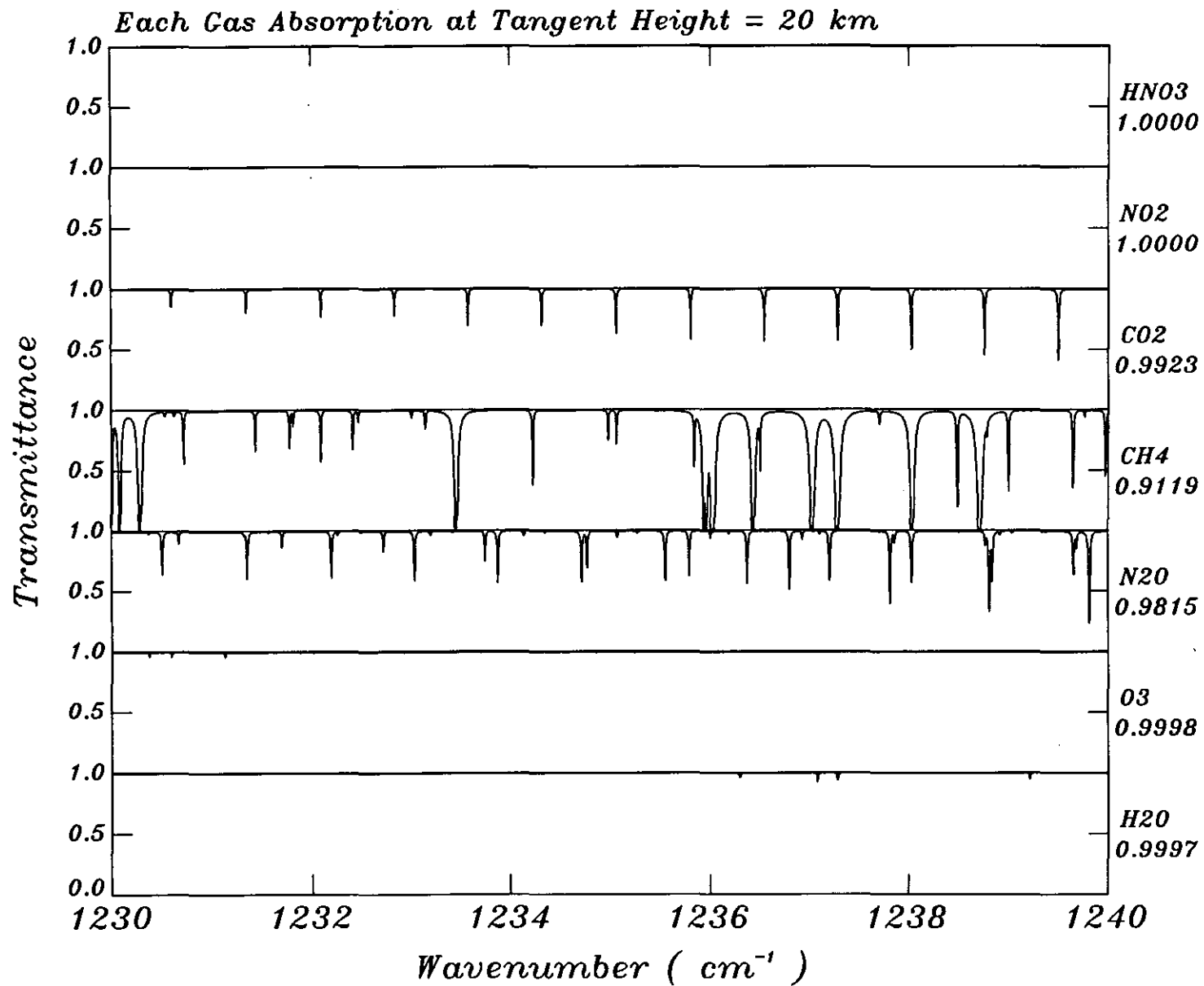


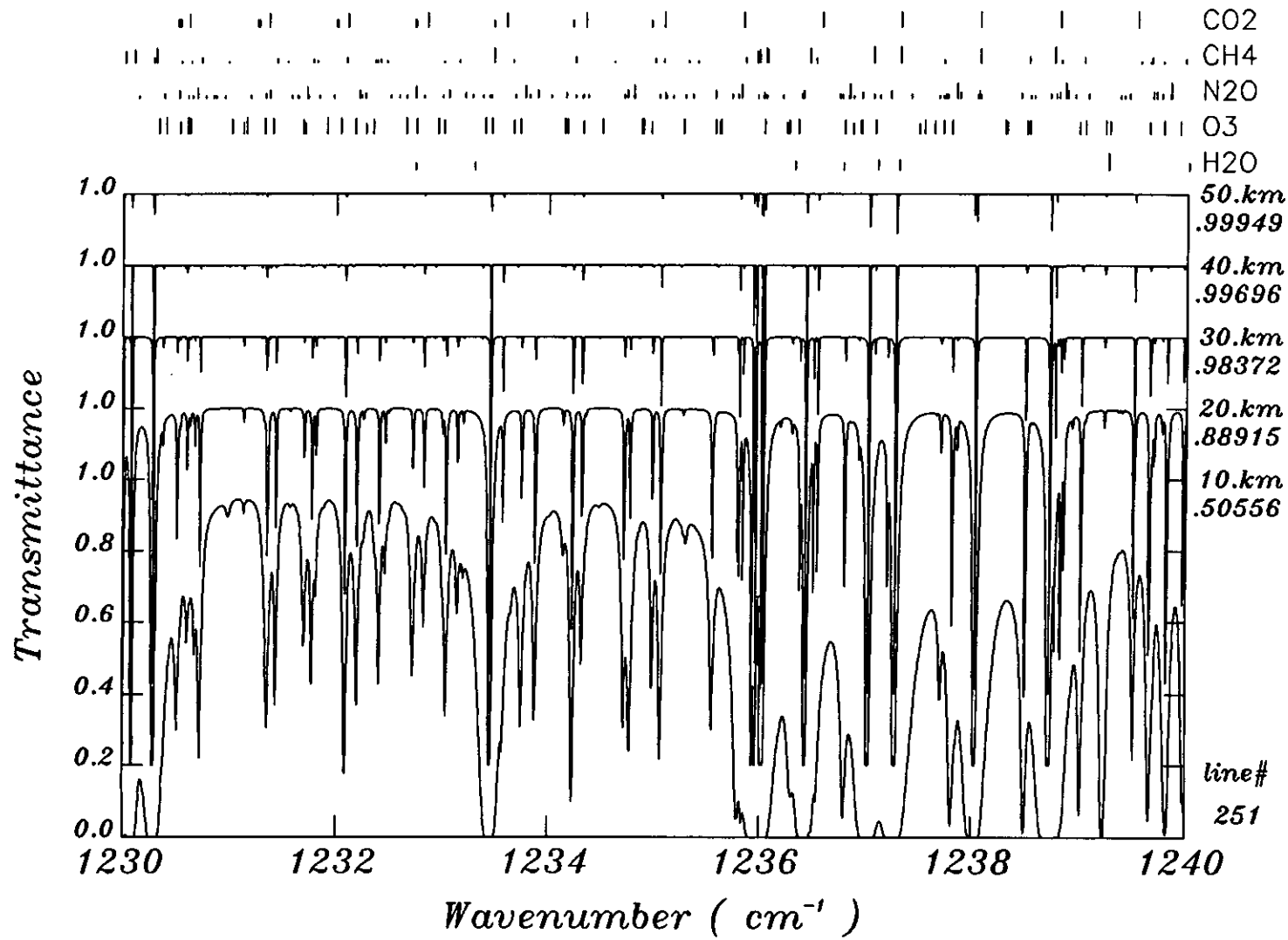




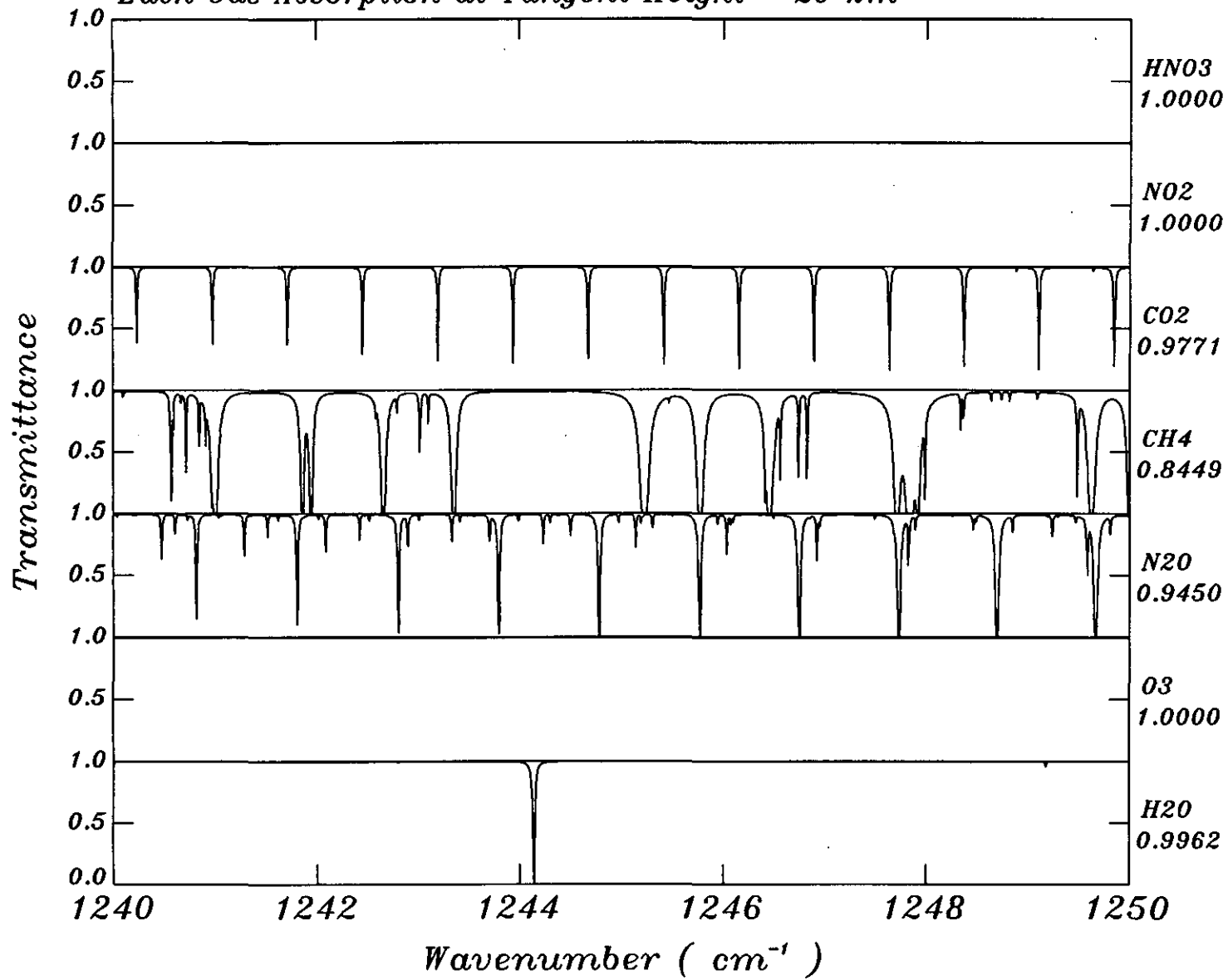


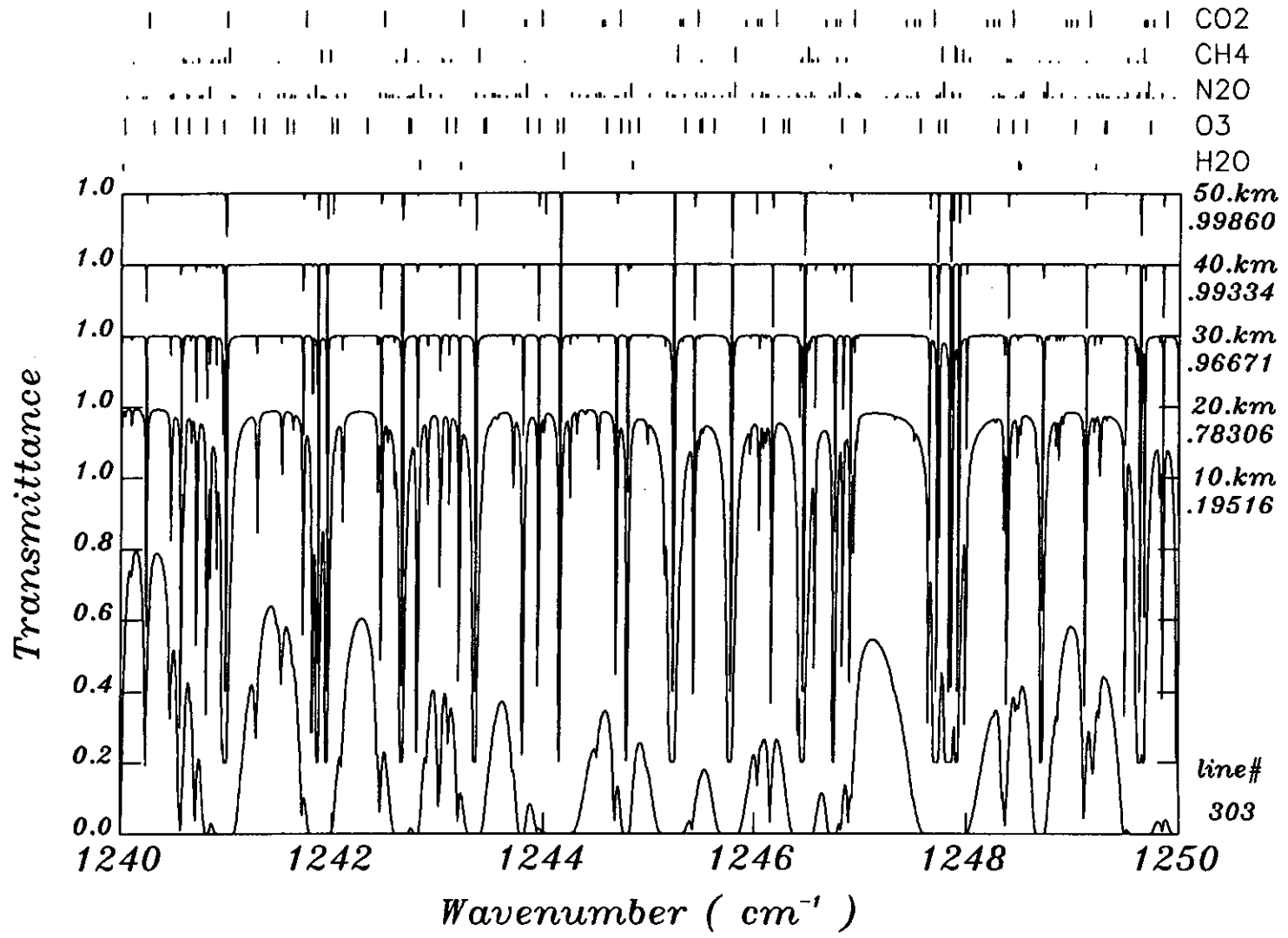




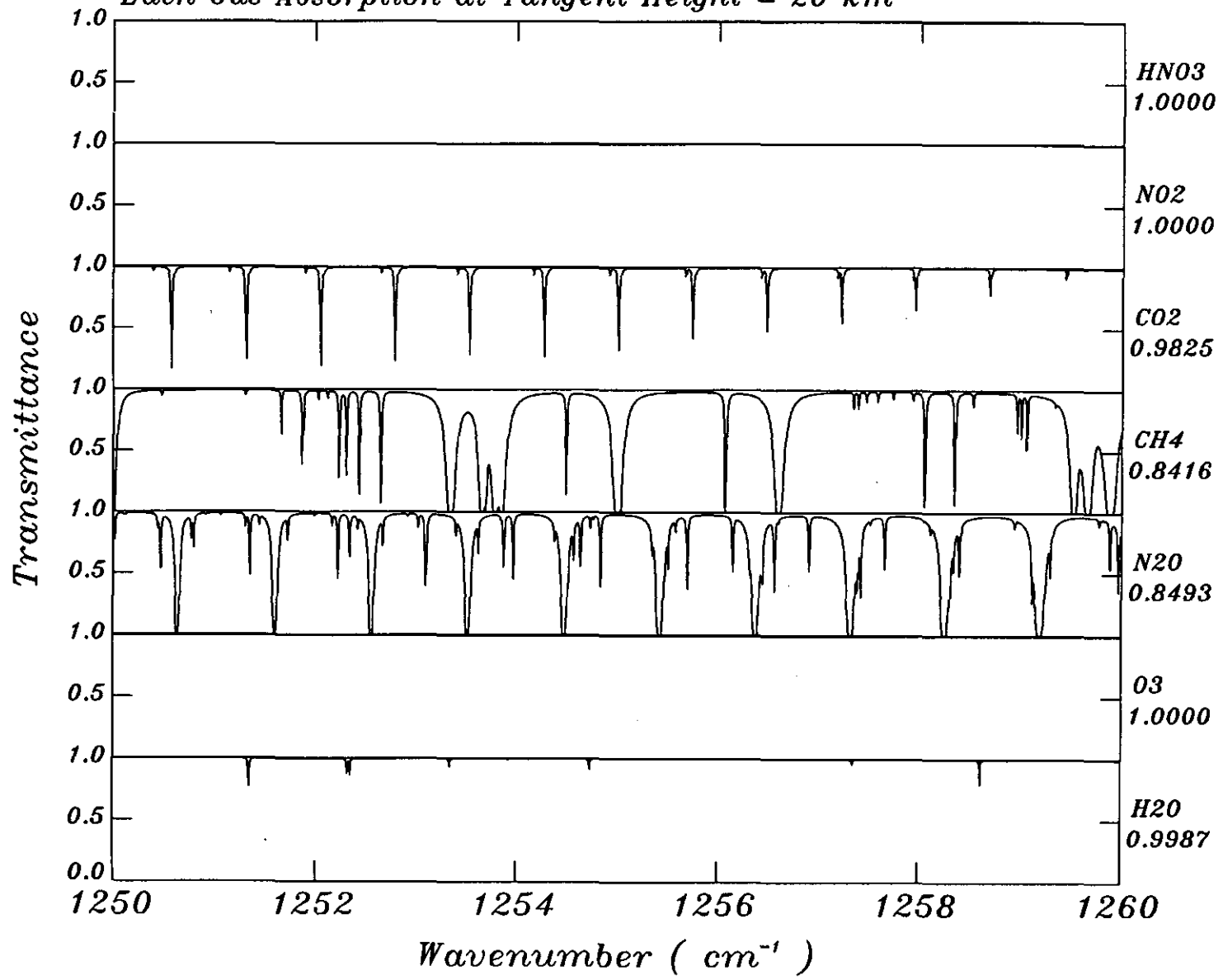


Each Gas Absorption at Tangent Height = 20 km

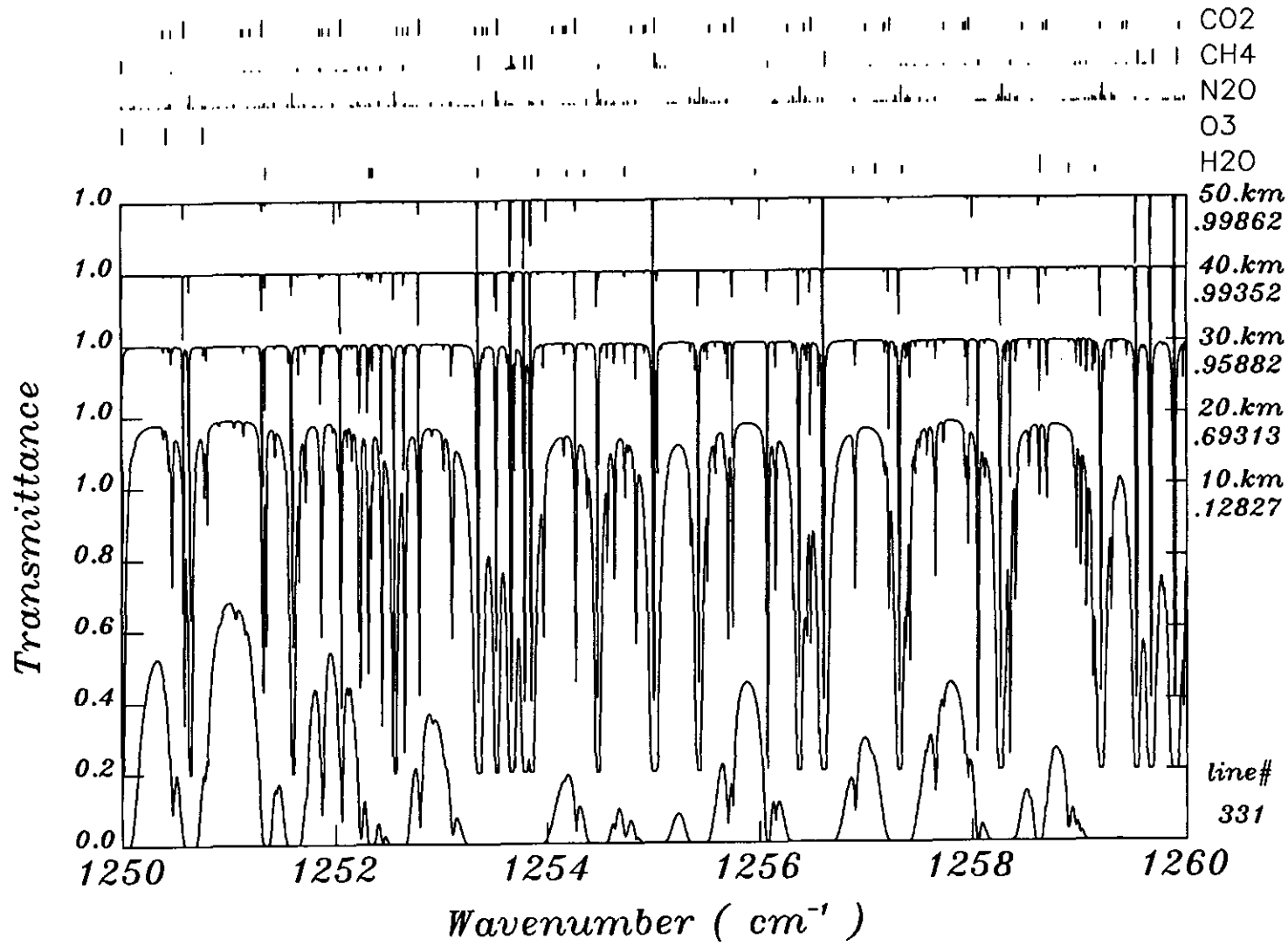




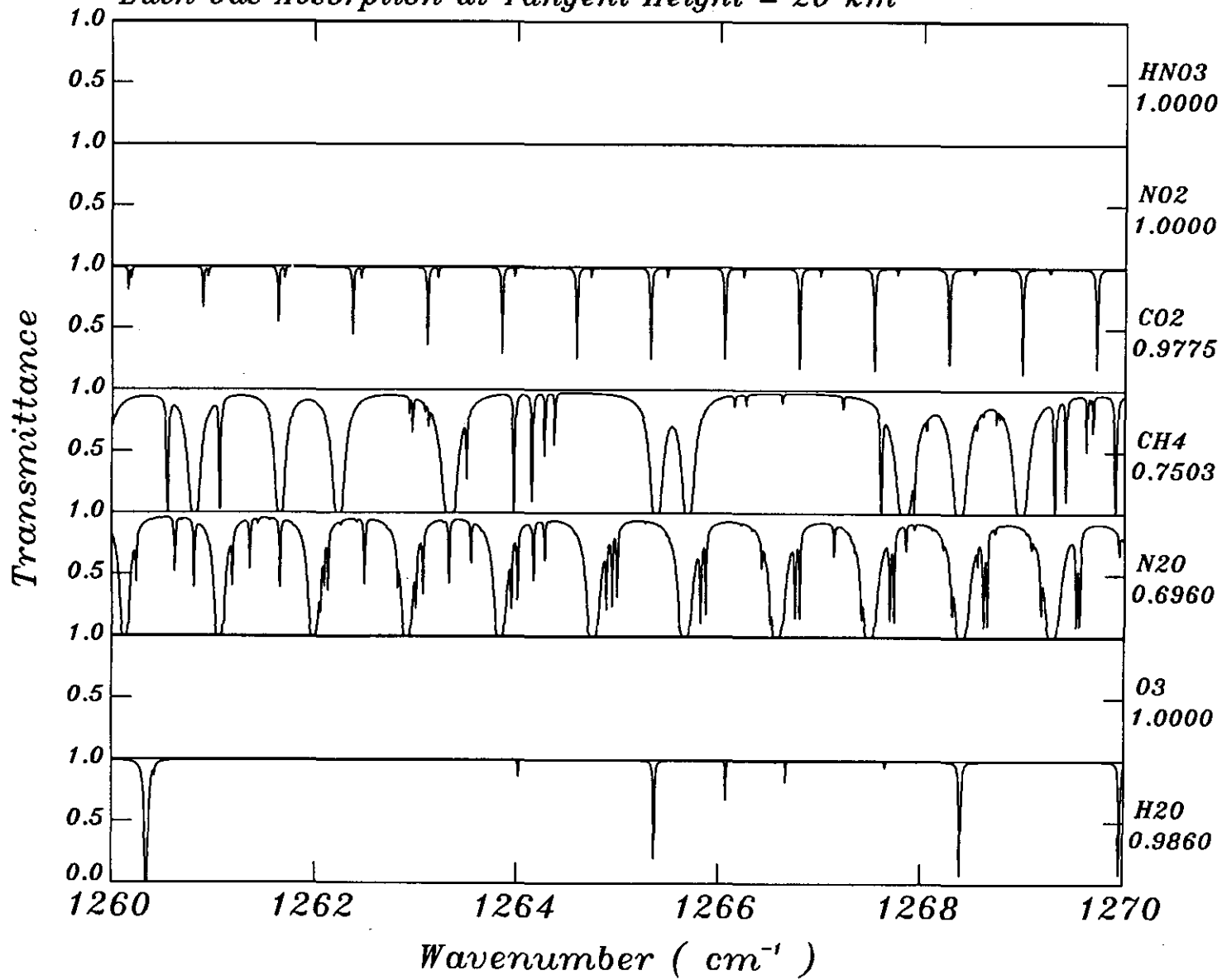
Each Gas Absorption at Tangent Height = 20 km



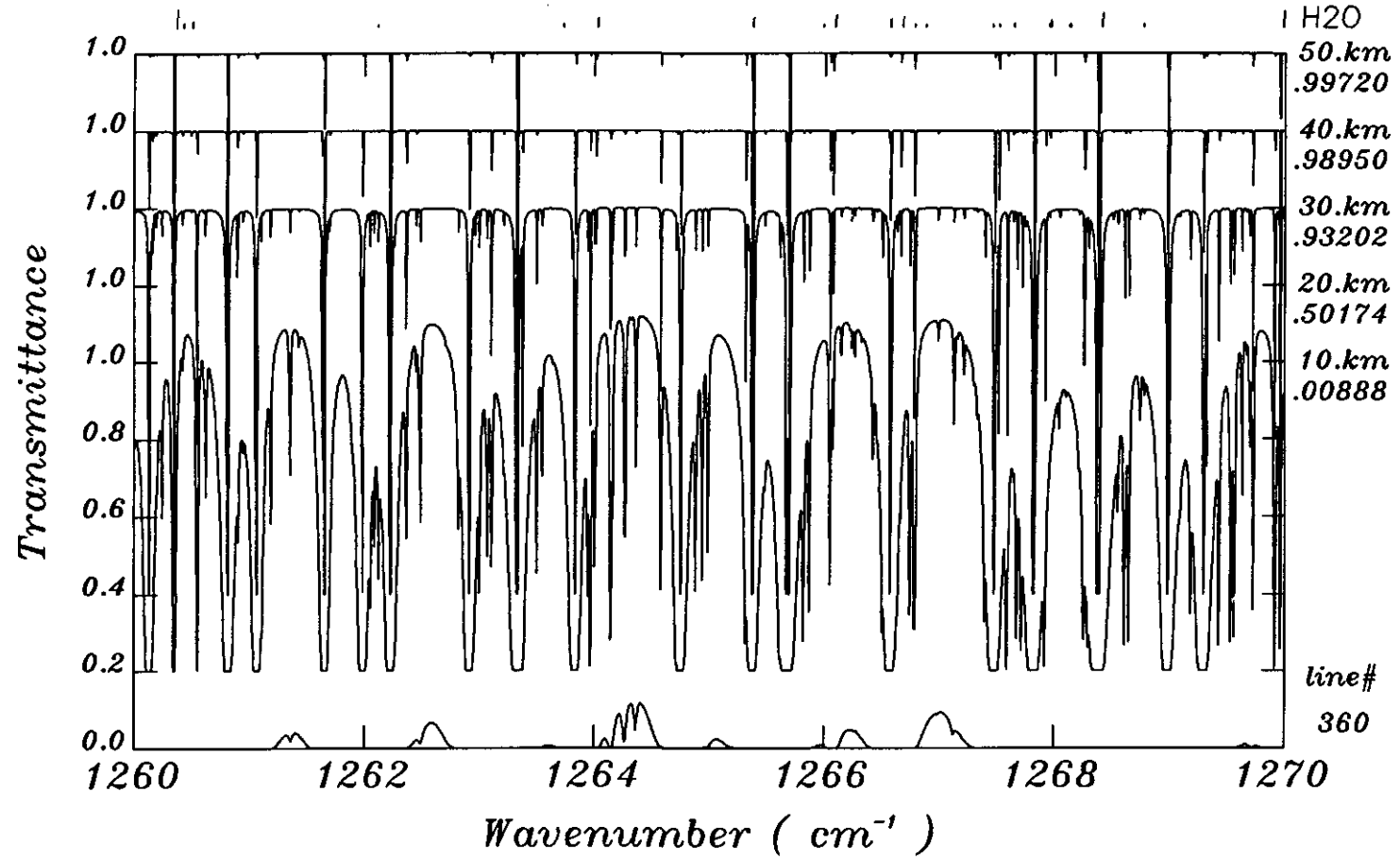


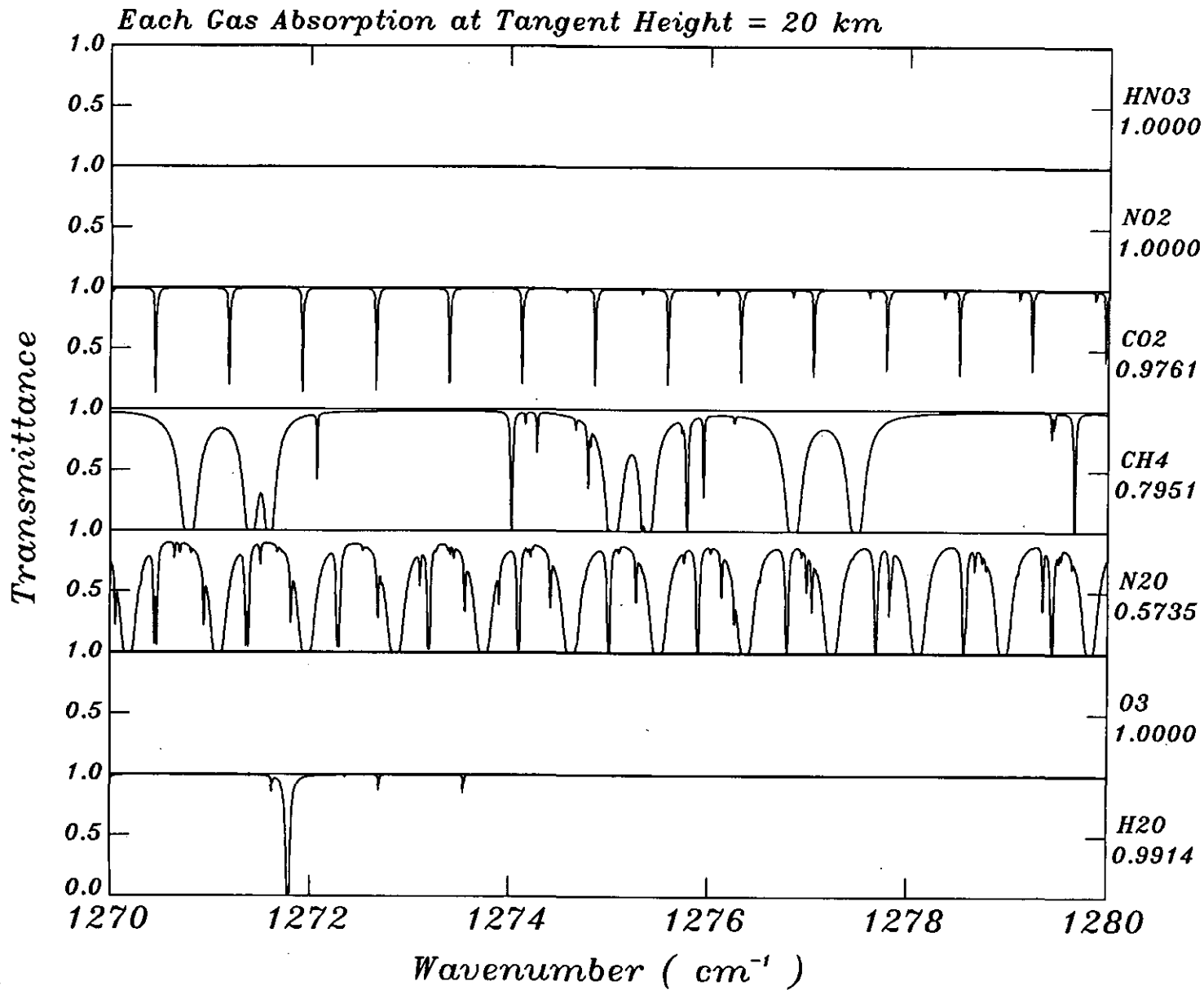


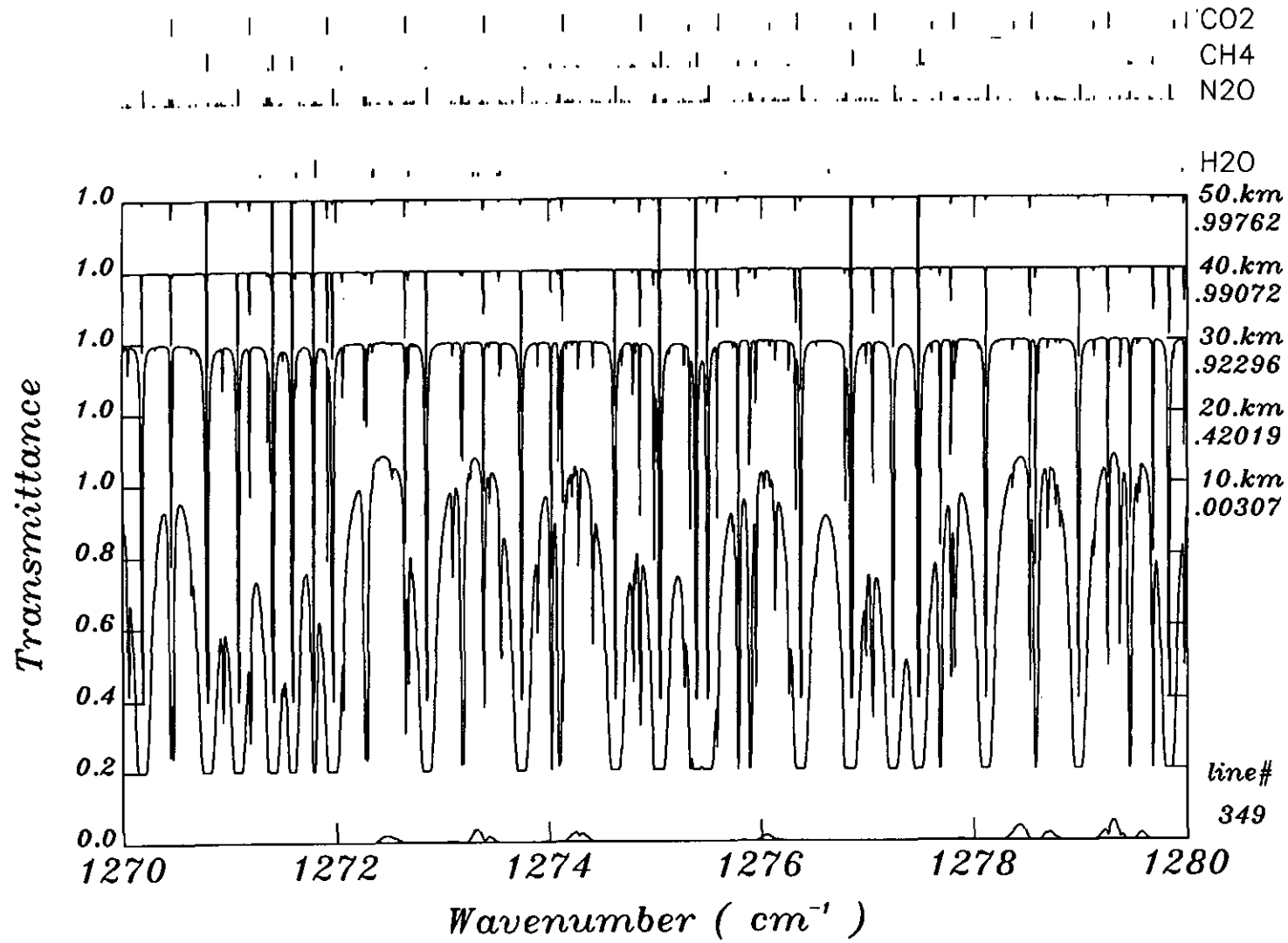
Each Gas Absorption at Tangent Height = 20 km

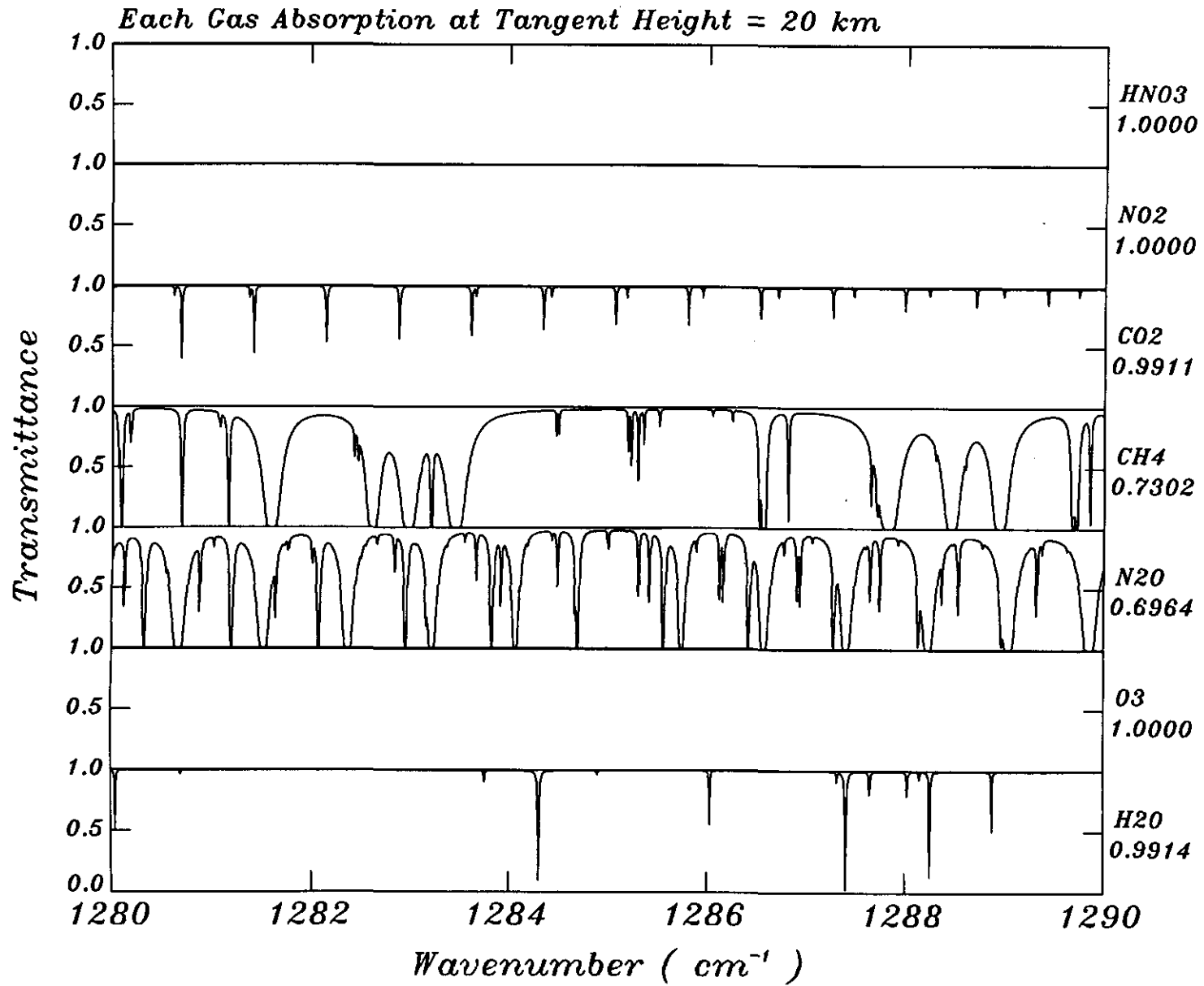


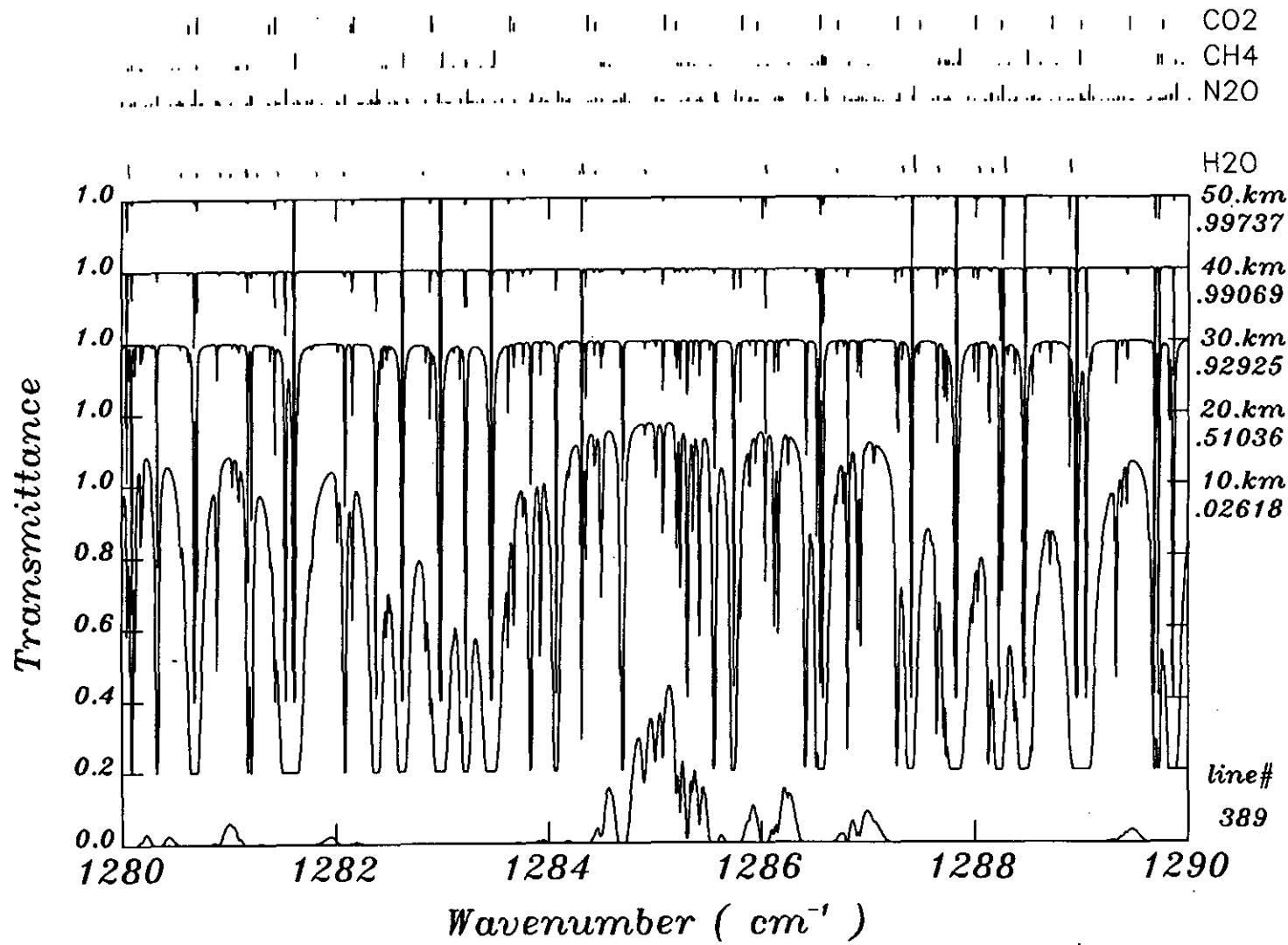
CO2  
CH4  
N2O



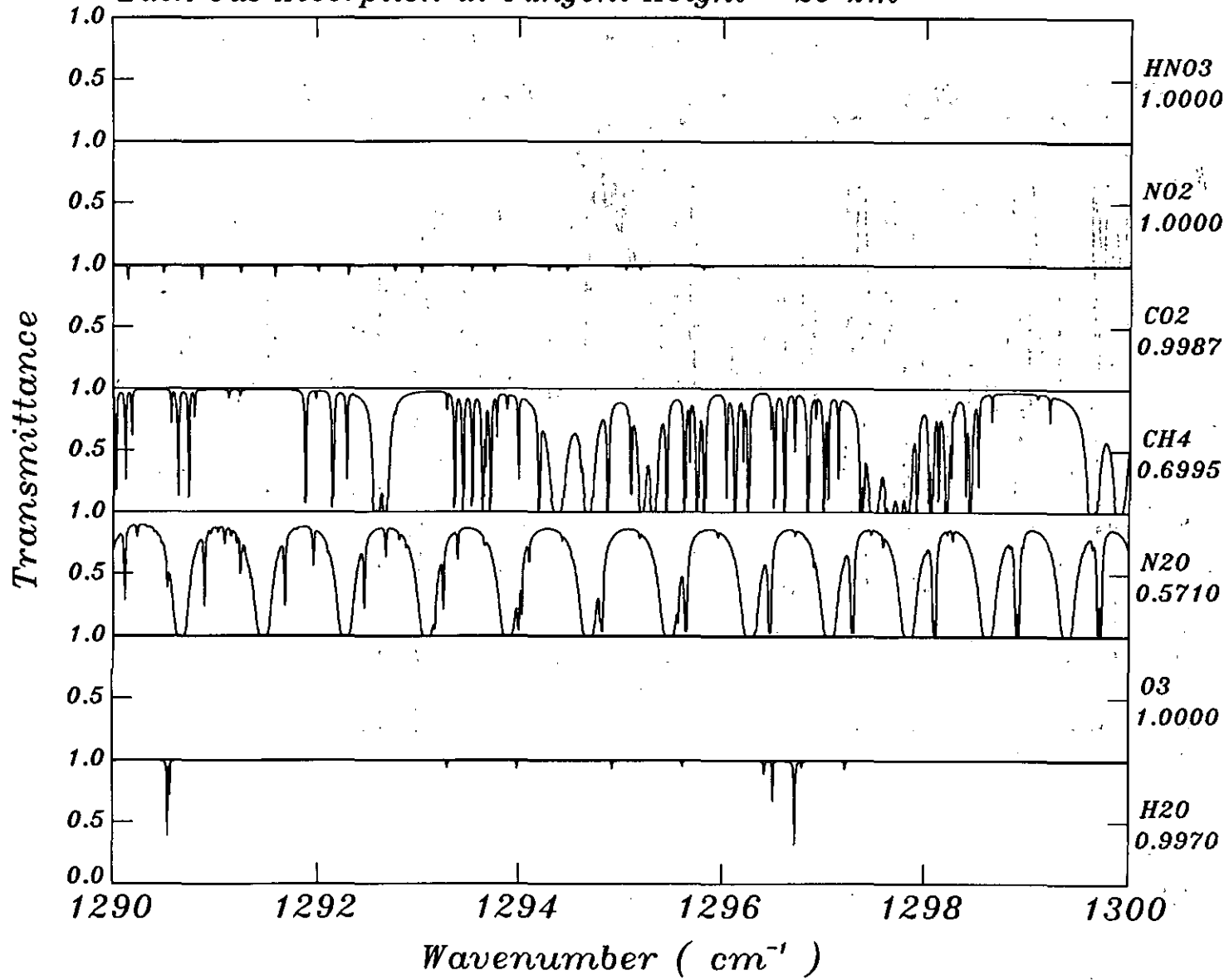




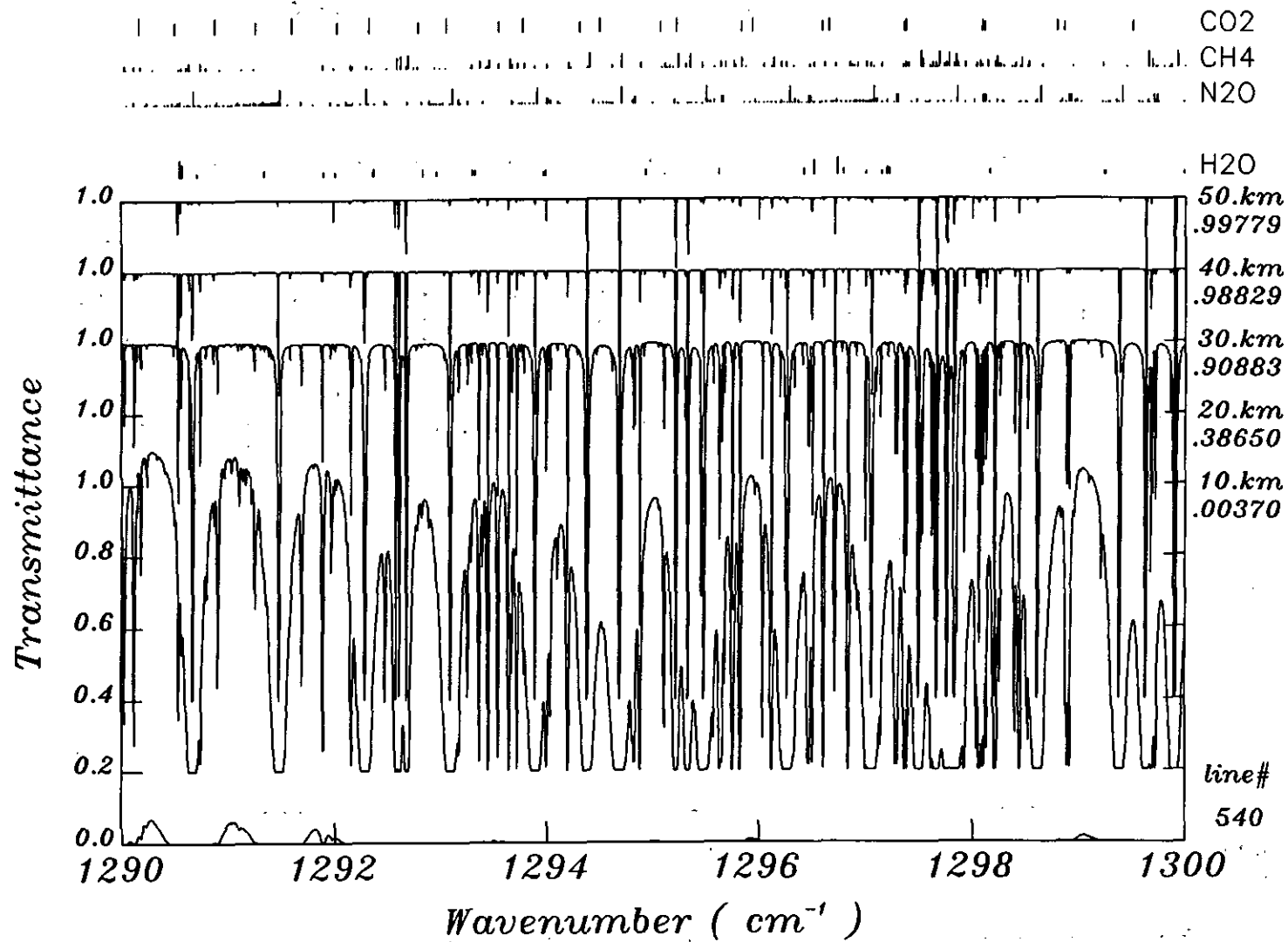




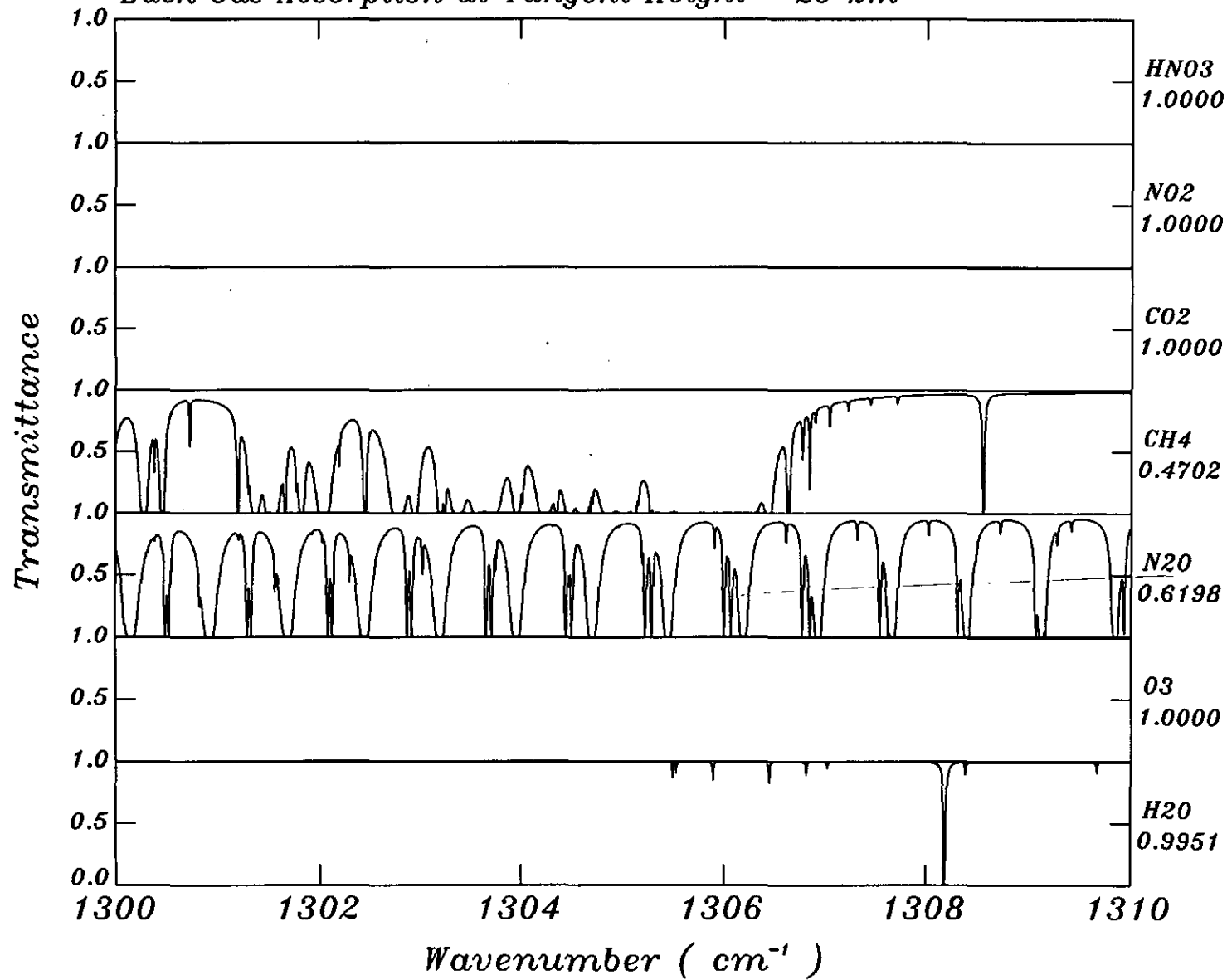
Each Gas Absorption at Tangent Height = 20 km

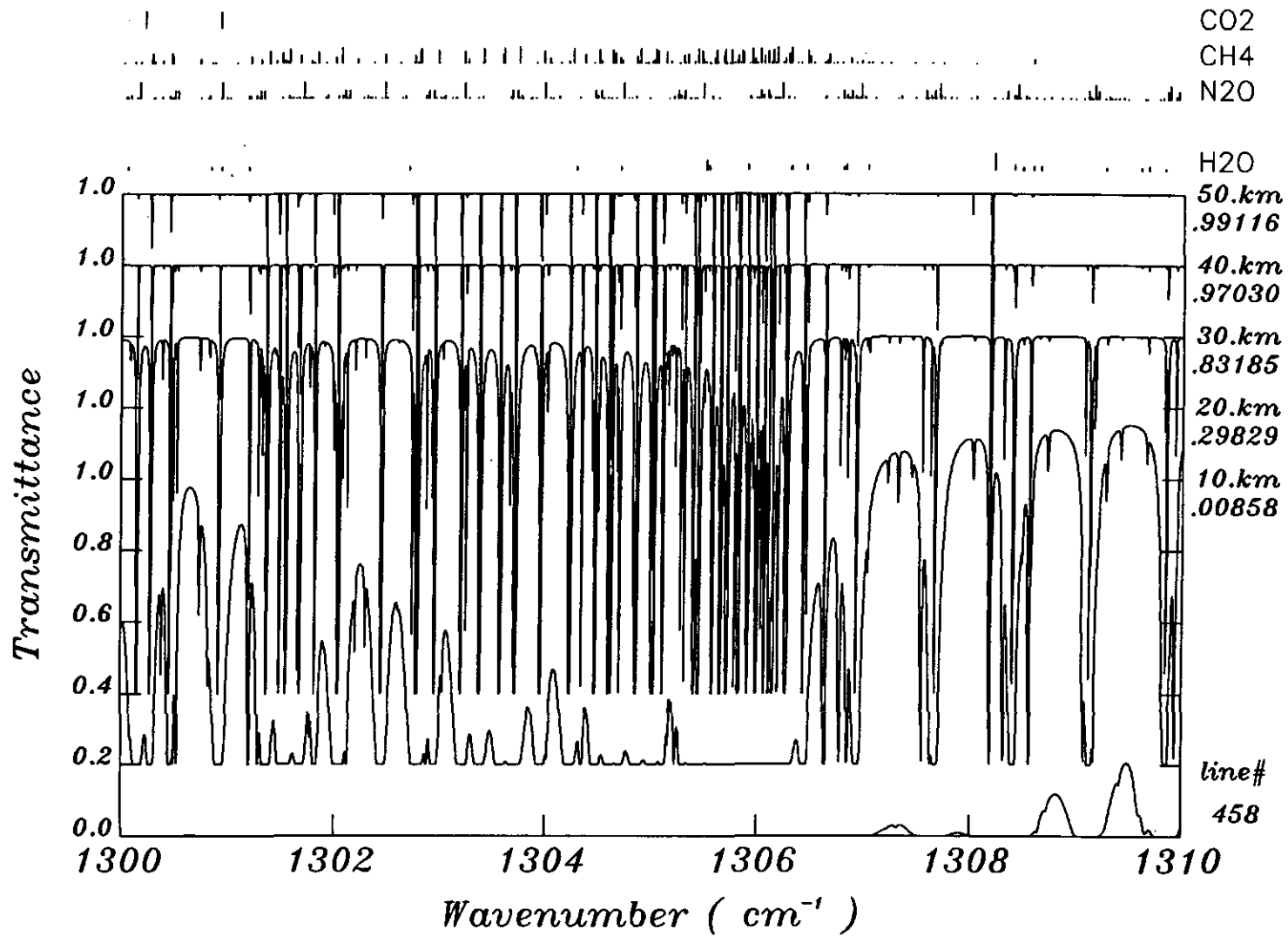


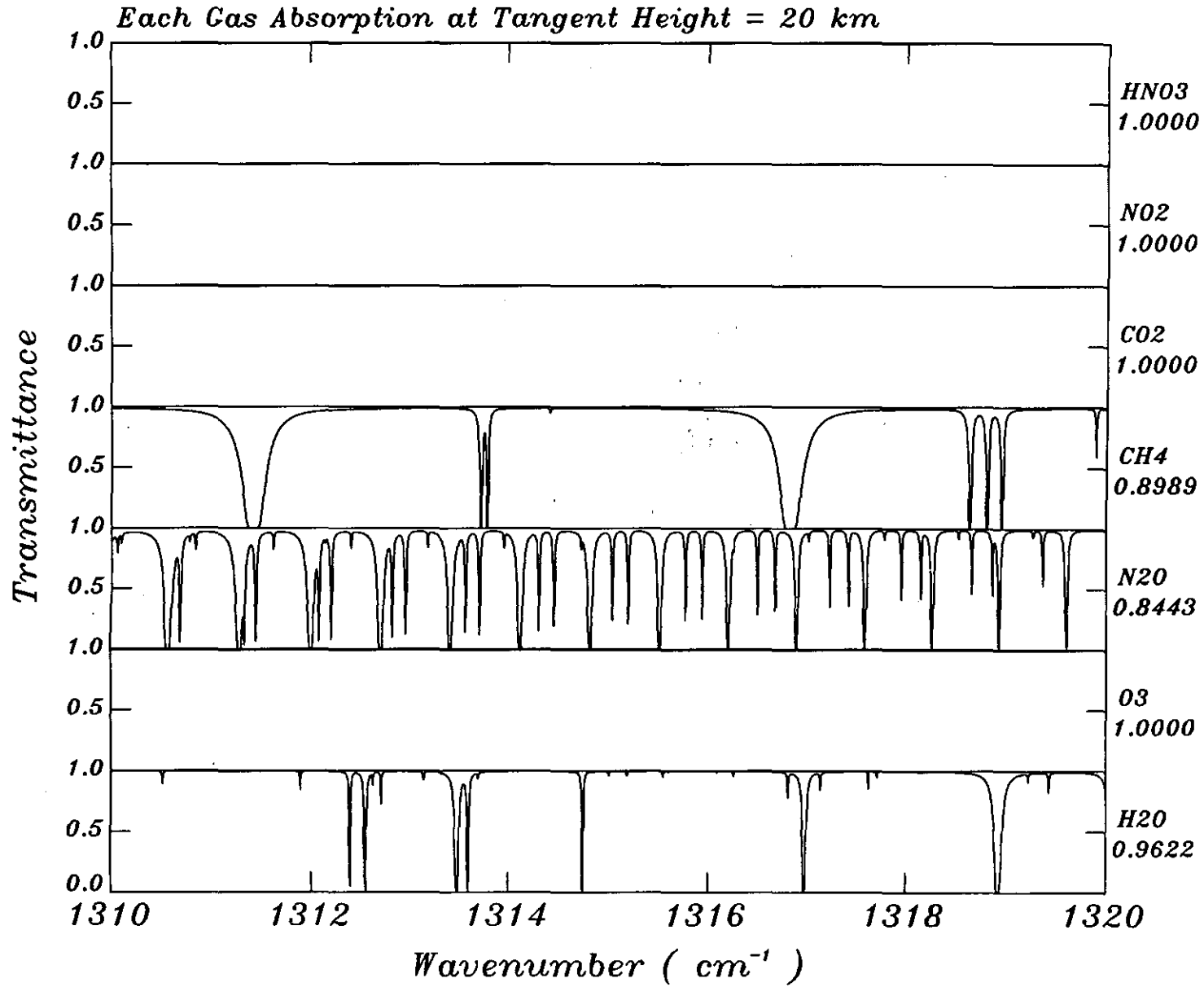


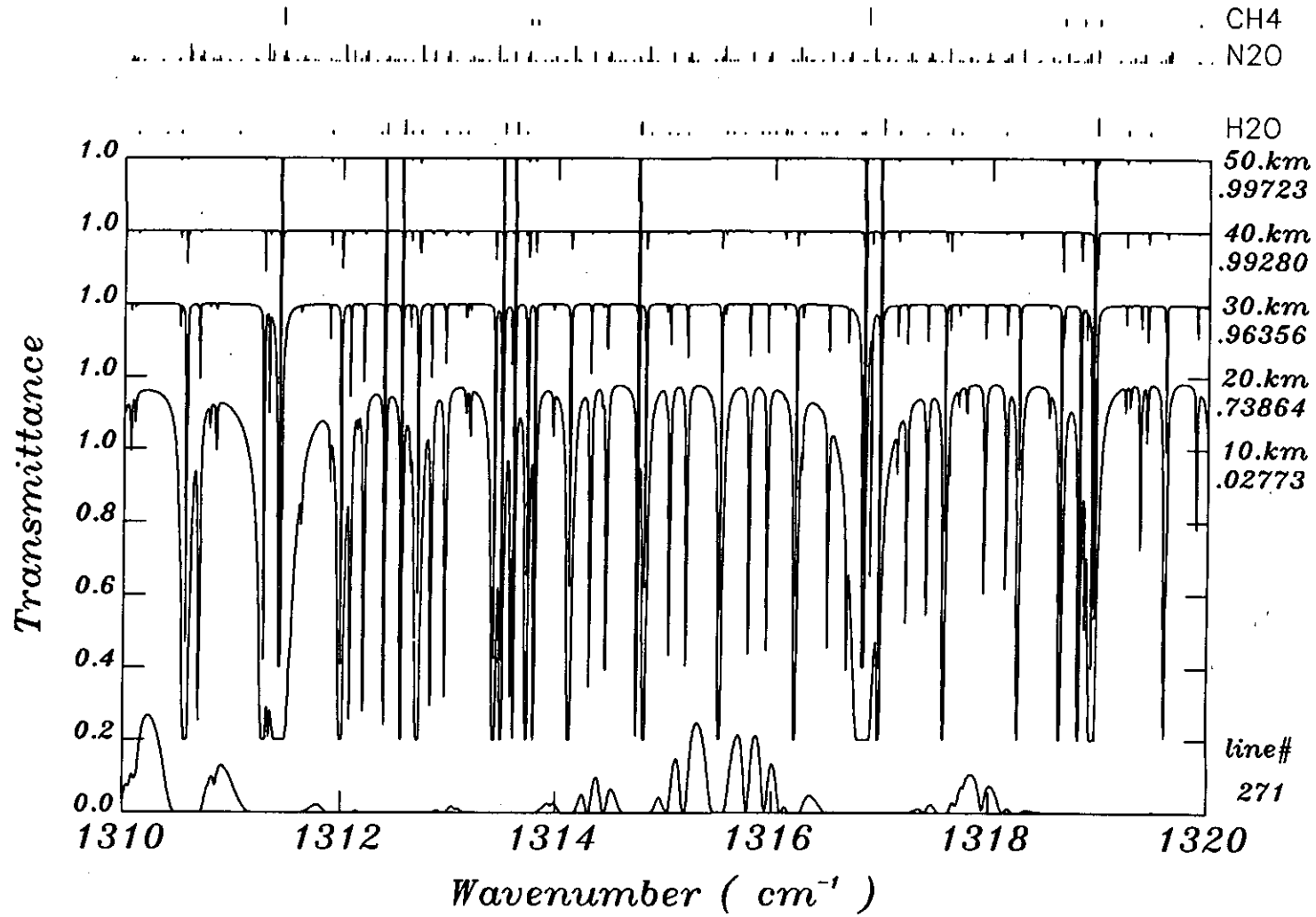


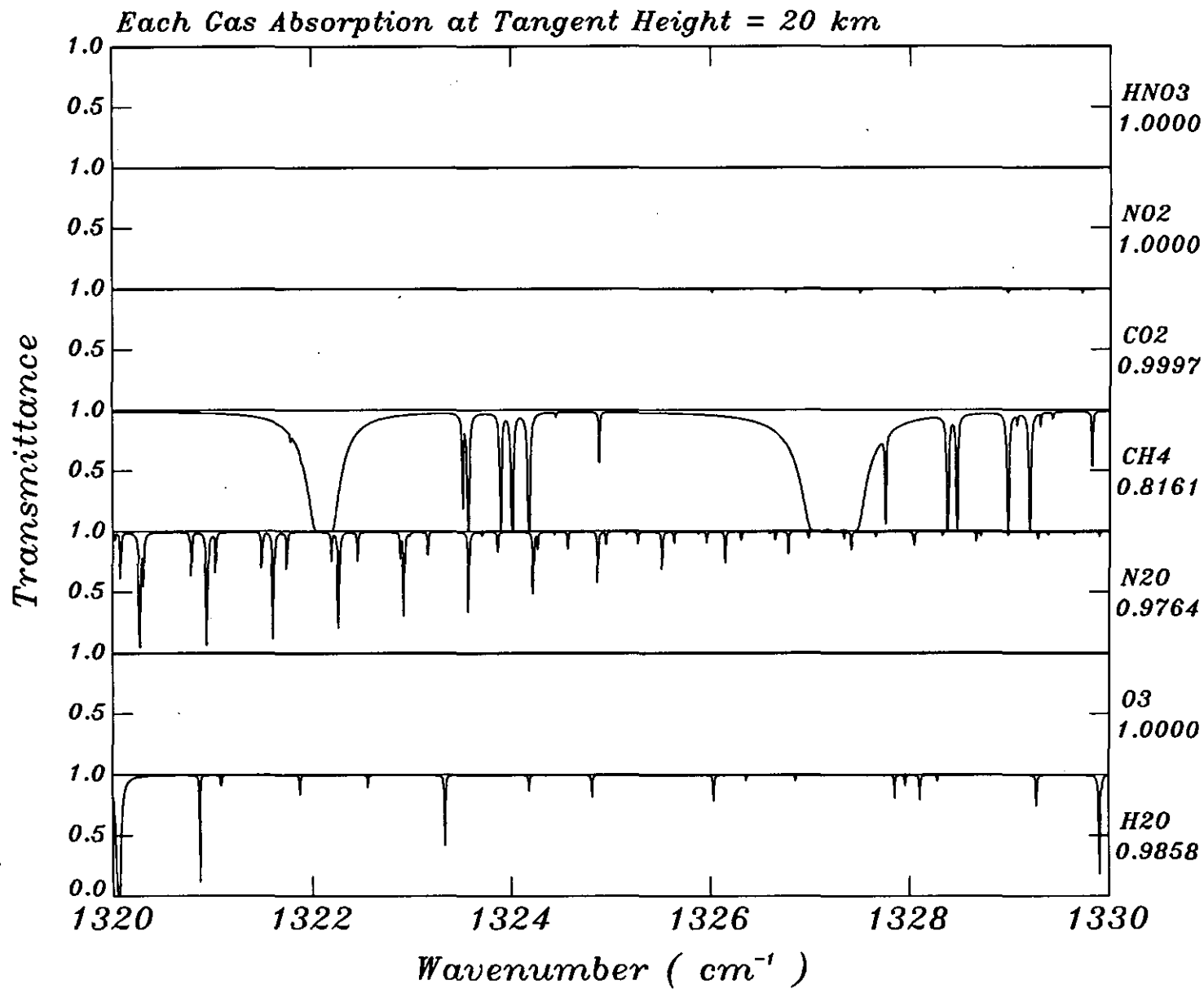
Each Gas Absorption at Tangent Height = 20 km

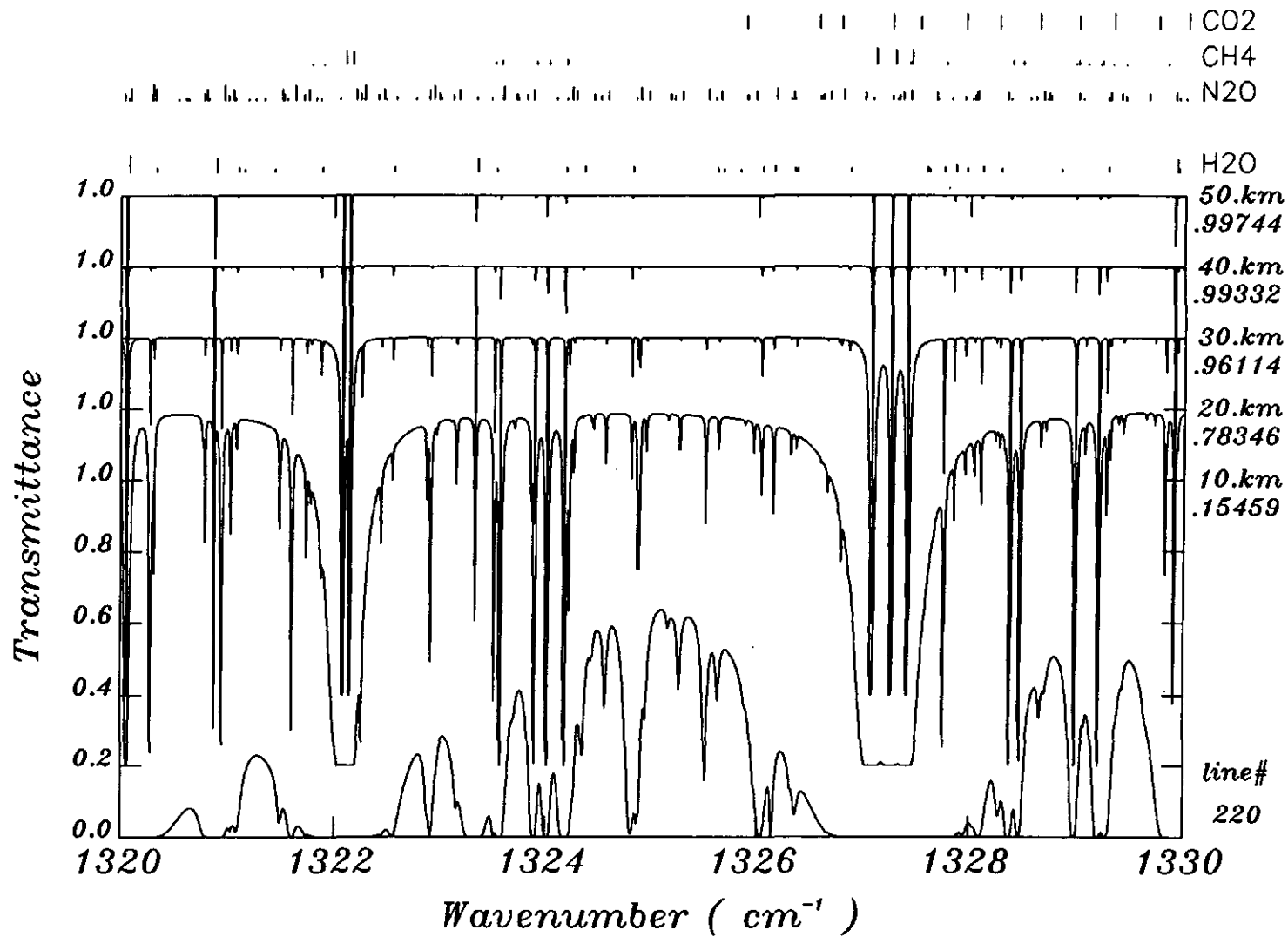


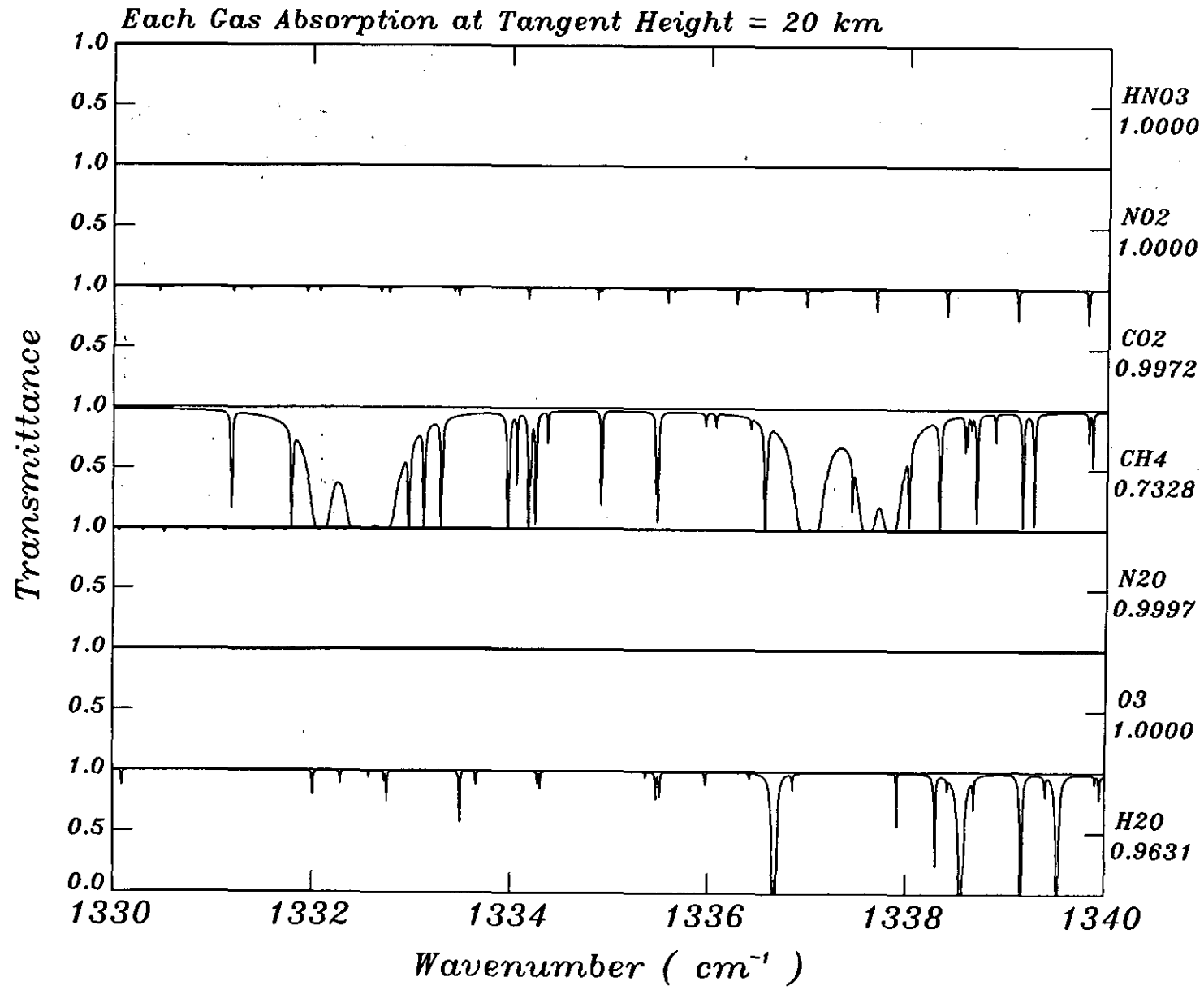




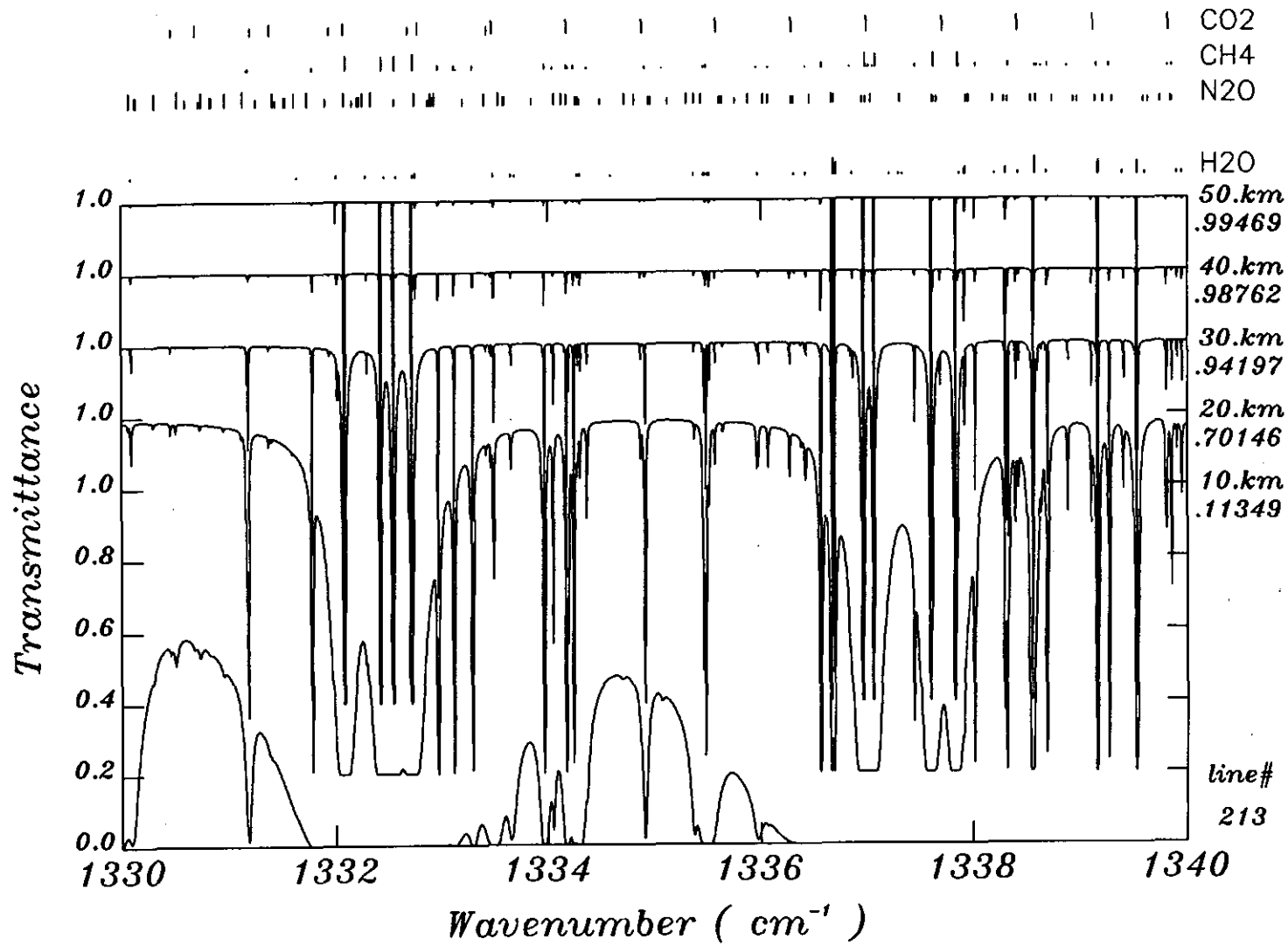




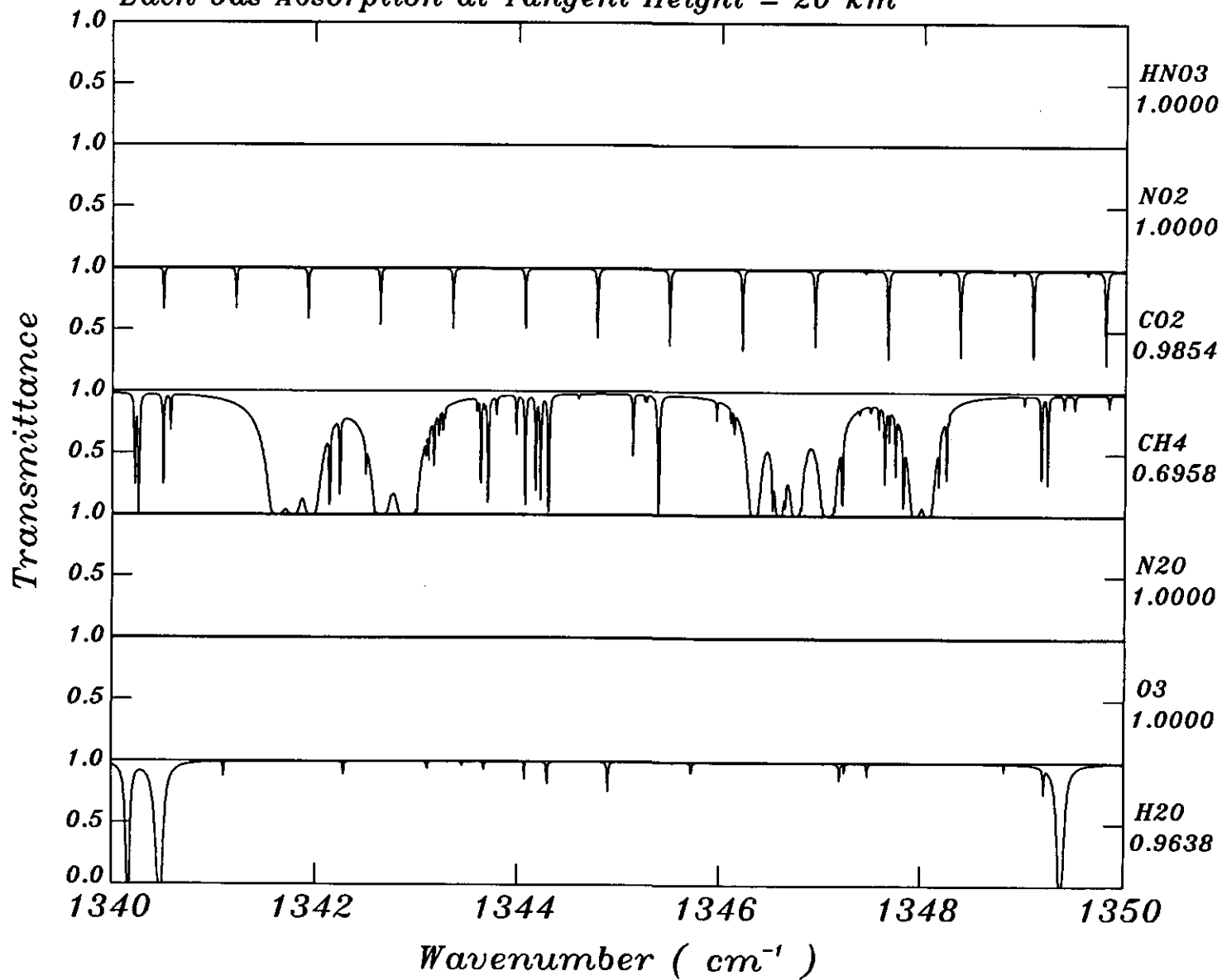


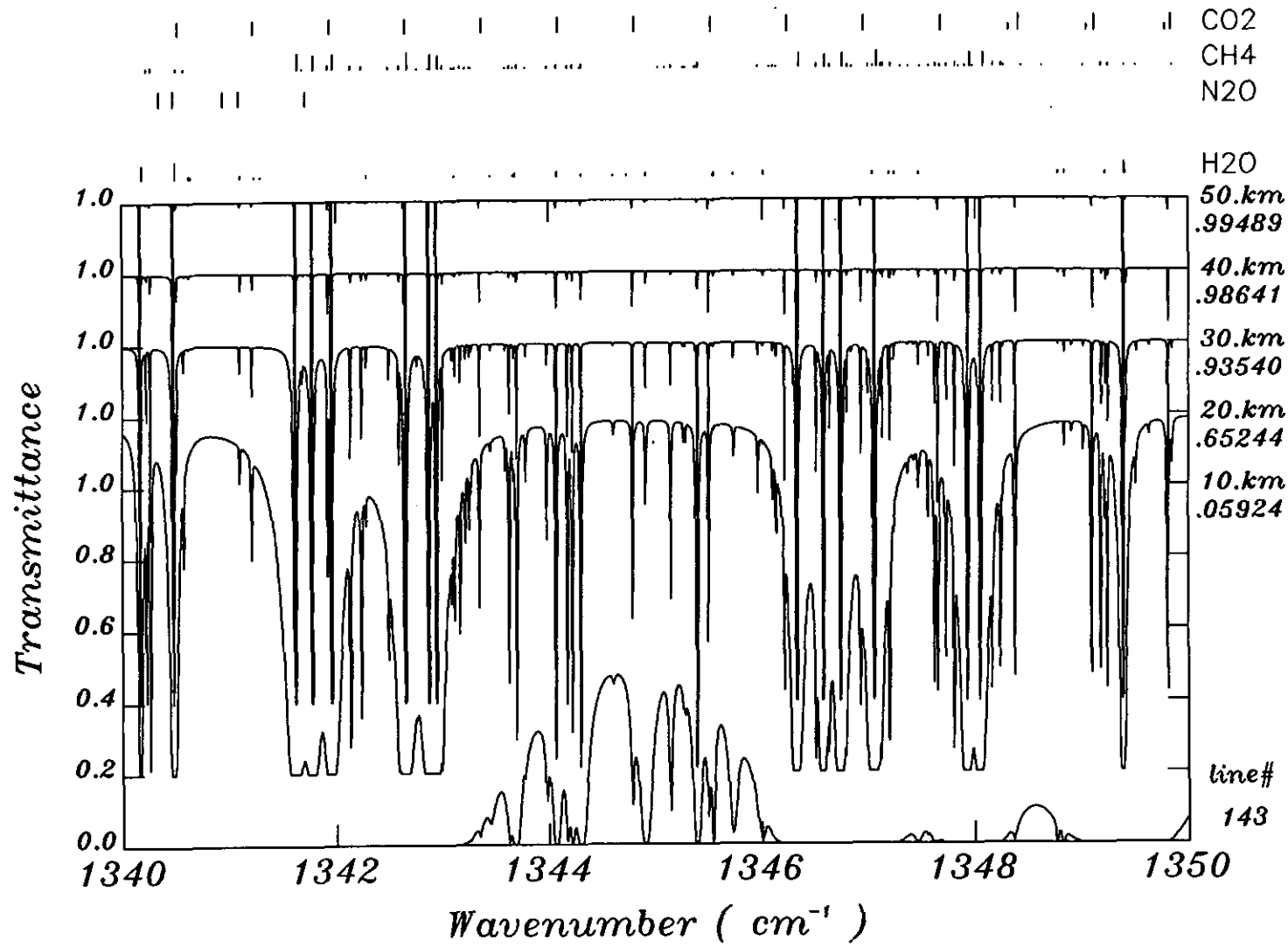




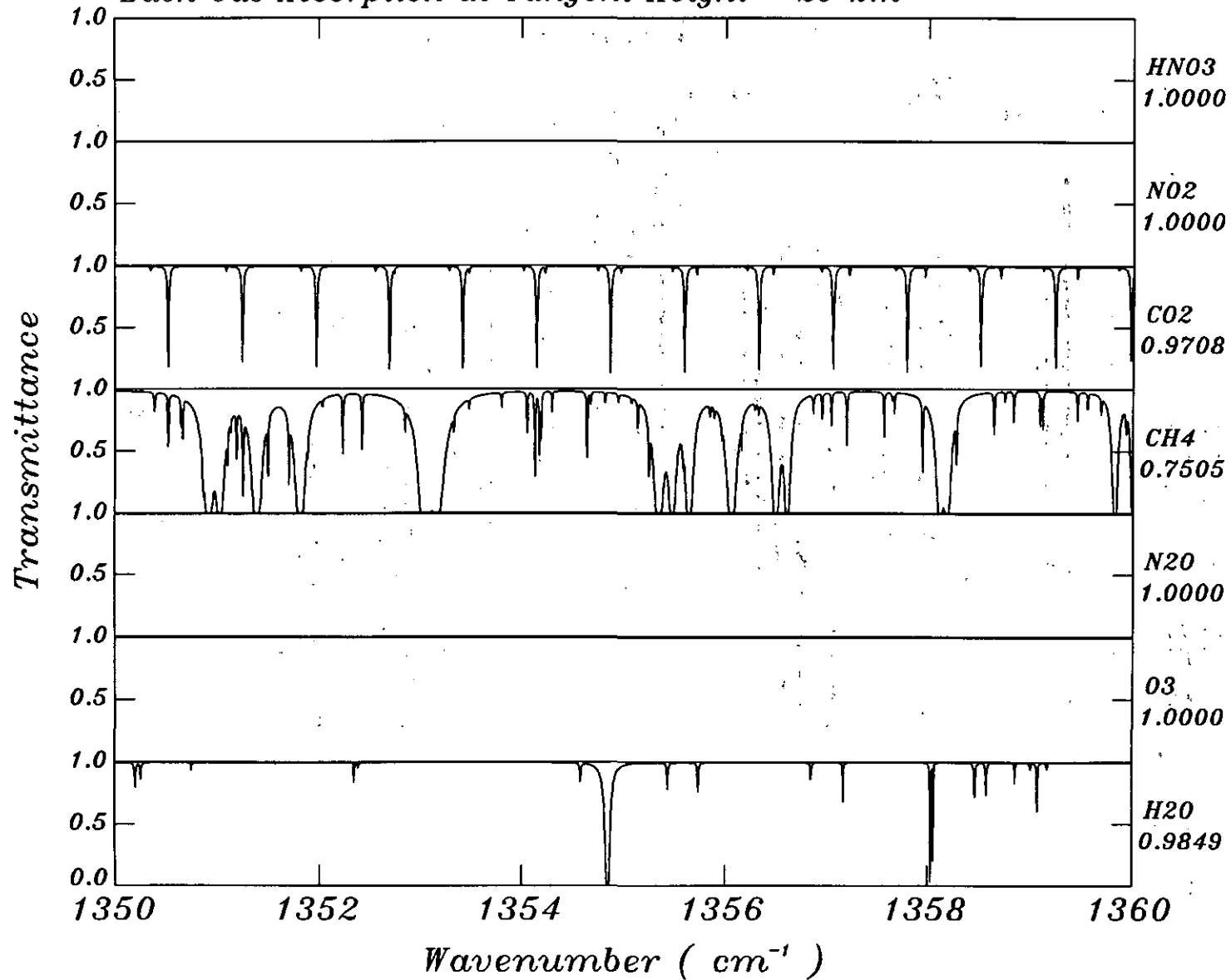


Each Gas Absorption at Tangent Height = 20 km

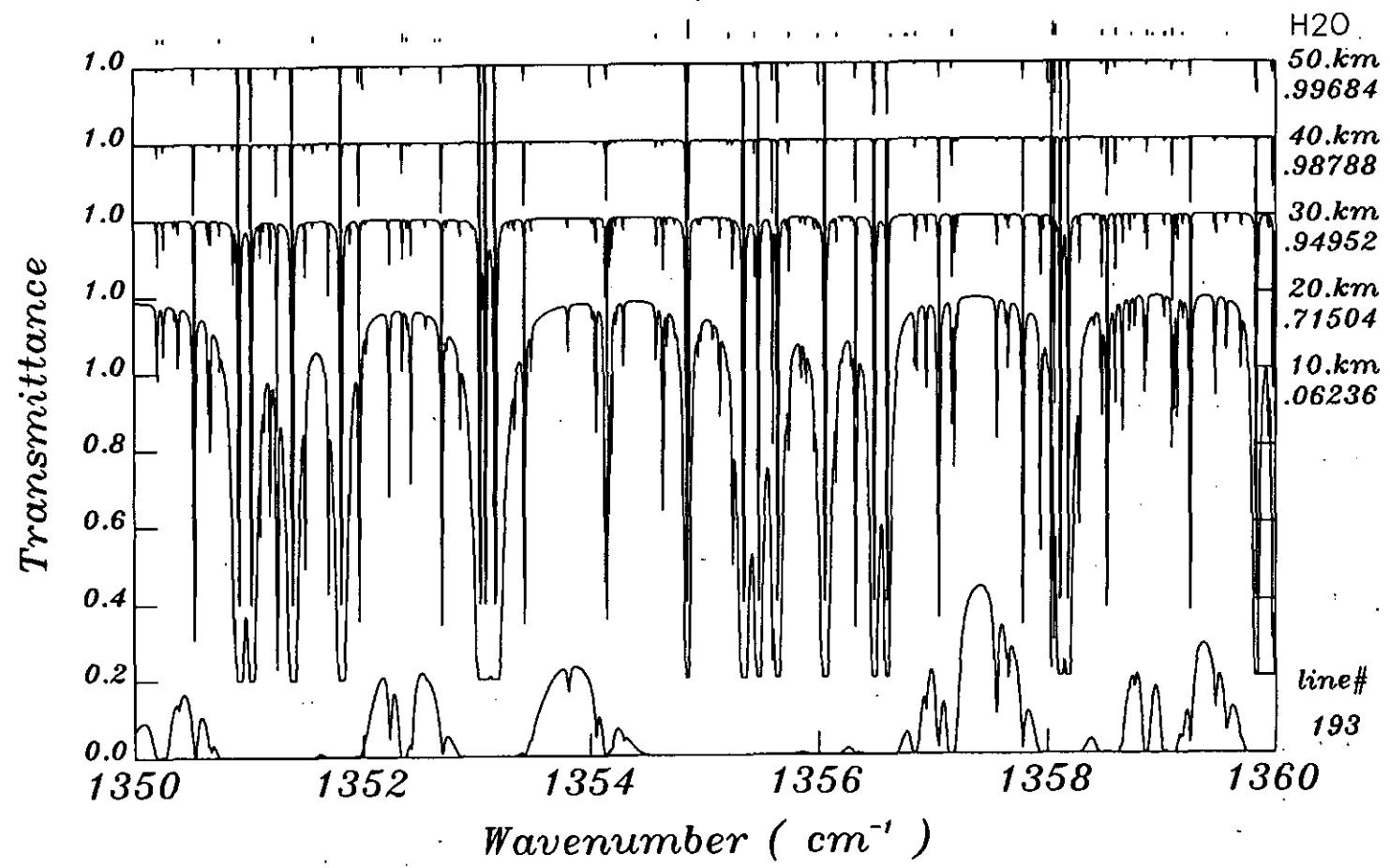


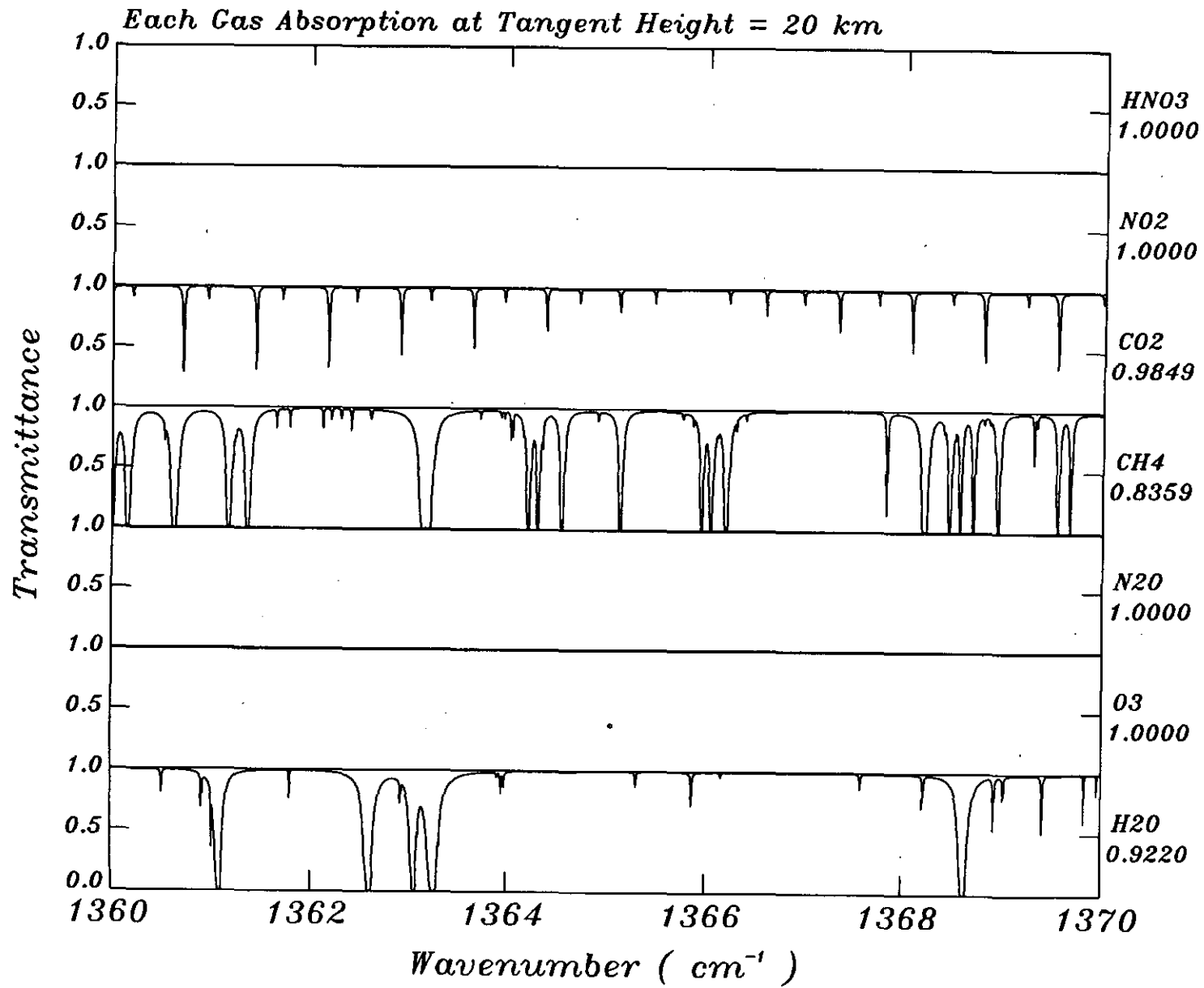


*Each Gas Absorption at Tangent Height = 20 km*

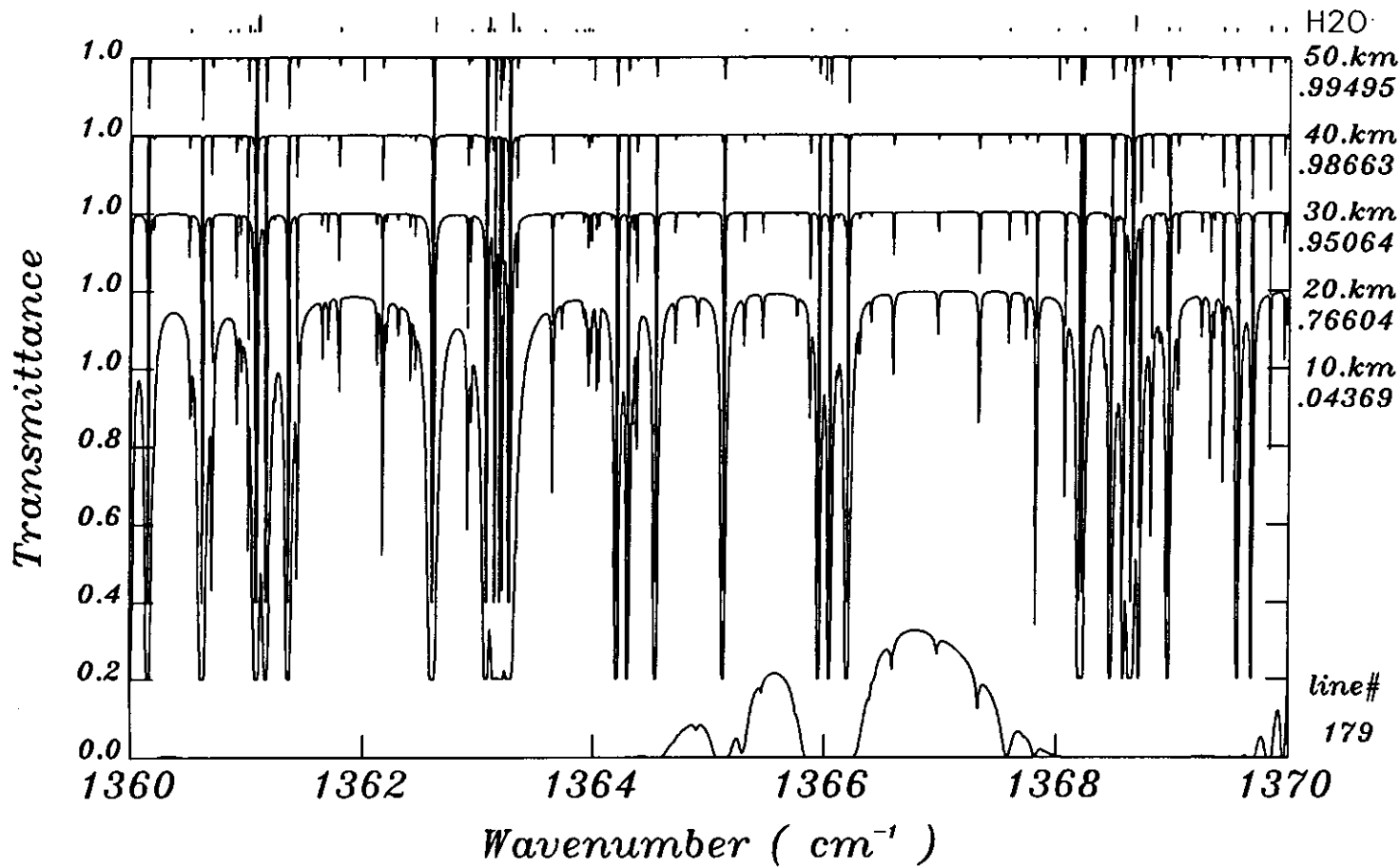


CO2  
CH4

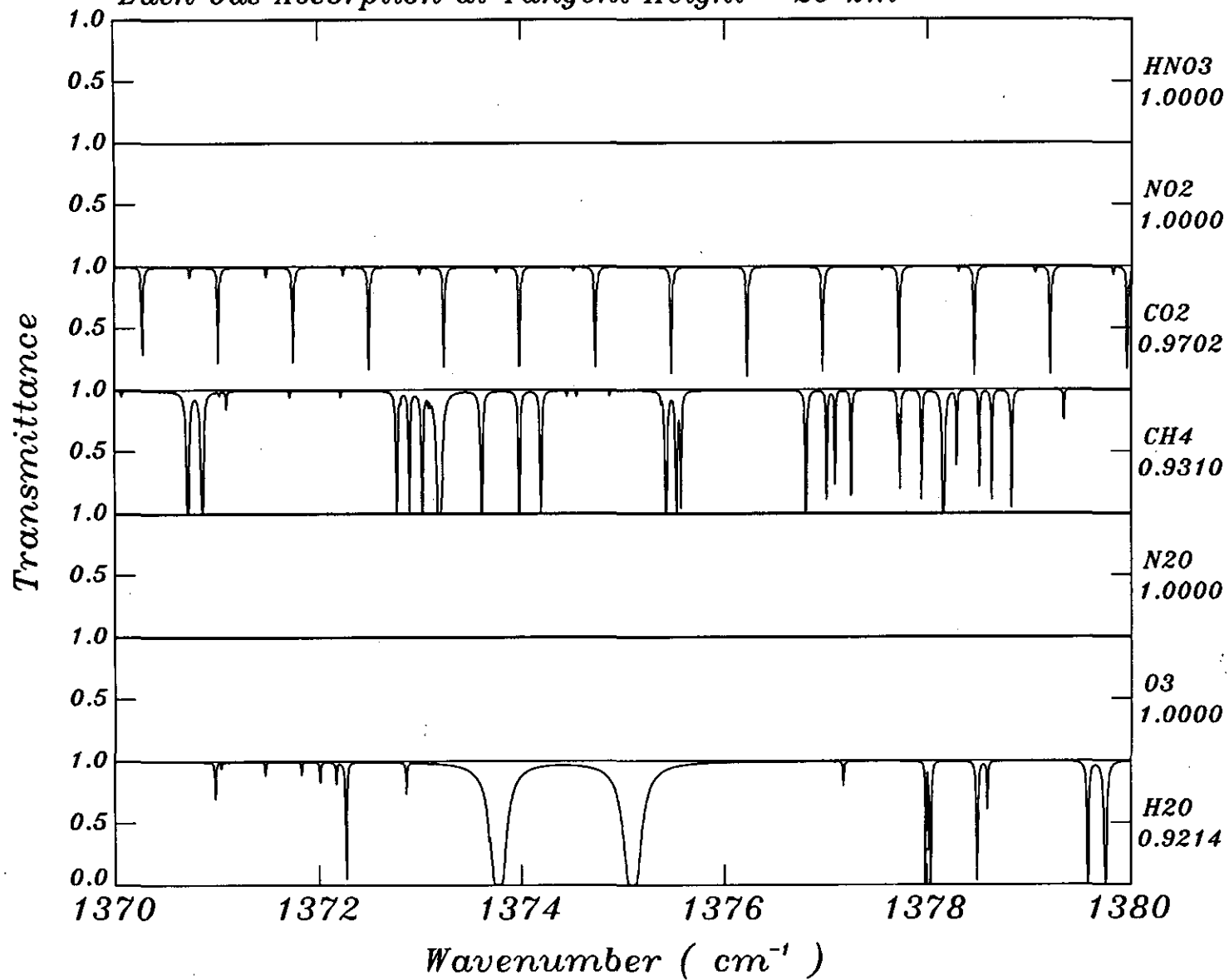




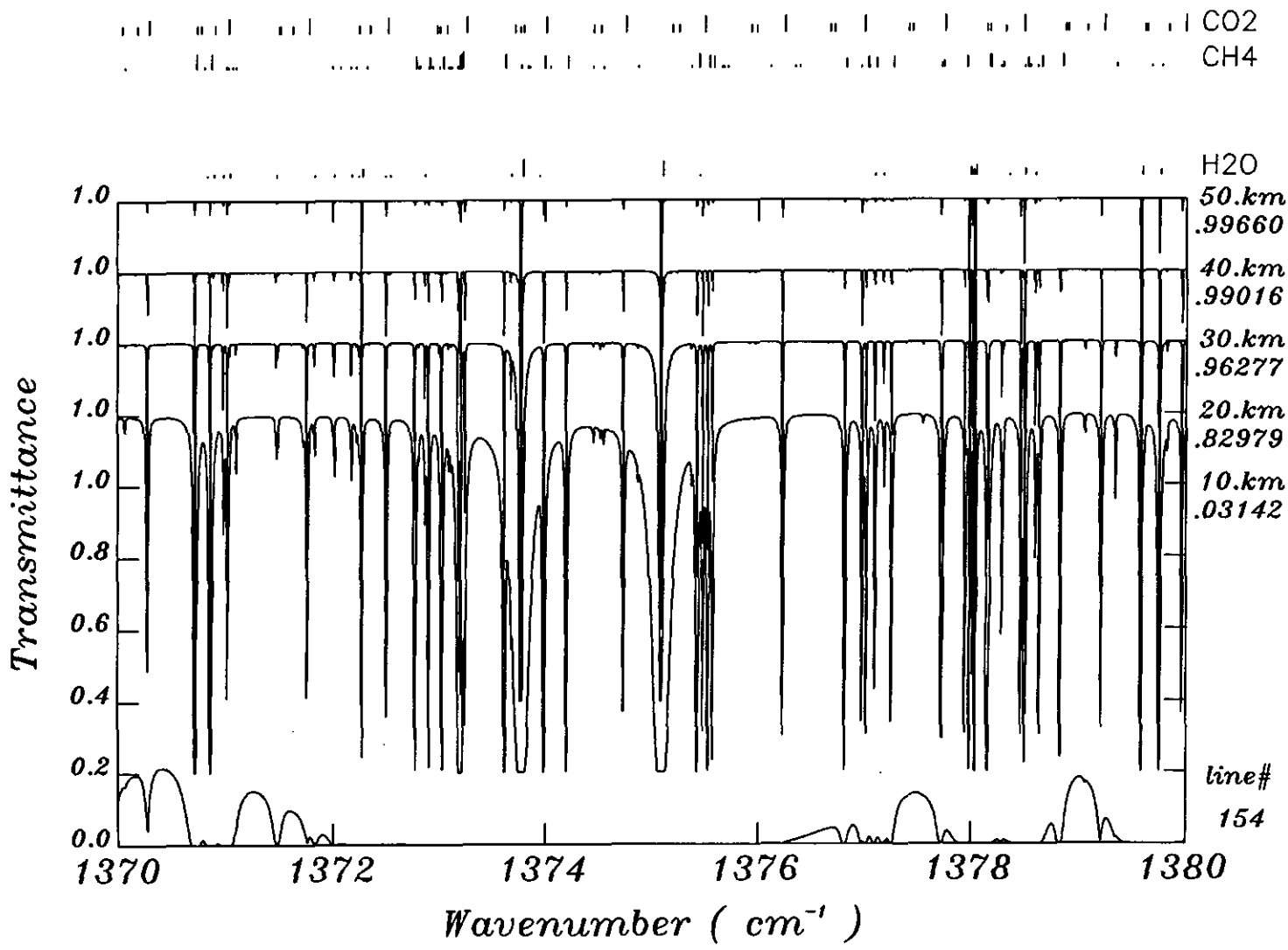
CO2  
CH4



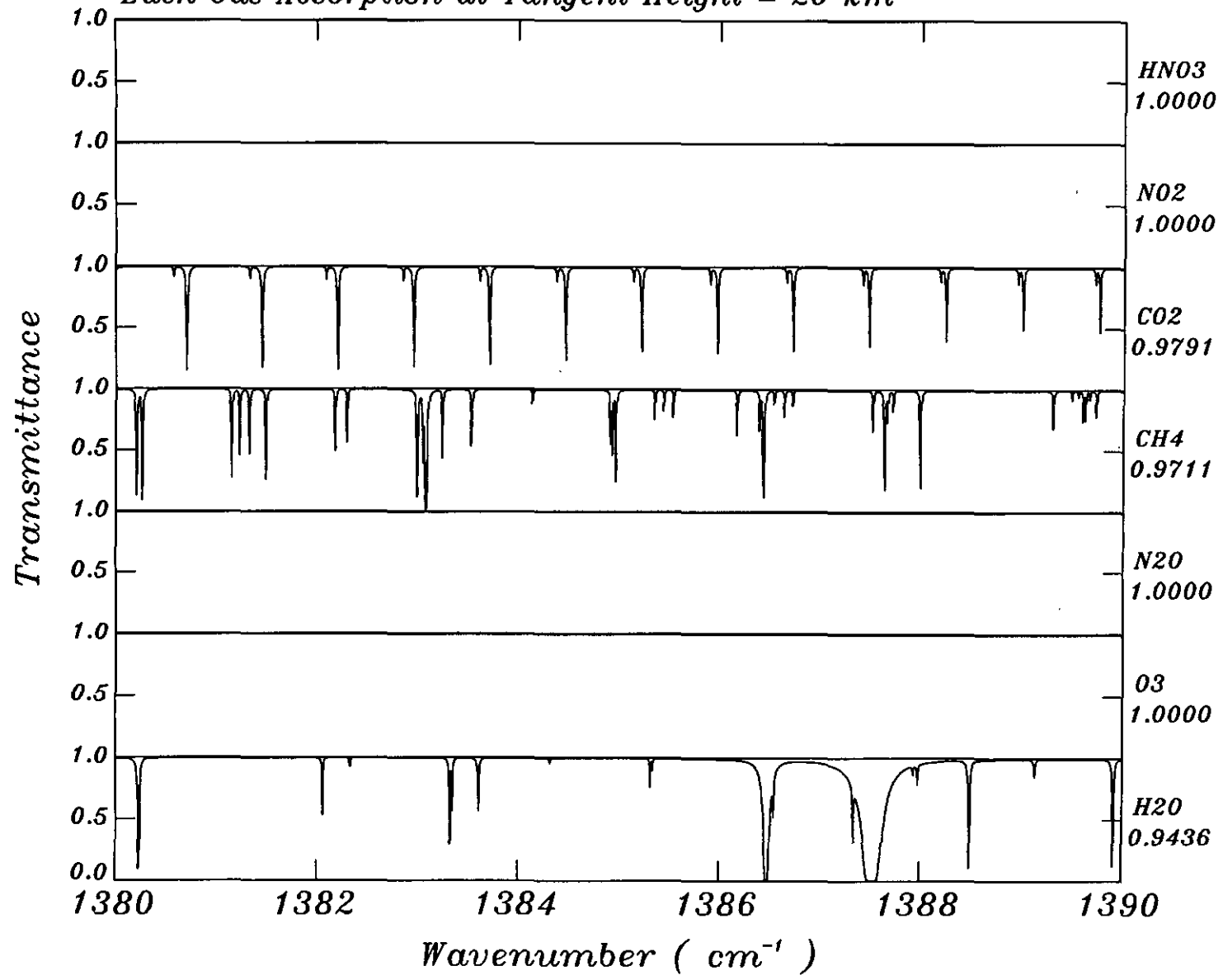
Each Gas Absorption at Tangent Height = 20 km



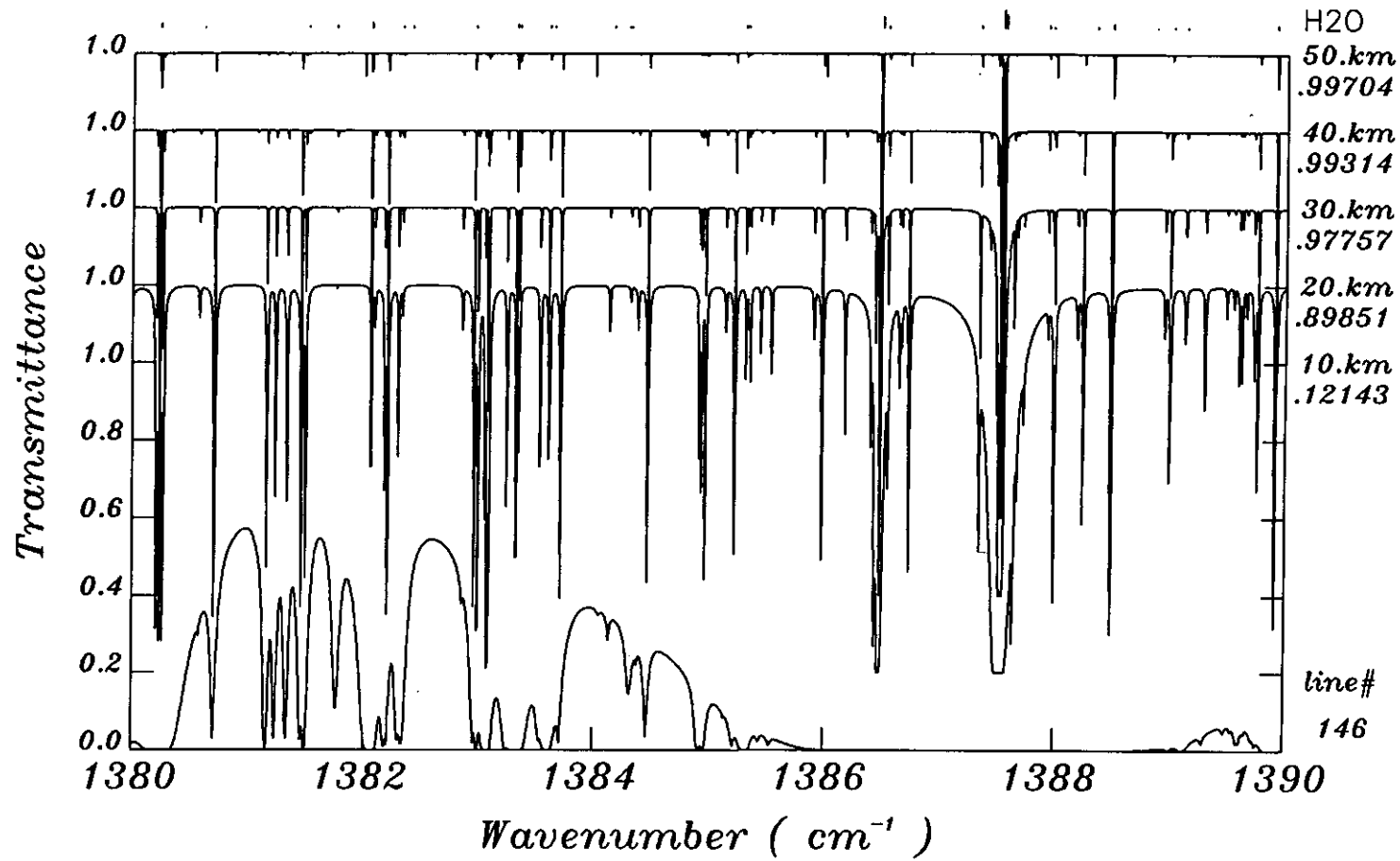


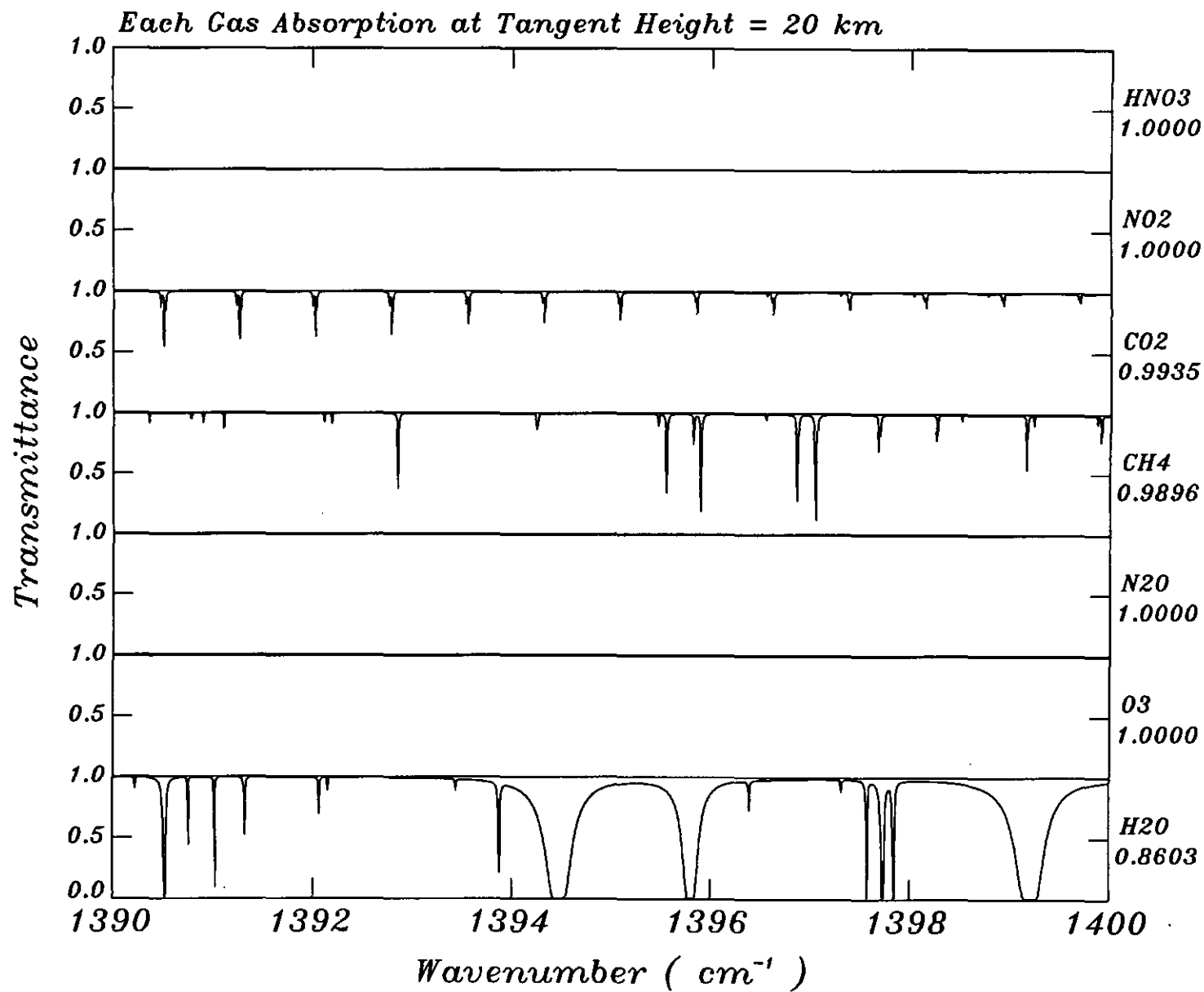


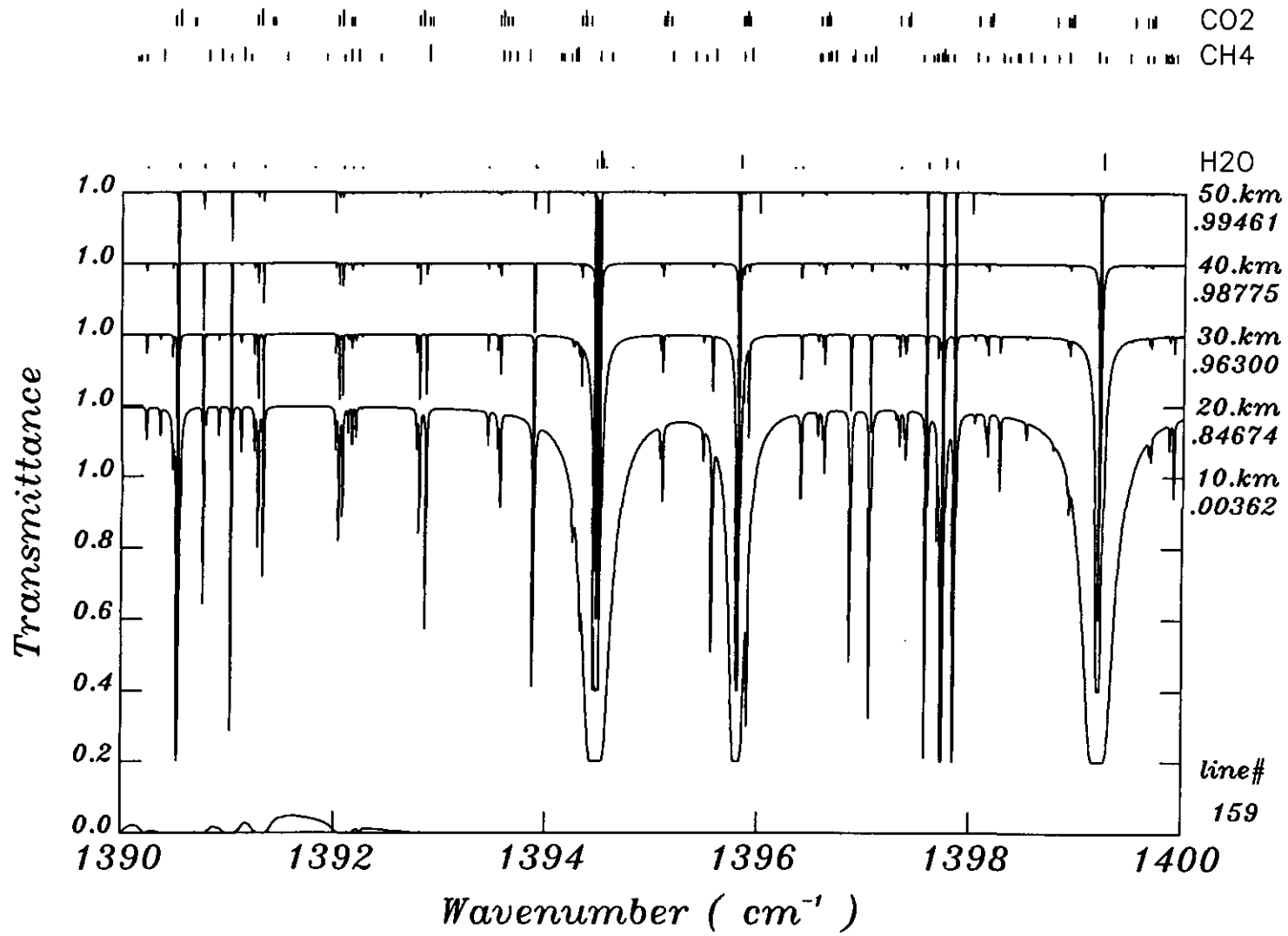
Each Gas Absorption at Tangent Height = 20 km

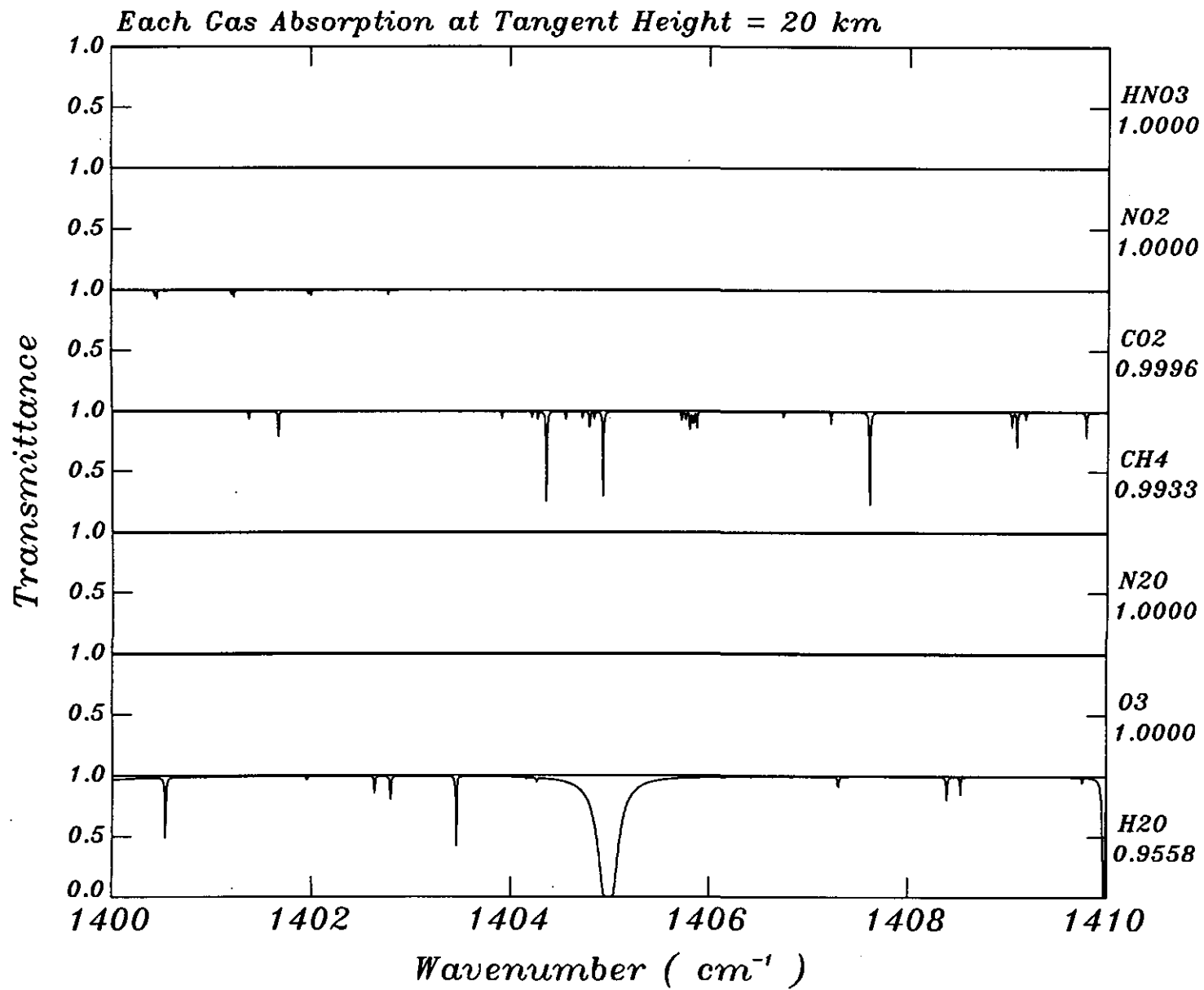


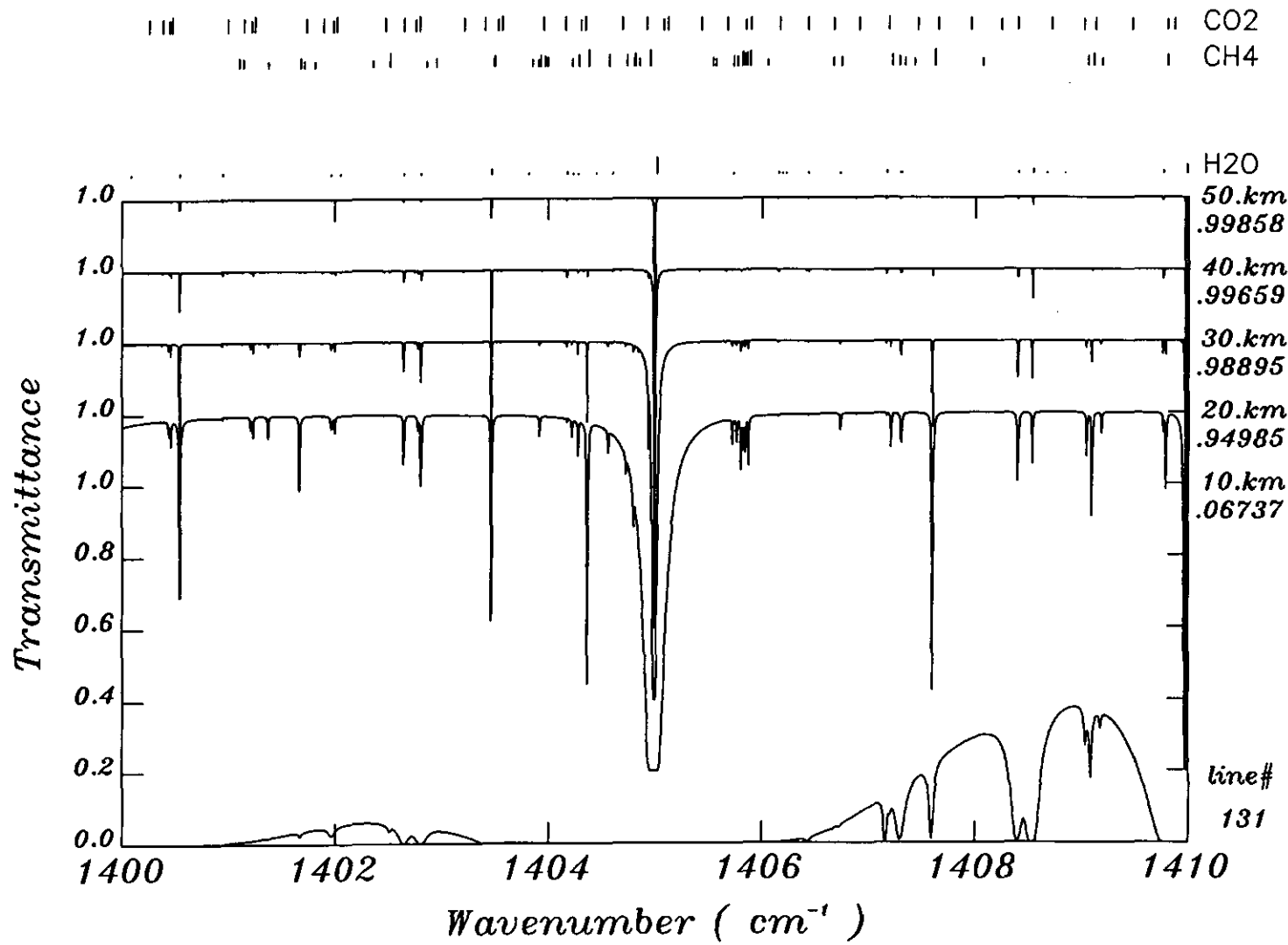
CO2  
CH4



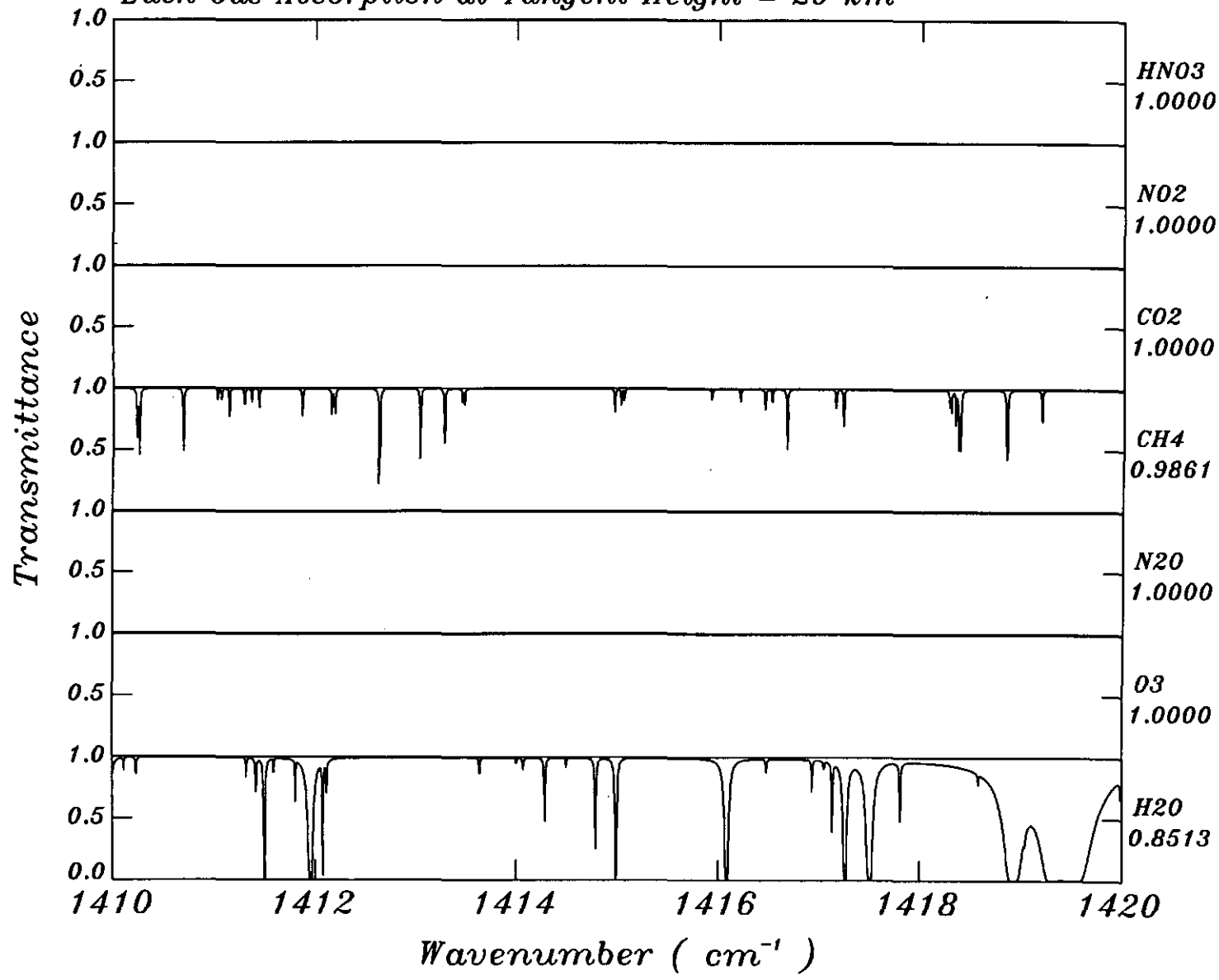




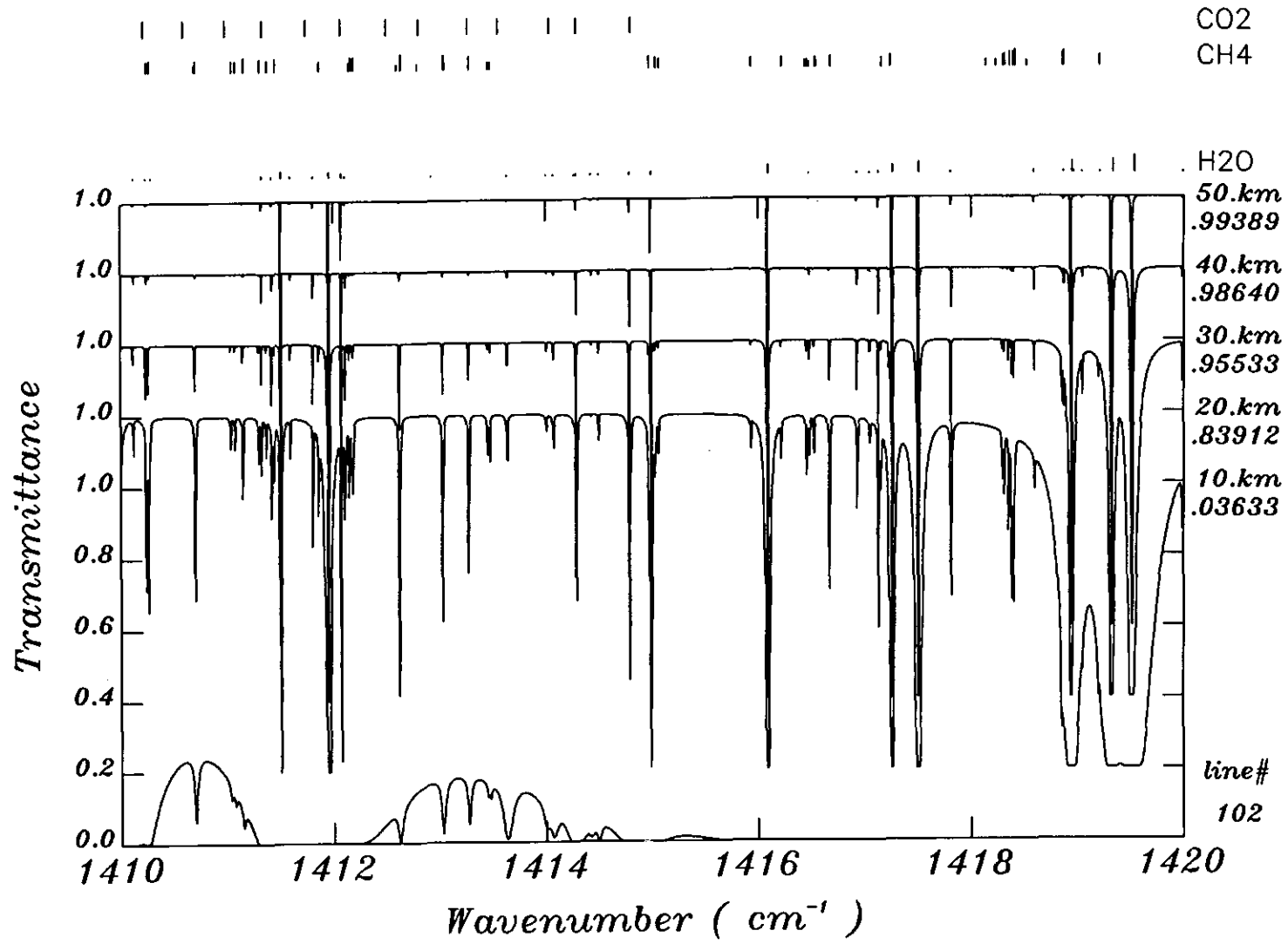




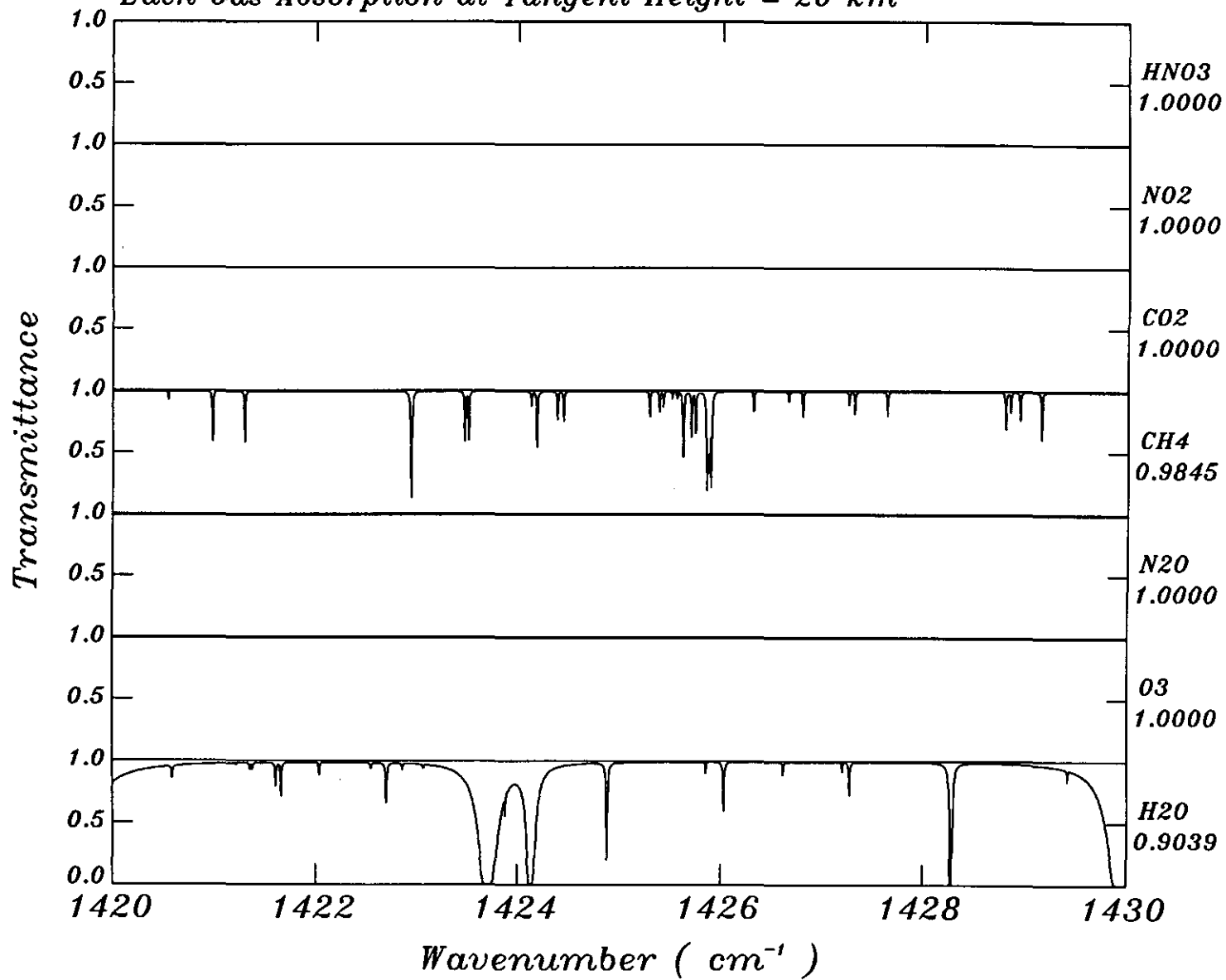
Each Gas Absorption at Tangent Height = 20 km



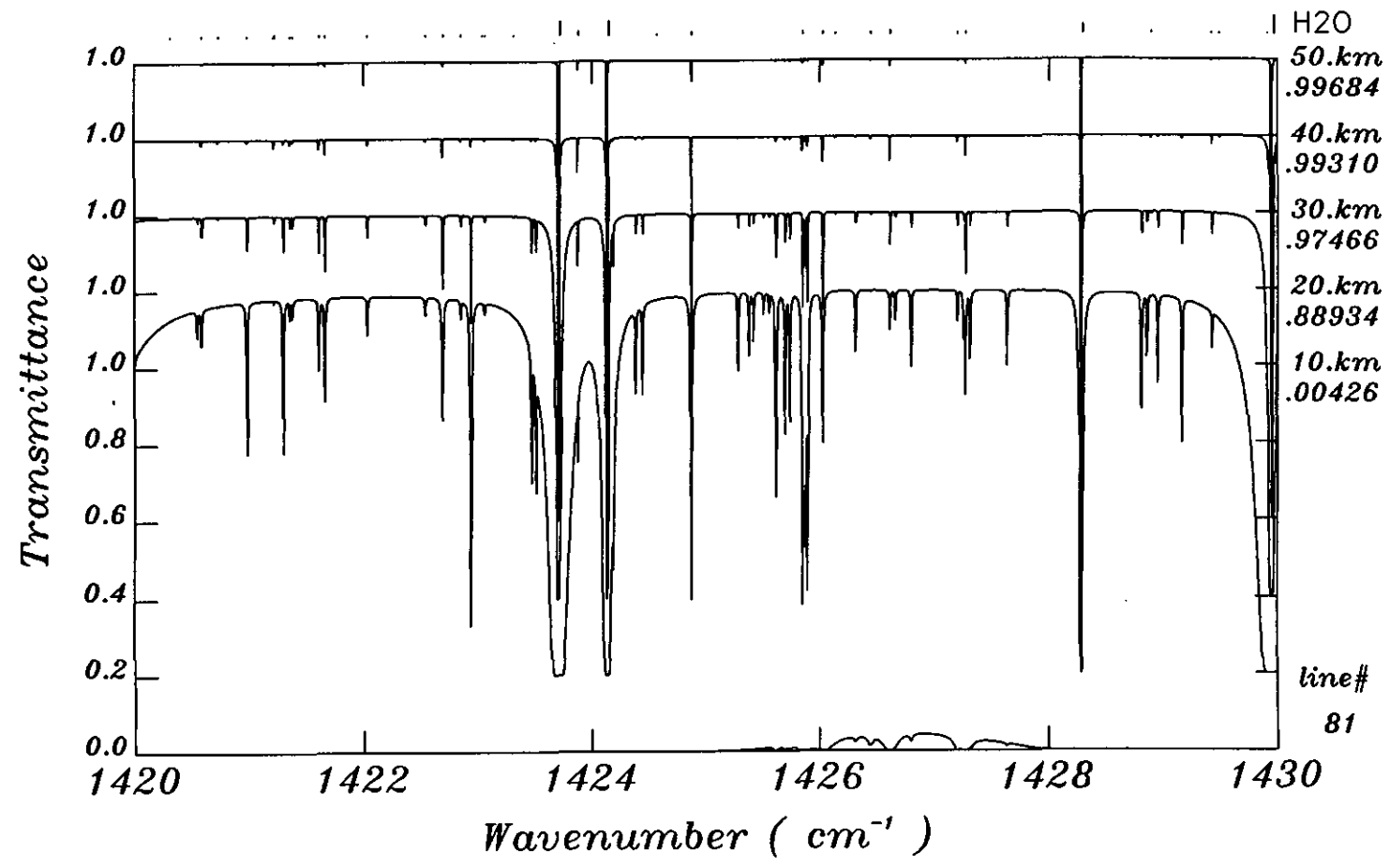


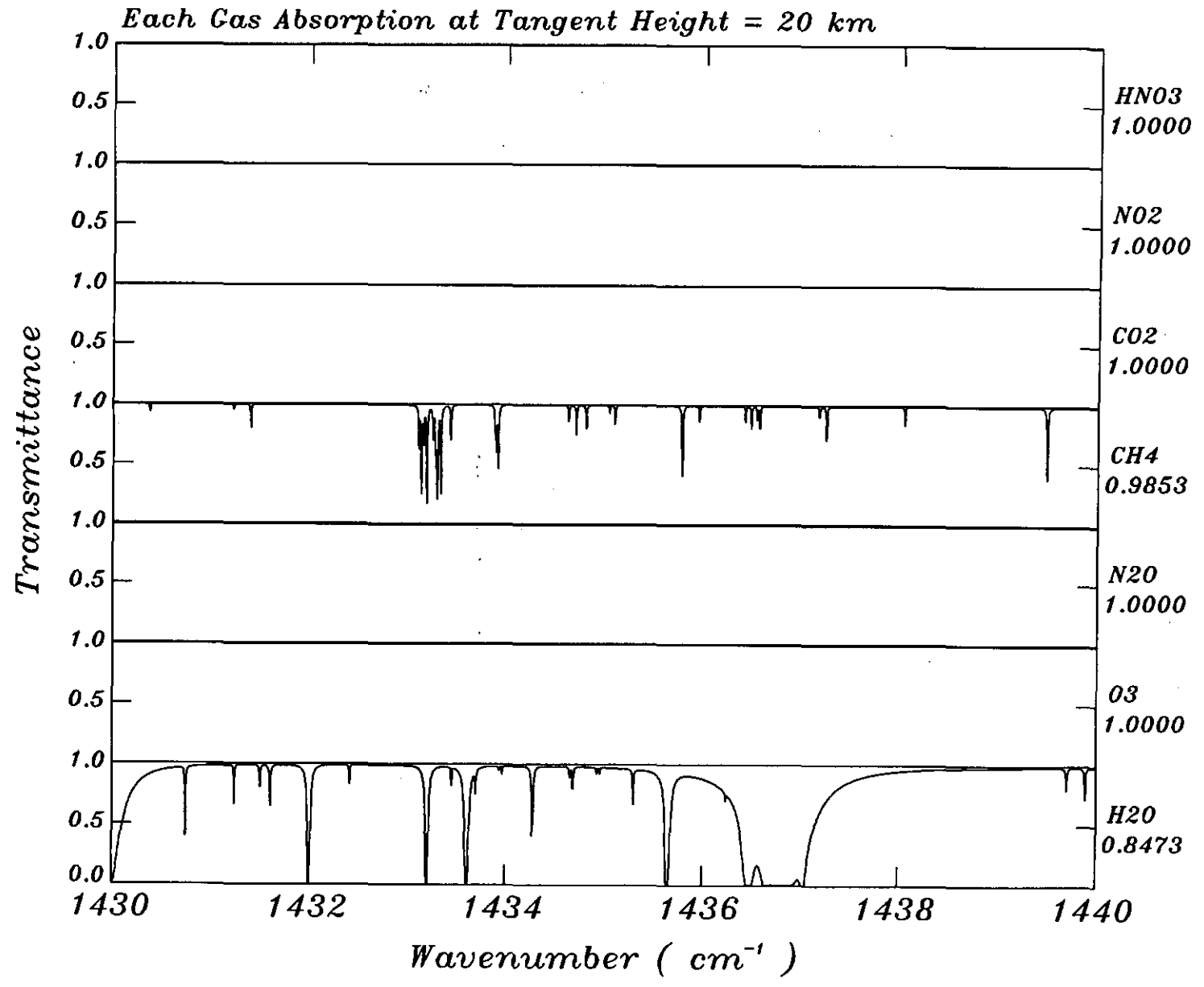


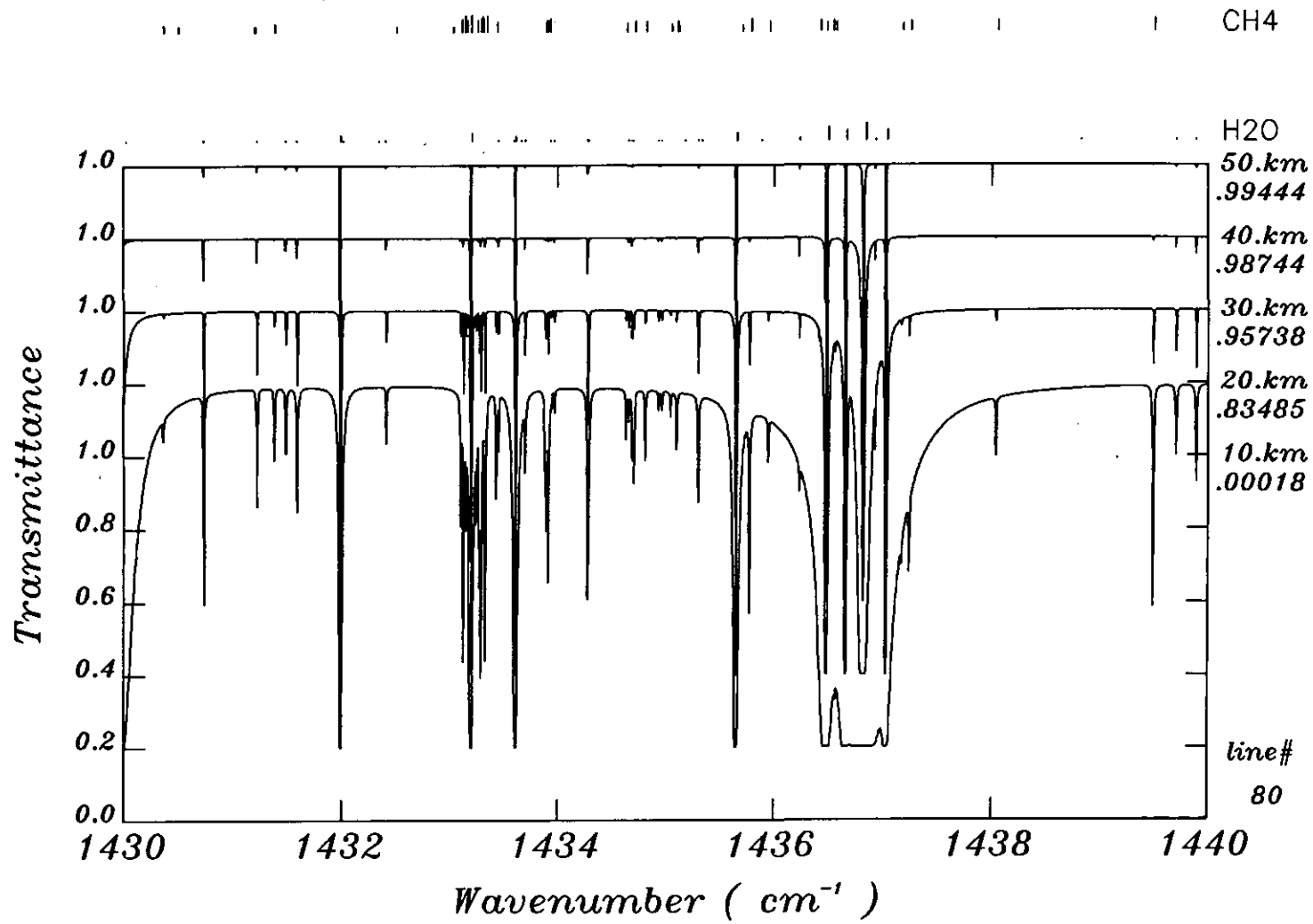
Each Gas Absorption at Tangent Height = 20 km

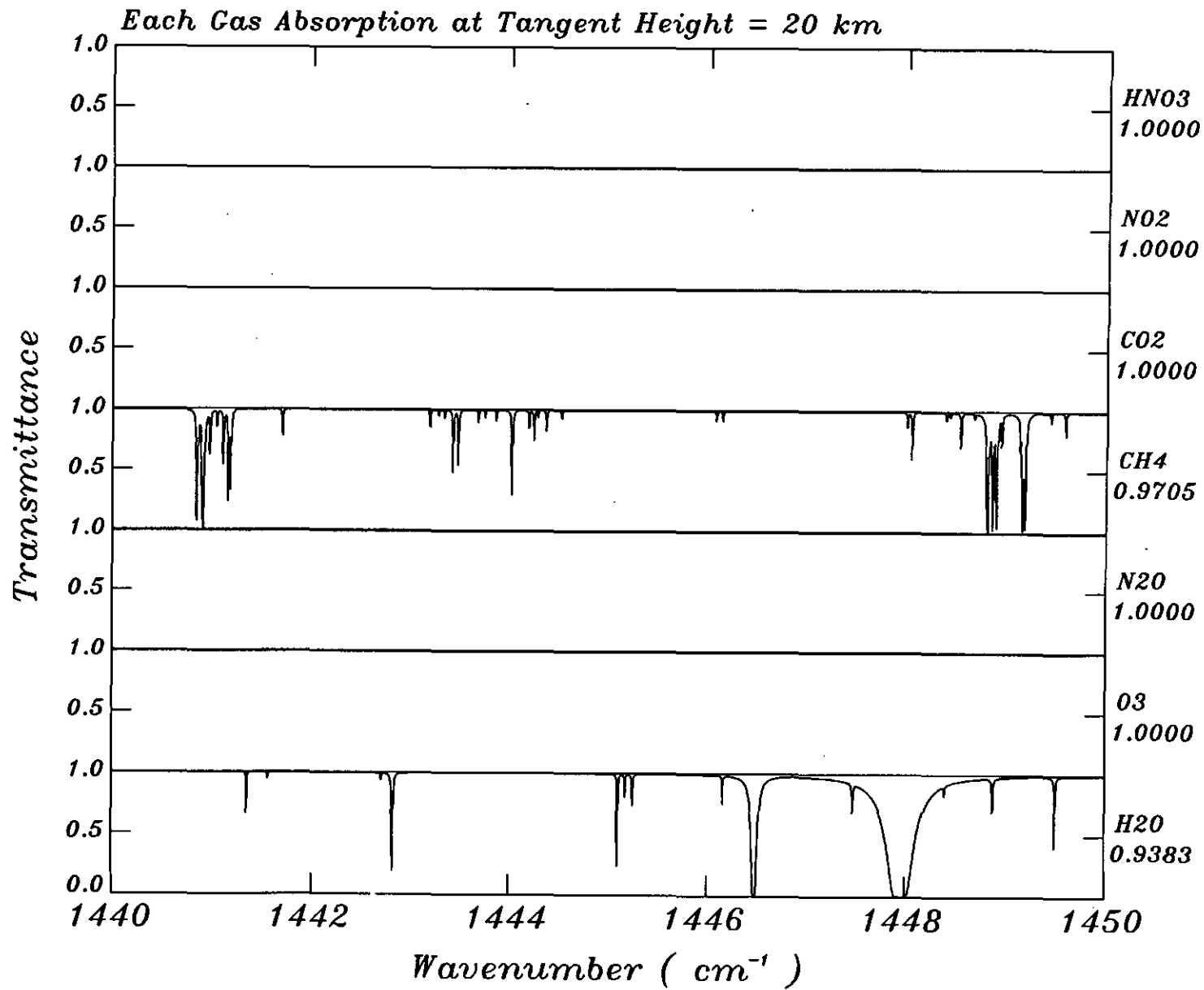


CH4

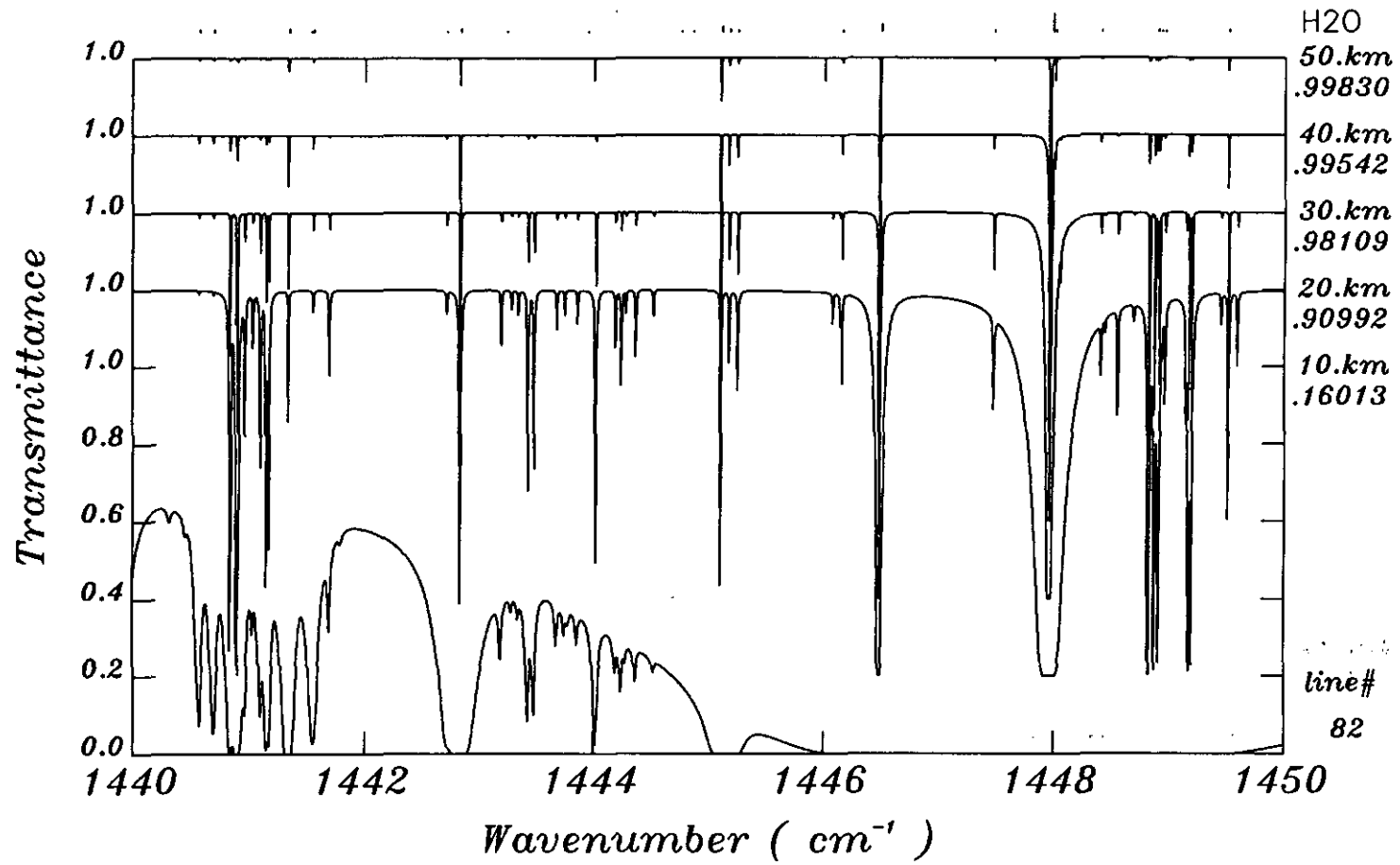




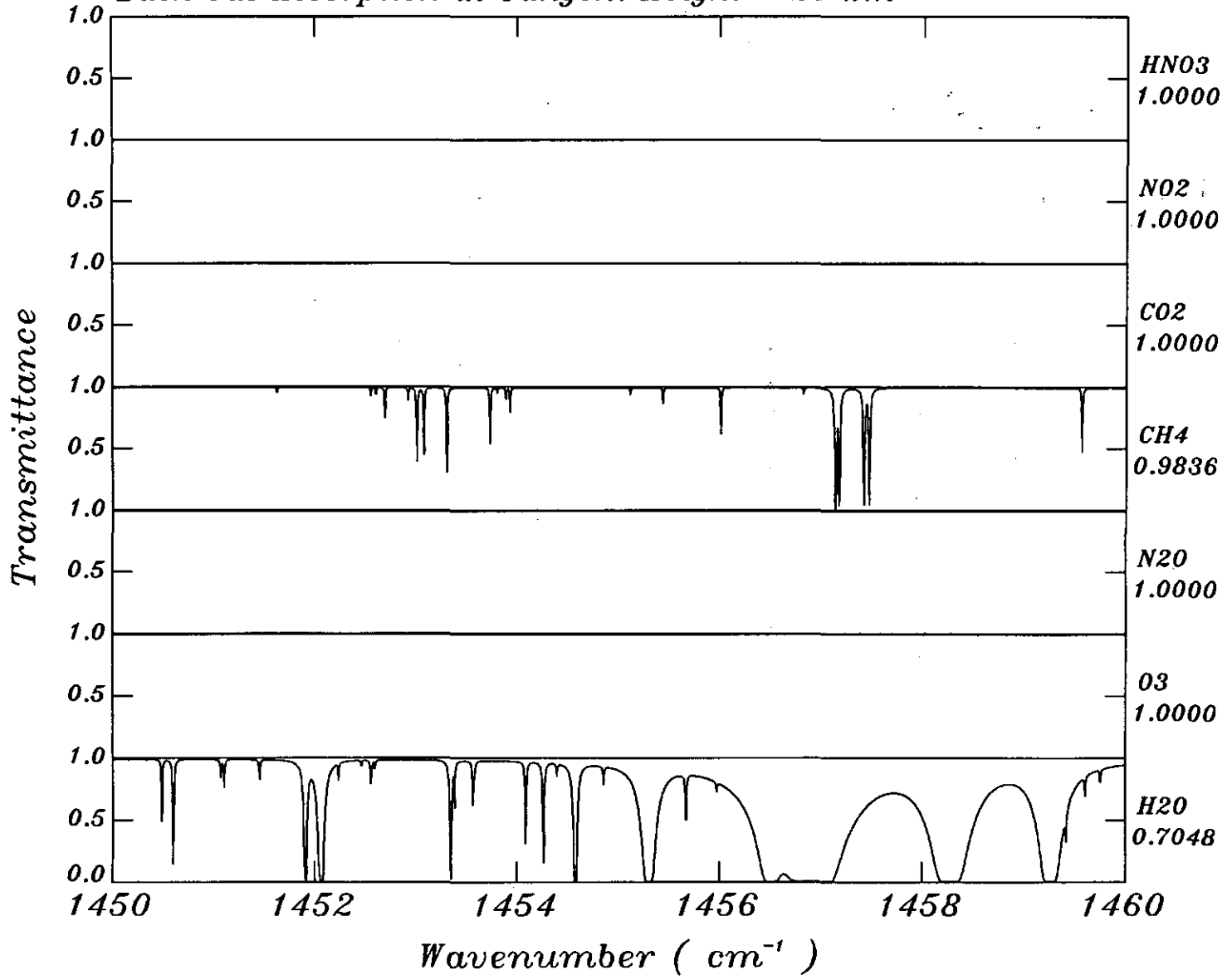




CH4

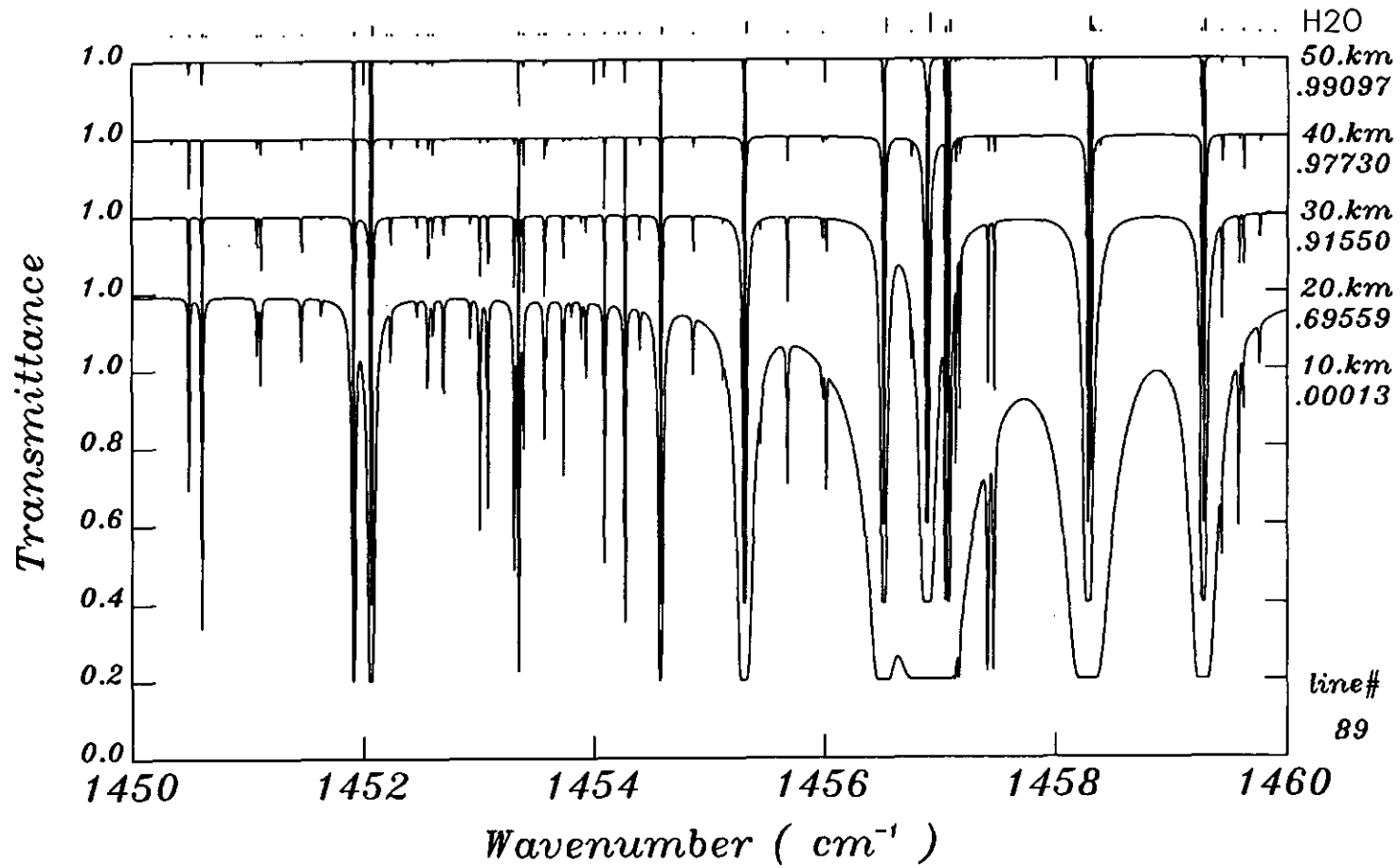


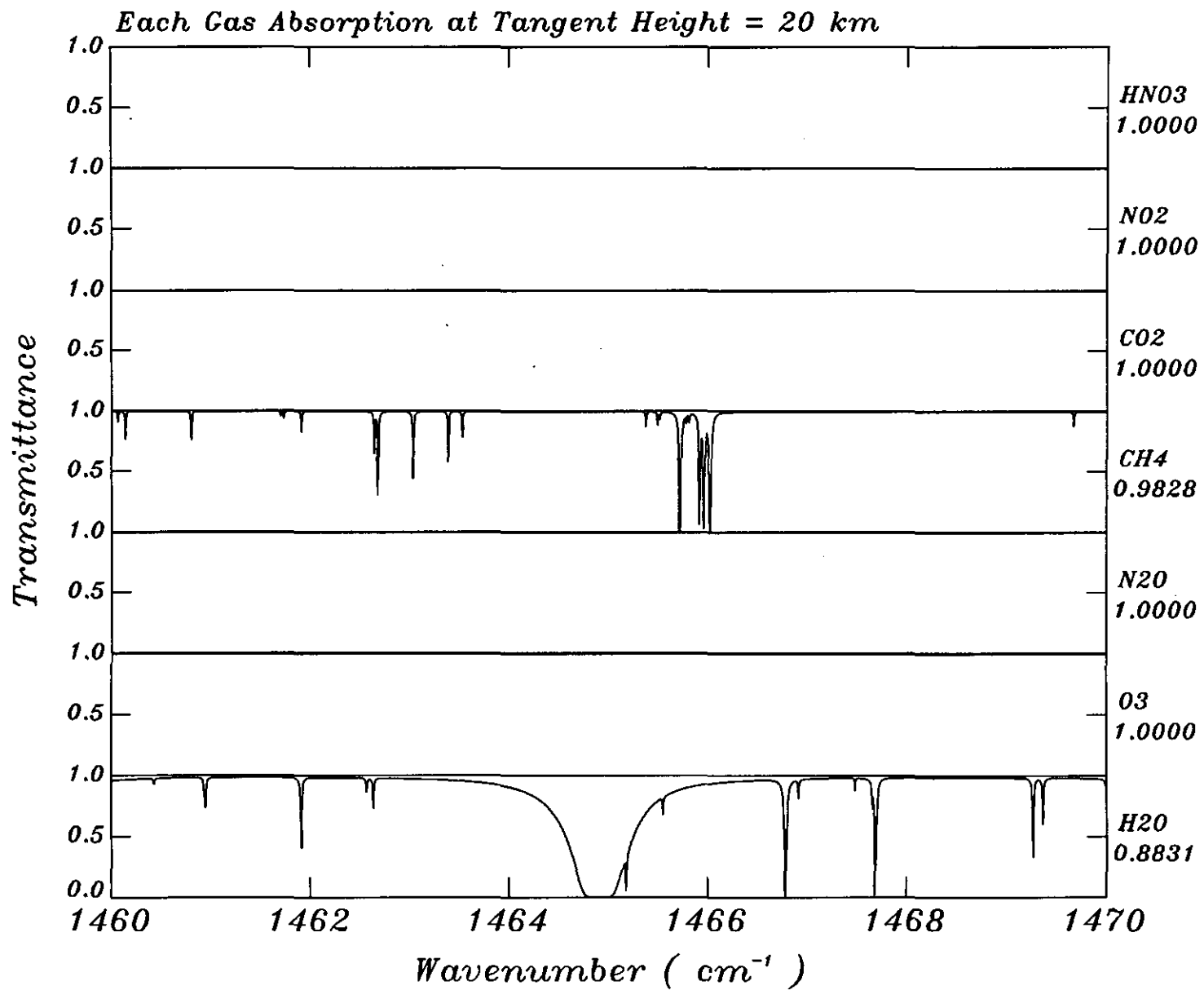
Each Gas Absorption at Tangent Height = 20 km

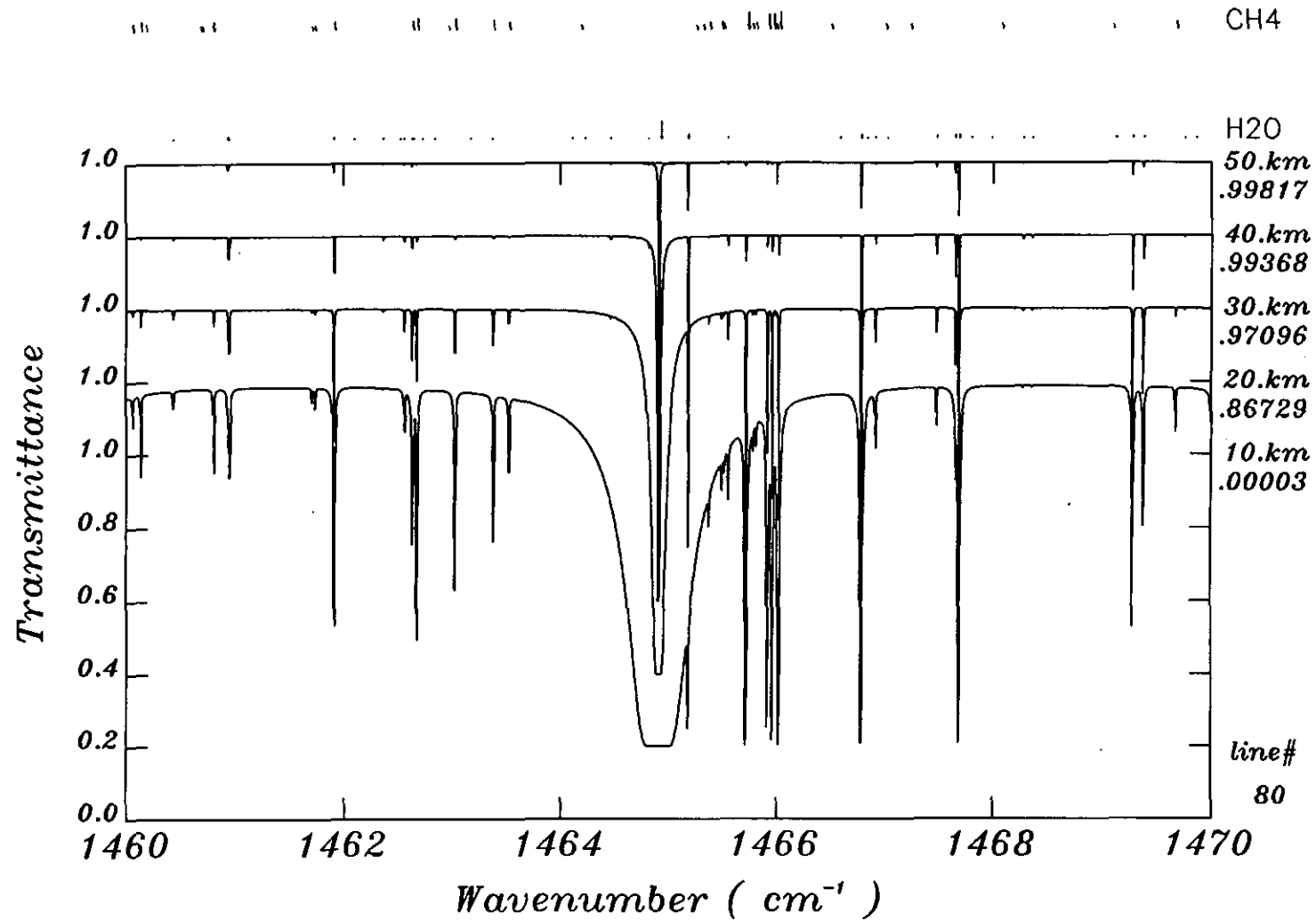




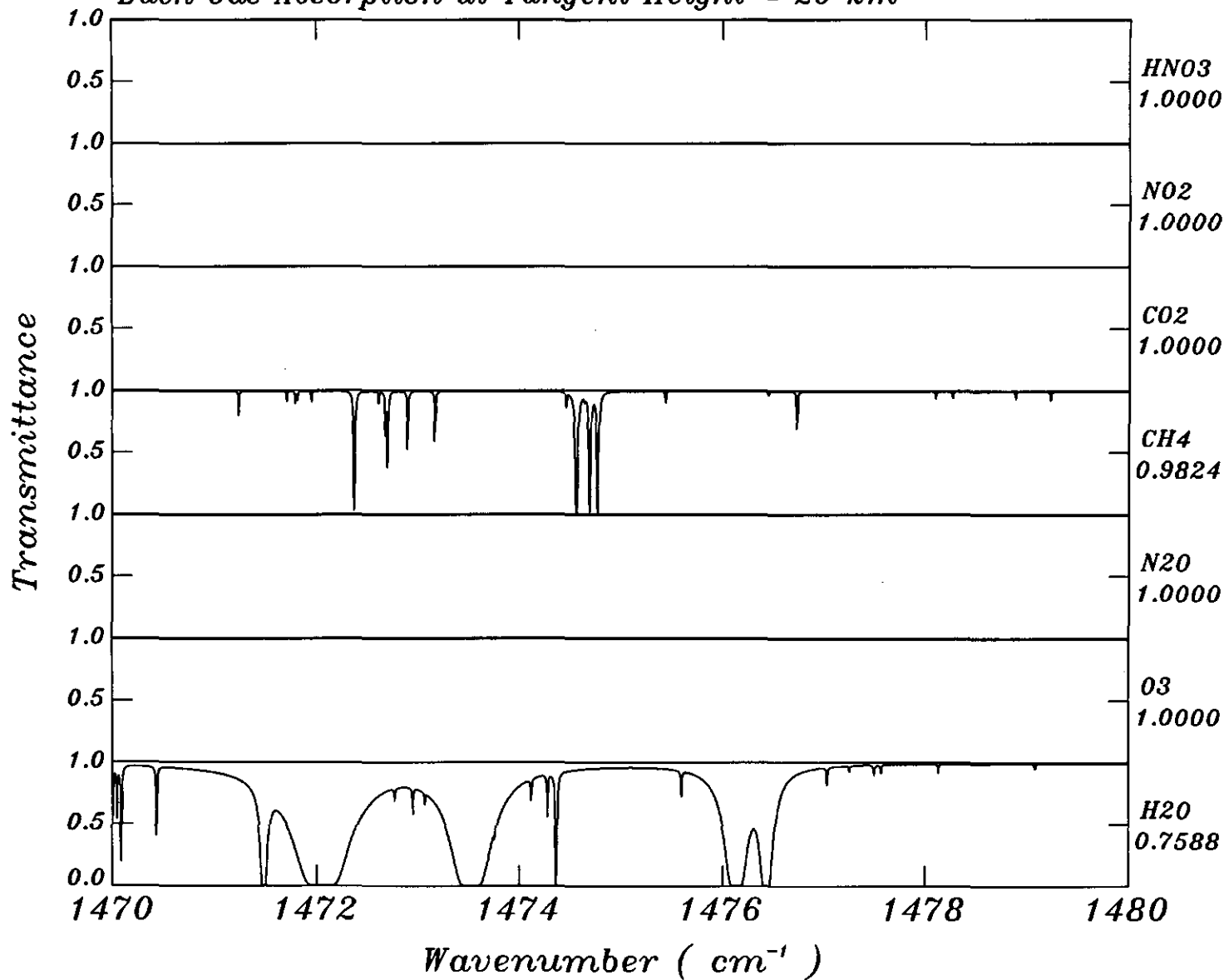
CH4

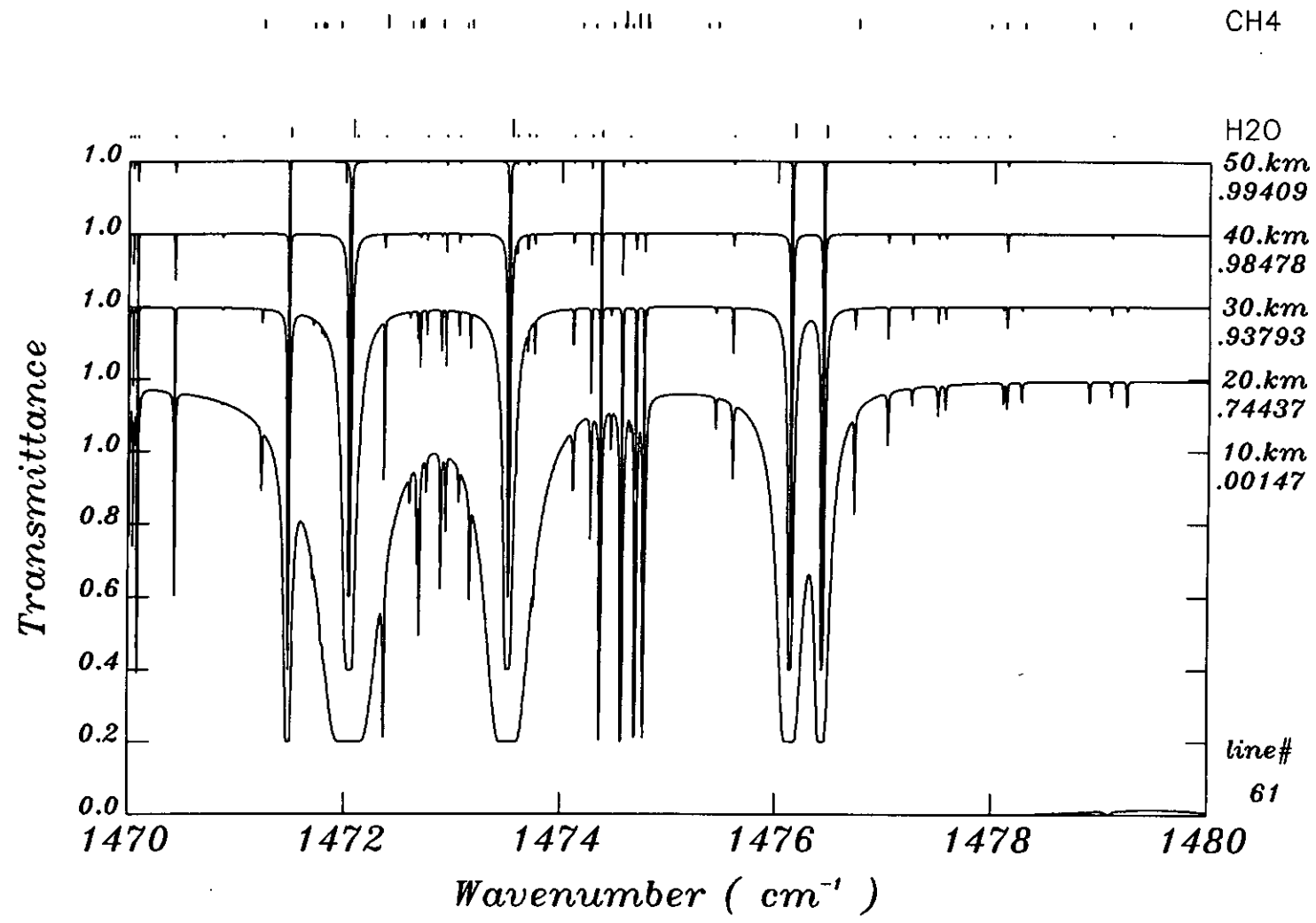




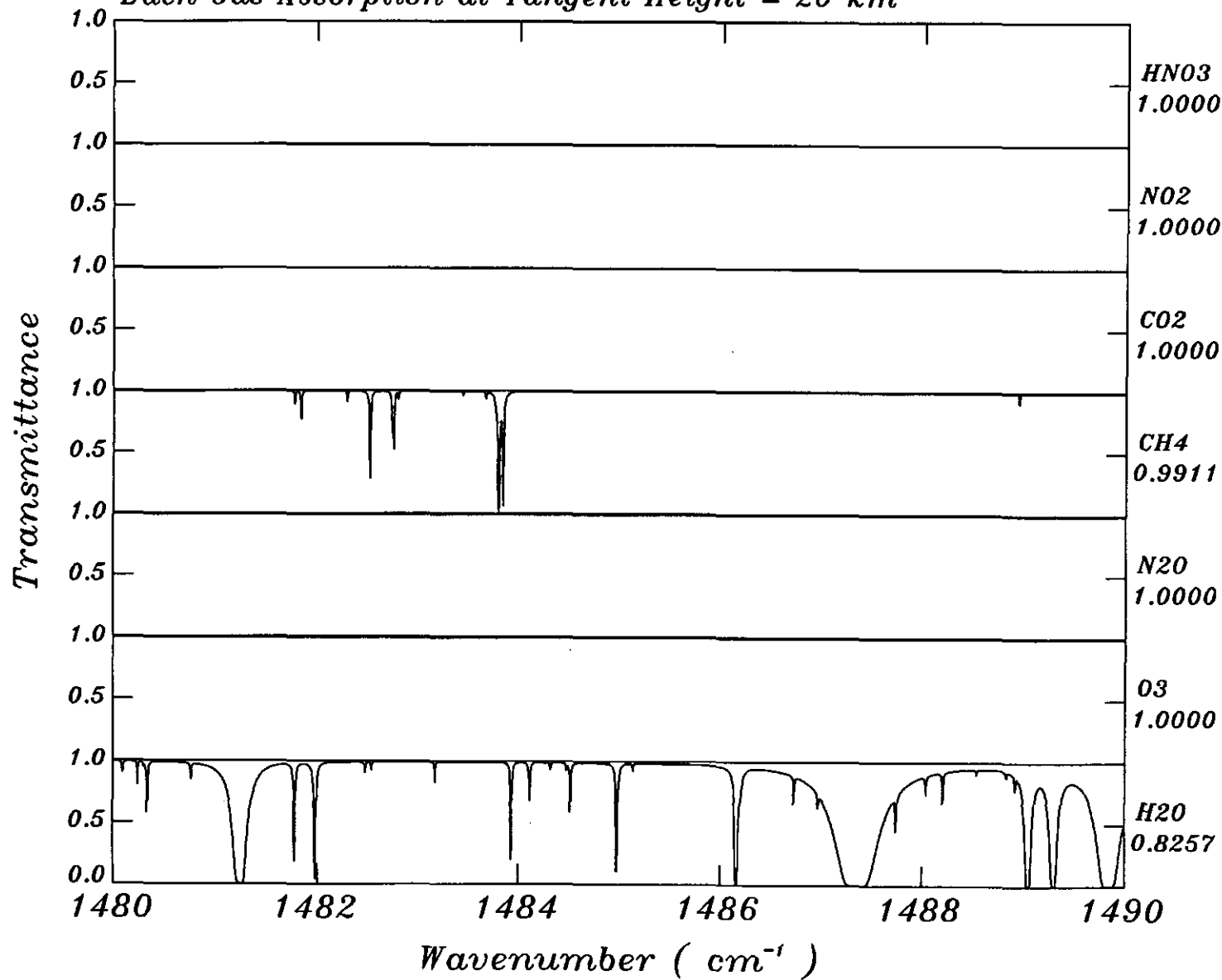


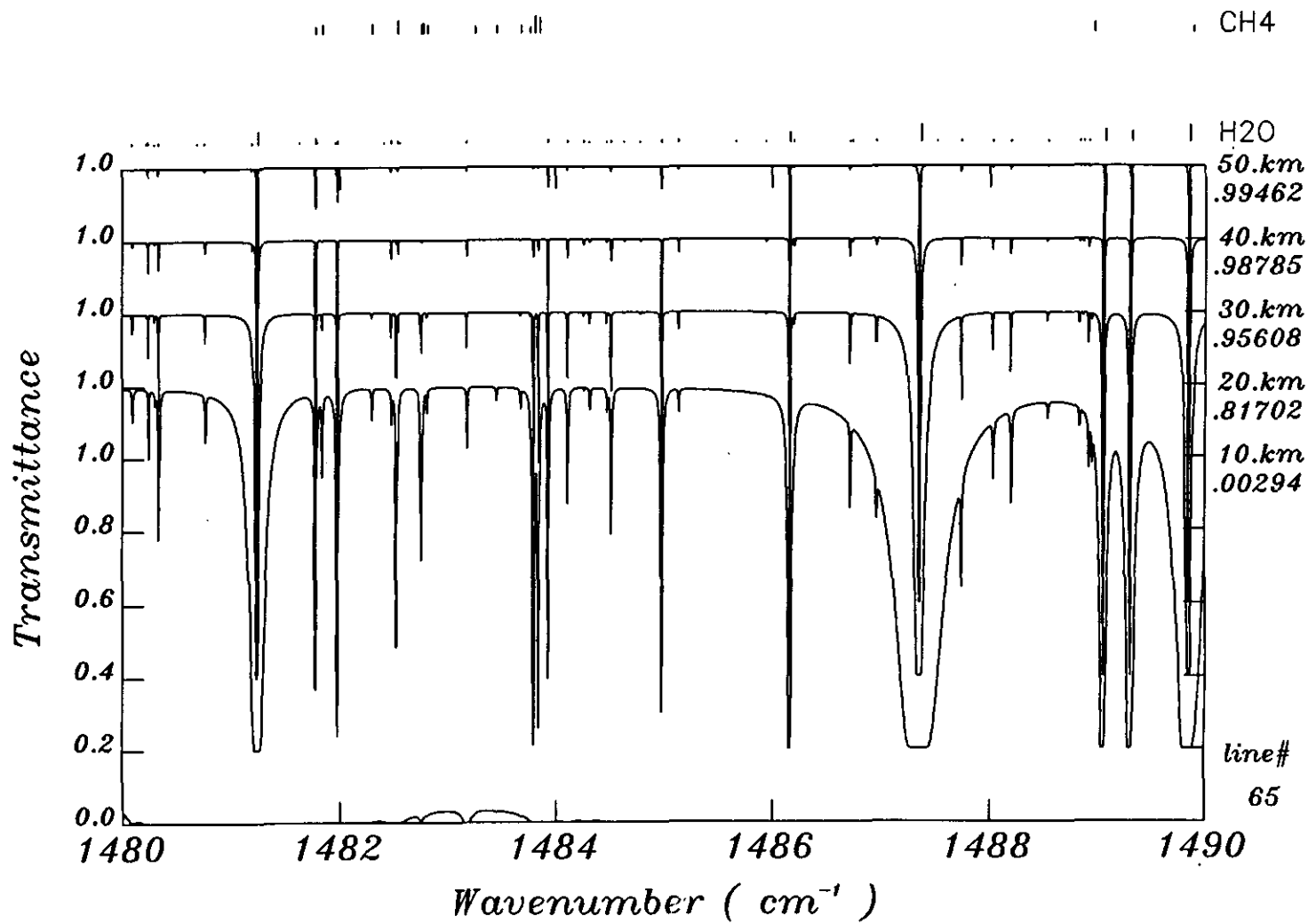
Each Gas Absorption at Tangent Height = 20 km



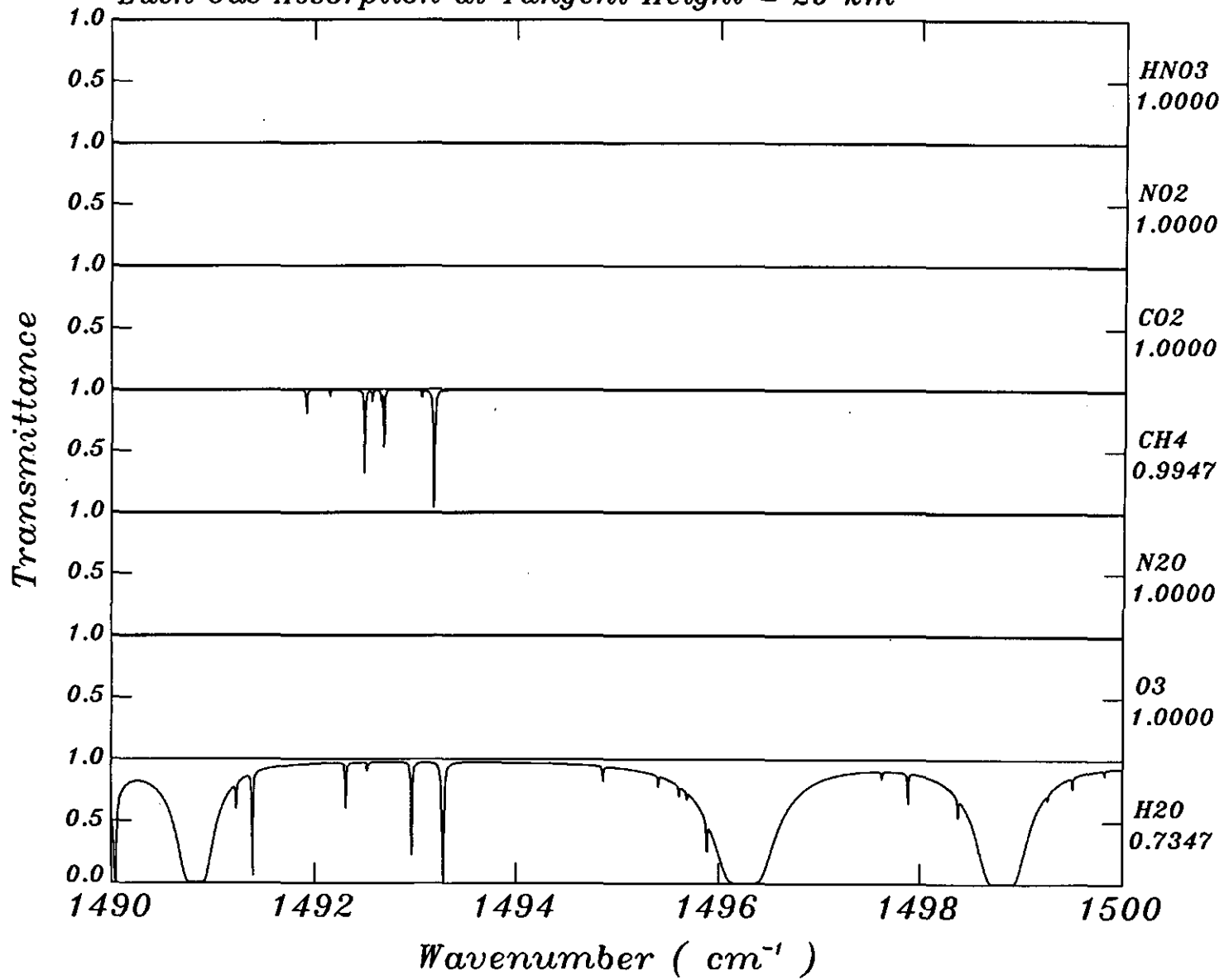


Each Gas Absorption at Tangent Height = 20 km

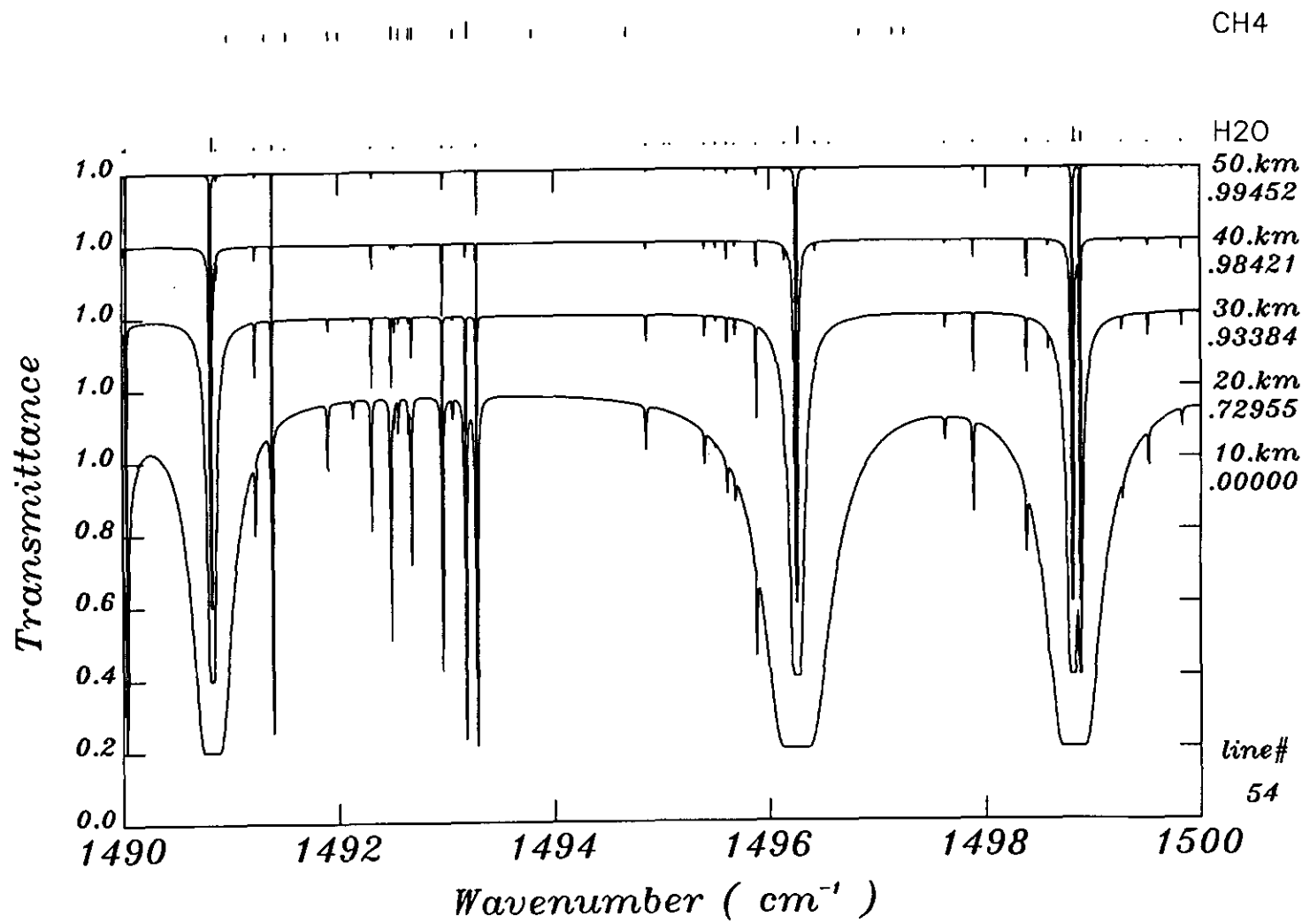




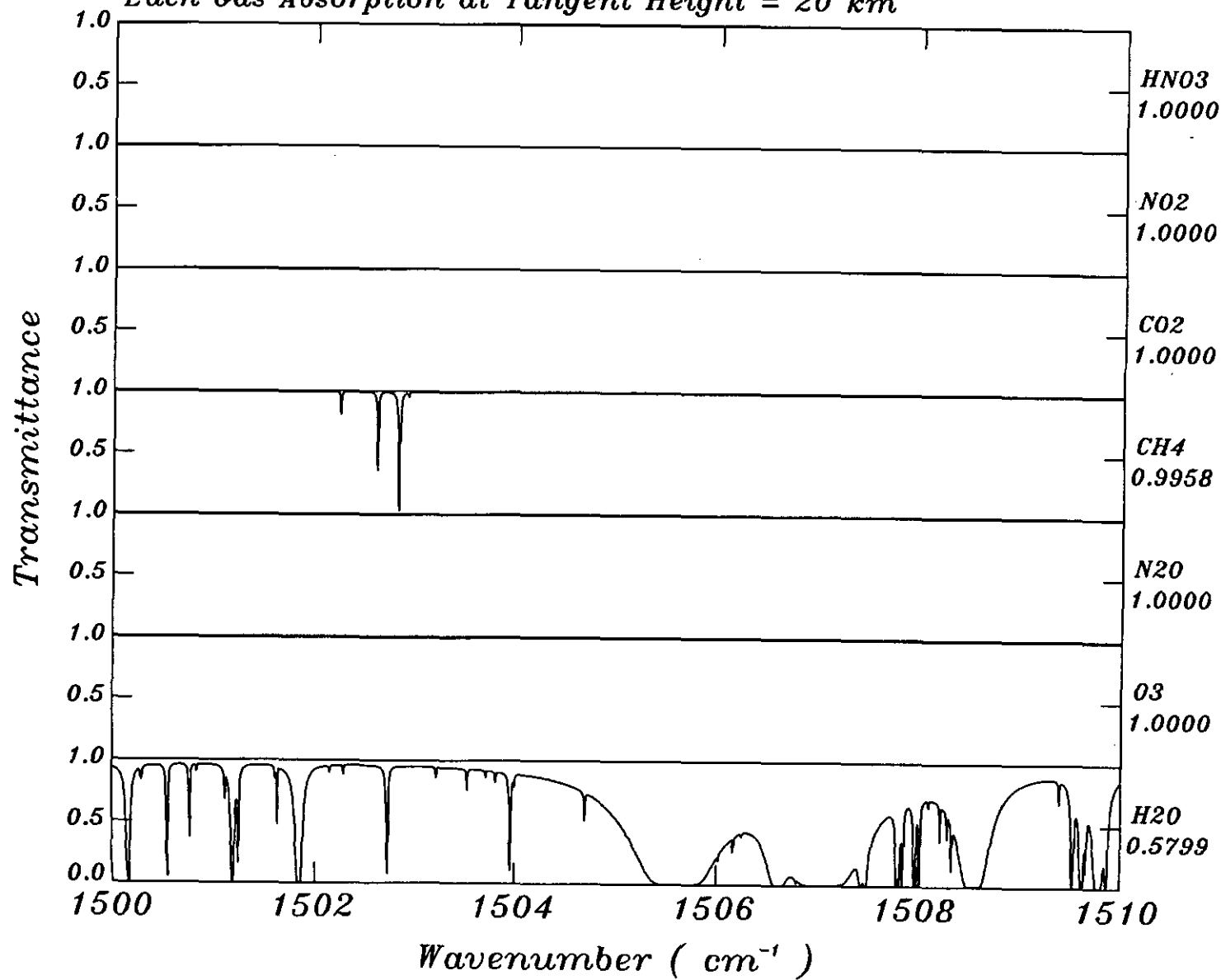
Each Gas Absorption at Tangent Height = 20 km

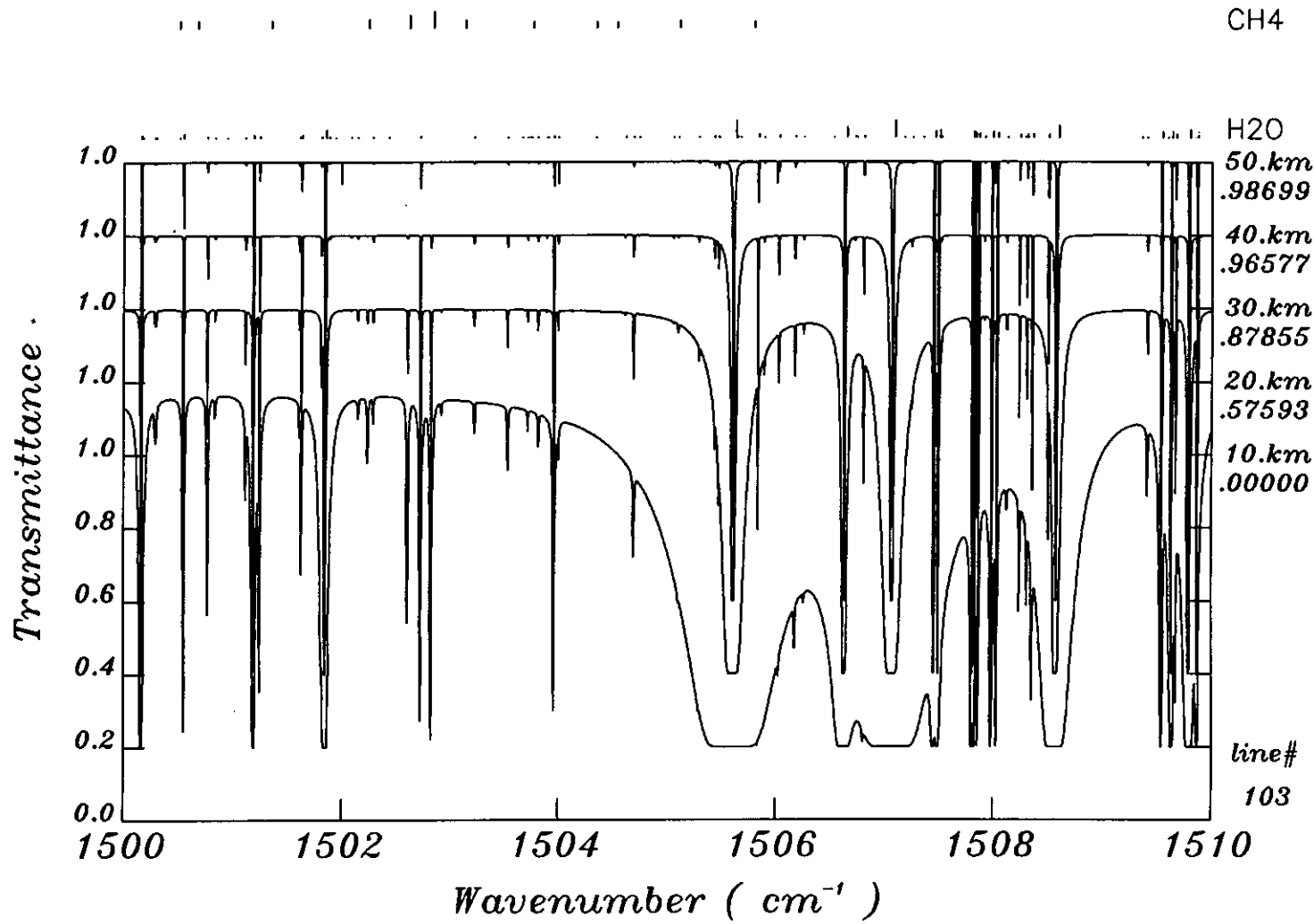




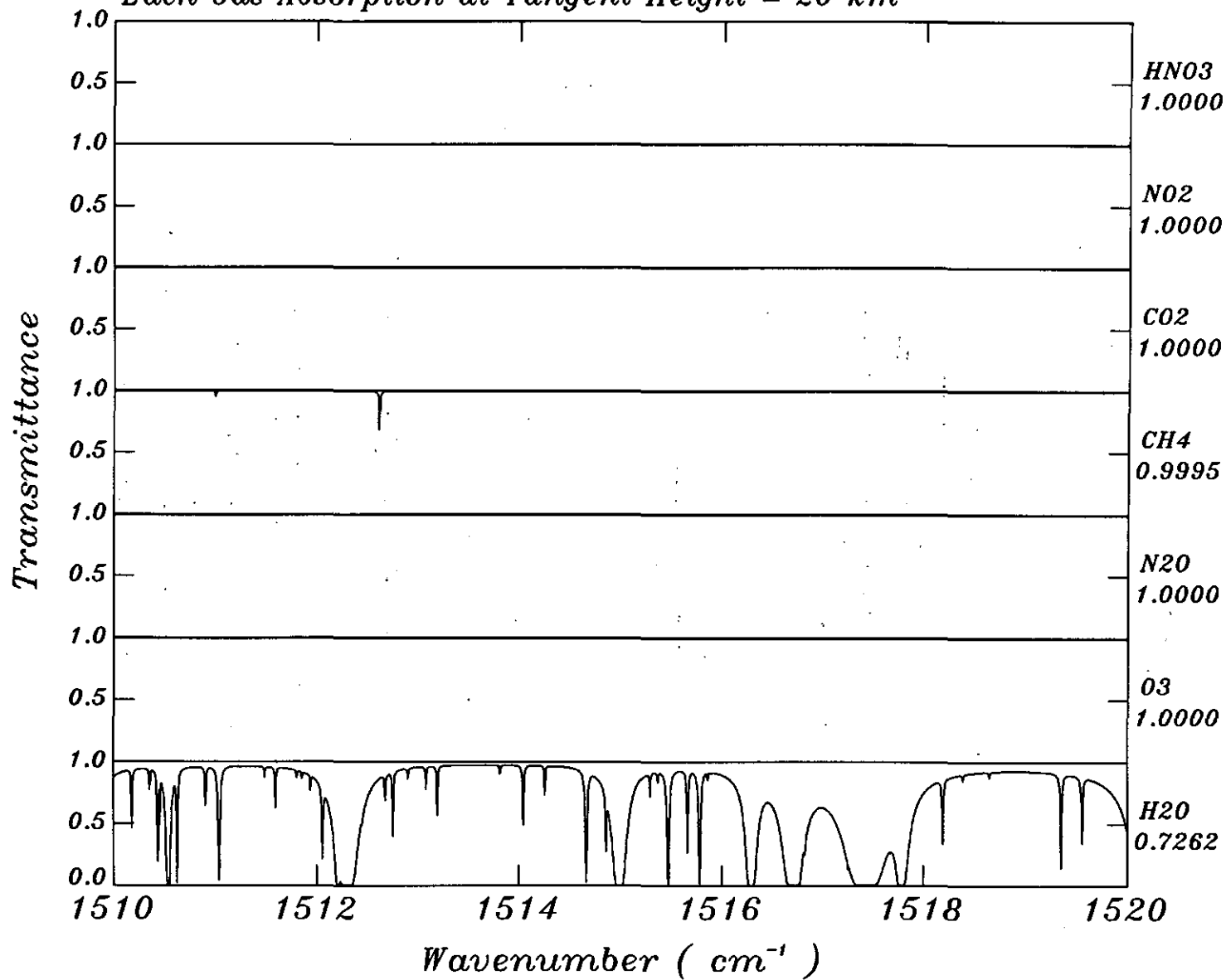


Each Gas Absorption at Tangent Height = 20 km

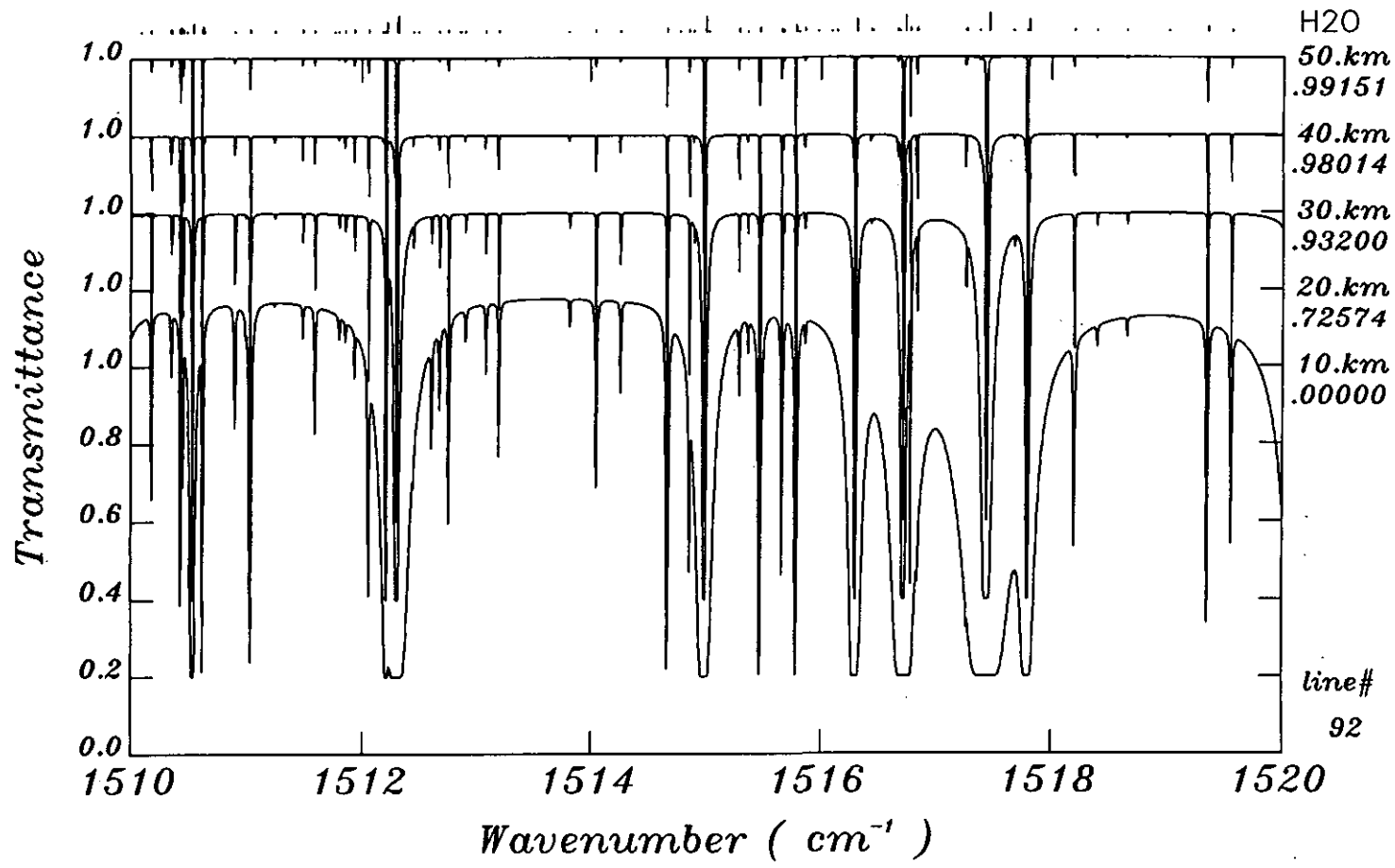


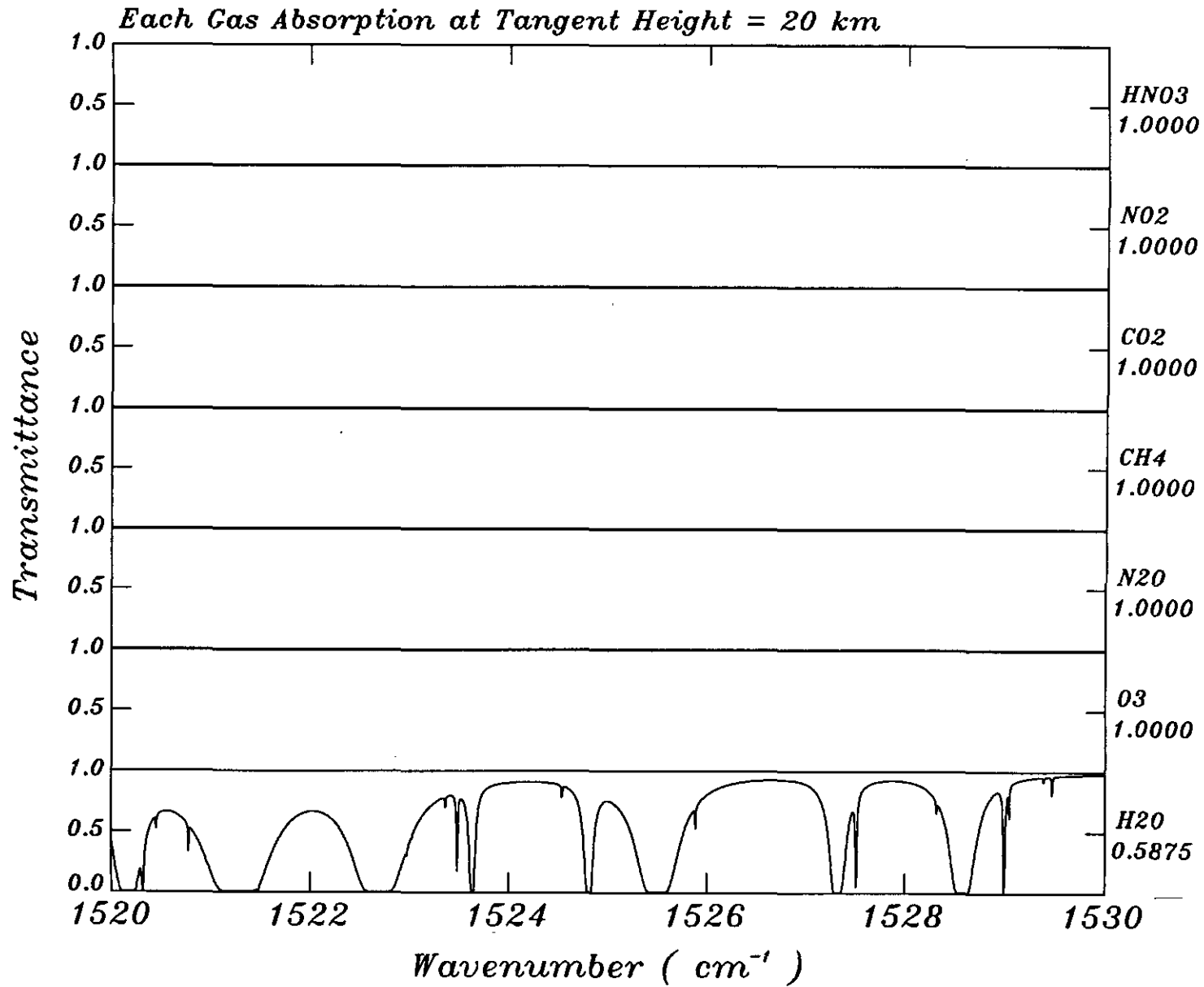


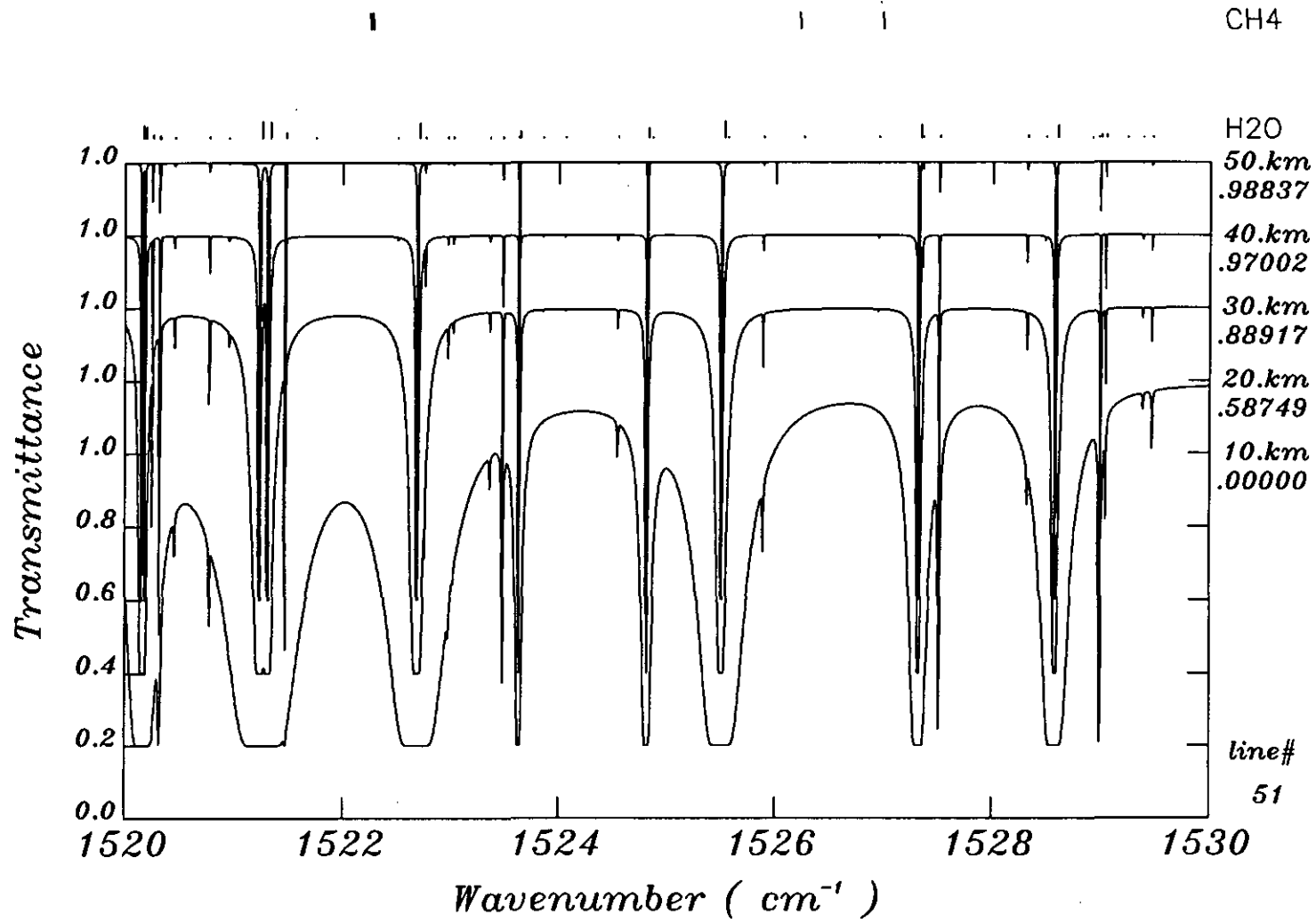
Each Gas Absorption at Tangent Height = 20 km

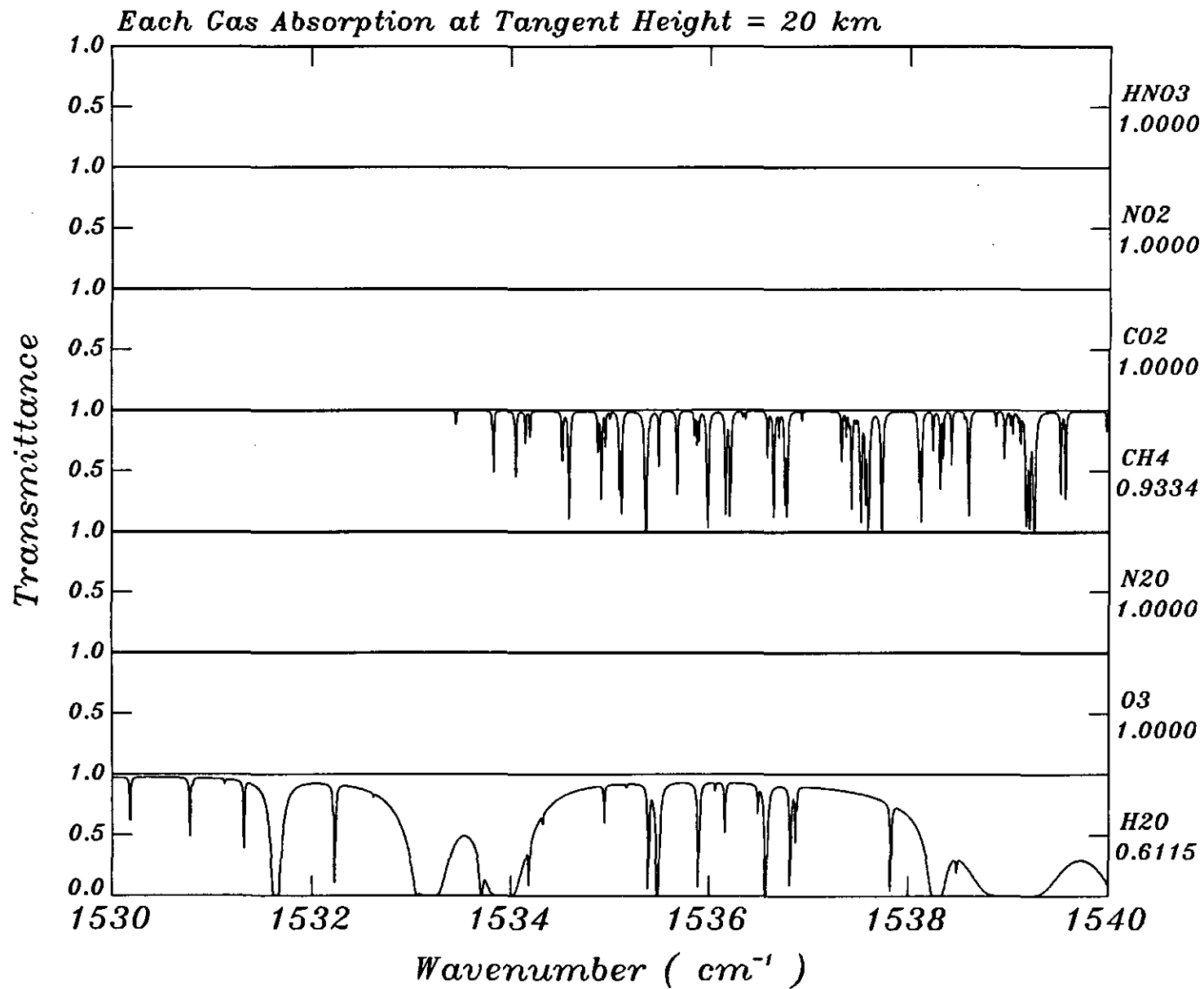


CH4



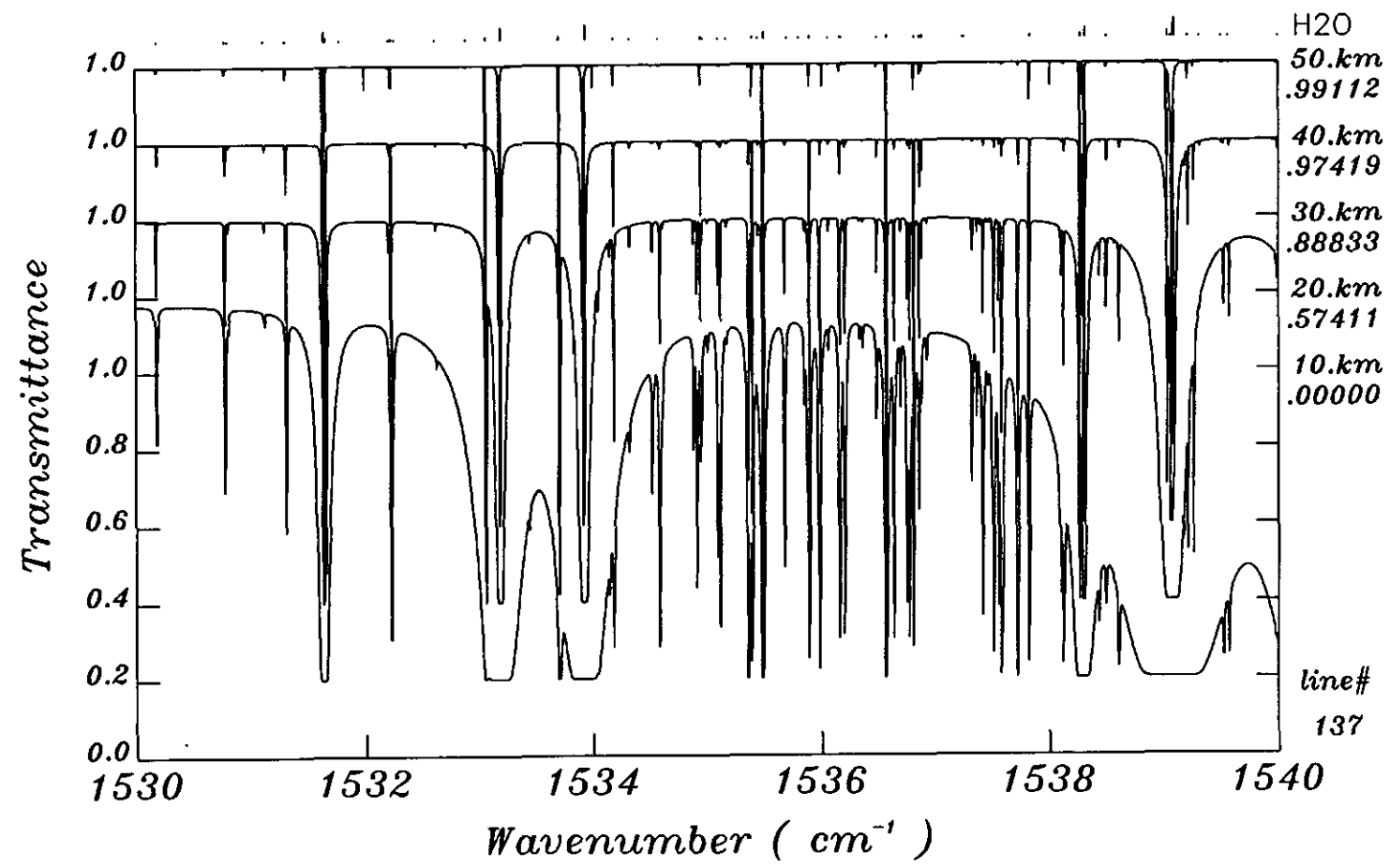


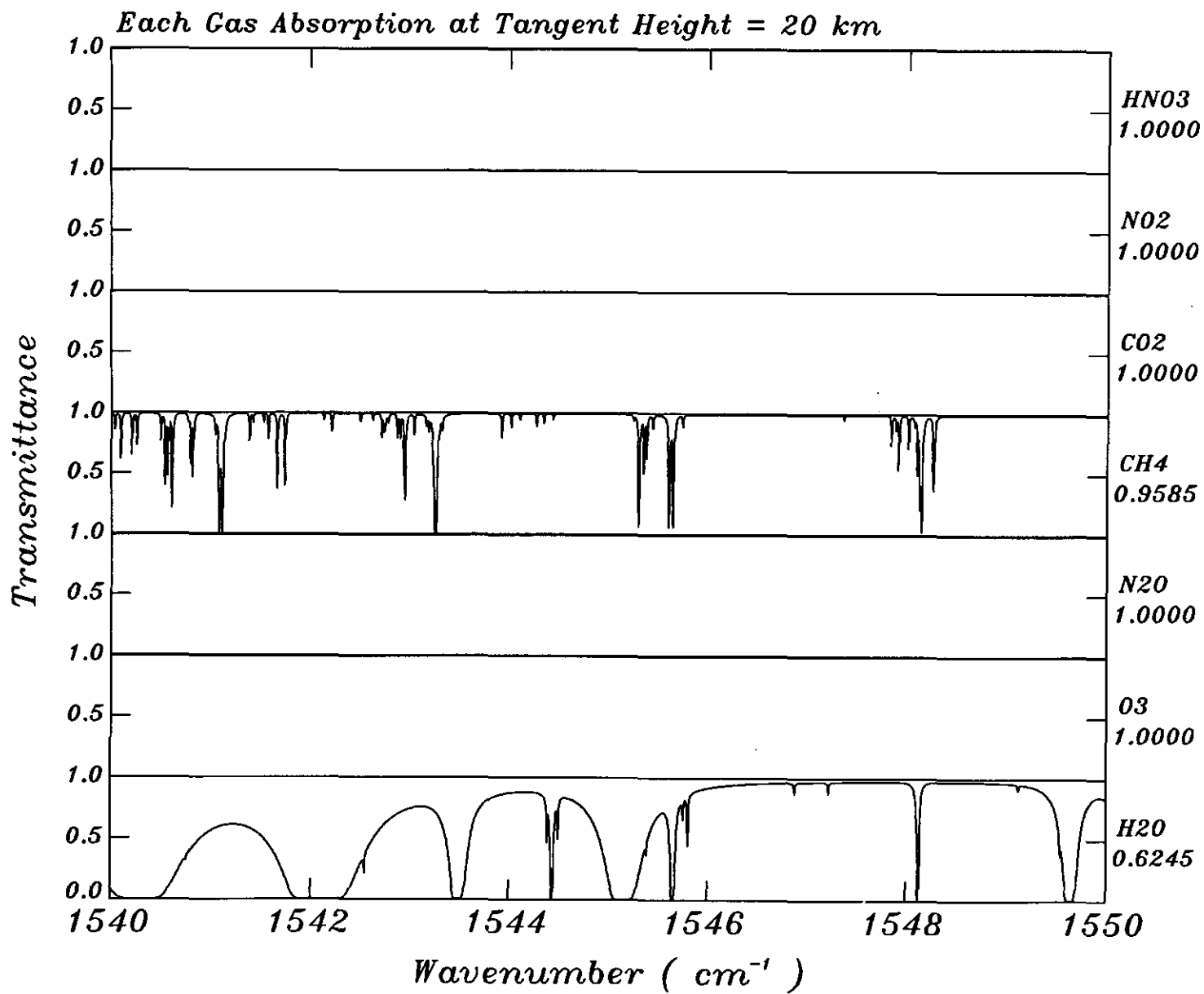


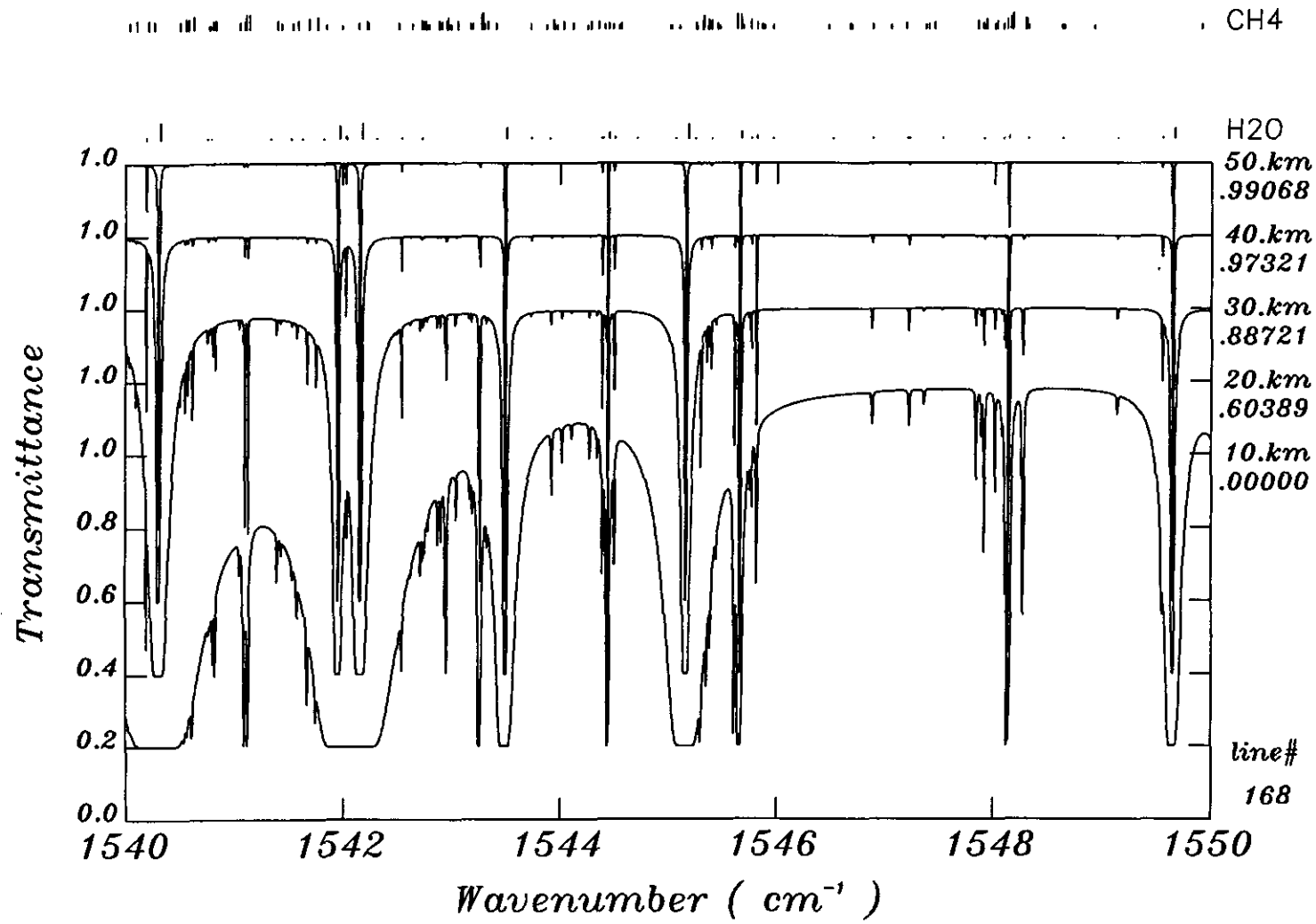




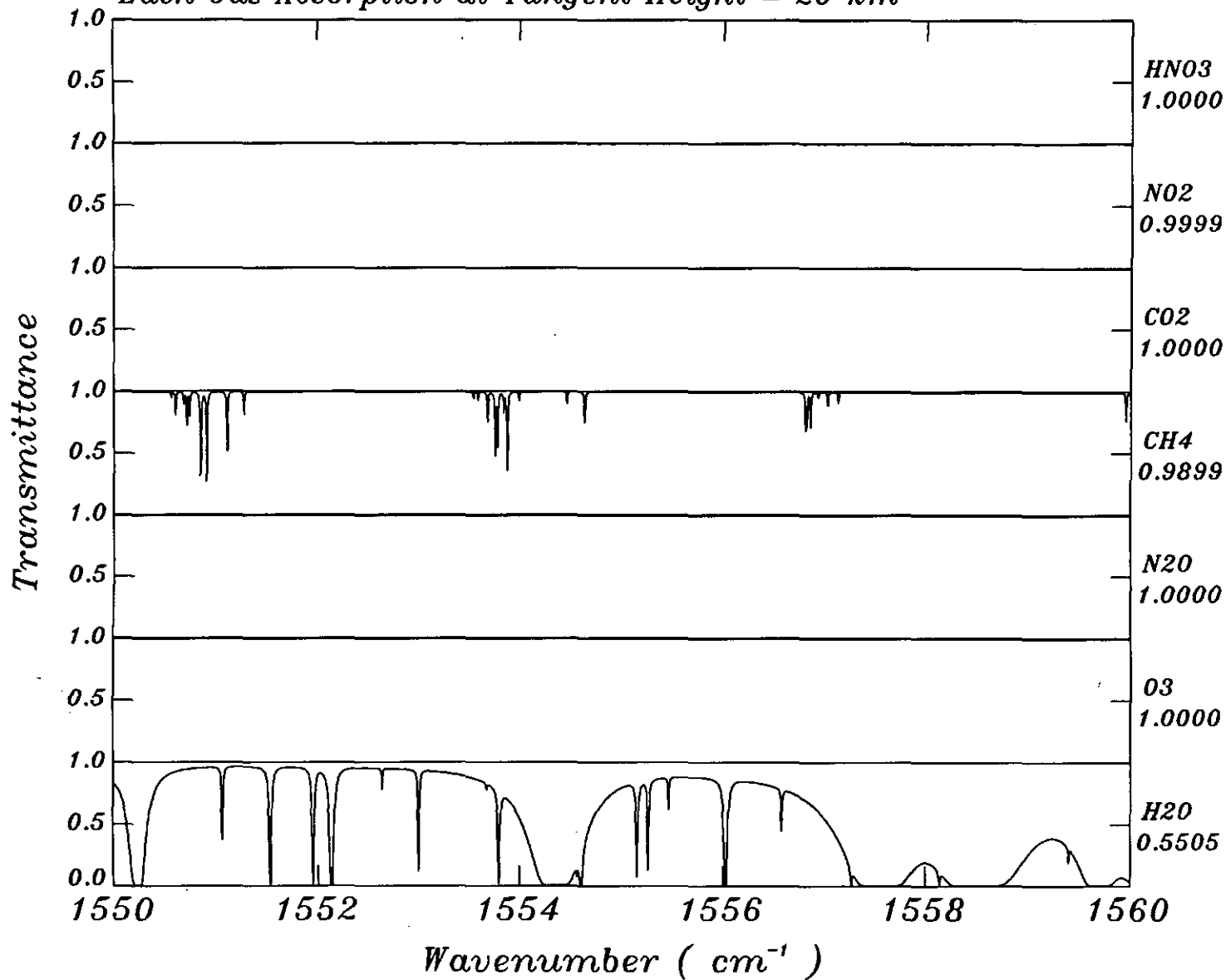
CH4

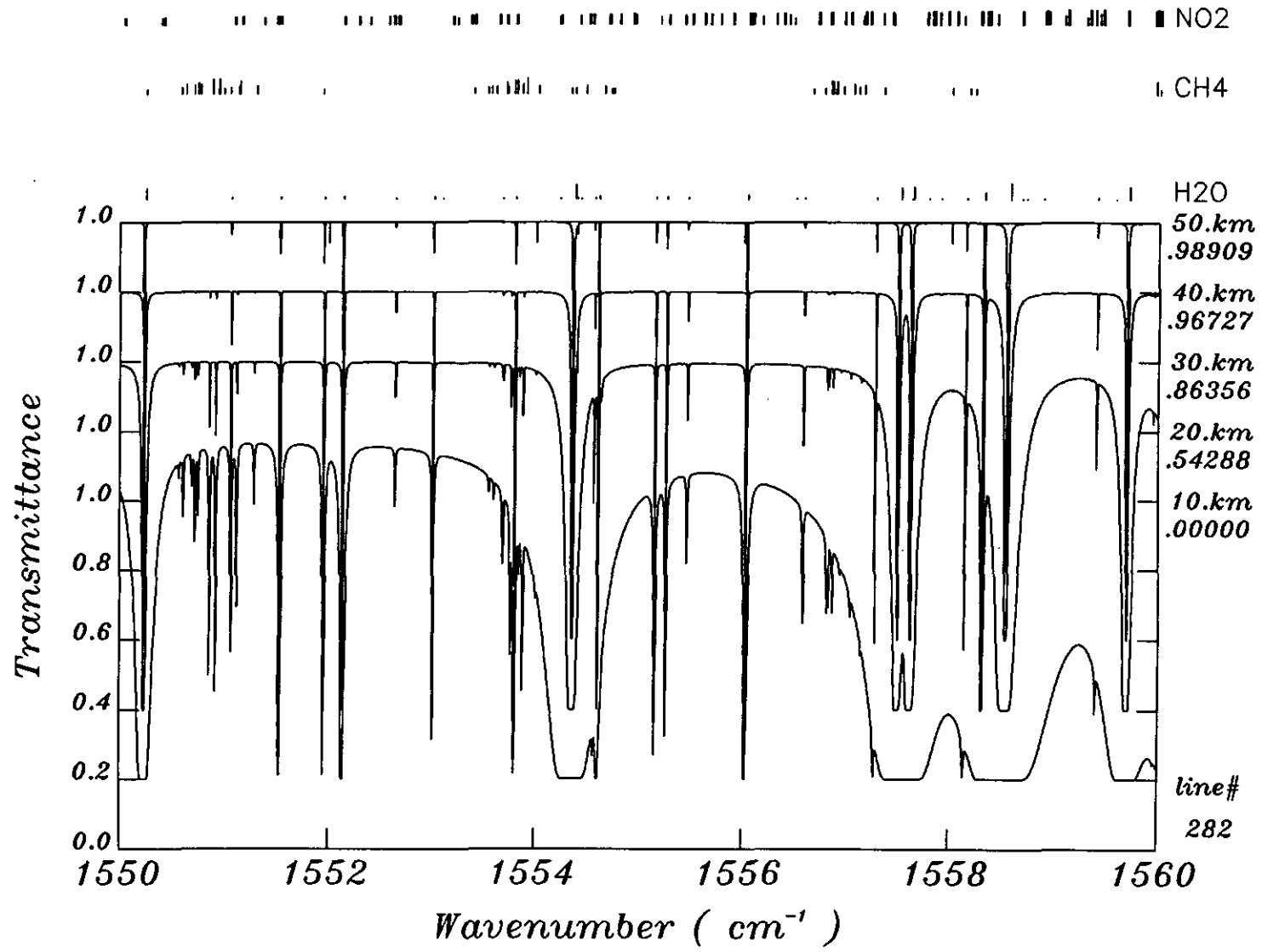


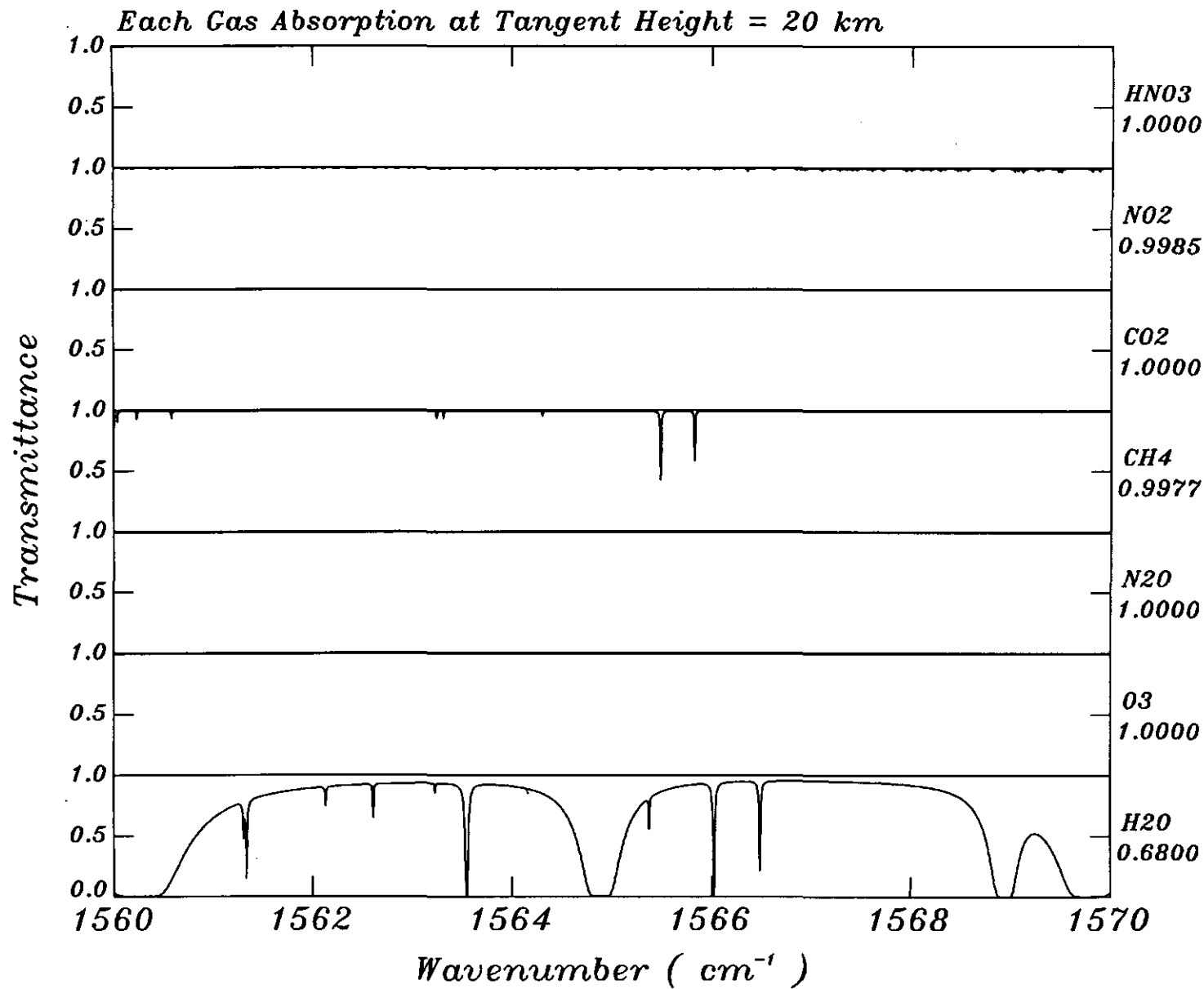


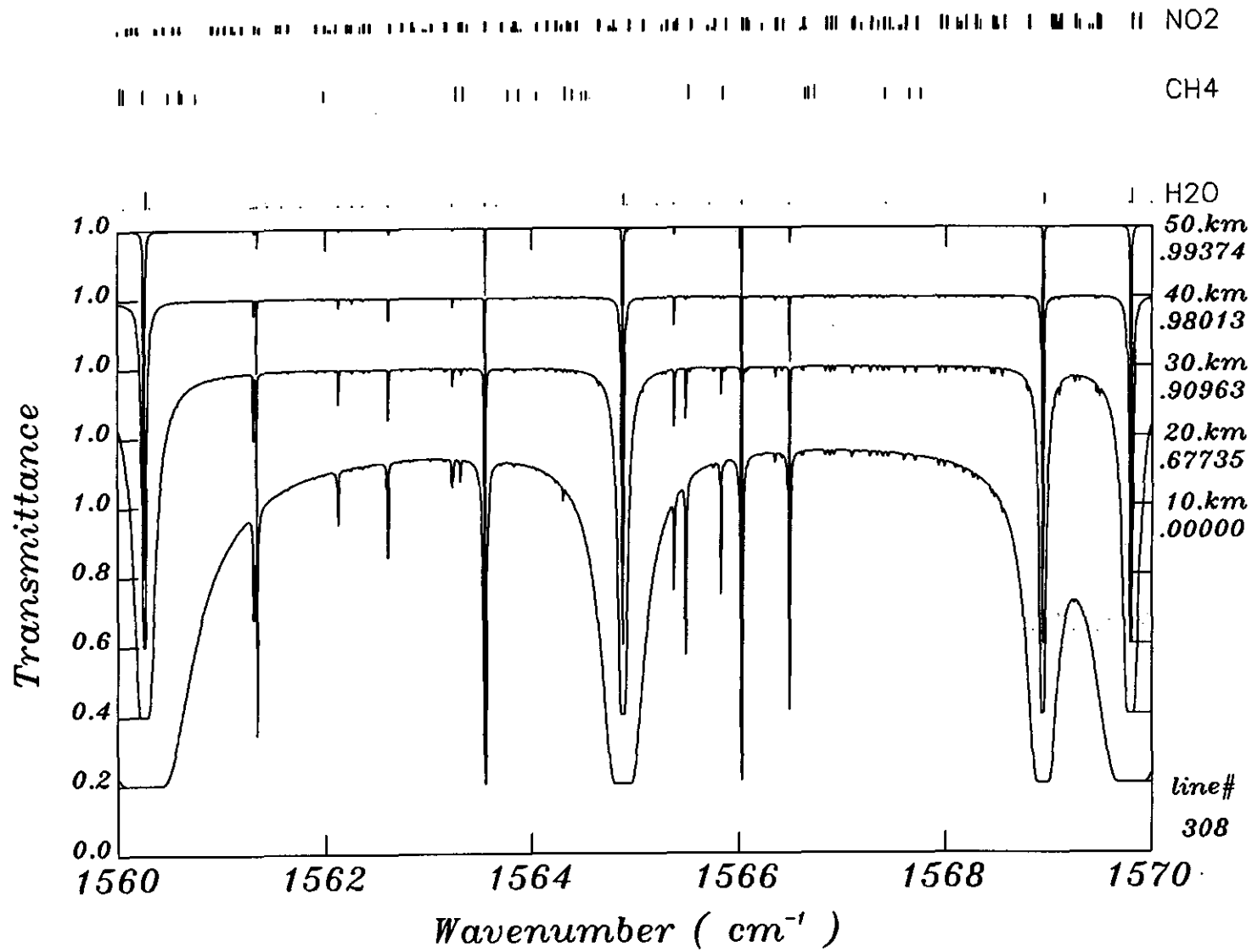


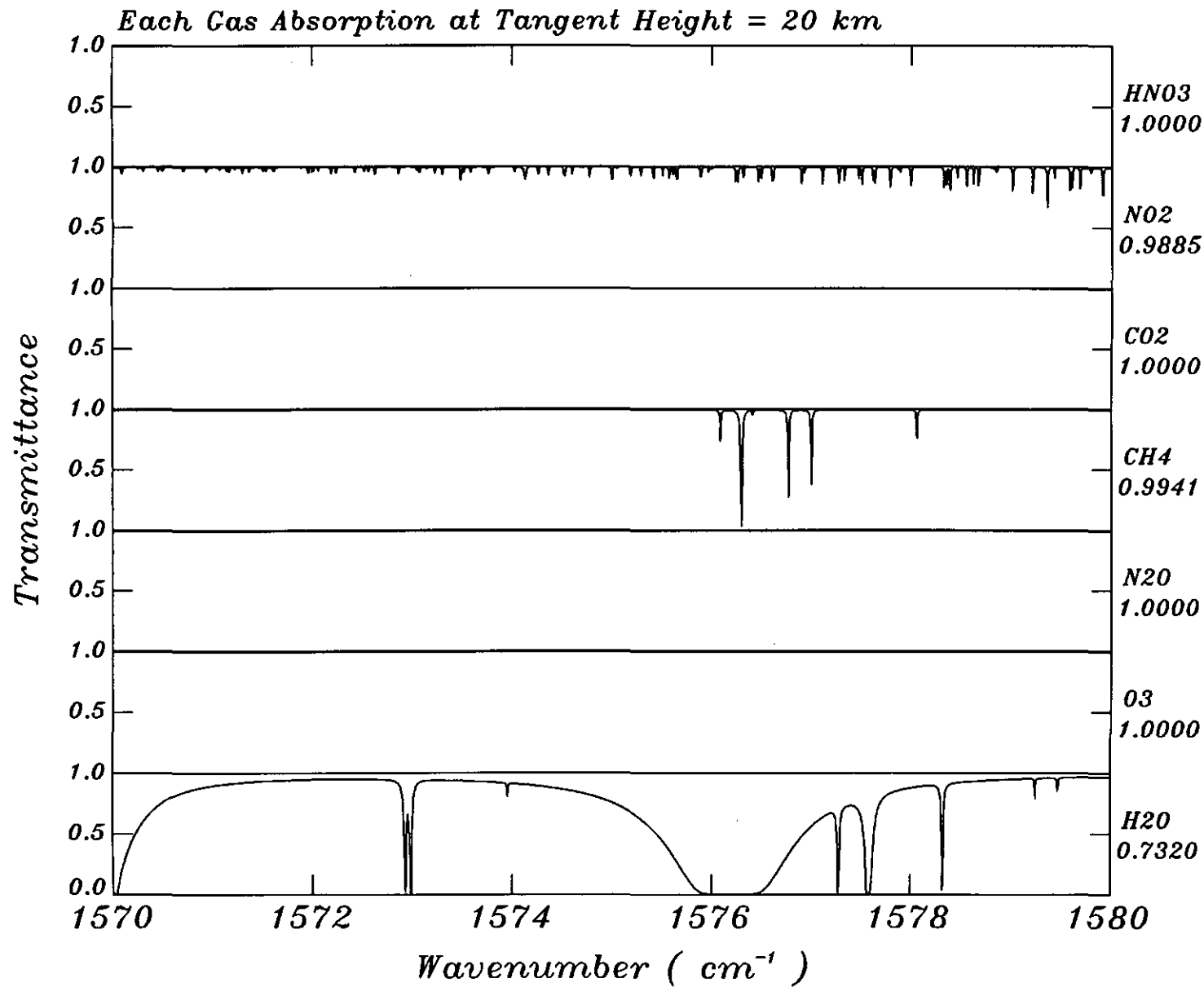
Each Gas Absorption at Tangent Height = 20 km







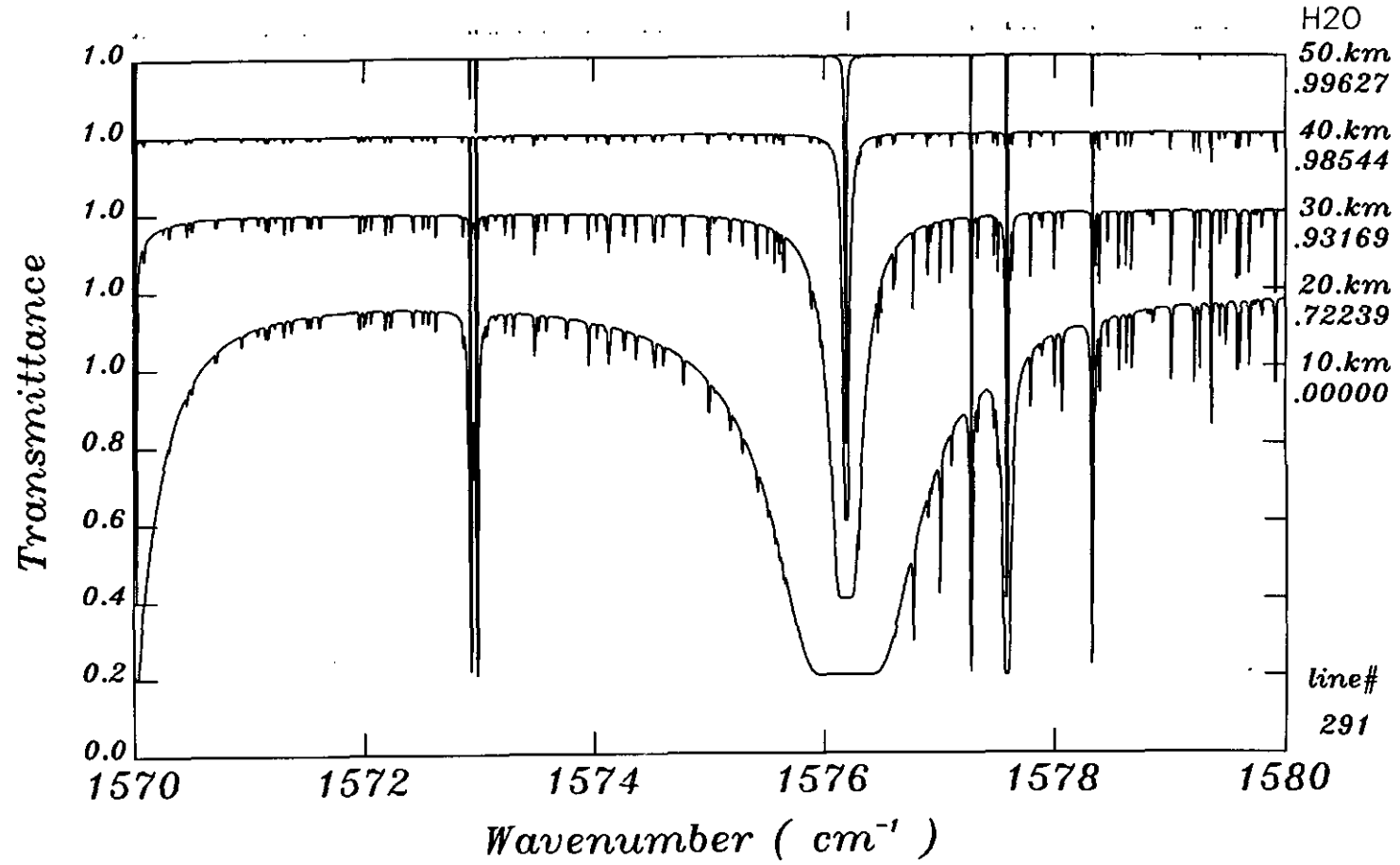


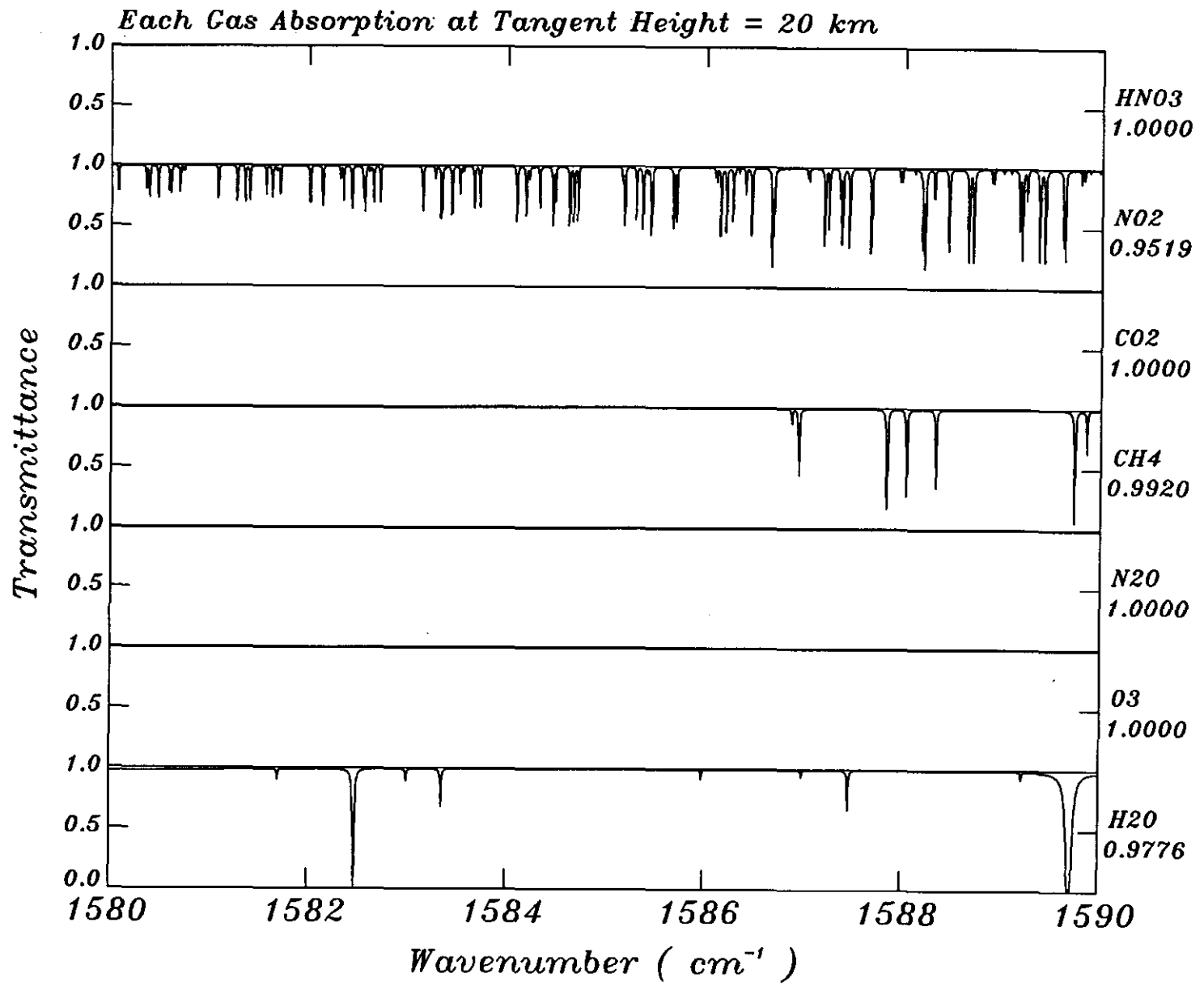




NO2

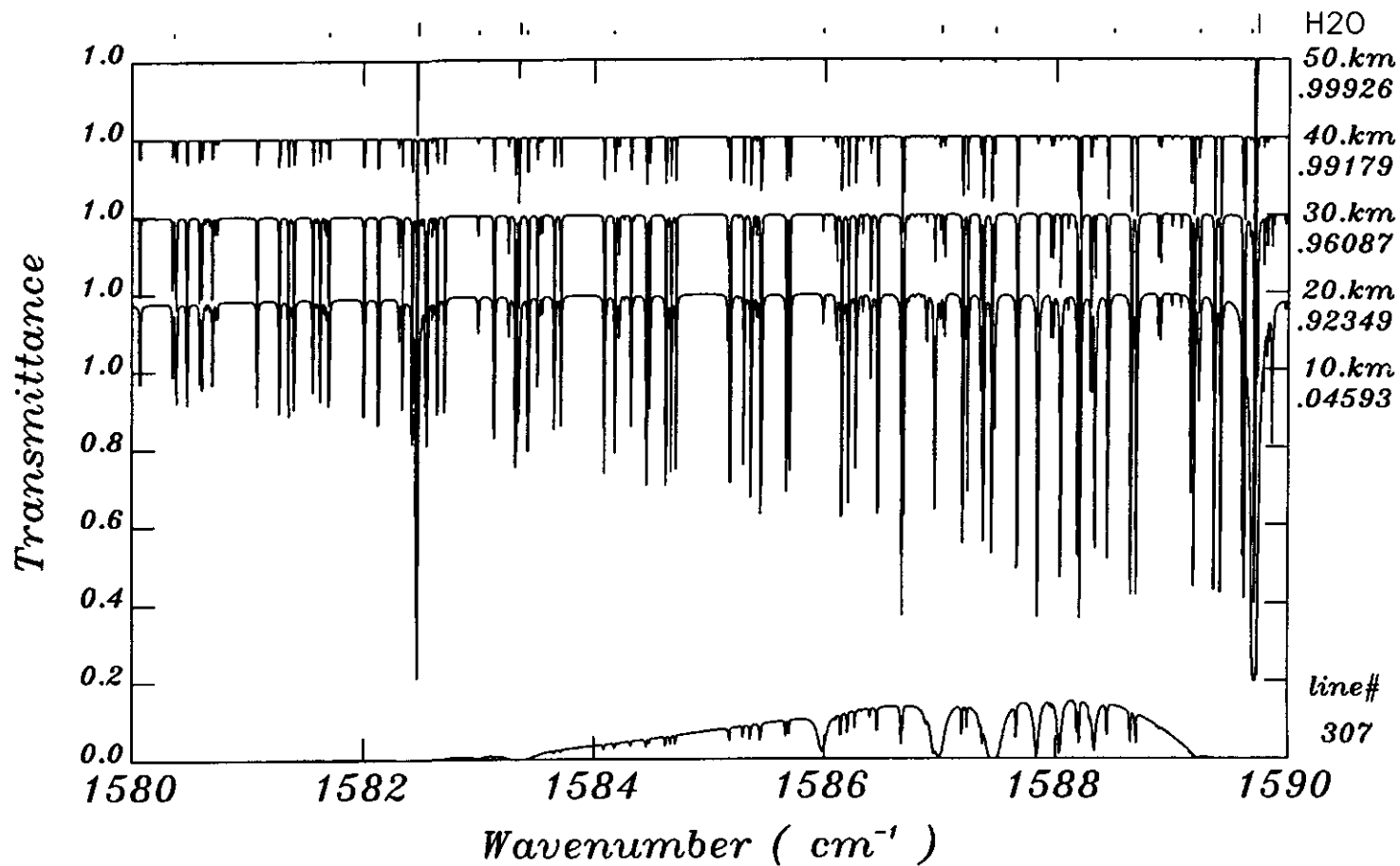
CH4

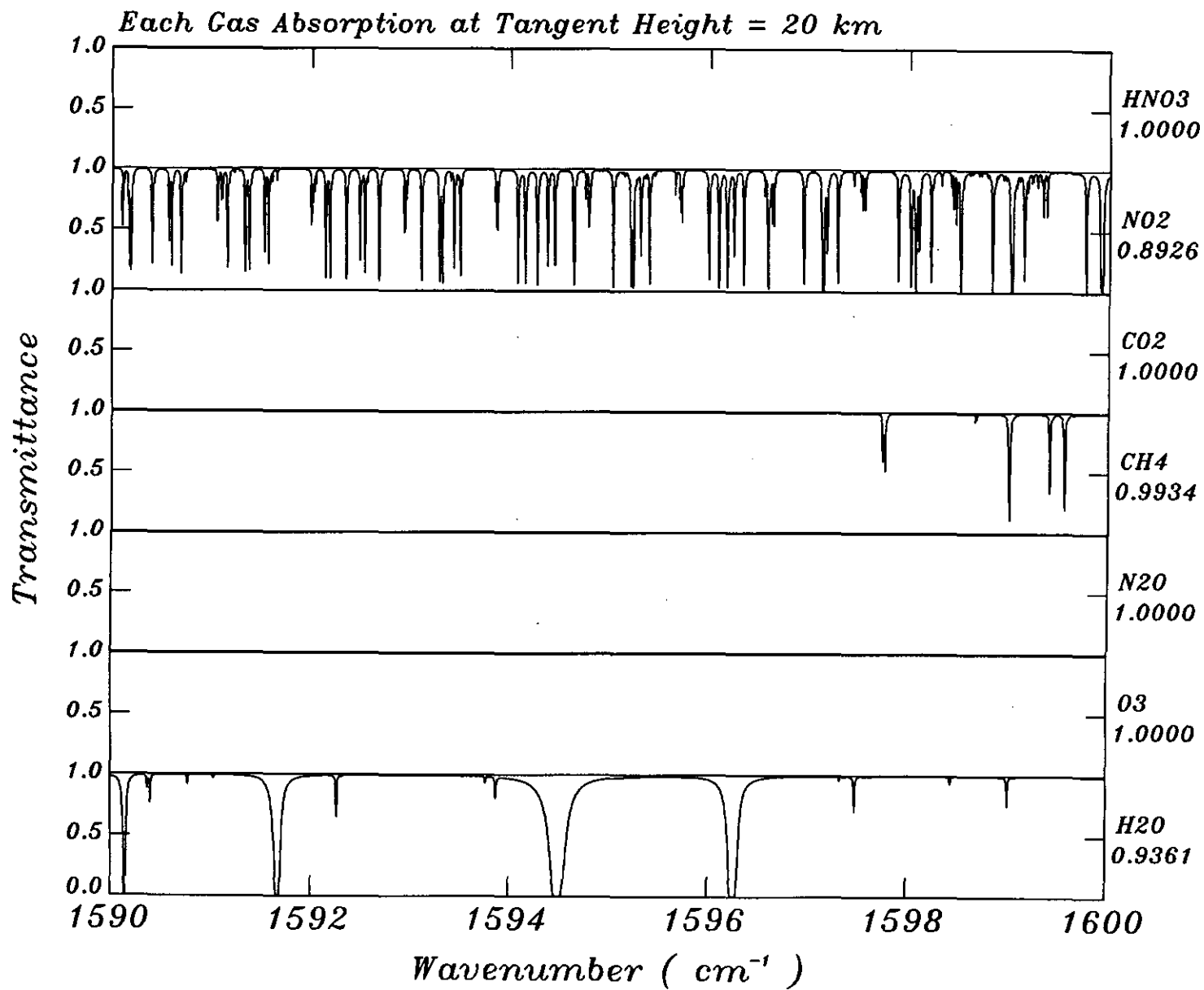




NO2

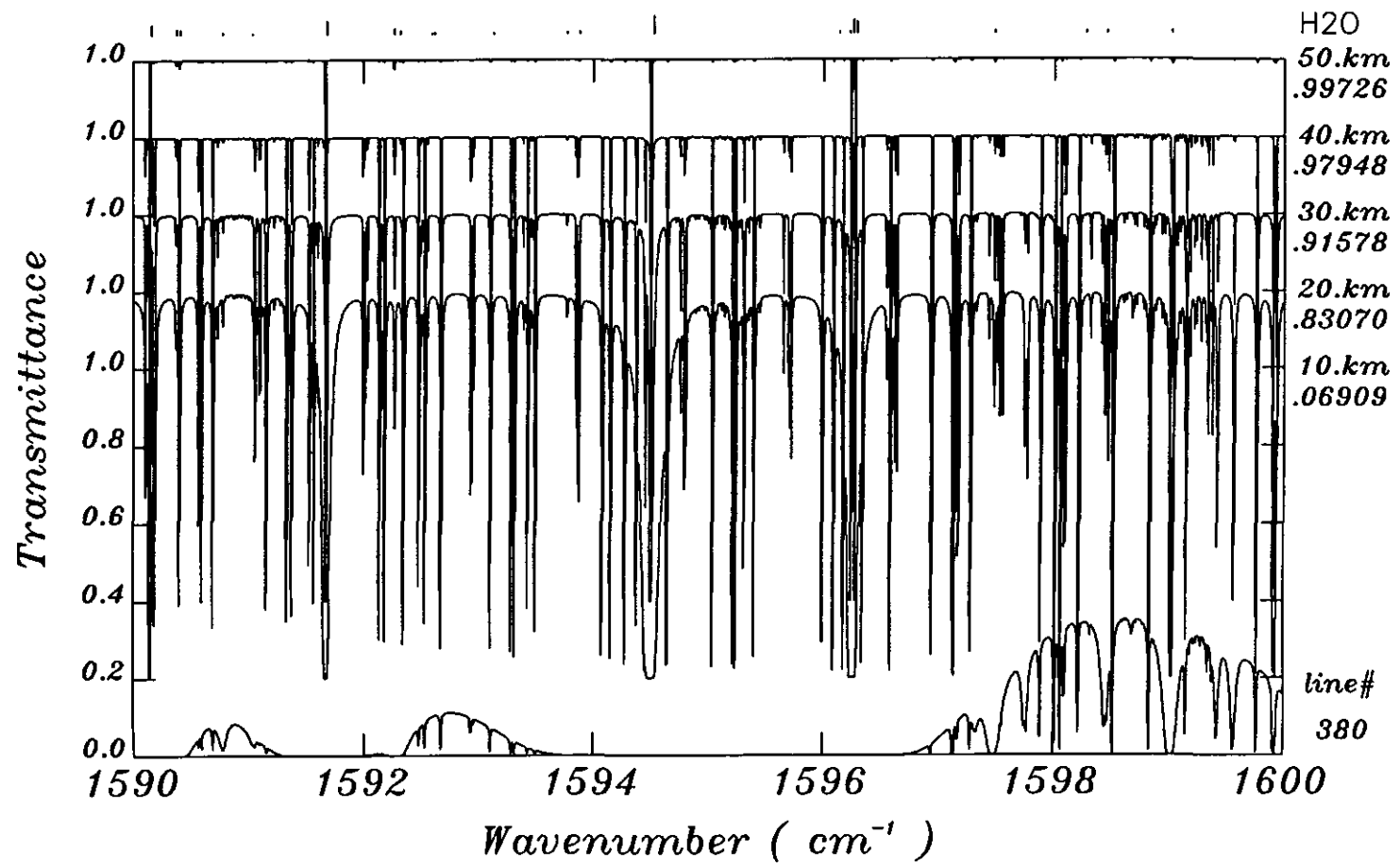
CH4

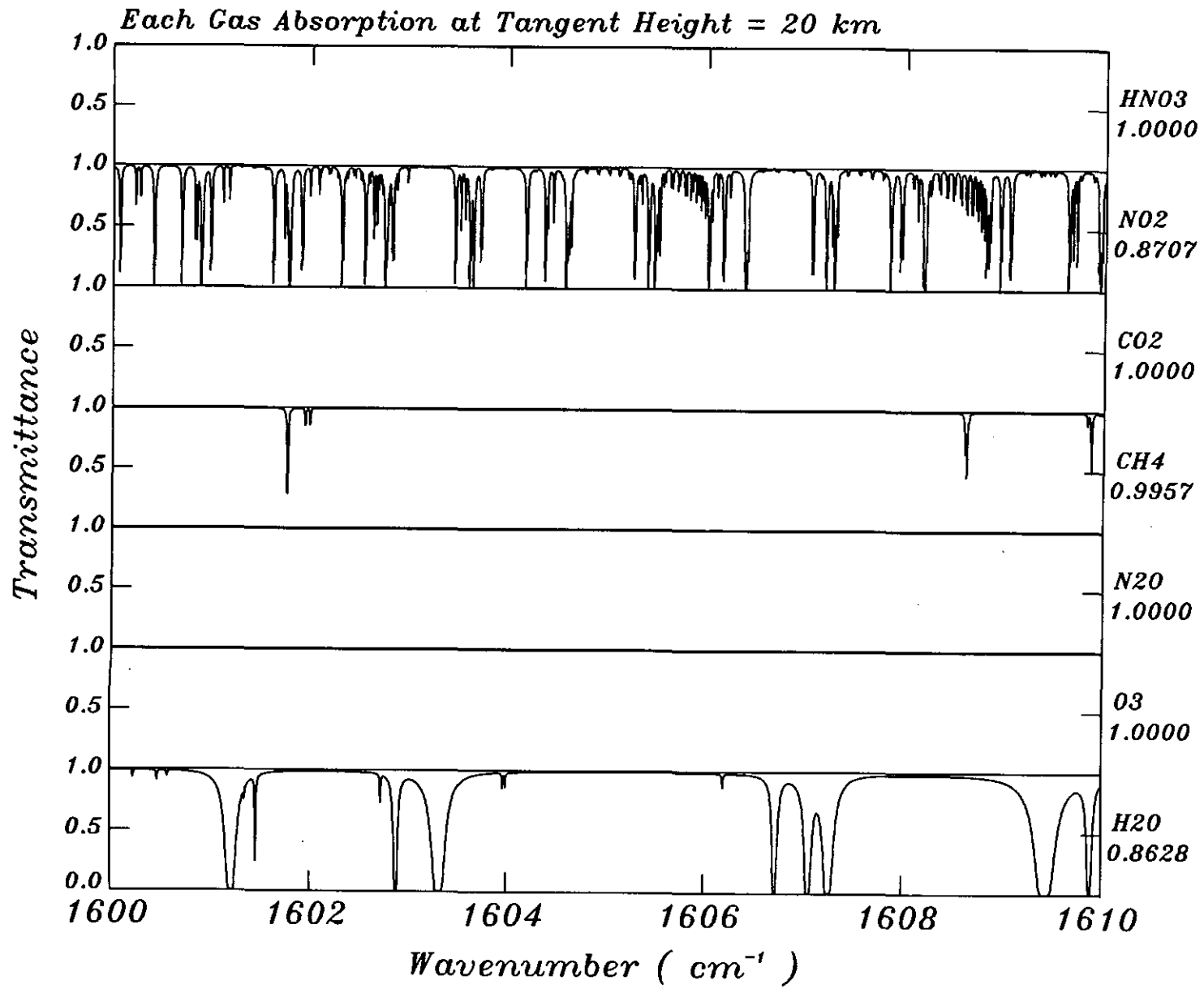


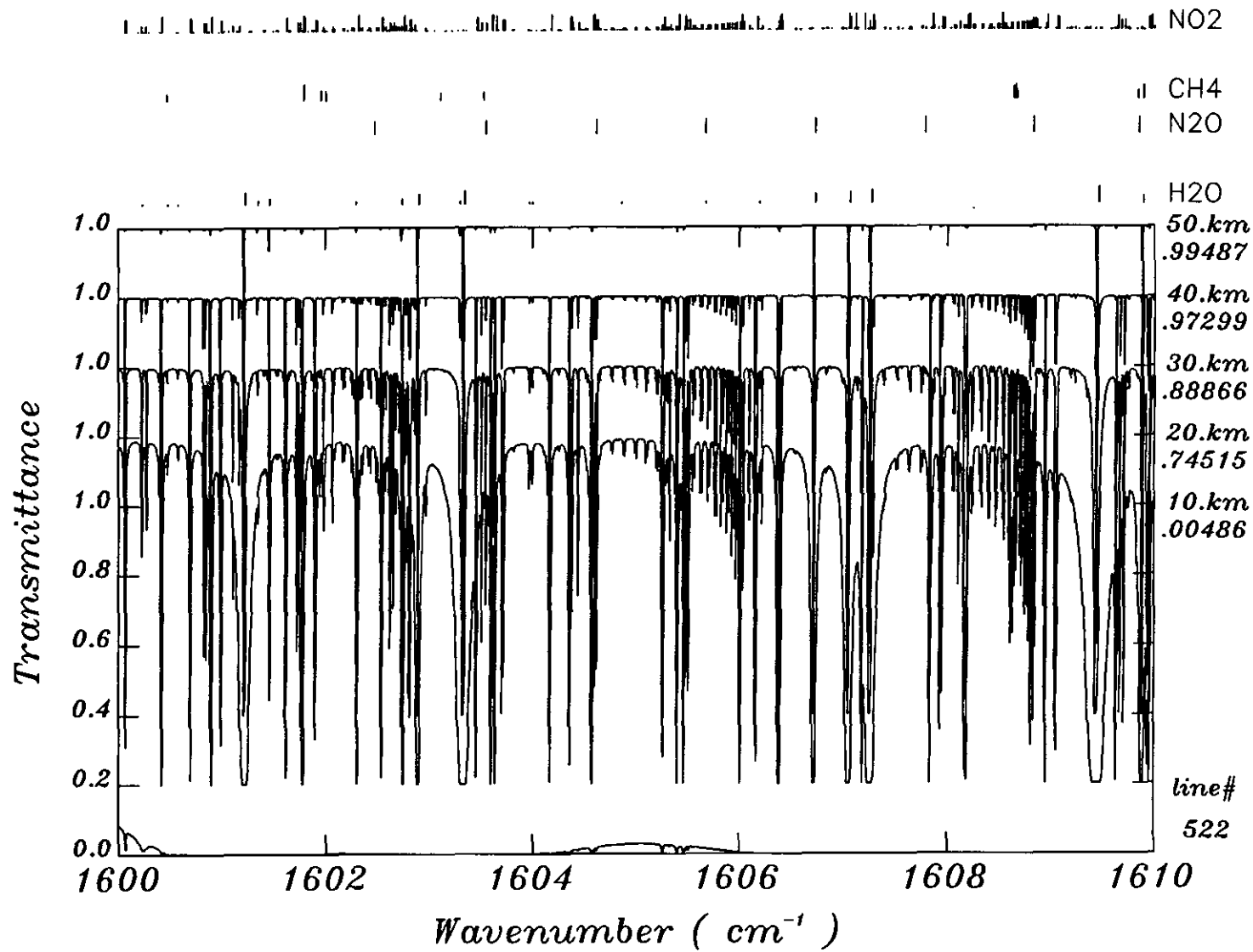


NO2

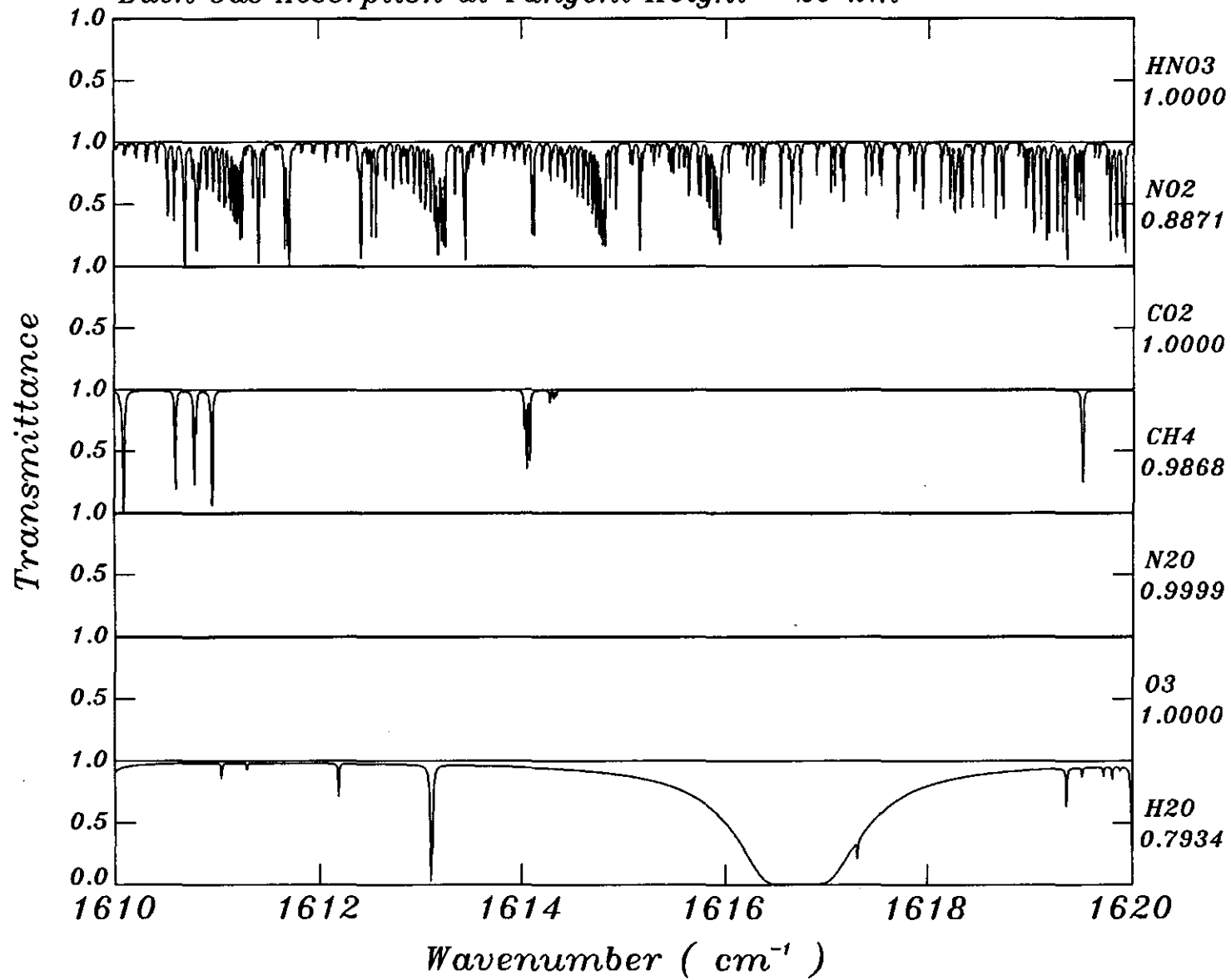
CH4



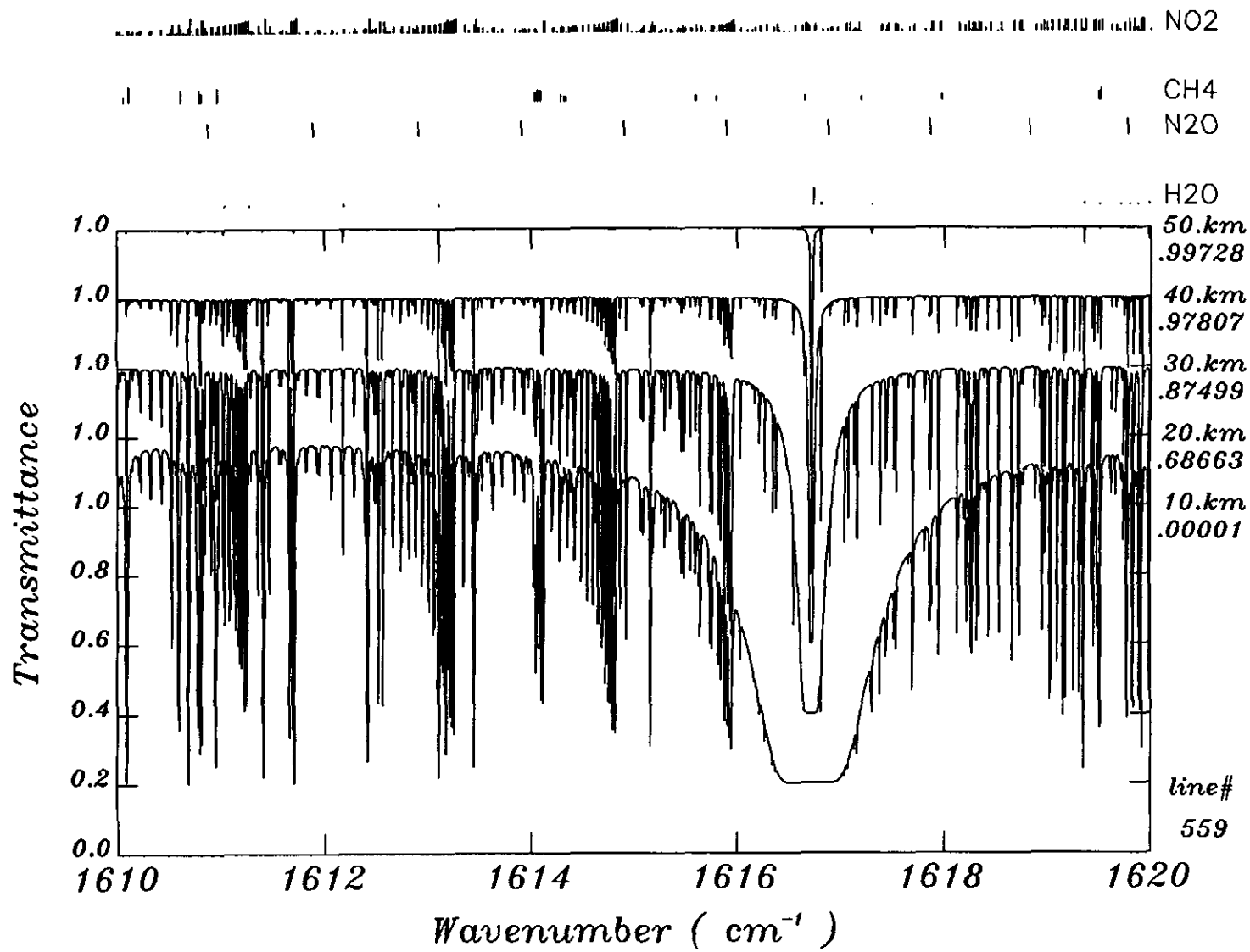




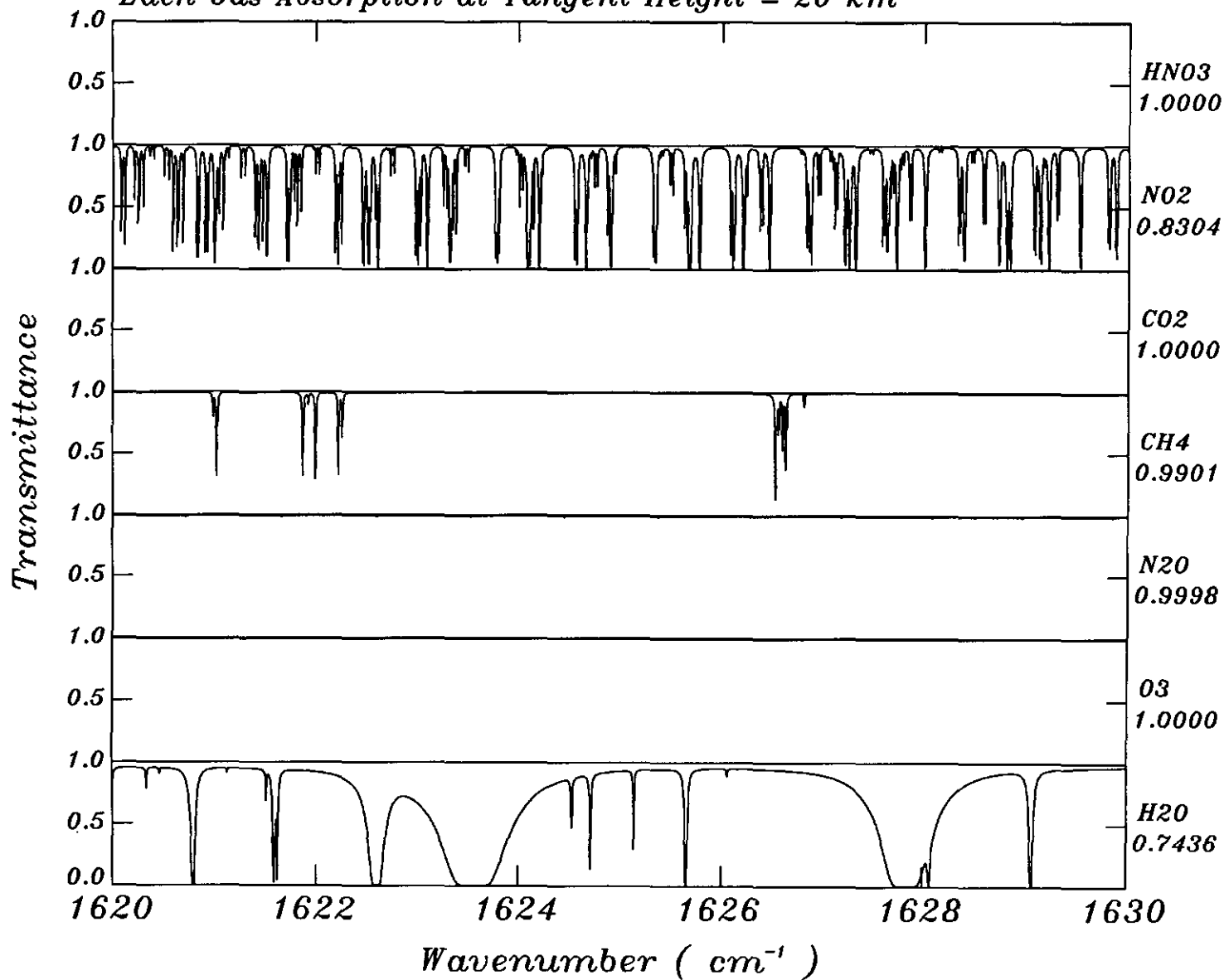
Each Gas Absorption at Tangent Height = 20 km

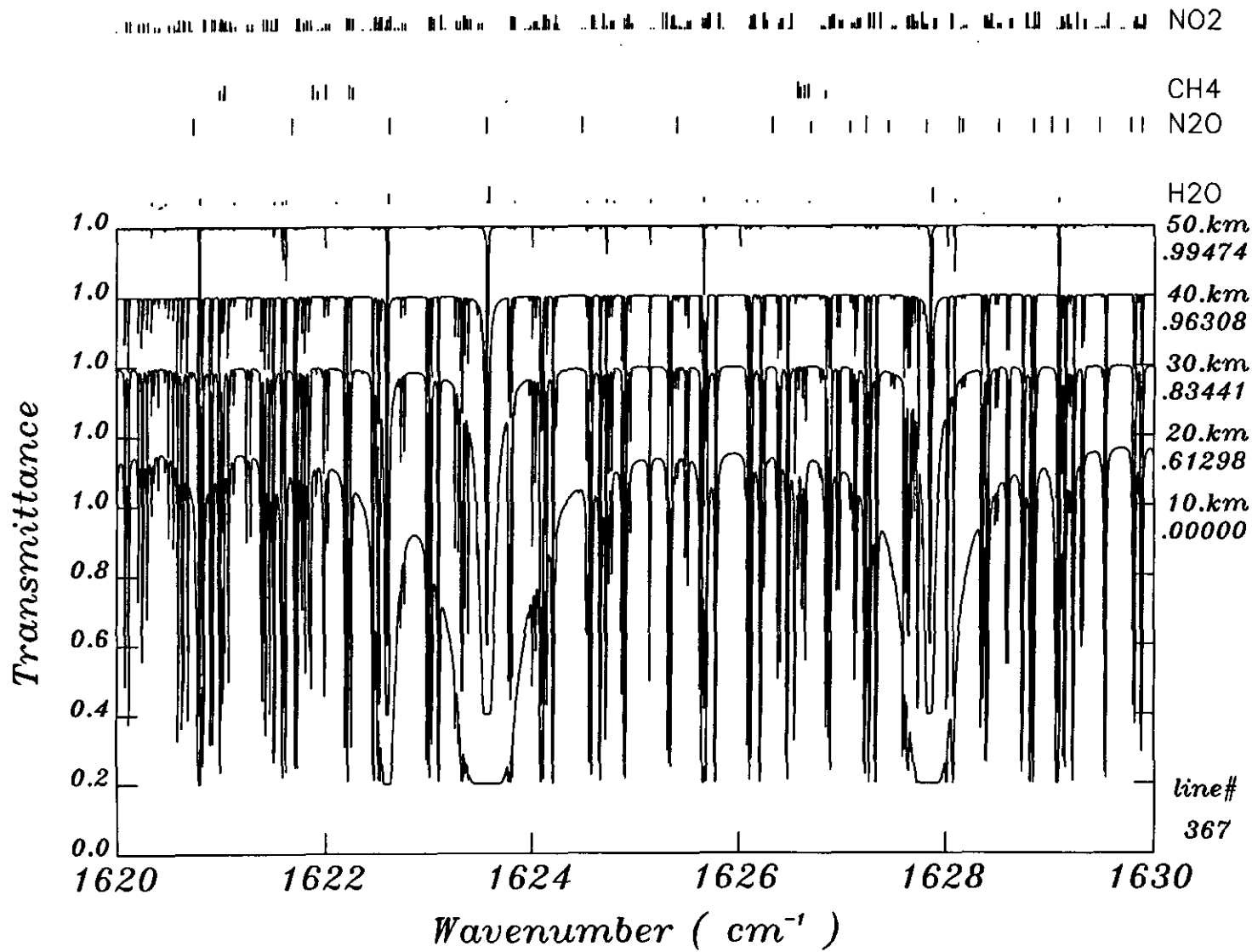




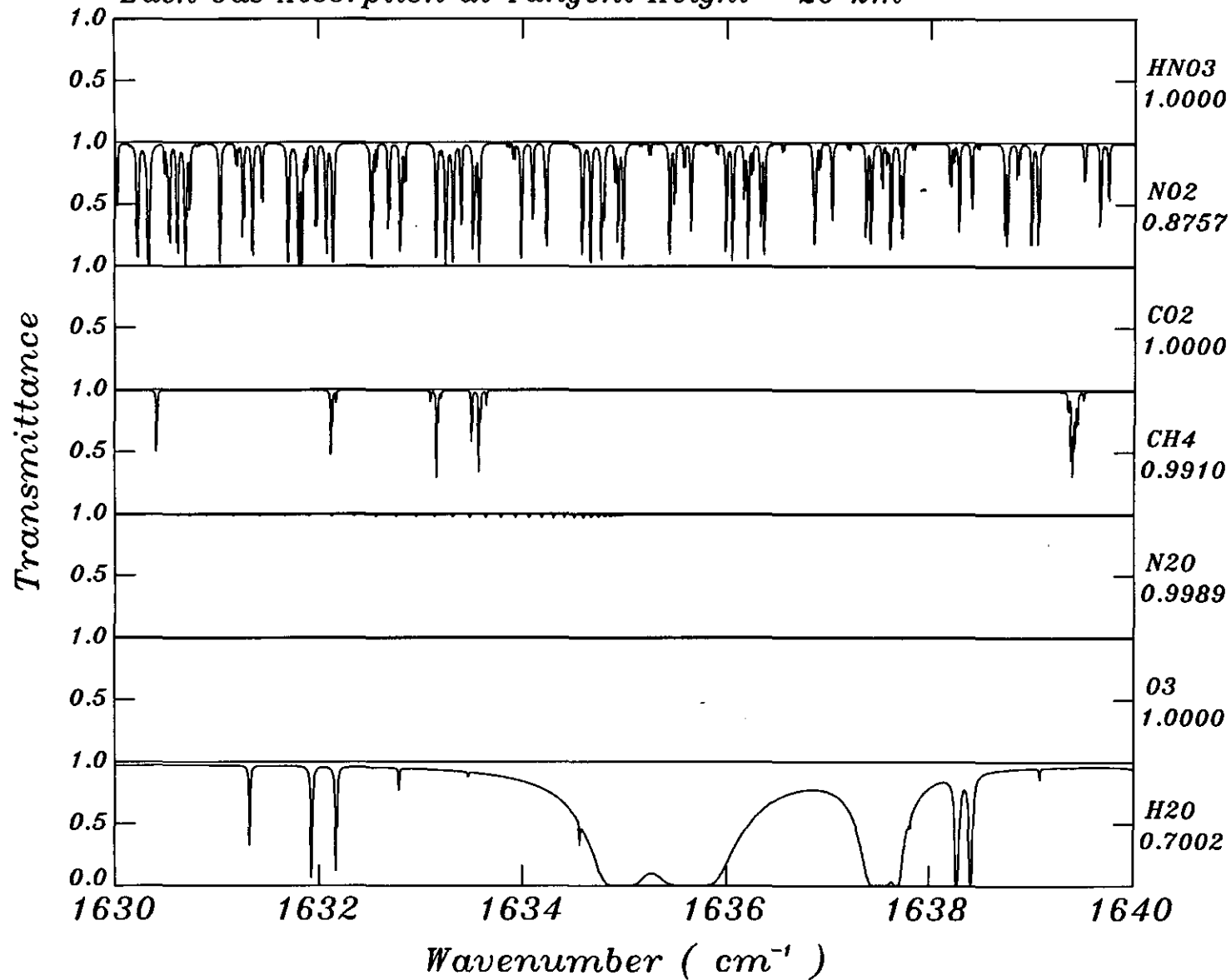


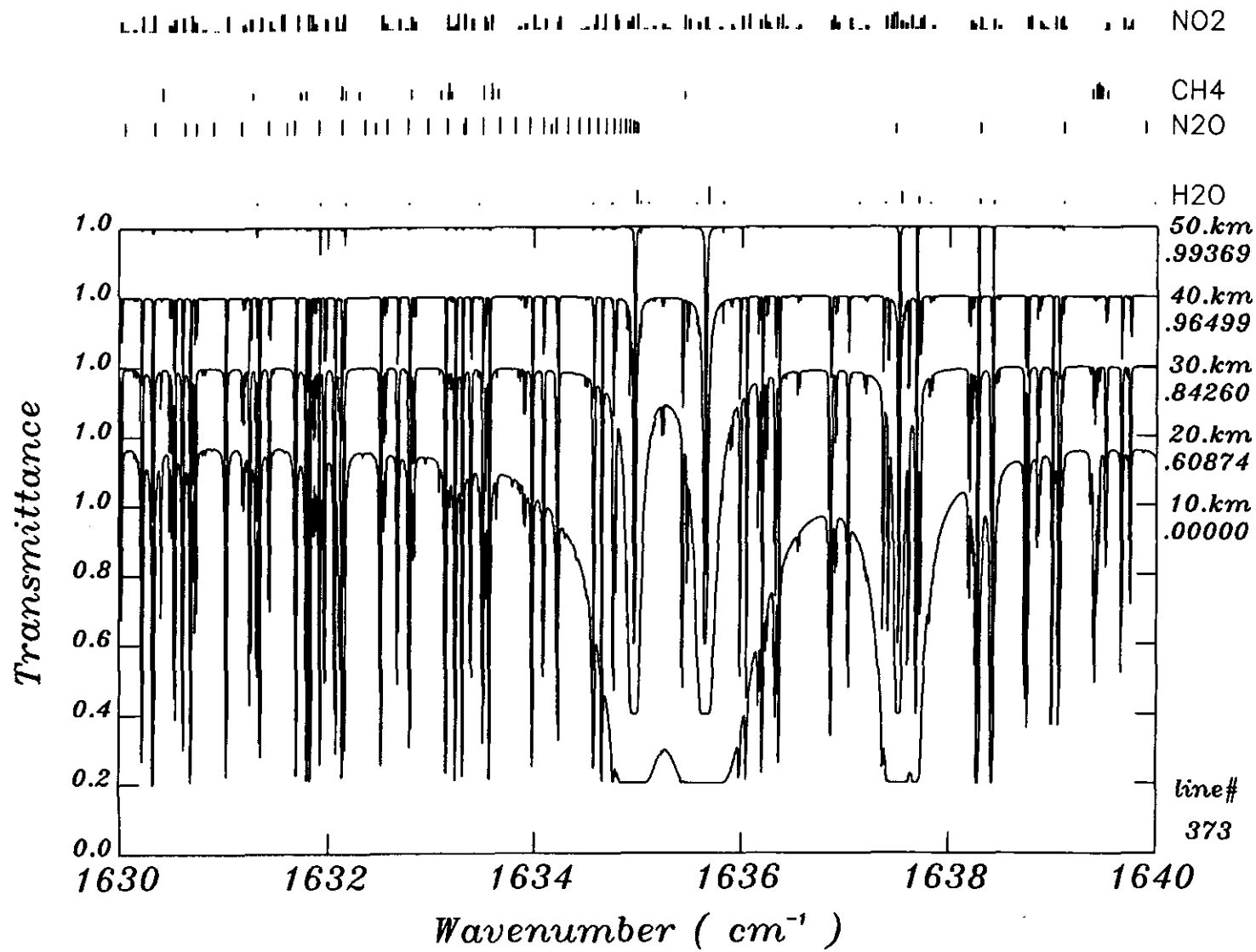
Each Gas Absorption at Tangent Height = 20 km

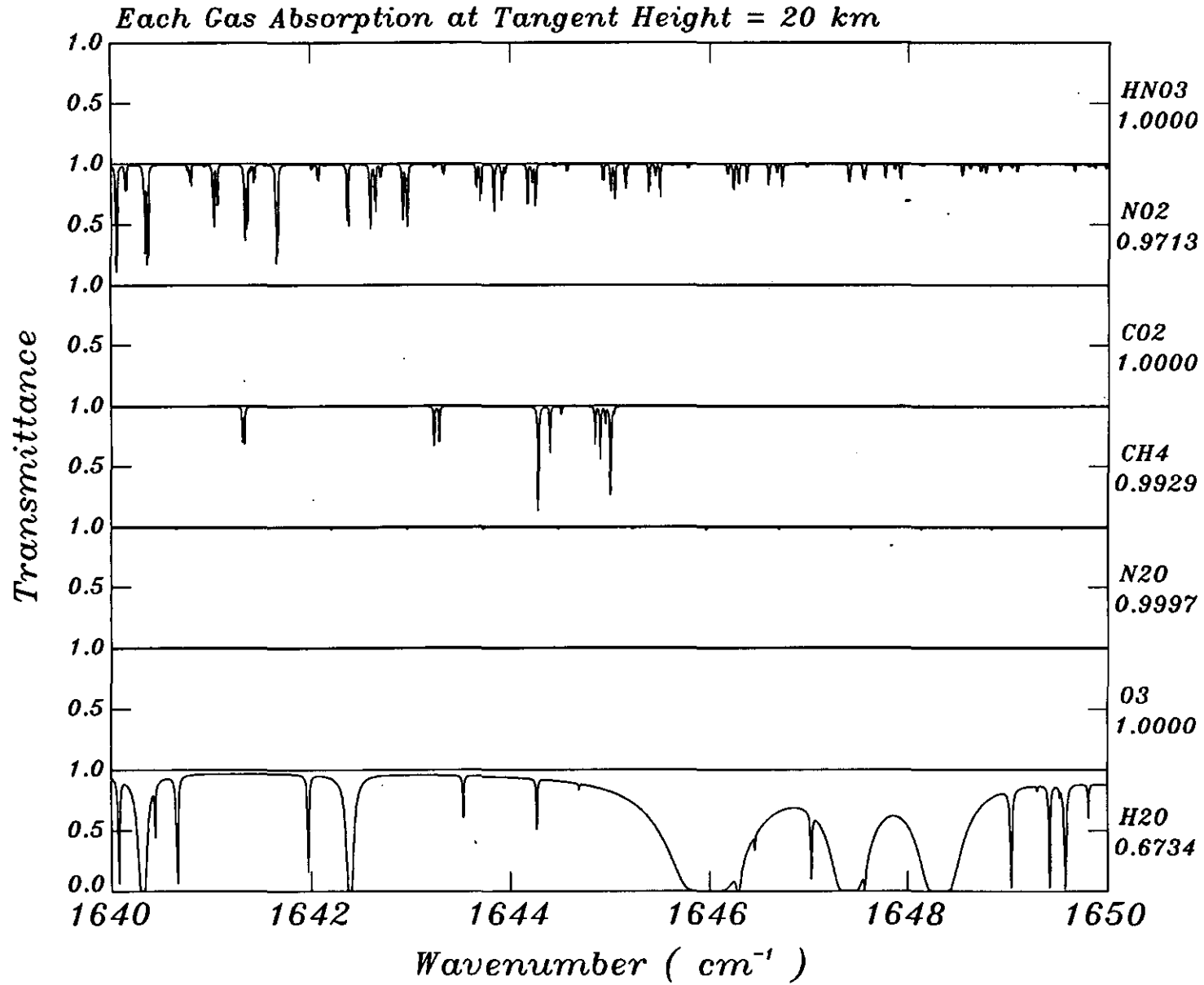


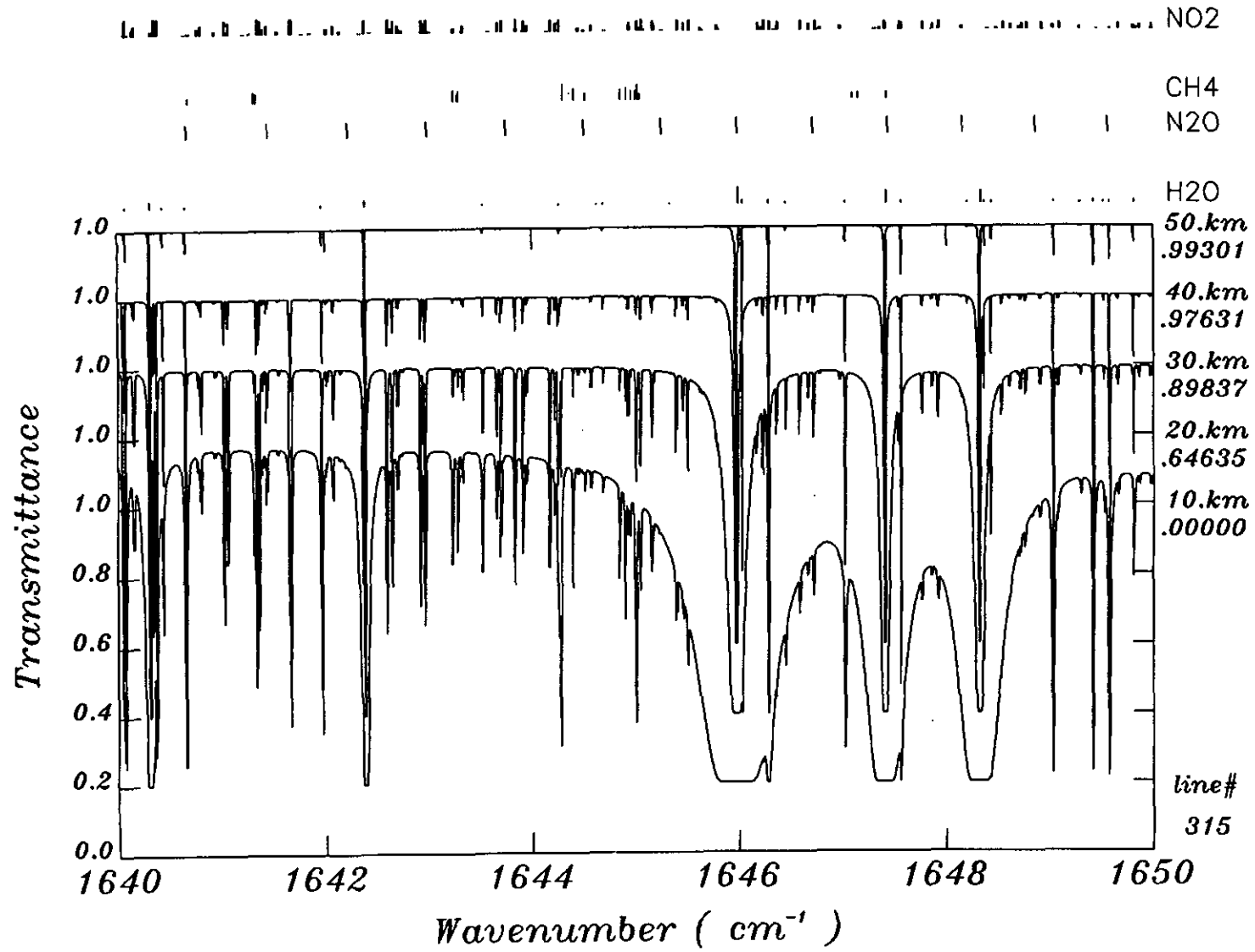


Each Gas Absorption at Tangent Height = 20 km









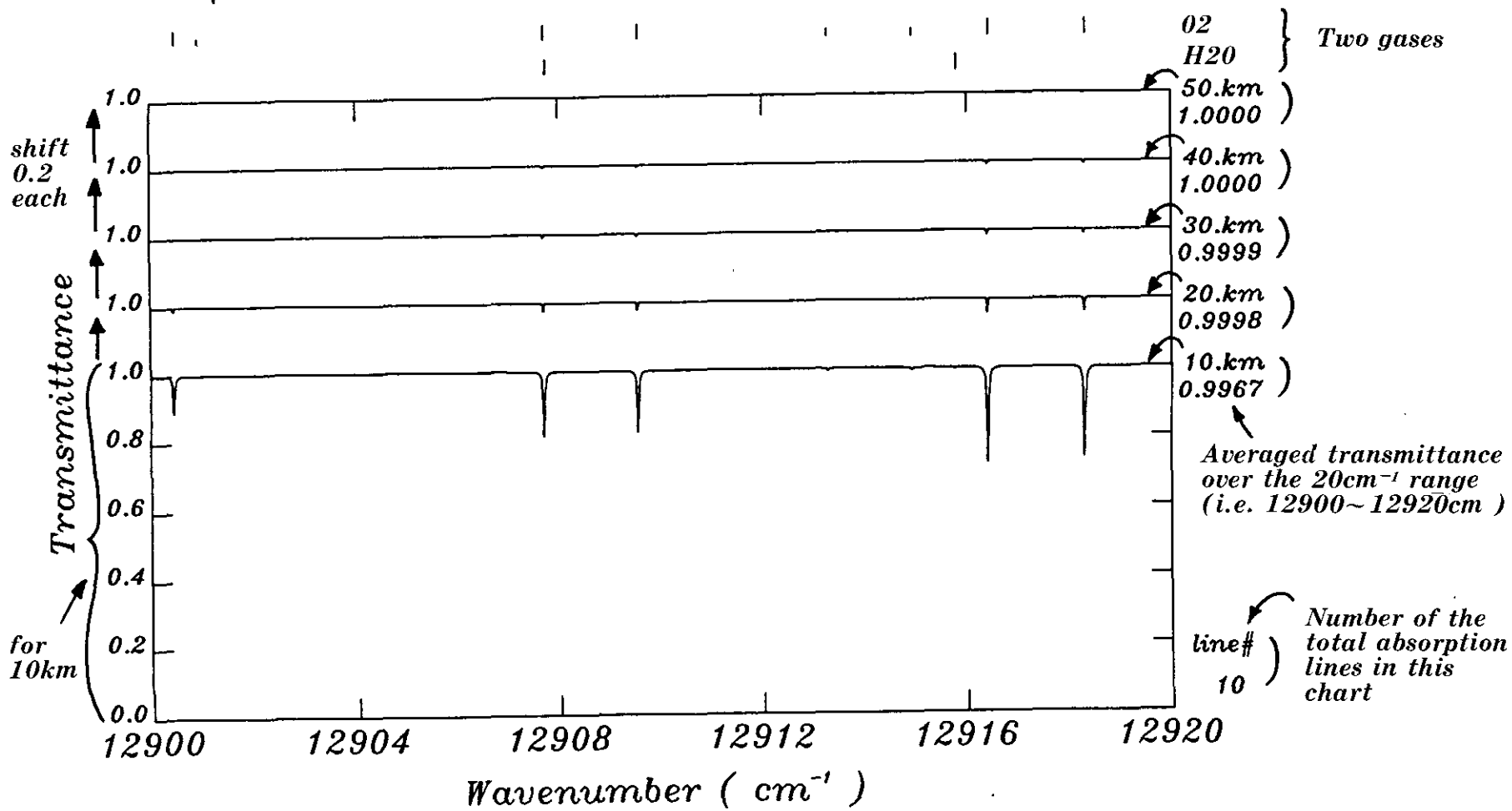
Atlas of the Visible O<sub>2</sub>

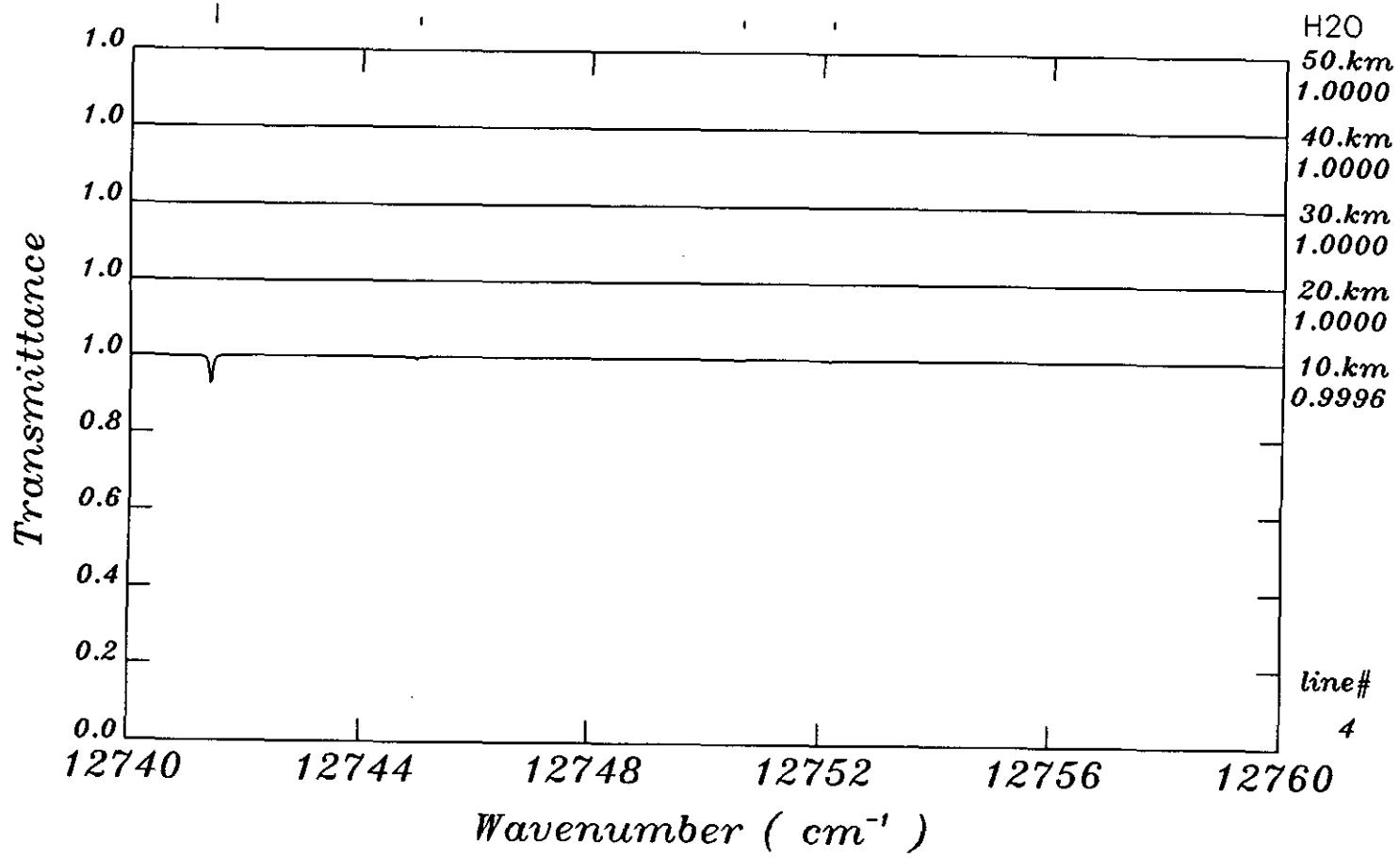
Absorption Spectrum

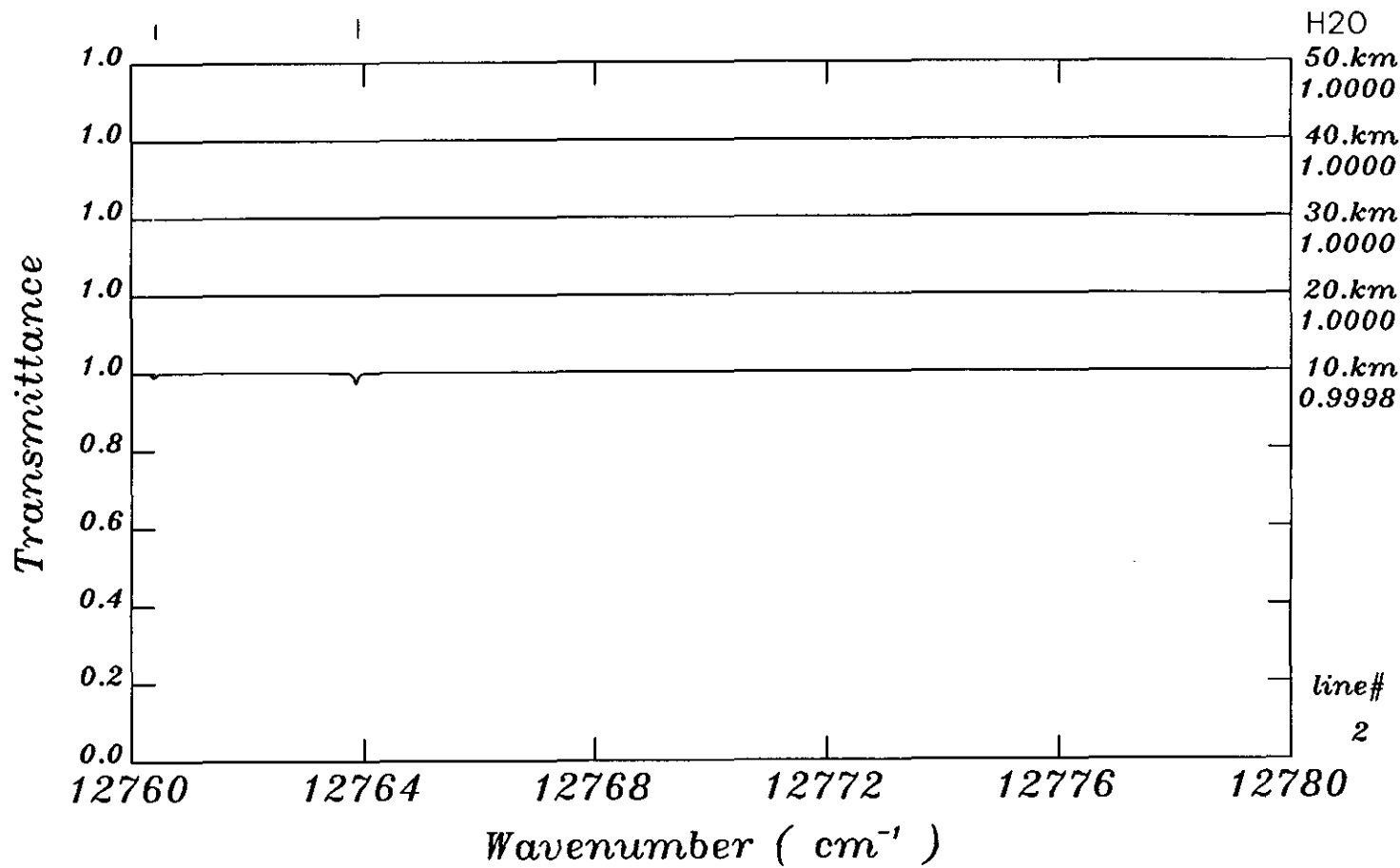


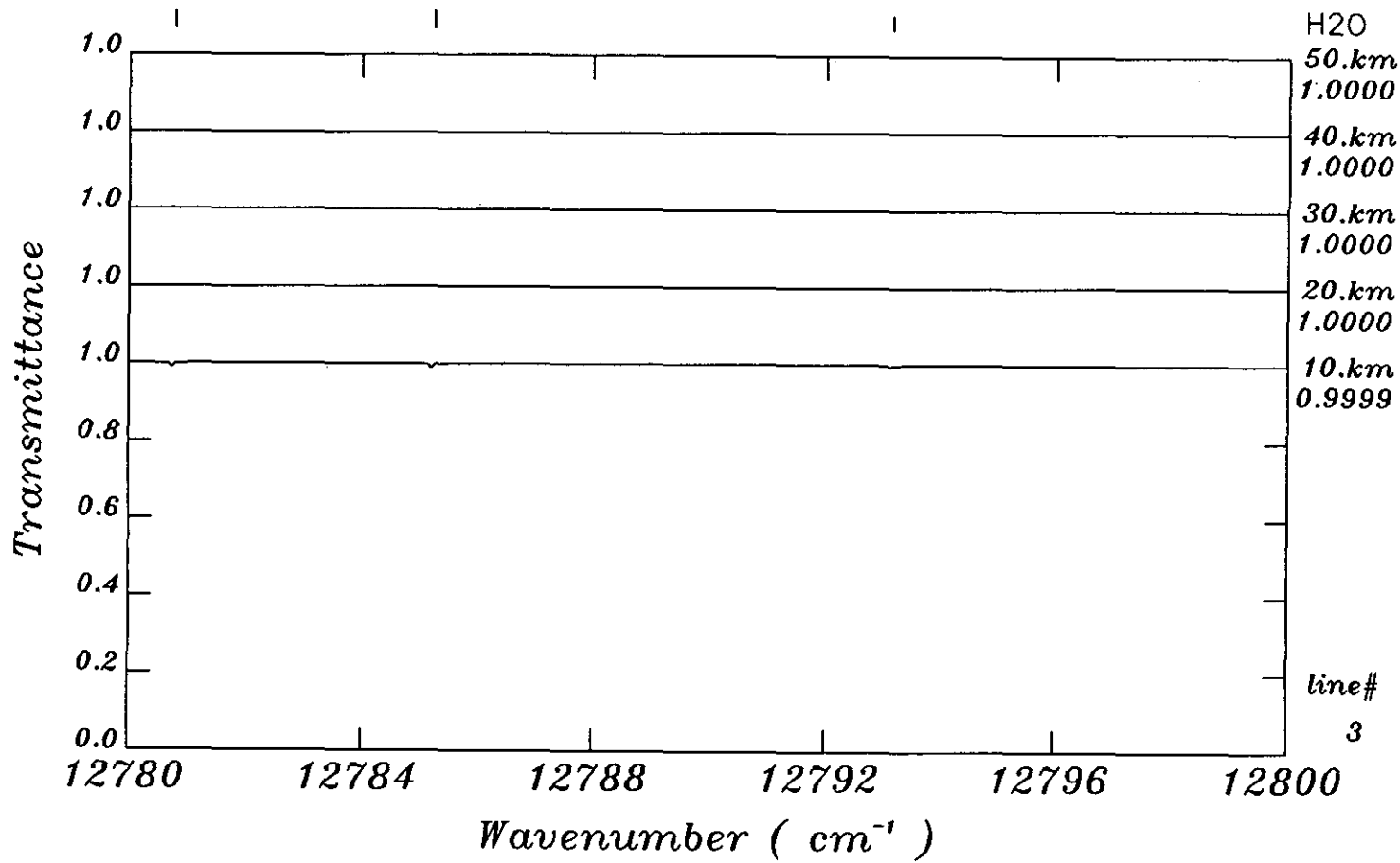
(Sample)

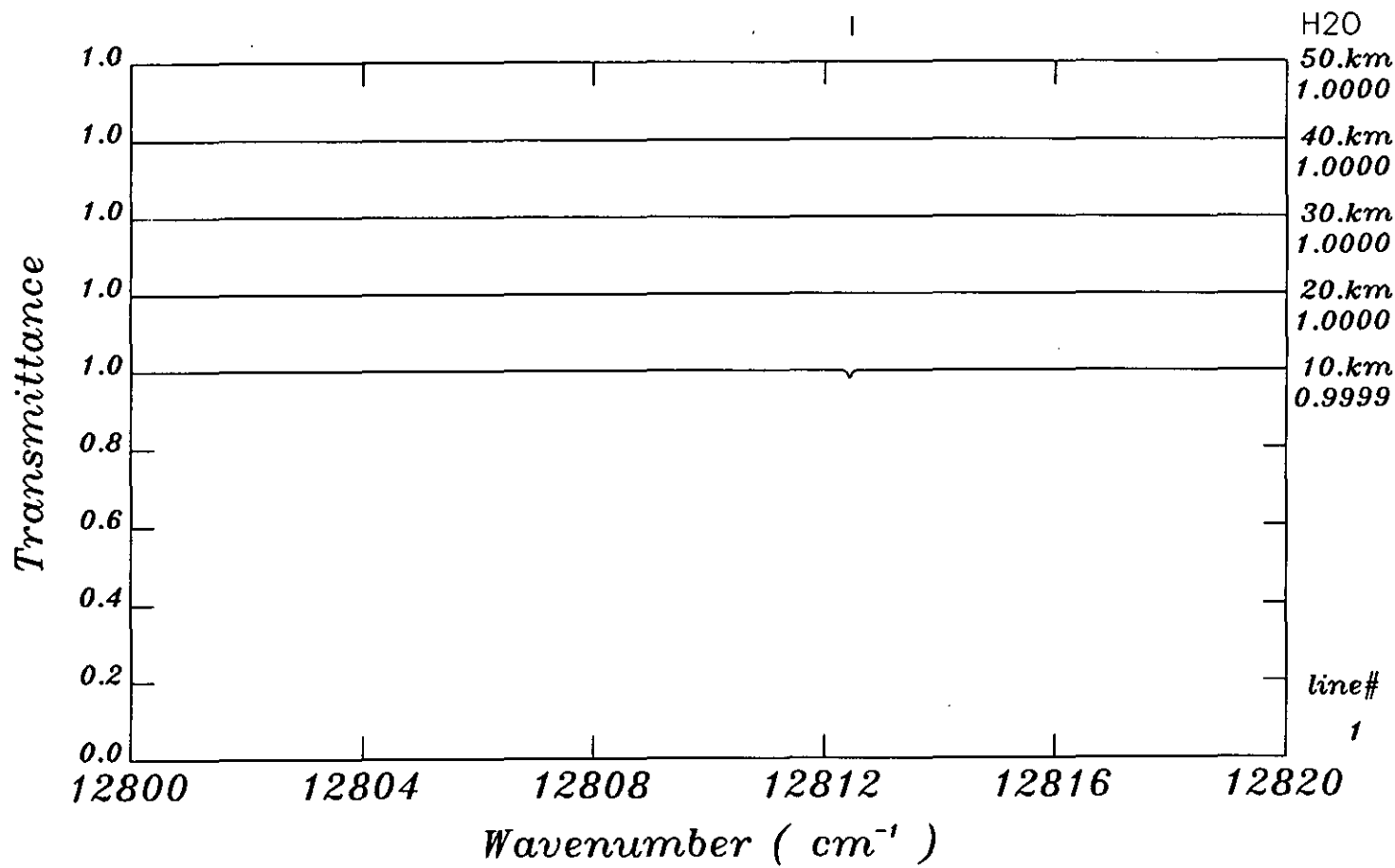
All line positions and strengths

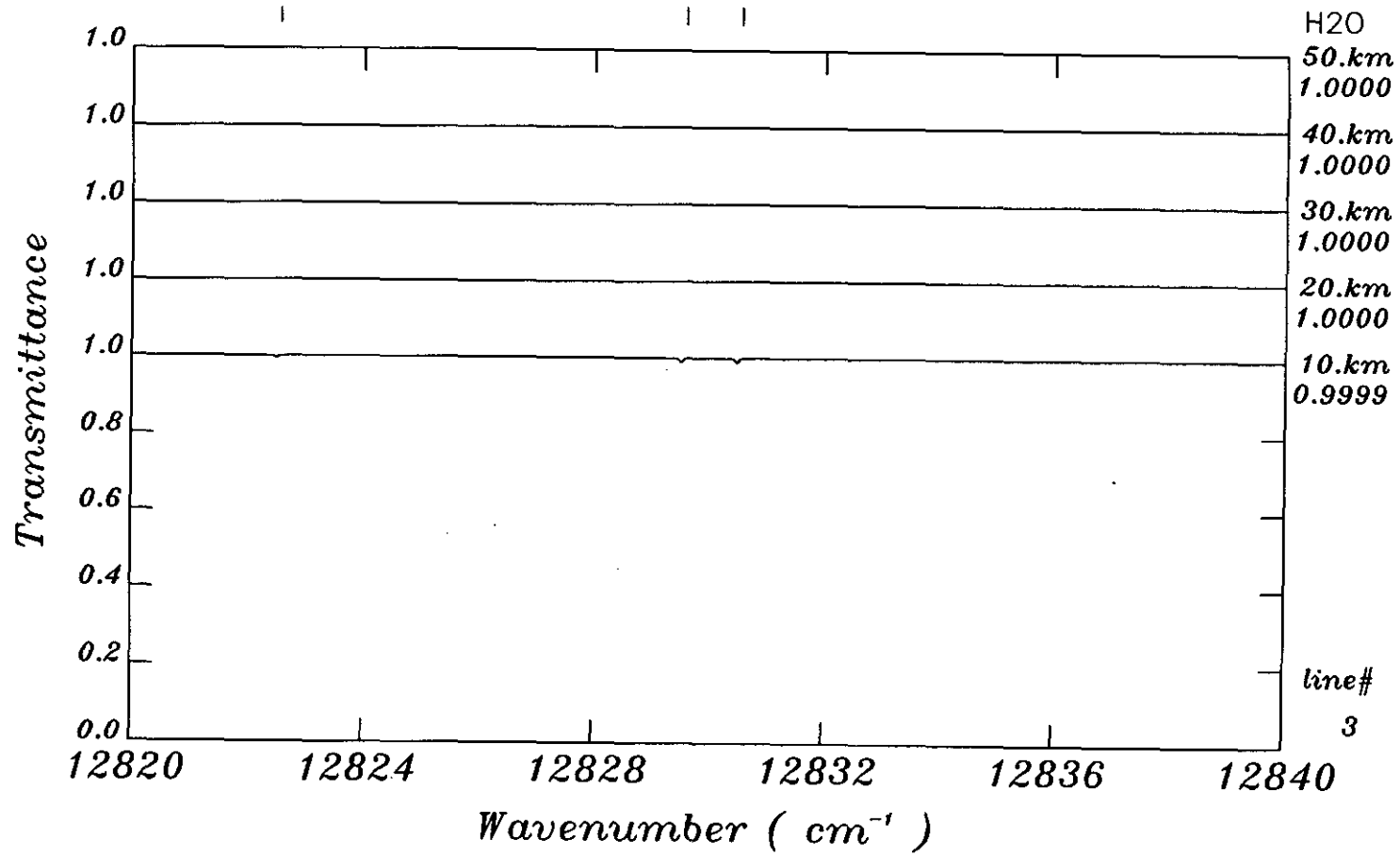


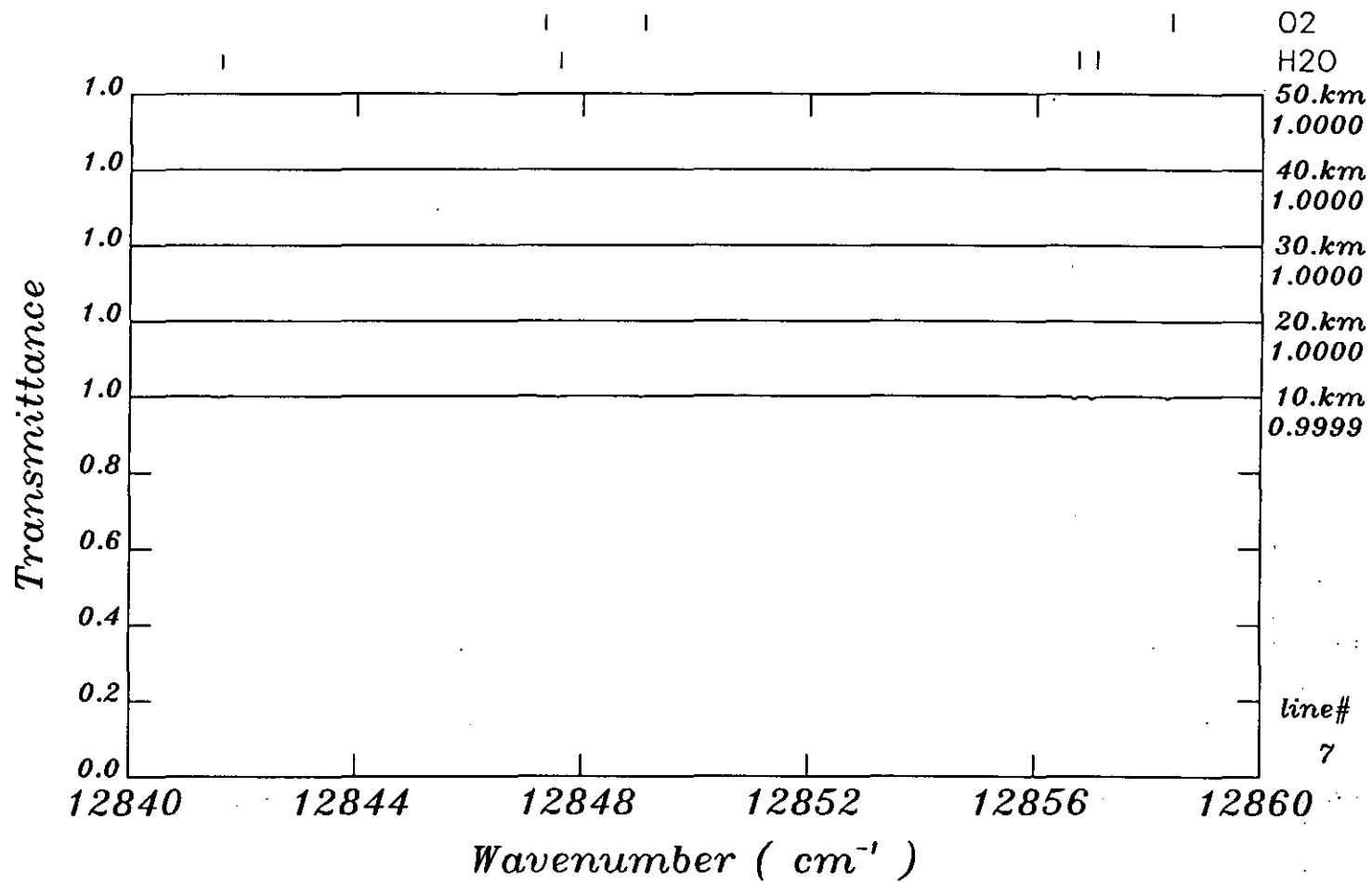


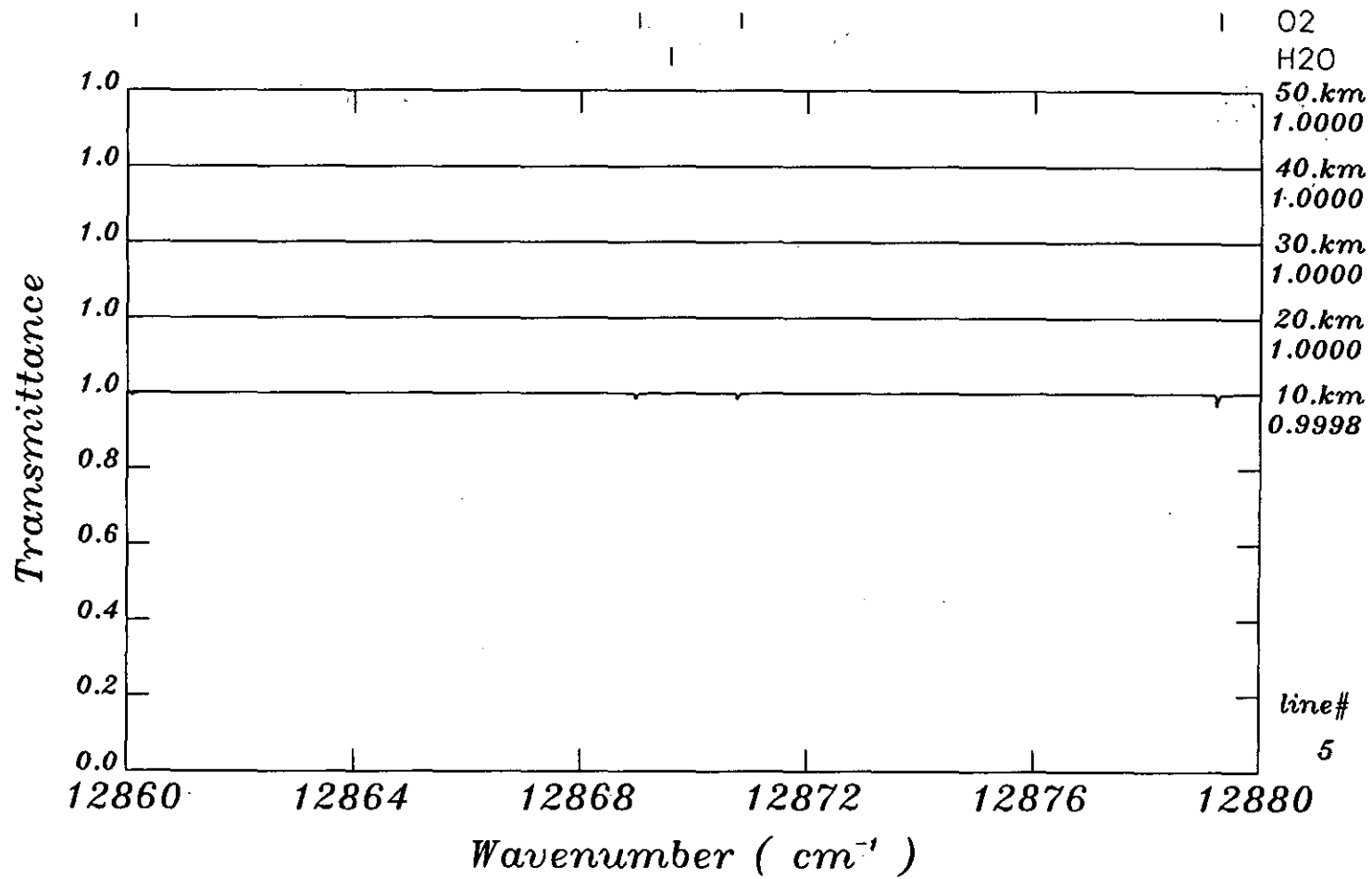




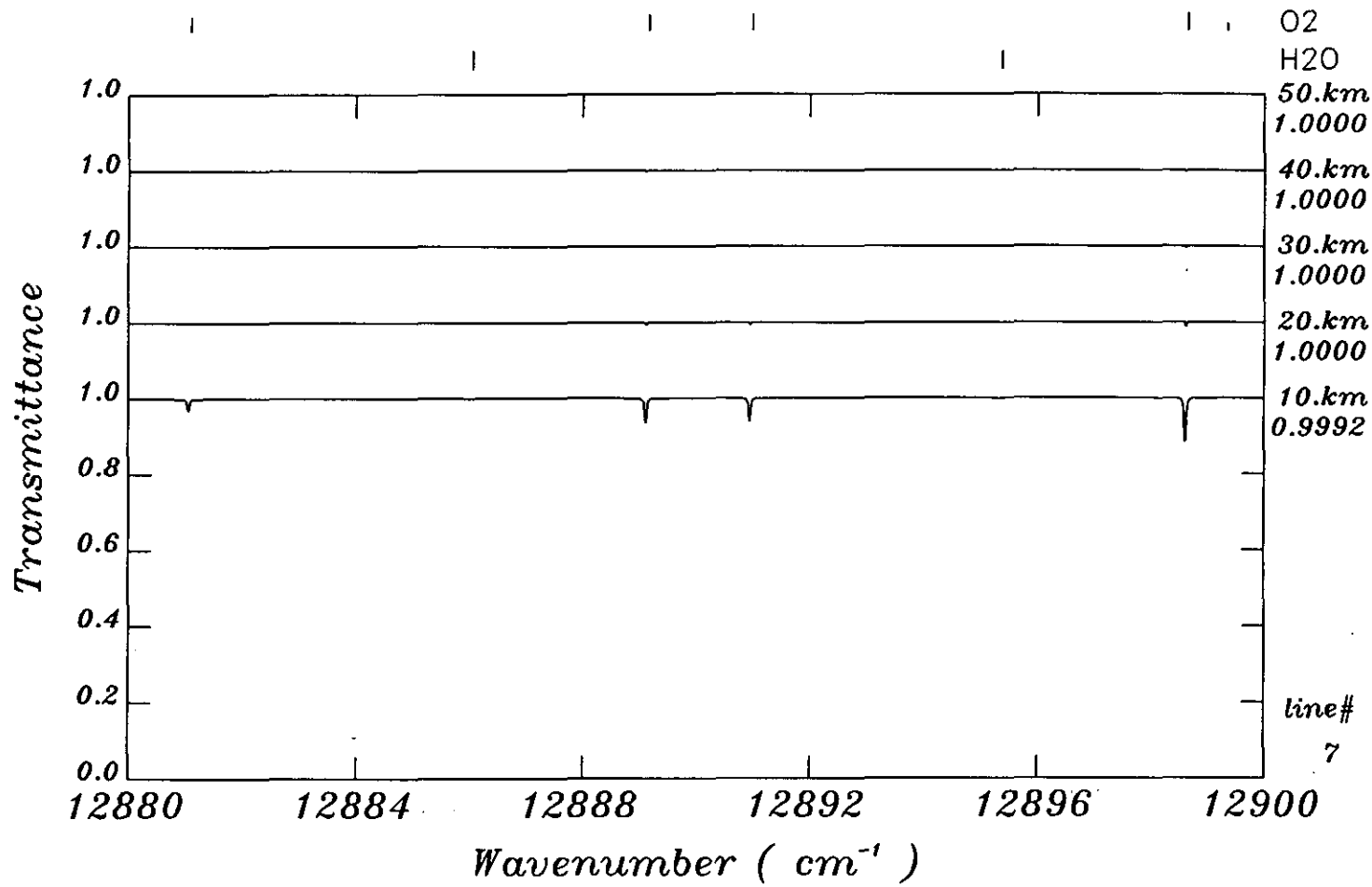


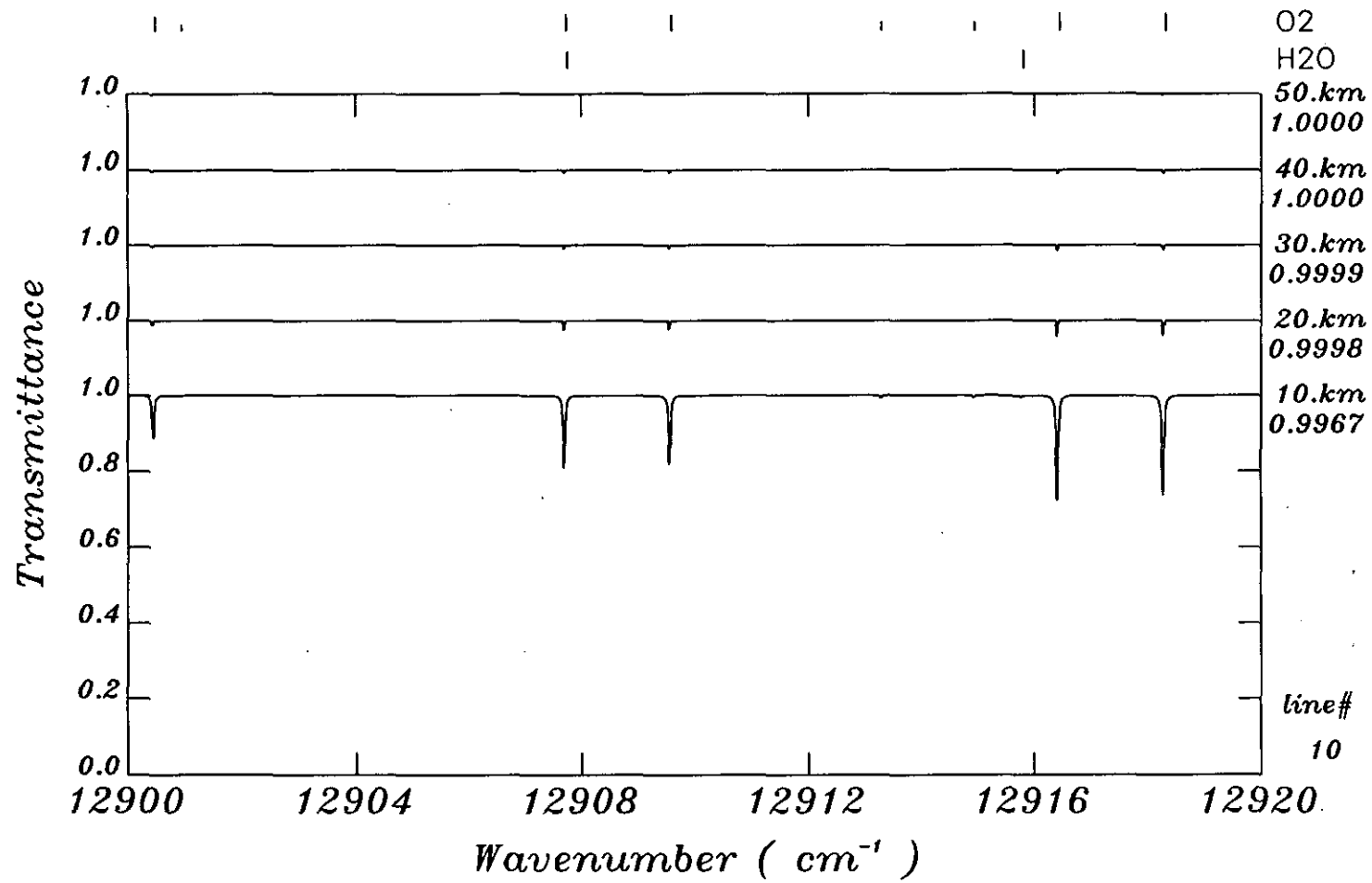


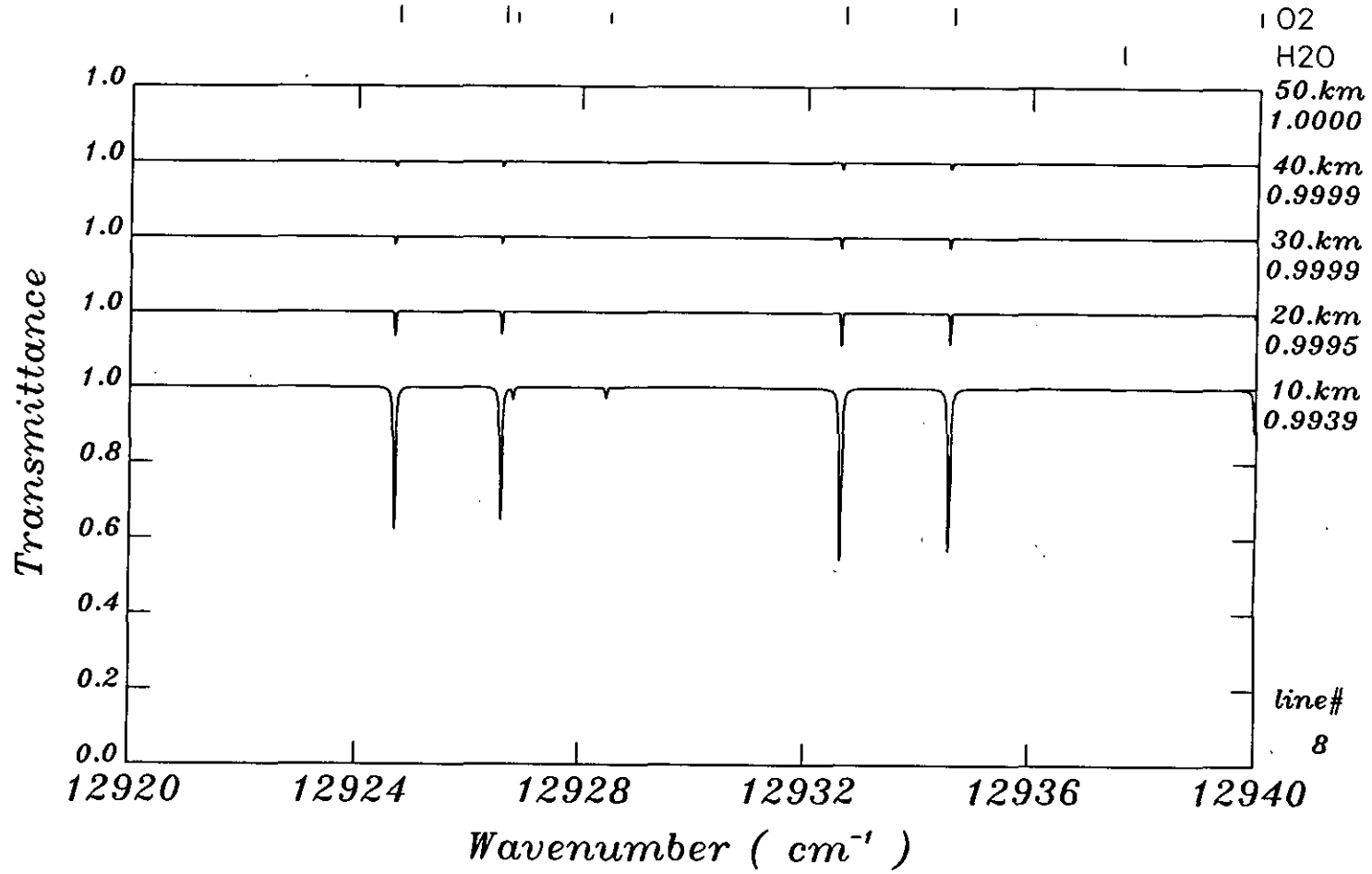


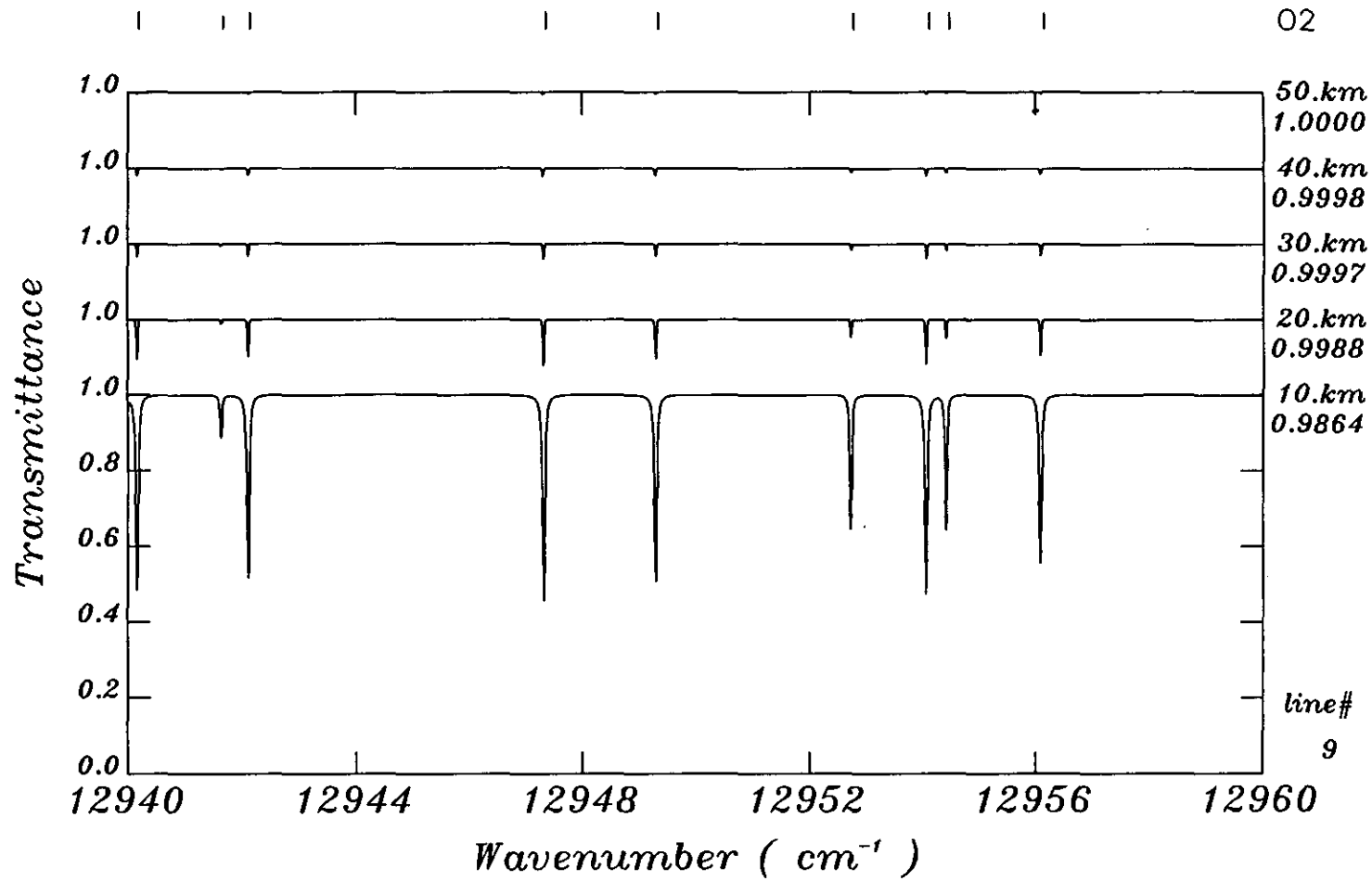


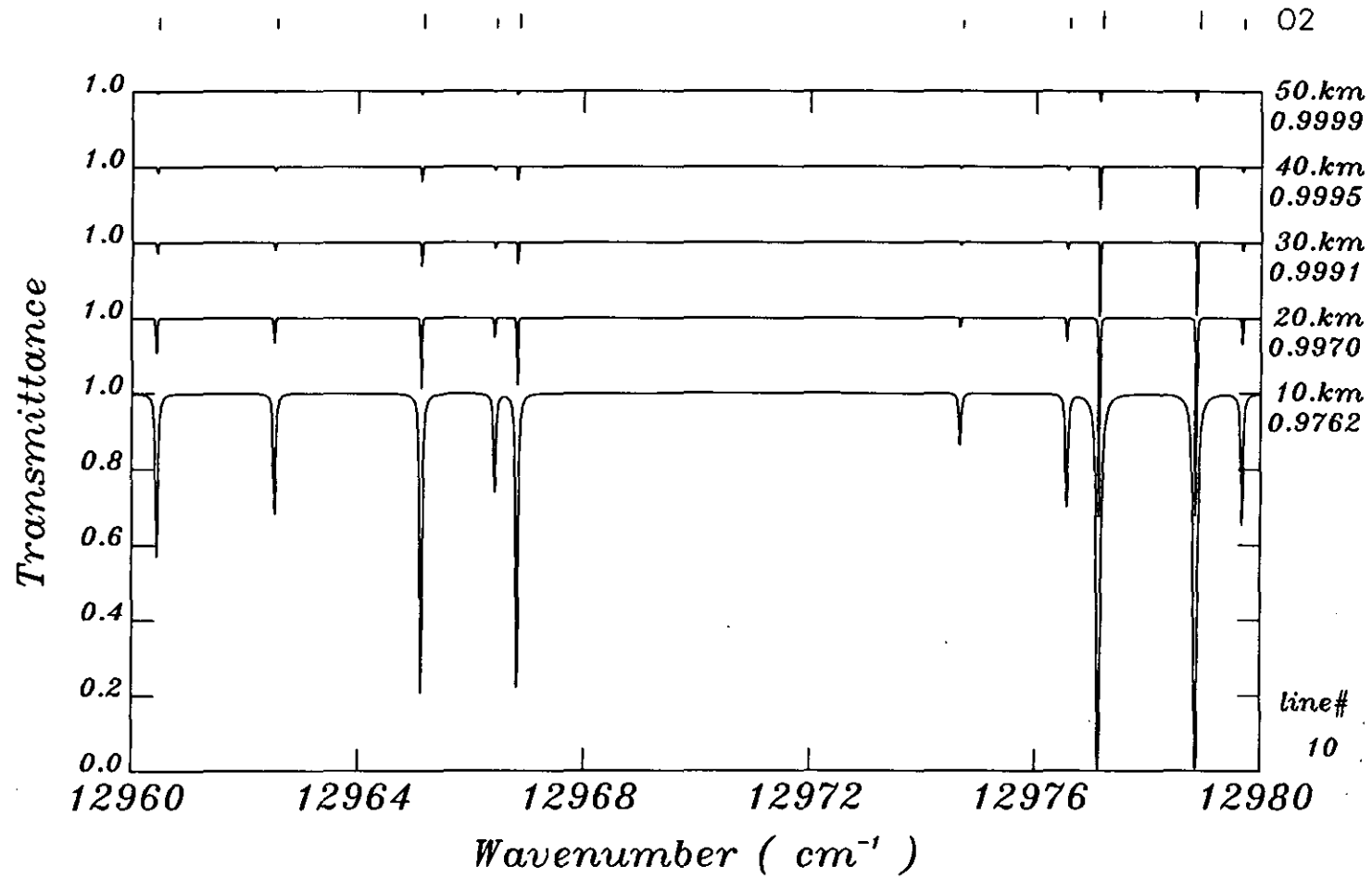


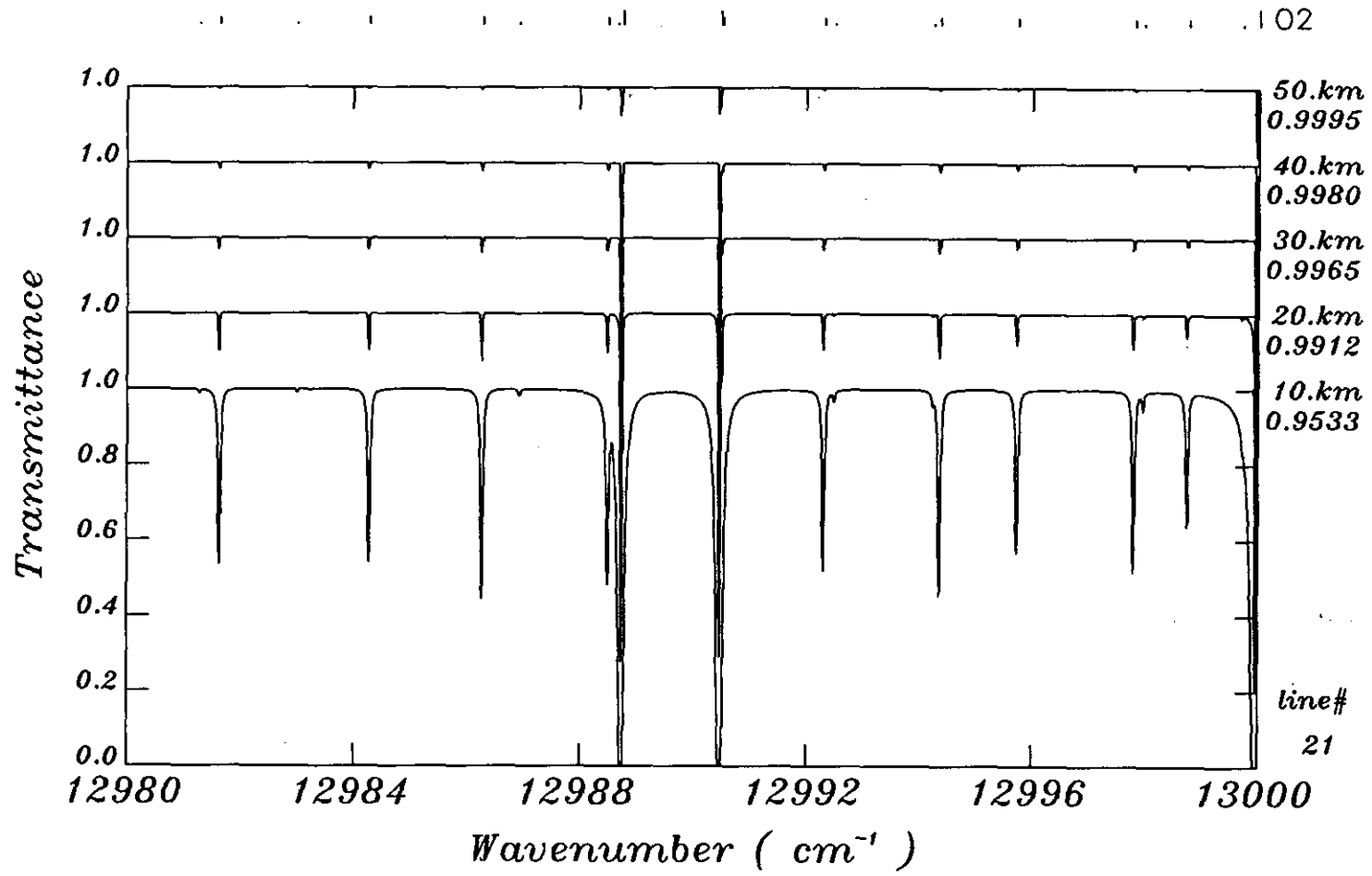


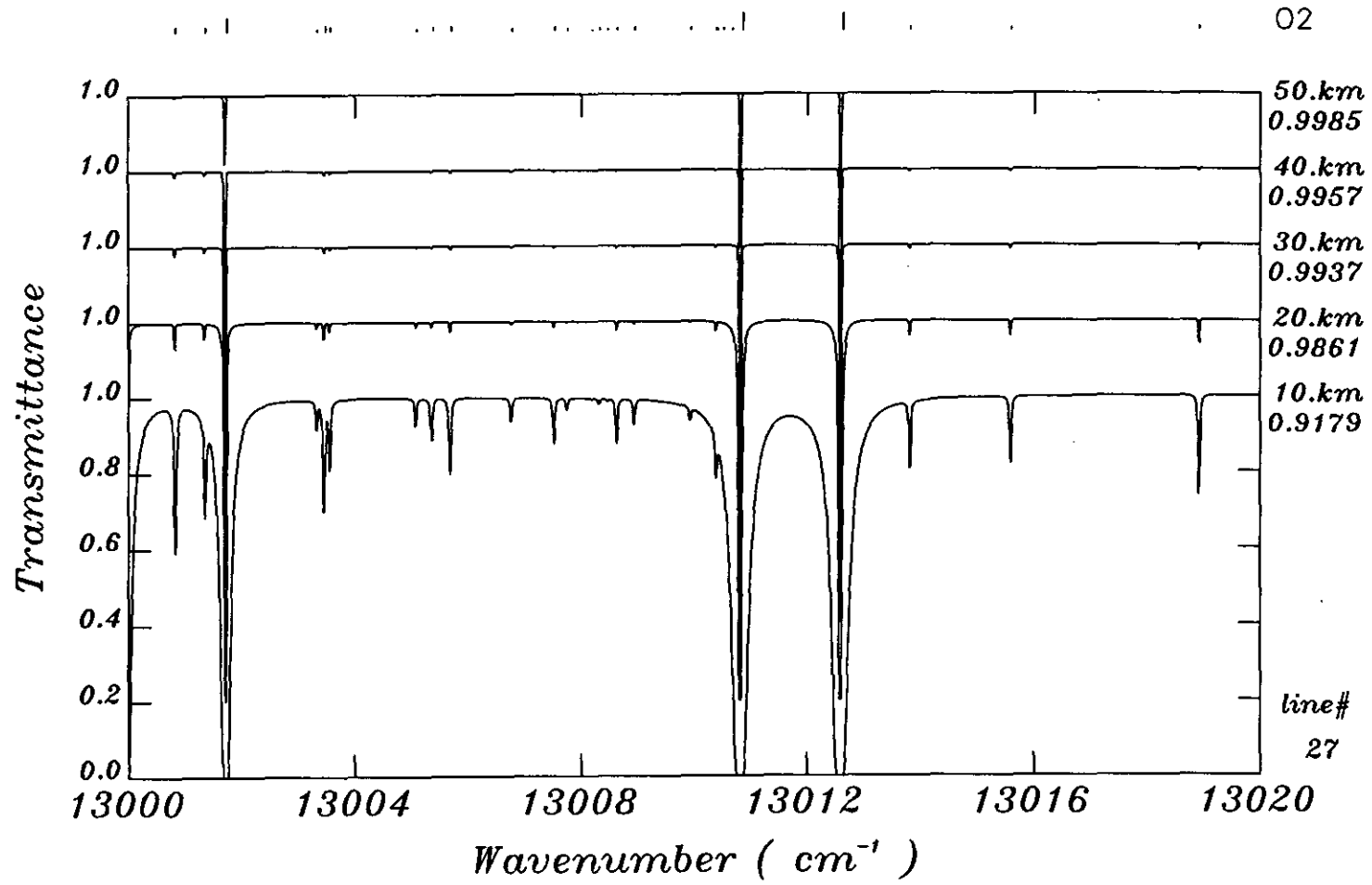


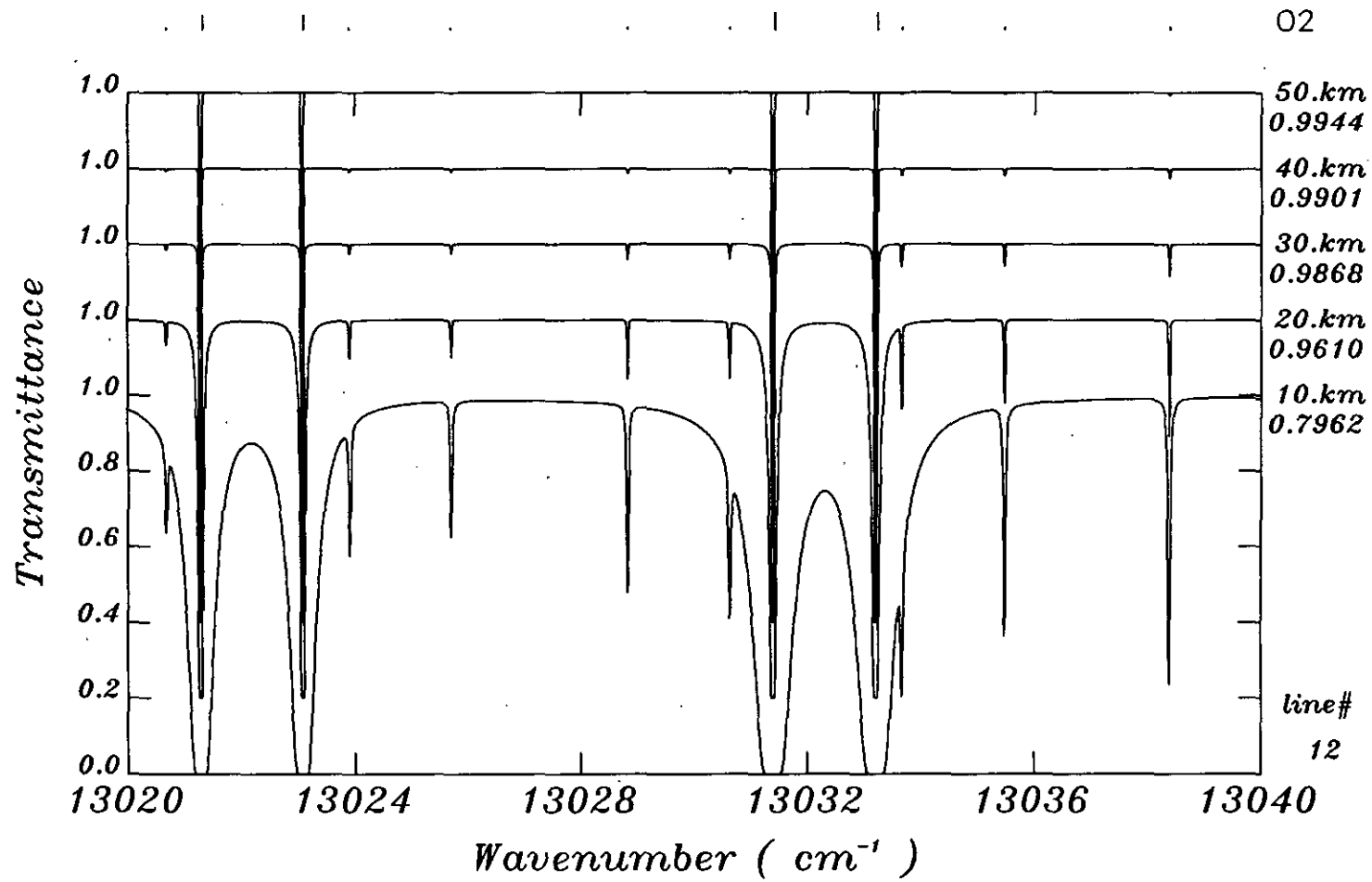




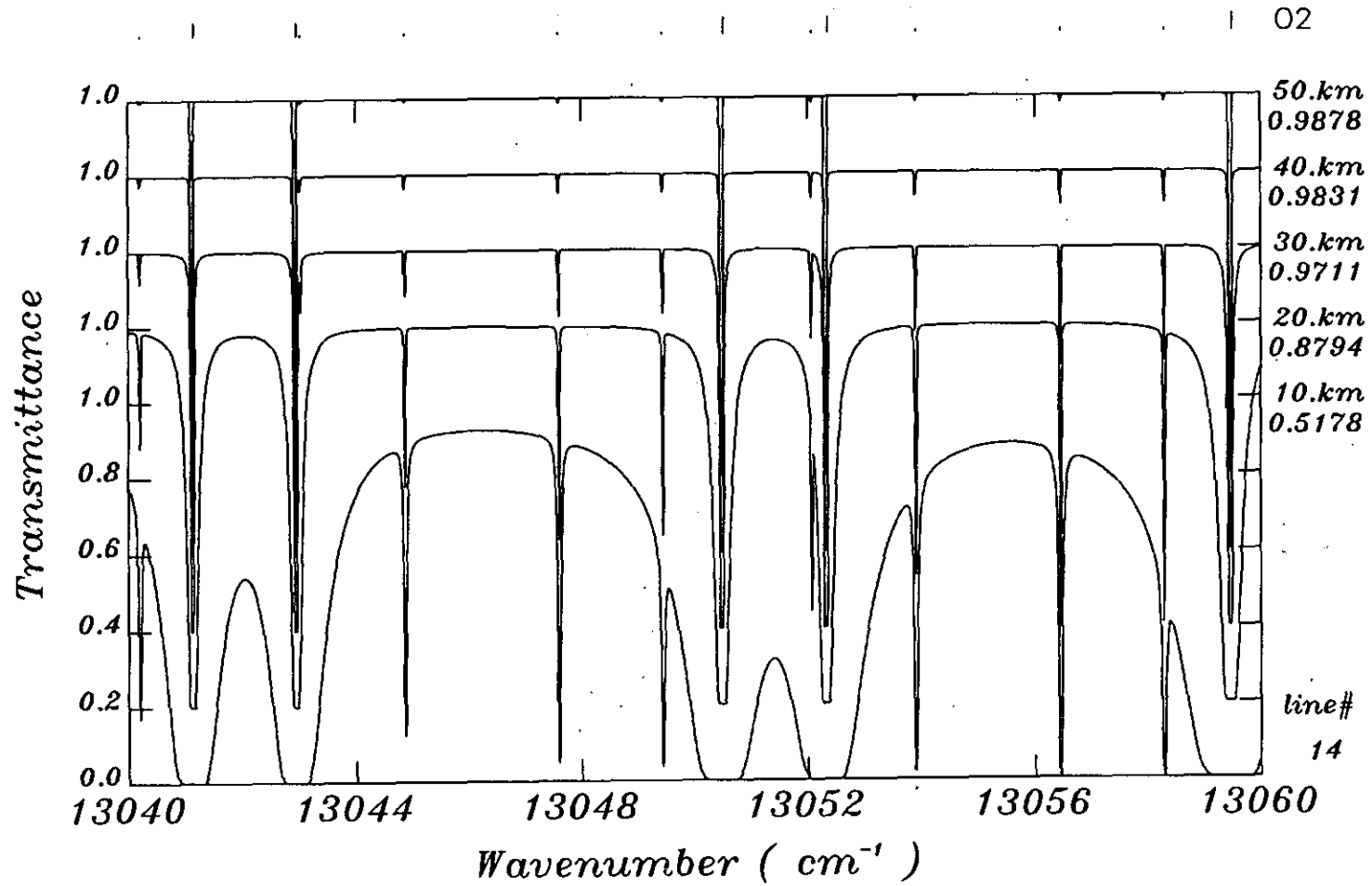


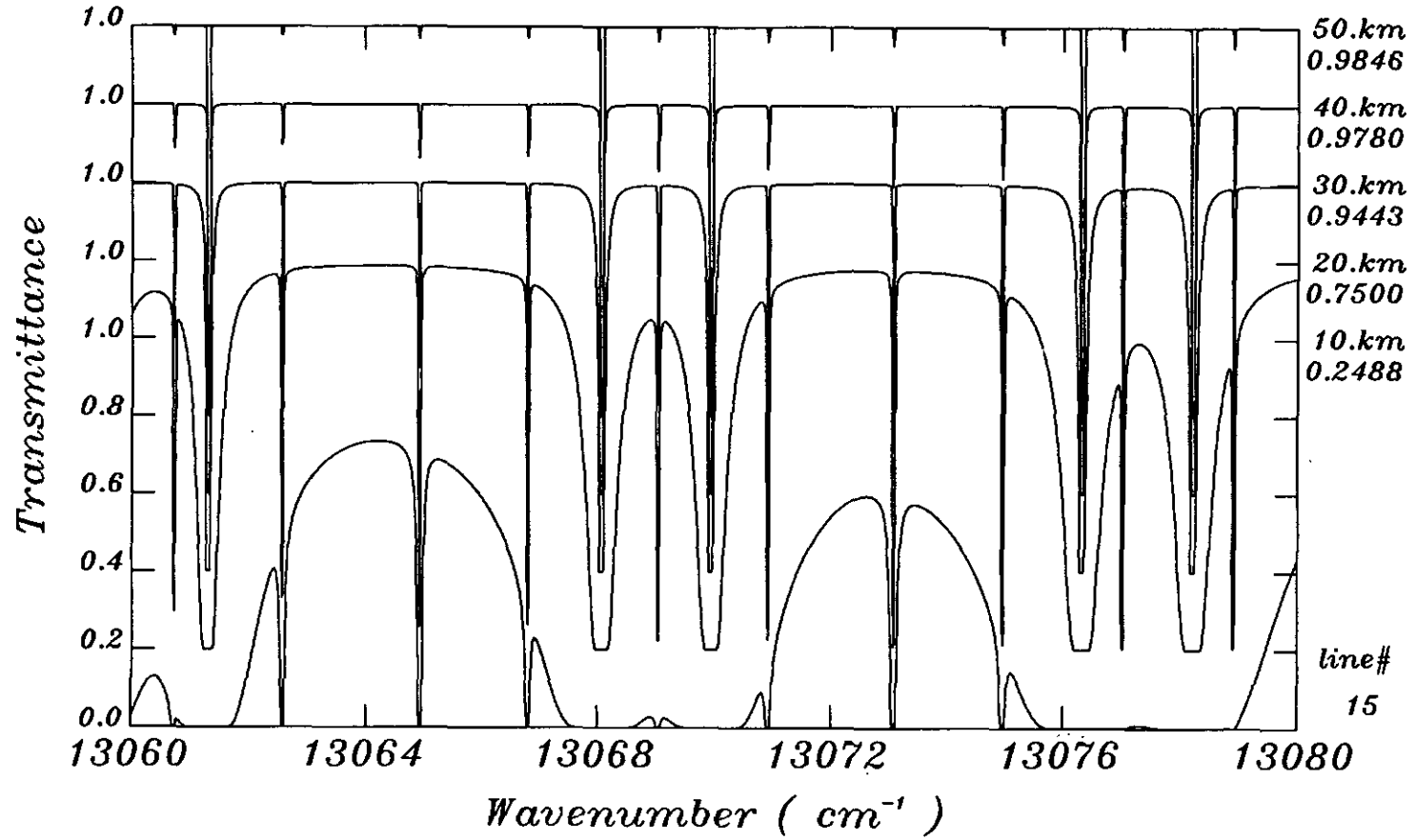


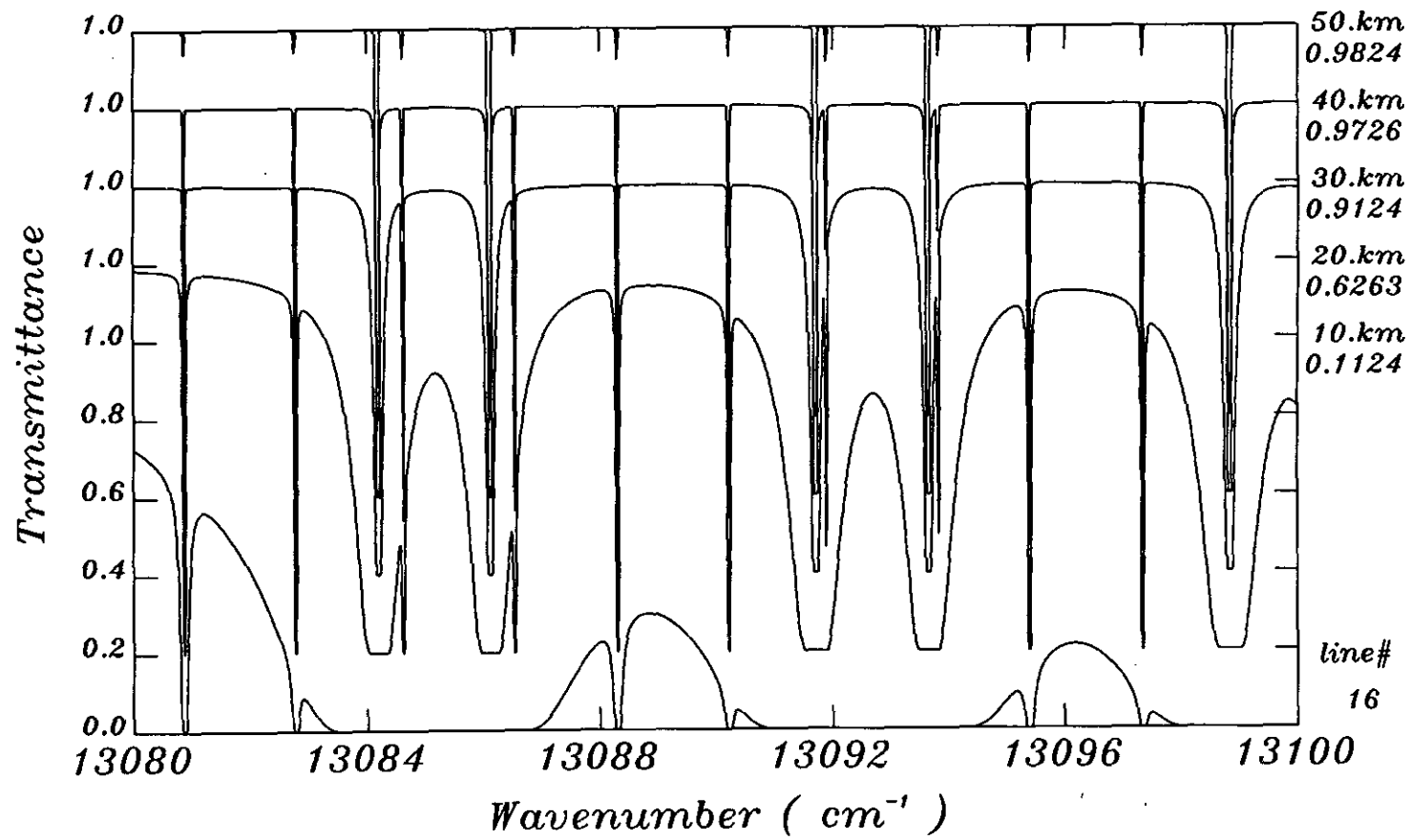


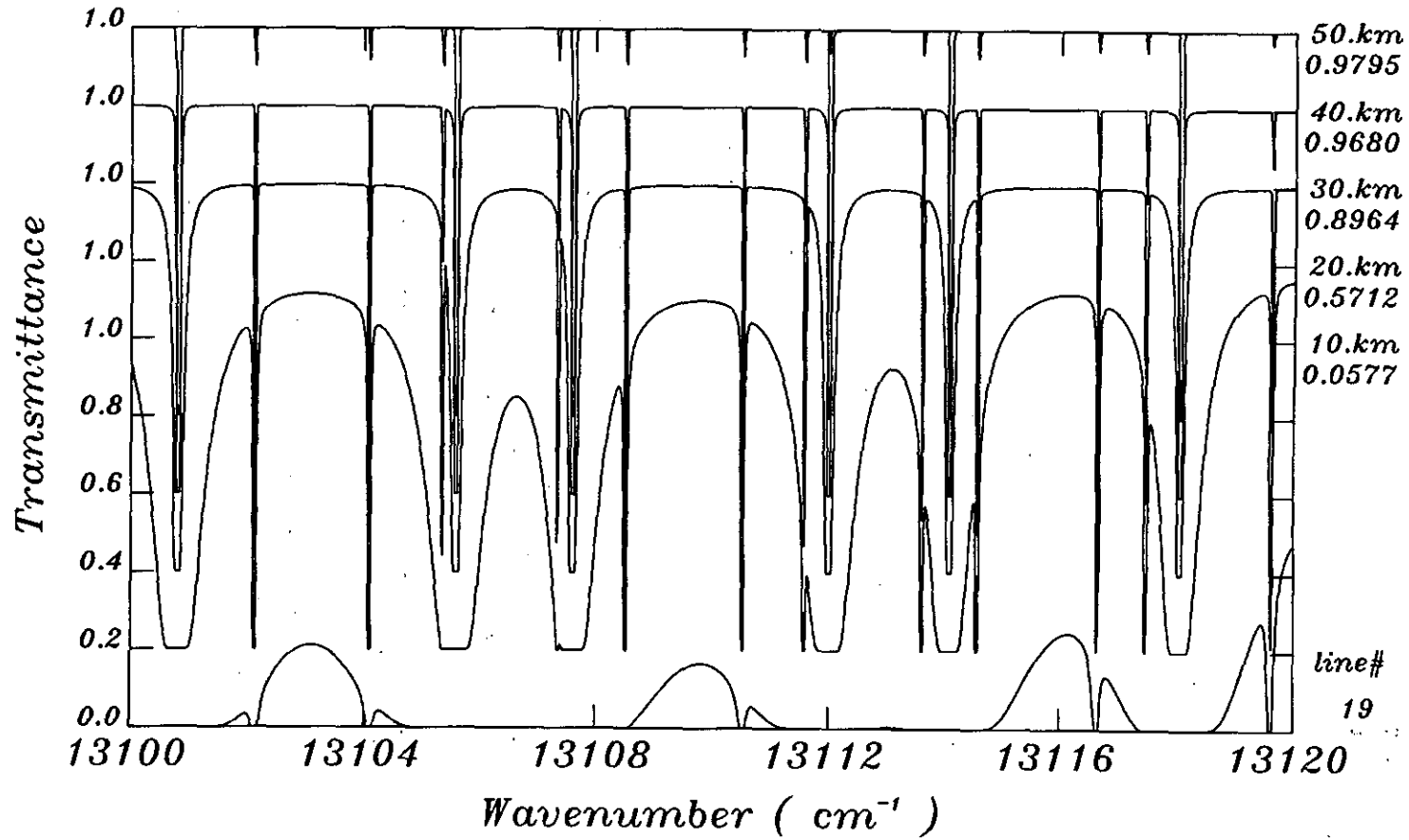


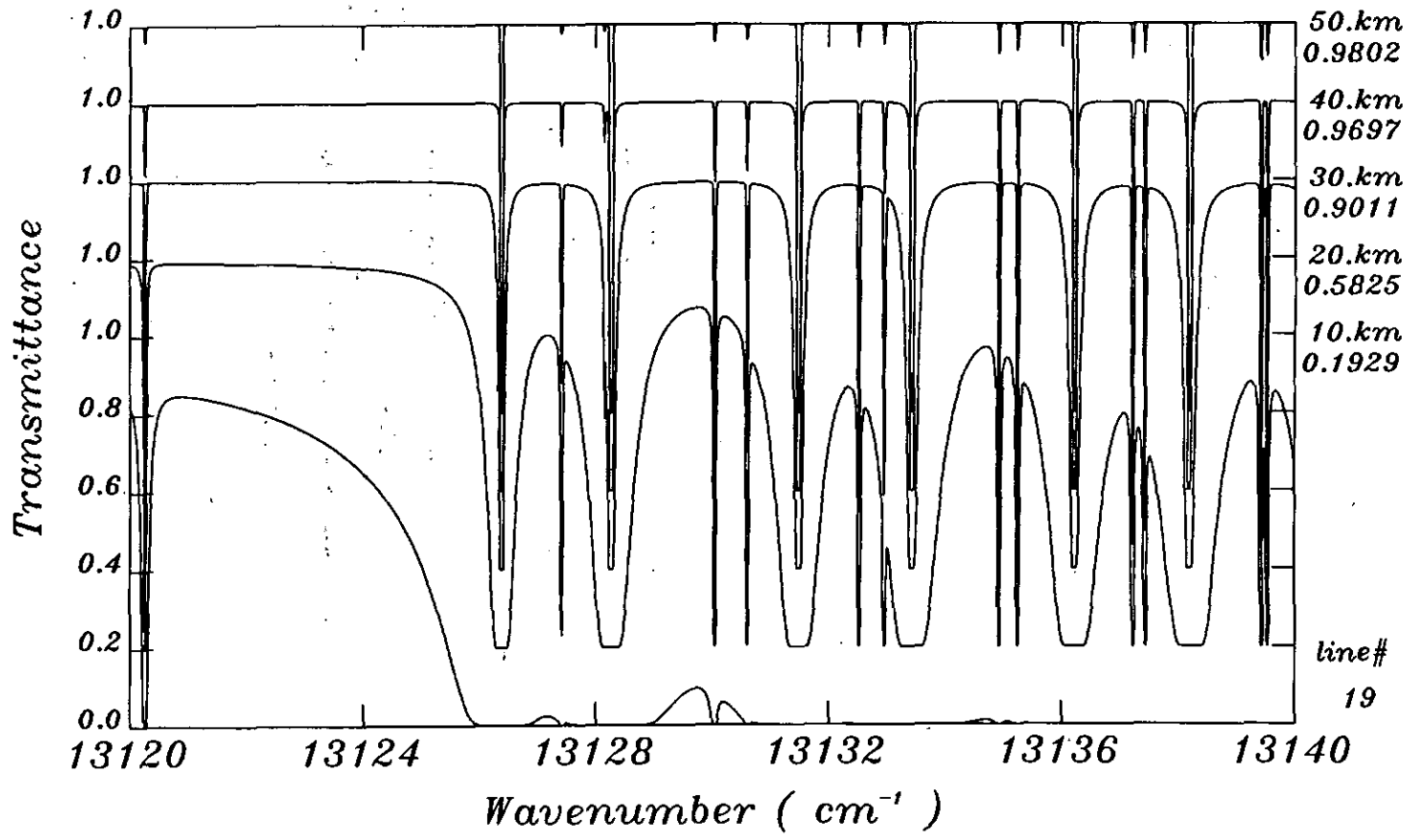


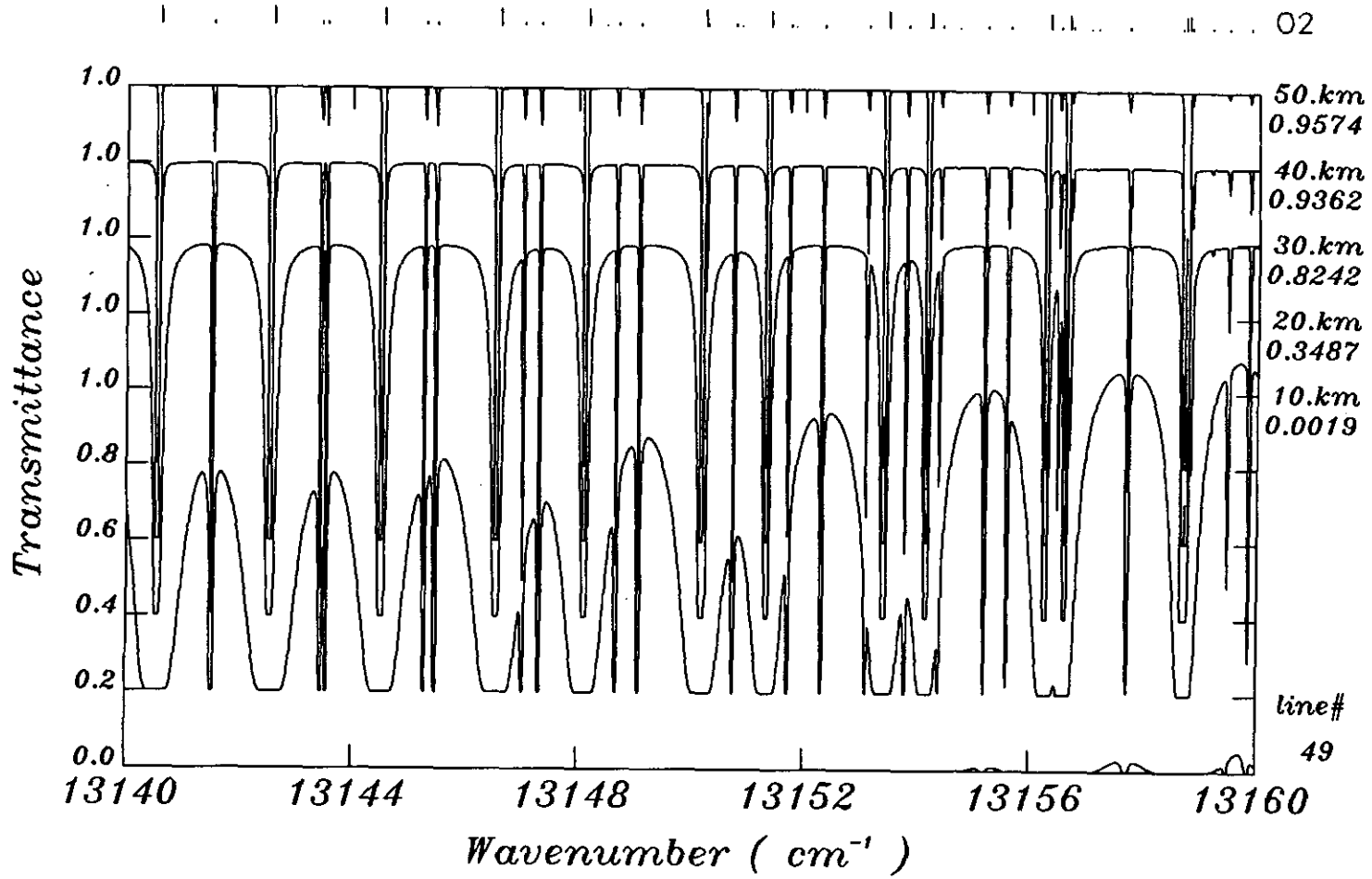




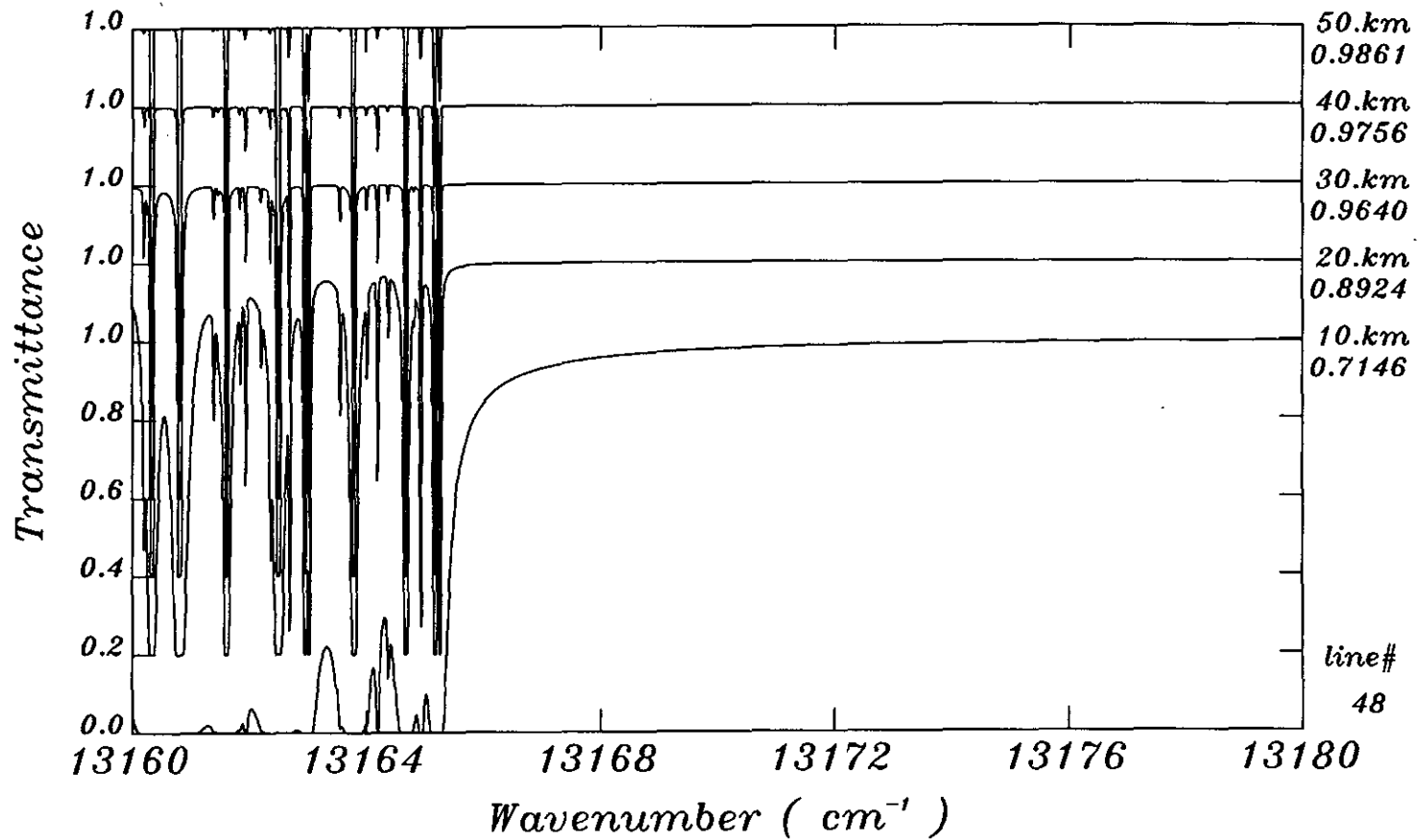


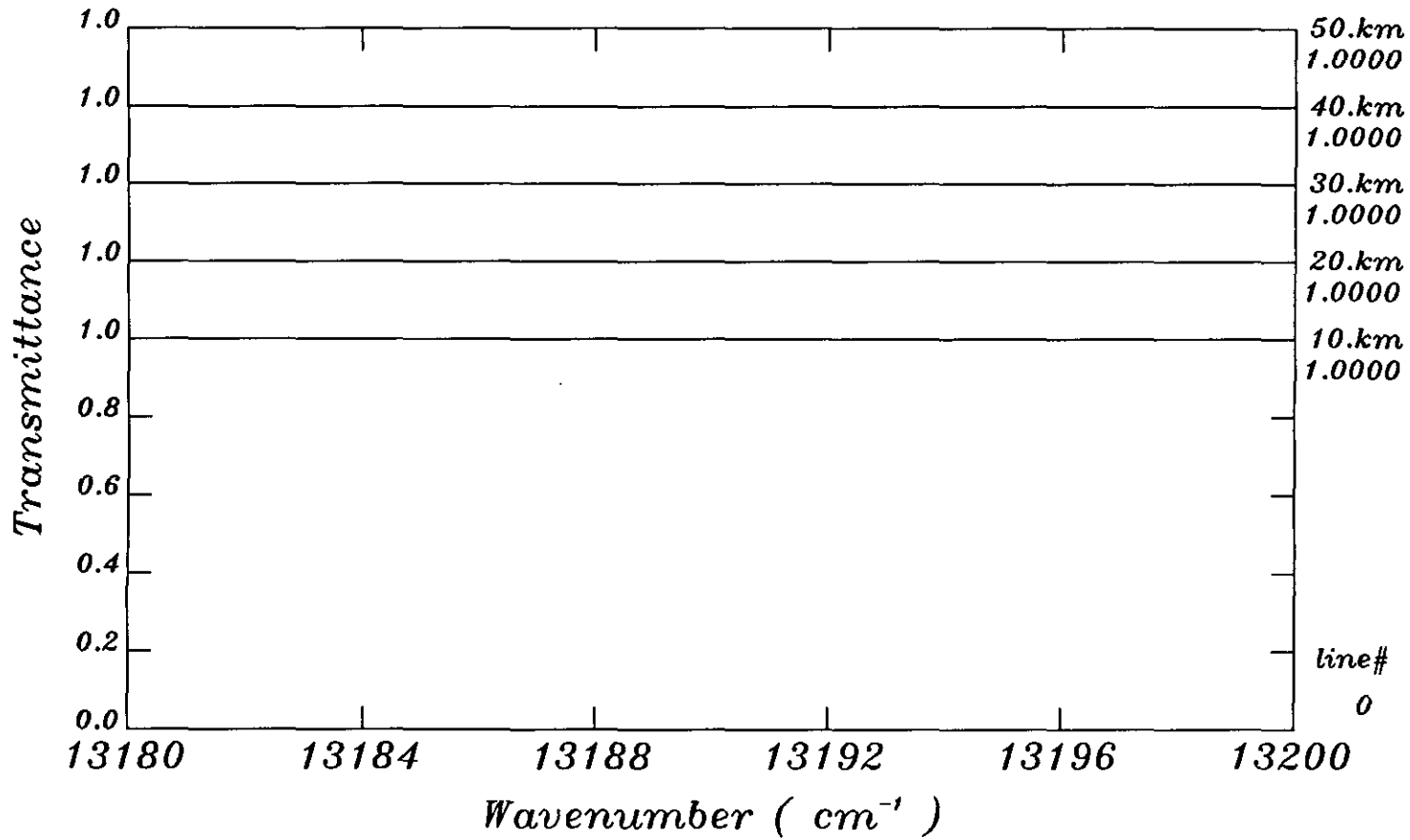




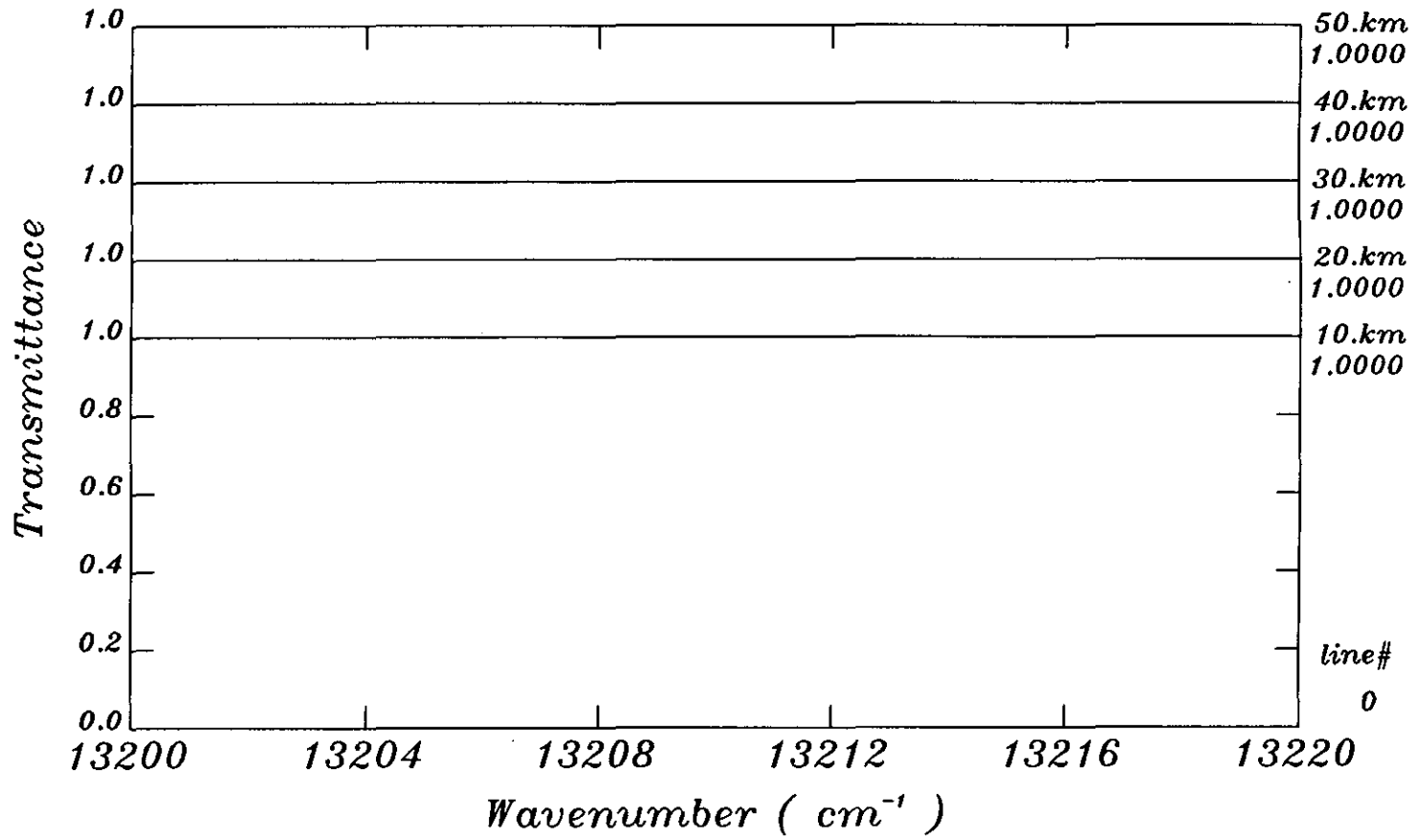


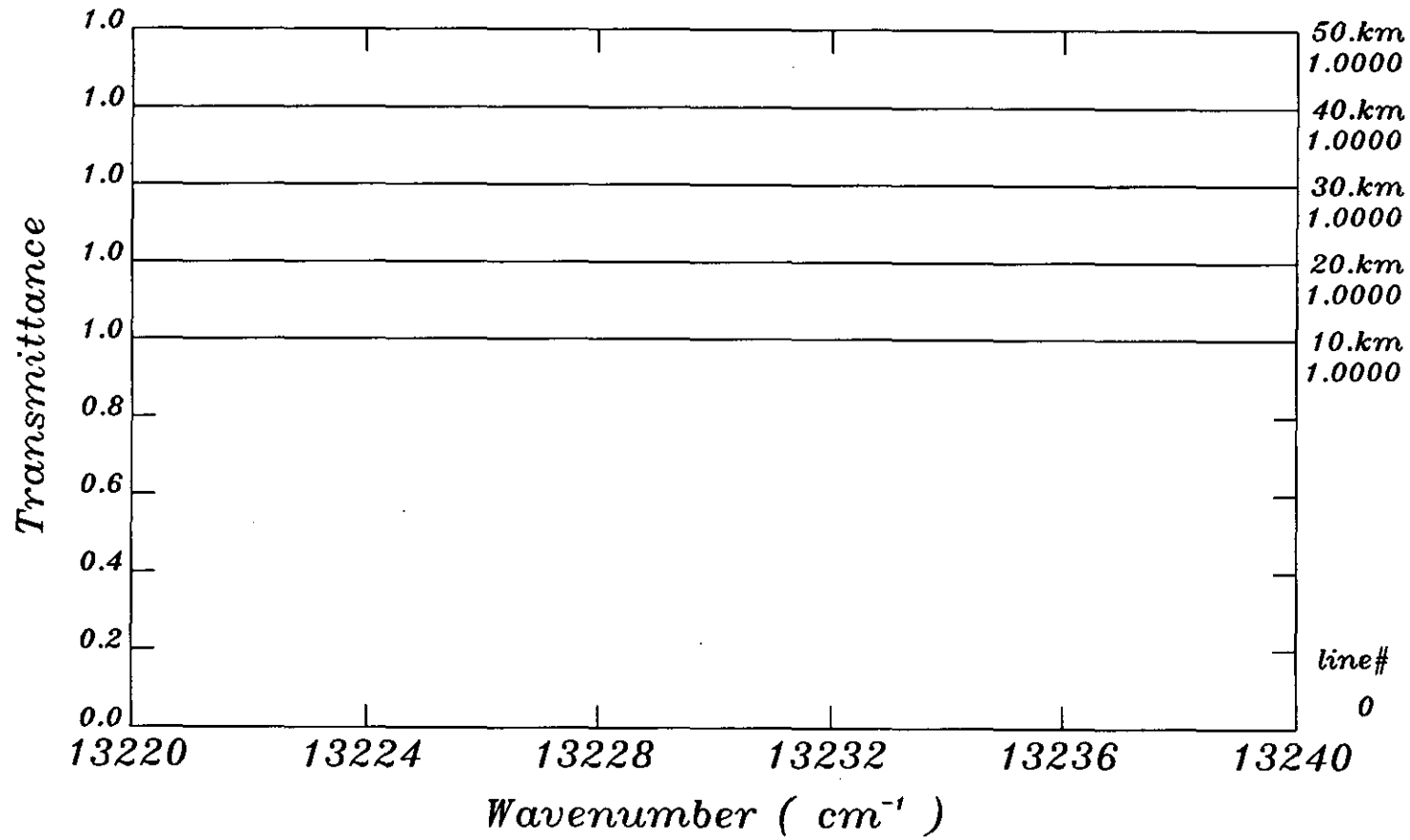
02

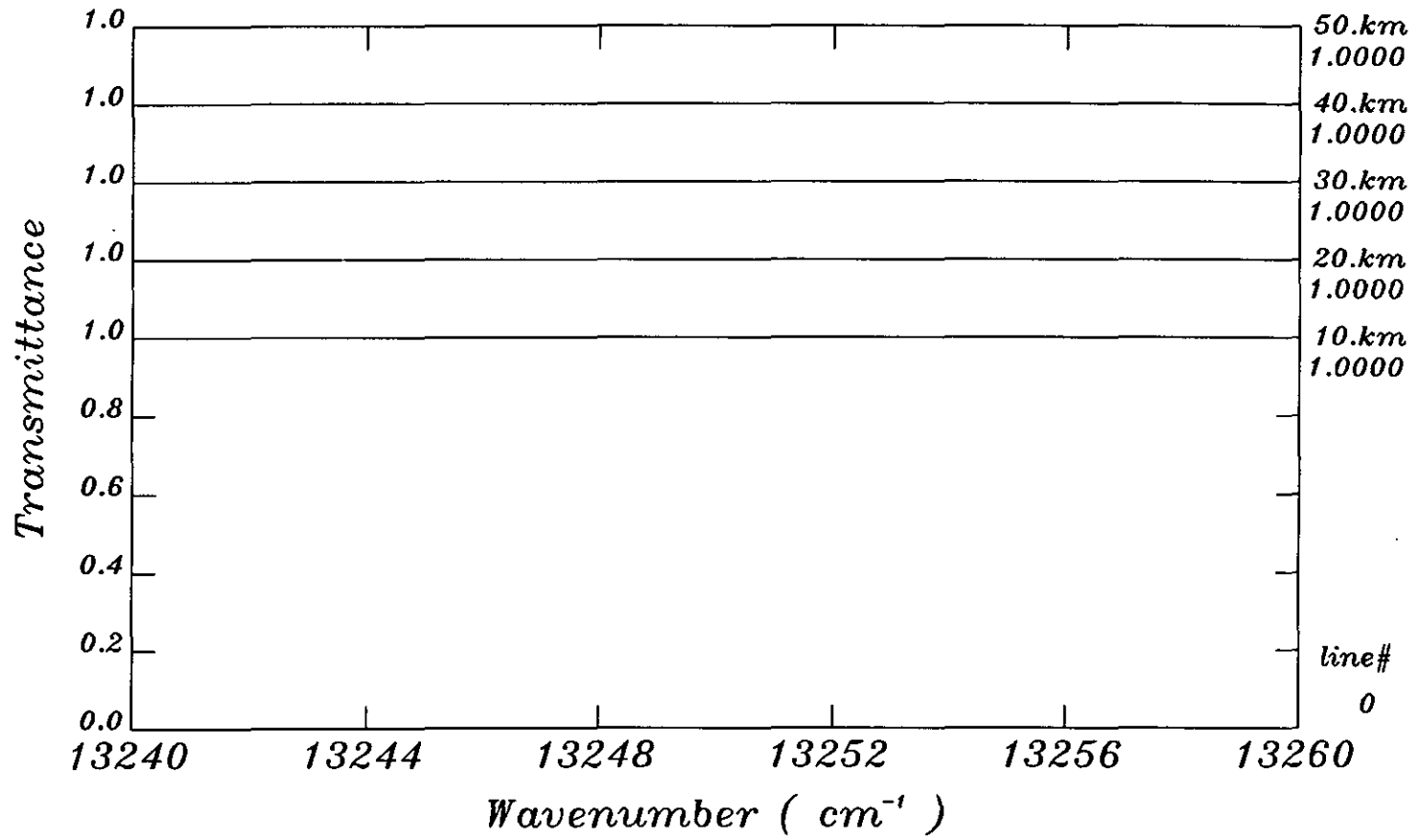


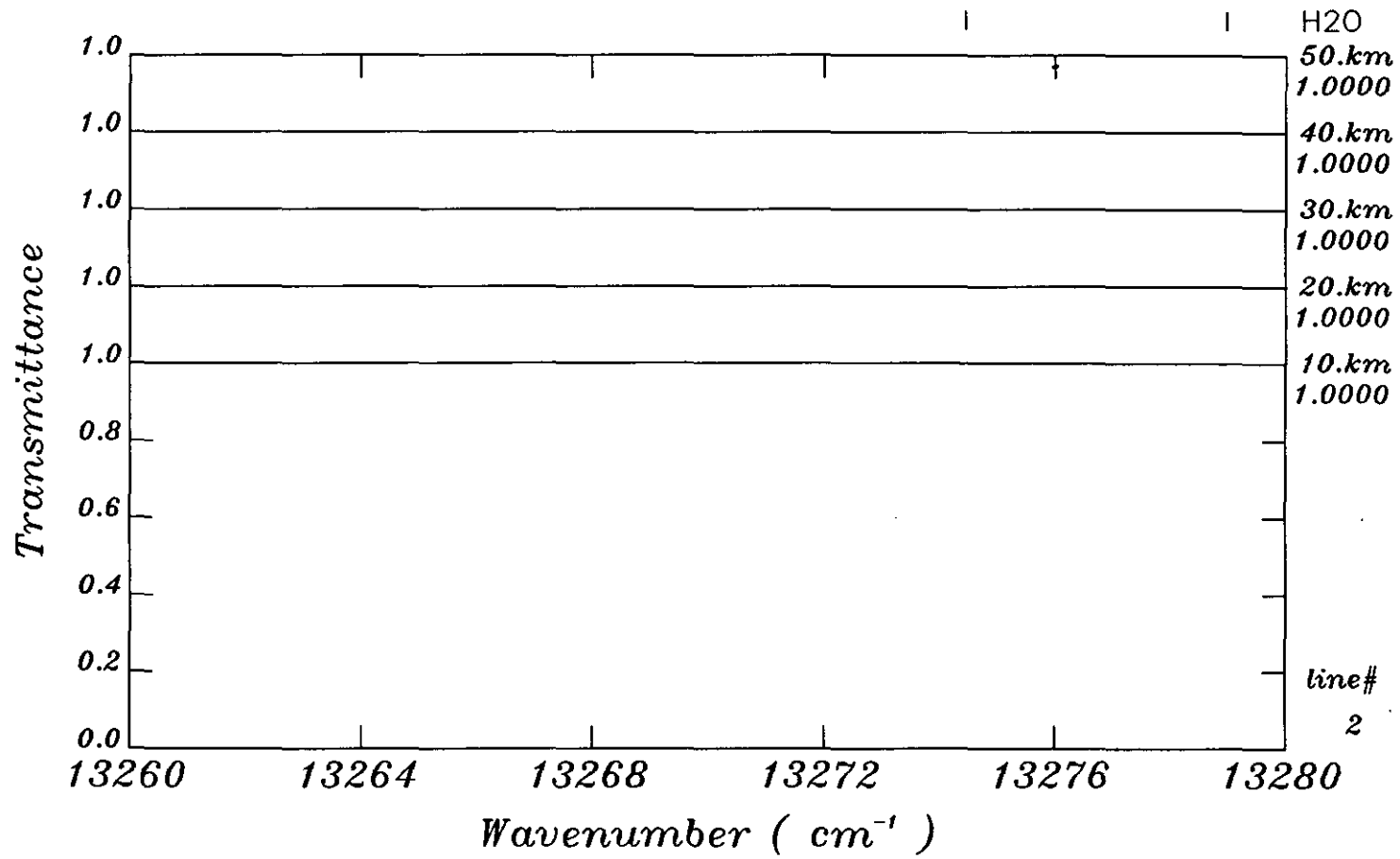












[ Appendix A ] ( Infrared calculation )

Charged Time for the Simulations on VAX 11/785 System  
(except for the program compilation time)

Wavenumber (cm <sup>-1</sup> )	TRN.FOR;50			TRNS.FOR;51		
	Date	CPU Time	Elapsed Time	Date	CPU Time	Elapsed Time
0830 - 0850	8/08	1: 00' 51"	1: 57' 33"	-	-	-
0850 - 0900	5/21	11: 25' 35"	27: 46' 40"	5/22	23' 18.27"	1: 01' 47"
0900 - 0940	5/22	3: 39' 21"	11: 17' 03"	5/22	17' 09.33"	1: 09' 31"
0940 - 0980	5/22	1: 24' 44"	4: 54' 48"	5/22	20' 23.27"	39' 46"
0980 - 1020	5/23	3: 40' 06"	12: 30' 05"	5/23	19' 13.61"	1: 04' 56"
1020 - 1060	5/24	4: 38' 11"	13: 58' 49"	5/24	19' 30.58"	24' 45"
1060 - 1100	5/24	2: 22' 13"	9: 27' 21"	5/24	20' 46.02"	38' 23"
1100 - 1180	5/25	3: 33' 46"	10: 14' 00"	5/25	44' 23.49"	1: 18' 00"
1150 - 1250	5/16	3: 21' 20"	3: 49' 50"	5/16	56' 00.85"	1: 03' 24"
1250 - 1350	5/07	2: 59' 12"	6: 54' 24"	5/10	55' 43.97"	1: 12' 03"
1350 - 1450	5/08	2: 17' 44"	5: 15' 58"	5/11	54' 12.36"	1: 05' 57"
1450 - 1550	5/09	2: 14' 10"	5: 18' 13"	5/11	52' 55.71"	1: 49' 05"
1550 - 1650	5/15	4: 53' 46"	5: 50' 40"	5/16	54' 52.98"	1: 52' 13"

\* TRN.FOR;50 is used for cross section calculation and its file output and plot data output of the total transmittances.

\* TRNS.FOR;51 is used for each gas transmittance calculations at 20 km altitude with reading the cross section file.

[ **Appendix B** ] ( Infrared re-calculation including CFC-11 and CFC-12 )

Charged Time for the Simulations on VAX 11/785 System  
(except for the program compilation time)

Wavenumber (cm <sup>-1</sup> )	TRNF.FOR;55			TRNFS.FOR;54		
	Date	CPU Time	Elapsed Time	Date	CPU Time	Elapsed Time
0830 - 0850	8/09	12' 33"	2: 10' 01"	8/09	11' 58.43"	34' 30"
0850 - 0860	7/30	7' 42"	29' 50"	7/30	6' 04.19"	20' 57"
0860 - 0900	8/07	39' 12"	48' 23"	8/07	24' 00.61"	34' 41"
0900 - 0940	8/08	31' 36"	39' 32"	8/08	20' 14.30"	55' 25"
1060 - 1070	8/08	9' 45"	13' 07"	8/08	5' 55.54"	7' 50"
1070 - 1100	8/09	33' 43"	1: 06' 58"	8/09	22' 33.15"	49' 59"
1100 - 1180	8/09	1: 19' 54"	2: 12' 47"	8/09	49' 14.96"	2: 49' 43"

\* TRNF.FOR;55 is used for transmittance calculation with reading cross section files including CFC-11 & CFC-12, and plot data output of the total transmittances.

\* TRNFS.FOR;54 is used for each gas transmittance calculations at 20 km altitude with reading the cross section file including CFC-11 & CFC-12.

[ Appendix C ] ( Visible calculation )

Charged Time for the Simulations on VAX 11/785 System  
(except for the program compilation time)

Temperature condition	TRNV.FOR;54		
	Date	CPU Time	Elapsed Time
Standard ( $\Delta T = 0$ )	7/03	43' 02"	57' 47"
$\Delta T = +10$	7/10	43' 04"	56' 44"
$\Delta T = -10$	7/10	42' 51"	1: 32' 54"

- \* TRNV.FOR;54 is used for cross section calculation and plot data output of the total transmittances.
- \* Temperatures in all atmospheric layers are shifted at the amount of  $\Delta T$ .  
Pressure in each layer is automatically re-calculated from temperature by the hydrostatics relation in the program TRNV.FOR.